Title
Coexistence and complex population dynamics

Author
Johnson, Evan

Publication Date
2022

Peer reviewed|Thesis/dissertation

Coexistence and complex population dynamics

By

EVAN C. JOHNSON
DISSERTATION

Submitted in partial satisfaction of the requirements for the degree of

DOCTOR OF PHILOSOPHY

in

Population Biology

in the

OFFICE OF GRADUATE STUDIES

of the

UNIVERSITY OF CALIFORNIA

DAVIS

Approved:

Alan Hastings, Chair

Andrew Latimer

Sebastian Schreiber

Committee in Charge

2022

To Mom, Dad, Logan, and Alan.

Abstract

Against the backdrop of resource competition, ecological coexistence appears mysterious: if species must specialize in order to exist, how can dozen of similar species inhabit the same environment? Many explanations have been put forward, but efforts have remained primarily theoretical, with simple models demonstrating coexistence via simple mechanisms. Therein lies the problem — explanations are simple by design, but nature is complex. Here, we improve upon *Modern Coexistence Theory*, a mathematical framework that can be used to measure the *relative importance* of different explanations for coexistence. Innovations range from the methodological to the conceptual.

Additionally, we attempt to understand the causes of unexpected population crashes, also known as catastrophes or ecological "black swan" events. Many such crashes do not fit the common explanation of tipping points resulting from changing environmental conditions. We provide an alternative and general mechanism for population crashes in a static environment, namely stochasticity (of any variety) combined with multiple episodes of density dependence. This explanation is confirmed in experimental microcosms of the red flour beetle, and connections to real-world population crashes are discussed.

Contents

Introduction

Community ecologists have put forward many explanations for coexistence, the most prominent of which are are specialized natural enemies (Nicholson, 1937; Holt, 1977; Holt et al., 1994; Holt and Lawton, 1994), a trade-off between competition and colonization (Levins and Culver, 1971; Sousa, 1979; Hastings, 1980; Tilman, 1994), the Janzen-Connell Hypothesis (Janzen, 1970; Connell, 1971; Stump and Chesson, 2015); the partitioning of resources across space (MacArthur, 1958;Hutchinson, 1961; Tilman, 1982; Holt, 1984); opportunist-gleaner tradeoffs (Fredrickson and Stephanopoulos, 1981); seasonal variation in resource supply (Stewart and Levin, 1973; Grover, 1997) or endogenously cyclical resource-consumer dynamics (Armstrong and McGehee, 1976; 1980), temporal partitioning of the environment (Loreau, 1989; Loreau, 1992; Klausmeier, 2010), the storage effect (Chesson and Warner, 1981, Chesson, 2003), and neutral theory (cite: Caswell, 1976; Hubbell, 2001, Kalyuzhny et al., 2015). Each explanation, having emerged from simple models (e.g., Levins and Culver, 1971), experiments (e.g., Paine, 1966), or curious patterns in field data (e.g., Janzen, 1970), are certainly *partial explanations*. Real ecological communities are complex, and many of the above phenomena may be operating at once. Spectacularly, each of these partial explanations can be grouped into natural categories called *coexistence mechanisms* and assigned a measure of relative importance. *Modern Coexistence Theory* (MCT) is the framework that makes this possible.

MCT has been widely successful. It has been the basis of important conceptual and theoretical advances (e.g., Chesson and Huntly, 1997; Stump and Chesson, 2015; Snyder and Chesson, 2003; Chesson and Kuang, 2008; Chesson and Kuang, 2010; Schreiber, 2021), and several attempts to infer the mechanisms of coexistence in real communities (Cáceres, 1997; Venable et al., 1993; Pake and Venable, 1995; Pake and Venable, 1996; Adler et al., 2006; Sears and Chesson, 2007; Descamps-Julien and Gonzalez, 2005; Facelli et al., 2005; Angert et al., 2009; Adler et al., 2010; Usinowicz et al., 2012; Chesson et al., 2012; Chu and Adler, 2015; Usinowicz et al., 2017; Ignace et al., 2018; Hallett et al., 2019; Armitage and Jones, 2019; Armitage and Jones, 2020; Zepeda and Martorell, 2019; Zepeda and Martorell, 2019; Towers et al., 2020; Holt and Chesson, 2014; Ellner et al., 2016) or laboratory microcosms (Jiang and Morin, 2007; Letten et al., 2018). Additionally, MCT unifies seemingly dissimilar explanations for coexistence through categorization into coexistence

mechanisms, thus organizing a scattered literature and highlighting similarities, such as the symmetrical role (with regards to coexistence) of resource specialization and specialist predators (Chesson and Kuang, 2008).

We perceive of MCT as a broad edifice (Fig. 1) that relates real coexistence (i.e., coexistence in real ecological communities) to simple yet incomplete explanations for coexistence (i.e., simple models in which coexistence has been demonstrated). The edifice is composed of three kinds of relationships, each corresponding to a level of arrows in Figure 1: 1) the relationship between coexistence and invasion growth rates, 2) the relationships between the invasion growth rate and coexistence mechanisms 3) the relationship between coexistence mechanisms and simple explanations for coexistence.

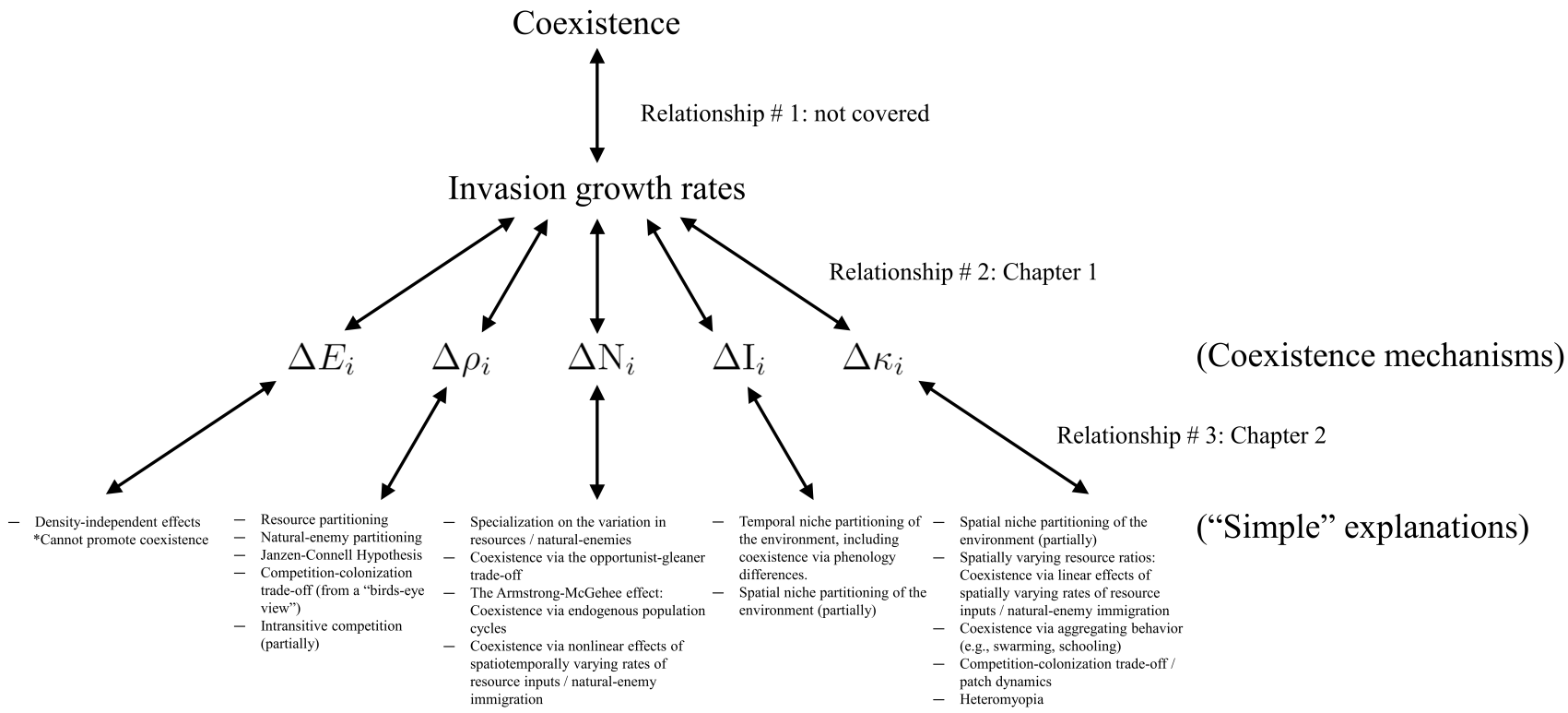

Figure 1: The goal of Modern Coexistence Theory: connecting *actual coexistence* to *simple explanations for coexistence*

This dissertation attempts to bridge the gaps in Figure 1, and in doing so, enable better inferences about ecological coexistence. In Chapter 1, we tackle relationship # 3, the connection between invasion growth rates and coexistence mechanisms. Specifically, we show how coexistence mechanisms can be measured measured in realistic models with spatiotemporal variation (Section 1.2). Additionally, we provide alternatives to the problematic and infamously confusing *scaling factors* (Section 1.1). In Chapter 2, we focus on relationship #3, the connection between coexistence mechanisms and fine-grained explanations of coexistence. Specifically, we discuss the biological meaning of the *storage effect* (Section 2.1) and other fluctuation-dependent mechanisms (Section 2.2). Relationship #1 is left to future research.

Chapter 3 focuses on a different topic: single-species population dynamics. Using experimental microcosms (of the red flour beetle, *Tribolium castaneum*) and stochastic models, we infer a novel mechanism of population crashes. The mechanism is connected to real-world populations, and the general utility of microcosm experiments is discussed. The composition of density dependence at successive life stages, all within a single generation, produces a variety of complex population dynamics, including chaos. Each section of this dissertation is presented as a stand-alone manuscript, complete with appendices and references.

References

Adler, P. B., Ellner, S. P., & Levine, J. M. (2010). Coexistence of perennial plants: An embarrassment of niches. *Ecology Letters*, *13*(8), 1019–1029.

Adler, P. B., HilleRisLambers, J., Kyriakidis, P. C., Guan, Q., & Levine, J. M. (2006). Climate variability has a stabilizing effect on the coexistence of prairie grasses. *Proceedings of the National Academy of Sciences*, *103*(34), 12793–12798.

Angert, A. L., Huxman, T. E., Chesson, P., & Venable, D. L. (2009). Functional tradeoffs determine species coexistence via the storage effect. *Proceedings of the National Academy of Sciences*, *106*(28), 11641–11645.

Armitage, D. W., & Jones, S. E. (2019). Negative frequency-dependent growth underlies the stable coexistence of two cosmopolitan aquatic plants. *Ecology*, *100*(5), e02657.

Armitage, D. W., & Jones, S. E. (2020). Coexistence barriers confine the poleward range of a globally distributed plant. *Ecology Letters*, *23*(12), 1838–1848.

Armstrong, R. A., & McGehee, R. (1976). Coexistence of species competing for shared resources. *Theoretical Population Biology*, *9*(3), 317–328.

Armstrong, R. A., & McGehee, R. (1980). Competitive exclusion. *The American Naturalist*, *115*(2), 151–170.

Cáceres, C. E. (1997). Temporal variation, dormancy, and coexistence: A field test of the storage effect. *Proceedings of the National Academy of Sciences*, *94*(17), 9171–9175.

Caswell, H. (1976). Community structure: A neutral model analysis. *Ecological monographs*, *46*(3), 327–354.

Chesson, P. (2003). Quantifying and testing coexistence mechanisms arising from recruitment fluctuations. *Theoretical Population Biology*, *64*(3), 345–357.

Chesson, P., & Huntly, N. (1997). The roles of harsh and fluctuating conditions in the dynamics of ecological communities. *The American Naturalist*, *150*(5), 519–553.

Chesson, P., Huntly, N. J., Roxburgh, S. H., Pantastico-Caldas, M., & Facelli, J. M. (2012). The storage effect: Definition and tests in two plant communities. In *Temporal dynamics and ecological process* (pp. 11–40). Cambridge University Press.

Chesson, P., & Kuang, J. J. (2008). The interaction between predation and competition. *Nature*, *456*(7219), 235–238.

Chesson, P., & Kuang, J. J. (2010). The storage effect due to frequency-dependent predation in multispecies plant communities. *Theoretical Population Biology*, *78*(2), 148–164.

Chesson, P. L., & Warner, R. R. (1981). Environmental variability promotes coexistence in lottery competitive systems. *The American Naturalist*, *117*(6), 923–943.

Chu, C., & Adler, P. B. (2015). Large niche differences emerge at the recruitment stage to stabilize grassland coexistence. *Ecological Monographs*, *85*(3), 373–392.

Connell, J. H. (1971). On the role of natural enemies in preventing competitive exclusion in some marine animals and in rain forest trees. In *Dynamics of populations* (pp. 298–312). Wageningen, The Netherlands.

Descamps-Julien, B., & Gonzalez, A. (2005). Stable coexistence in a fluctuating environment: An experimental demonstration. *Ecology*, *86*(10), 2815–2824.

Ellner, S. P., Snyder, R. E., & Adler, P. B. (2016). How to quantify the temporal storage effect using simulations instead of math. *Ecology letters*, *19*(11), 1333–1342.

Facelli, J. M., Chesson, P., & Barnes, N. (2005). Differences in seed biology of annual plants in arid lands: A key ingredient of the storage effect. *Ecology*, *86*(11), 2998–3006.

Fredrickson, A., & Stephanopoulos, G. (1981). Microbial competition. *Science*, *213*(4511), 972–979.

Grover, J. P. (1997). *Resource competition*. Springer.

Hallett, L. M., Shoemaker, L. G., White, C. T., & Suding, K. N. (2019). Rainfall variability maintains grass-forb species coexistence. *Ecology Letters*, *22*(10), 1658–1667.

Hastings, A. (1980). Disturbance, coexistence, history, and competition for space. *Theoretical Population Biology*, *18*(3), 363–373.

Holt, G., & Chesson, P. (2014). Variation in moisture duration as a driver of coexistence by the storage effect in desert annual plants. *Theoretical Population Biology*, *92*, 36–50.

Holt, R. a., & Lawton, J. (1994). The ecological consequences of shared natural enemies. *Annual review of Ecology and Systematics*, *25*(1), 495–520.

Holt, R. D. (1977). Predation, apparent competition, and the structure of prey communities. *Theoretical Population Biology*, *12*(2), 197–229.

Holt, R. D. (1984). Spatial heterogeneity, indirect interactions, and the coexistence of prey species. *The American Naturalist*, *124*(3), 377–406.

Holt, R. D., Grover, J., & Tilman, D. (1994). Simple rules for interspecific dominance in systems with exploitative and apparent competition. *The American Naturalist*, *144*(5), 741–771.

Hubbell, S. P. (2001). *The unified neutral theory of biodiversity and biogeography*. Princeton University Press.

Hutchinson, G. E. (1961). The paradox of the plankton. *The American Naturalist*, *95*(882), 137–145.

Ignace, D. D., Huntly, N., & Chesson, P. (2018). The role of climate in the dynamics of annual plants in a chihuahuan desert ecosystem. *Evolutionary Ecology Research*, *19*(3), 279–297.

Janzen, D. H. (1970). Herbivores and the number of tree species in tropical forests. *The American Naturalist*, *104*(940), 501–528.

Jiang, L., & Morin, P. J. (2007). Temperature fluctuation facilitates coexistence of competing species in experimental microbial communities. *Journal of Animal Ecology*, *76*(4), 660–668.

Kalyuzhny, M., Kadmon, R., & Shnerb, N. M. (2015). A neutral theory with environmental stochasticity explains static and dynamic properties of ecological communities. *Ecology letters*, *18*(6), 572–580.

Klausmeier, C. A. (2010). Successional state dynamics: A novel approach to modeling nonequilibrium food-web dynamics. *Journal of Theoretical Biology*, *262*(4), 584–595.

Letten, A. D., Dhami, M. K., Ke, P.-J., & Fukami, T. (2018). Species coexistence through simultaneous fluctuation-dependent mechanisms. *Proceedings of the National Academy of Sciences*, *115*(26), 6745–6750.

Levins, R., & Culver, D. (1971). Regional coexistence of species and competition between rare species. *Proceedings of the National Academy of Sciences*, *68*(6), 1246–1248.

Loreau, M. (1989). Coexistence of temporally segregated competitors in a cyclic environment. *Theoretical Population Biology*, *36*(2), 181–201.

Loreau, M. (1992). Time scale of resource dynamics and coexistence through time partitioning. *Theoretical Population Biology*, *41*(3), 401–412.

MacArthur, R. H. (1958). Population ecology of some warblers of northeastern coniferous forests. *Ecology*, *39*(4), 599–619.

Nicholson, A. (1937). The role of competition in determining animal populations. *Journal of the Council for Scientific and Industrial Research*, 101–106.

Paine, R. T. (1966). Food web complexity and species diversity. *The American Naturalist*, *100*(910), 65–75.

Pake, C. E., & Venable, D. L. (1995). Is coexistence of sonoran desert annuals mediated by temporal variability reproductive success. *Ecology*, *76*(1), 246–261.

Pake, C. E., & Venable, D. L. (1996). Seed banks in desert annuals: Implications for persistence and coexistence in variable environments. *Ecology*, *77*(5), 1427–1435.

Schreiber, S. J. (2021). Positively and negatively autocorrelated environmental fluctuations have opposing effects on species coexistence. *The American Naturalist*, *197*(4), 000–000.

Sears, A. L., & Chesson, P. (2007). New methods for quantifying the spatial storage effect: An illustration with desert annuals. *Ecology*, *88*(9), 2240–2247.

Snyder, R. E., & Chesson, P. (2003). Local dispersal can facilitate coexistence in the presence of permanent spatial heterogeneity. *Ecology letters*, *6*(4), 301–309.

Sousa, W. P. (1979). Disturbance in Marine Intertidal Boulder Fields: The Nonequilibrium Maintenance of Species Diversity. *Ecology*, *60*(6), 1225.

Stewart, F. M., & Levin, B. R. (1973). Partitioning of resources and the outcome of interspecific competition: A model and some general considerations. *The American Naturalist*, *107*(954), 171–198.

Stump, S. M., & Chesson, P. (2015). Distance-responsive predation is not necessary for the janzen–connell hypothesis. *Theoretical Population Biology*, *106*, 60–70.

Tilman, D. (1982). *Resource competition and community structure*. Princeton University Press.

Tilman, D. (1994). Competition and biodiversity in spatially structured habitats. *Ecology*, *75*(1), 2–16.

Towers, I. R., Bowler, C. H., Mayfield, M. M., & Dwyer, J. M. (2020). Requirements for the spatial storage effect are weakly evident for common species in natural annual plant assemblages. *Ecology*, *101*(12), e03185.

Usinowicz, J., Chang-Yang, C.-H., Chen, Y.-Y., Clark, J. S., Fletcher, C., Garwood, N. C., Hao, Z., Johnstone, J., Lin, Y., Metz, M. R., Masaki, T., Nakashizuka, T., Sun, I.-F., Valencia, R., Wang, Y., Zimmerman, J. K., Ives, A. R., & Wright, S. J. (2017). Temporal coexistence mechanisms contribute to the latitudinal gradient in forest diversity. *Nature*, *550*(7674), 105–108.

Usinowicz, J., Wright, S. J., & Ives, A. R. (2012). Coexistence in tropical forests through asynchronous variation in annual seed production. *Ecology*, *93*(9), 2073–2084.

Venable, D. L., Pake, C. E., & Caprio, A. C. (1993). Diversity and coexistence of sonoran desert winter annuals. *Plant Species Biology*, *8*(2-3), 207–216.

Zepeda, V., & Martorell, C. (2019). Fluctuation-independent niche differentiation and relative non-linearity drive coexistence in a species-rich grassland. *Ecology*, *100*(8), e02726.

Chapter 1

Measuring coexistence

Chapter Contents

1.1 Methods for calculating coexistence mechanisms: Beyond scaling factors

1.1.1 Abstract

How do species coexist? A framework known as Modern Coexistence Theory can "measure coexistence" by partitioning invasion growth rates into *coexistence mechanisms*, terms which correspond to classes of explanations for coexistence. There are several reasonable ways to define coexistence mechanisms, each depending on exactly how a species perturbed to low density (the *invader*) is compared to other species that remain at their typical densities (the *residents*). Using conceptual arguments and two case studies, we compare five methods for calculating coexistence mechanisms: i) *Scaling factors*, the traditional approach which attempts to eliminate the linear effects of regulating factors; ii) *The simple comparison*, which gives equal weight to all resident species; iii) *Generation time scaling*, a novel method which corrects for intrinsic differences in population-dynamical speed; iv) β *scaling*, where resident growth rates are scaled by a measure of relative sensitivity to competition; and v) *The invader–invader comparison*, a previously obscure method in which a focal species is compared to itself at high vs. low density. We find that the conventional scaling factors can lead to nonsensical results when species have strong and asymmetric niche differences; though scaling factors can be useful in certain theoretical studies, they are not recommended for explaining coexistence in real communities. Invader–invader comparisons are also problematic, as they do not effectively measure specialization or niche differentiation. The universally-applicable simple comparison often works well, but can give counterintuitive results when species have disparate generation times. The β scaling method often works well in simple models, but faces implementation problems in complex models. We tentatively recommend generation time scaling as the all-purpose method for calculating coexistence mechanisms.

1.1.2 Introduction

Determining the mechanisms of coexistence in any given community is a difficult task. The underlying problem is that nature is complex, but explanations for coexistence (being reductionistic, as all explanations are) are simple, often codified in two-species models and several paragraphs of commentary. Therefore, our task is to take a arbitrary, complex model (representing the real world), and extract the relative importance of several simple explanations. Modern Coexistence Theory (Chesson, 1994; Chesson, 2000a; Barabás et al., 2018) is a tool that makes this possible

Modern Coexistence Theory (MCT) is a framework for understanding coexistence. More specifically, MCT "measures coexistence" by quantifying *coexistence mechanisms*: processes (e.g., resource partitioning) that tend to increase species' per capita growth rates when rare. The ability of each species to recover from rarity is ostensibly related to the overall stability of the community – coexistence. Crucially, coexistence mechanisms are operationalized with an *invader–resident comparison*: processes that contribute the per capita growth rate of a species that has been perturbed to low density (the *invader*) are compared to corresponding processes for species at typical abundances (the *residents*).

However, to date, little attention has been paid to the interpretation of coexistence mechanisms. MCT is used unquestioningly in empirical applications, even though it was not originally designed to measure coexistence, but rather to produce theoretical insights about the role of fluctuations in coexistence (Barabás et al., 2018, p. 288; Chesson, 2020, p. 6). The absence of conceptual analysis is a problem: if our goal is to interpret the values of coexistence mechanisms as the relative importance of explanations for coexistence, then we must be sure of the correspondence between explanations and coexistence mechanisms. In other words, the exact definition of coexistence mechanisms is crucial to their interpretation, and thus crucial to how we understand coexistence.

One part of the definition of coexistence mechanisms is *scaling factors*, constants that re-scale the growth rates of residents. For many, the scaling factors are the most confusing part of MCT. They were introduced by Chesson (1994, p. 241) with little justification: "This choice is justified by the results that it gives. It leads to a clear partitioning of mechanisms of coexistence, as shown in subsection 4.2, below." A diligent reader may go onto infer that the purpose of the scaling factors is to eliminate a term in the mathematical expression for the invader's growth rate: "... linear terms in competition do not appear in this comparison ..." (Chesson, 1994, p. 247; also see equations 36 and 43). Decades later, Chesson (2020, p. 3) confirms, "The idea [of the scaling factors] is that the [invader–resident] comparison should eliminate common components of competition to highlight critical species differences." One is left wondering why the linear effects of competition cannot be the basis of a critical species difference.

Further complicating the usage of scaling factor is that fact that they cannot serve their purported purpose — eliminating the linear effects of competition — when there are more distinct regulating factors than resident species (Chesson, 1994; Barabás et al., 2018). Regulating factors (also known as limiting factors or internal variables), are variables that are involved in a feedback loop that regulates population density. Examples include resources, refugia, and natural enemies. When a regulating factor is *continuous* (e.g., seeds along a continuum of sizes, varying rates of resource supply across space), then there are technically an infinite number of regulating factors, and thus the scaling factors automatically cannot serve their purported purpose.

There are a slew of other problems with scaling factors. 1) When species' sensitivities to regulating factors are similar, small differences in species' sensitivities will lead to big differences in the scaling factors (due to inverting an ill-conditioned matrix; see Barabás et al., 2018, p. 295). This means that inferences from empirical applications of MCT can be sensitive to measurement error and/or parameter estimation error. 2) Scaling factors can switch from positive to negative, turning an invader–resident difference into a invader–resident sum (due to subtracting a negative; Snyder et al., 2005, p. E92); this is problematic because the invader–resident difference is what permits us to interpret coexistence mechanisms as a rare-species advantage. 3) When a certain assumption of the mathematical theory is not met (Assumption *a6* in Chesson, 1994), the scaling factors may not be uniquely determined, even when there are more residents than regulating factors. In this scenario, the analytic theory cannot be used to calculate scaling factors, and instead one must use one of several computationally-intensive work-arounds (see Ellner et al., 2016, SI.5).

Here, we argue that the primary function of the scaling factors — eliminating the linear effects of competition — is not desirable if one wants to use MCT to understand coexistence in real communities. Eliminating the linear effects of competition is effective at showing that not all species can coexist via classical mechanisms (i.e., fluctuation-independent mechanisms such as resource or natural-enemy partitioning), which can be useful in theoretical research. But, if one wants to "measure coexistence" (i.e., understand empirically how species coexist) then is desirable to be able to attribute coexistence to classical mechanisms.

However, it is not merely the case that scaling factors are unnecessary: they can also lead to incorrect inferences about how species are coexisting. Scaling factors are designed entirely to eliminate the linear effects of competition, but they necessarily weight resident growth rates in the calculation of other coexistence mechanisms. Consequentially, the scaling factors can modulate other coexistence mechanisms, sometimes in a way that is nonsensical.

The obvious alternative to scaling factors is a simple average over resident species, which we call the *simple comparison* method. To be more precise, each resident gets weighted by $1/(S-1)$ (where S is the number of species in the community), such that equal weight is given to the low density state (i.e., the

invader) and the high density state (i.e., the sum of residents). The simple comparison can work well, but it can also be problematic if some species have comparatively fast population dynamics; such species tend to dominate all other species in the invader–resident comparison.

Our proposed solution to the shortcomings of previous methods is to scale resident growth rates by ratios of generation times. Conceptually, this *generation time scaling* converts the intrinsic speed of resident population dynamics to that of the invader. Functionally, the generation time scaling prevent the invader–resident comparison from being dominated by terms corresponding to a handful of speedy species. Yet another solution is to replace the invader–resident comparison with an *invader–invader comparison*, wherein a single focal species is compared to itself at high vs. low density.

In this paper, we define and discuss the five aforementioned methods for calculating coexistence mechanisms: scaling factors (Section 1.1.3.2), the simple comparison (Section 1.1.3.3), generation time scaling (Section 1.1.3.4), β scaling (Section 1.1.3.5)and the invader–invader comparison (Section 1.1.3.6). We discuss the strengths and weakness of each method (see Table 1.3 in the *Discussion*), using both conceptual arguments and two case study (Section 1.1.4 & Appendix 1.1.C). We conclude that scaling factors and the invader–invader comparison should not be used in empirical applications of MCT. All other methods have their time and place, but we recommend generation time scaling as the best all-purpose method.

1.1.3 Methods

All methods for calculating coexistence mechanisms are rooted in Modern Coexistence Theory (MCT). For completeness, we offer a summary of MCT below; for those seeking detail or clarification, see Barabás et al., 2018.

1.1.3.1 A summary of Modern Coexistence Theory

The main innovation of MCT is the partition of invasion growth rates into *coexistence mechanisms*. This partition is obtained with two main steps: "decompose and compare" (Ellner et al., 2019).

1. **Decompose**.

   Consider a community composed of scalar populations (i.e., populations without age, stage, or spatial structure), subject to temporal variation in the environment, population densities, and regulating factors. The per capita growth rate of species j is denoted by $r_j(t) = dN_j(t)/(N_j(t)dt)$ in continuous time or $r_j(t) = \log(N_j(t+1)/N_j(t))$ in discrete time. Now, we perturb species i (the invader) to zero density and use the superscript "$\{-i\}$" to indicate quantities that must be evaluated in this context.

We represent the per capita growth rate as a function g_j of the environmental parameter $E_j(t)$, as well as a vector of L regulating factors, $\boldsymbol{F^{\{-i\}}(t)} = (F_1^{\{-i\}}(t), F_2^{\{-i\}}(t), ..., F_L^{\{-i\}}(t))$:

$$r_j^{\{-i\}}(t) = g_j(E_j(t), \boldsymbol{F^{\{-i\}}(t)}). \tag{1.1}$$

For notational simplicity, we will drop the explicit time-dependence. The parameter E_j is sometimes called the environmental response, or the environmentally-dependent parameter, or simply the environment. While it usually represents a demographic parameter that depends on the environment (e.g., the probability of seed germination), it more generally represents the influence of density-independent factors. The regulating factors $\boldsymbol{F}$ can be abiotic resources, biotic resources, species densities, natural enemies, refugia, light, etc.

Next, we approximate each species' per capita growth rate with a second order Taylor series expansion about the equilibrium values E_j^* and $\boldsymbol{F}^{*j}$, selected so that $r_j(E_j^*, \boldsymbol{F}^{*j}) = 0$. While the regulating factors $\boldsymbol{F}$ are not species-specific, the equilibrium values $\boldsymbol{F}^{*j} = (F_1^{*j}, F_2^{*j}, ..., F_L^{*j})$ may be species-specific (note the superscript "j"). There is no agreed upon method for determining the equilibrium parameters (a number of strategies are discussed in Appendix 1.1.A). In any case, they should be close to their respective temporal means, $\overline{E_j}$ and $\overline{\boldsymbol{F^{\{-i\}}}}$, in order for the Taylor series to be a good approximation (Barabás et al., 2018, p. 280).

After calculating the aforementioned Taylor series expansion, we take a temporal average in order to obtain an approximation of species j's *long-term* average growth rate. The quality of this approximation depends on the environmental parameter only experiencing small deviations from equilibrium (for the mathematical details, see Chesson, 1994; and Chesson, 2000a). These *small-noise assumptions* also allow us to replace $\overline{(E_j - E_j^*)(F_k^{\{-i\}} - F_k^{*j})}$ with $\text{Cov}\left(E_j, F_k^{\{-i\}}\right)$ and perform analogous replacements for other terms. The result is

$$\begin{aligned}
\overline{r_j^{\{-i\}}} \approx\ & \alpha_j^{(1)}(\overline{E_j} - E_j^*) + \frac{1}{2}\alpha_j^{(2)}\text{Var}(E_j) \\
& + \sum_{k=1}^{L} \phi_{jk}^{(1)}(\overline{F_k^{\{-i\}}} - F_k^{*j}) \\
& + \sum_{k=1}^{L}\sum_{m=1}^{L} \phi_{jkm}^{(2)}\text{Cov}\left(F_k^{\{-i\}}, F_m^{\{-i\}}\right) \\
& + \zeta_{jk}^{(1)} \sum_{k=1}^{L} \text{Cov}\left(E_j, F_k^{\{-i\}}\right),
\end{aligned} \tag{1.2}$$

where the coefficients of the Taylor series,

$$\alpha_j^{(1)} = \frac{\partial g_j(E_j^*, \boldsymbol{F}^{*j})}{\partial E_j}, \quad \phi_{jk}^{(1)} = \frac{\partial g_j(E_j^*, \boldsymbol{F}^{*j})}{\partial F_k}, \quad \alpha_j^{(2)} = \frac{\partial g_j(E_j^*, \boldsymbol{F}^{*j})}{\partial E_j}, \quad \phi_{jkm}^{(2)} = \frac{\partial^2 g(E_j^*, \boldsymbol{F}^{*j})}{\partial F_k \partial F_m}, \quad \zeta_{jk}^{(1)} = \frac{\partial^2 g(E_j^*, \boldsymbol{F}^{*j})}{\partial E_j \partial F_k}, \tag{1.3}$$

are all evaluated at $E_j = E_j^*$ and $\boldsymbol{F} = \boldsymbol{F}^{*j}$.

2. **Compare**

Resident species (denoted with subscript s) have a long-term average per capita growth rate of zero; otherwise, resident populations would go extinct or explode to infinity. Therefore, the value of the invasion growth rate is unaltered if we subtract a linear combination of the residents' average growth rates. That is, we can write the invasion growth rate of species i as

$$\overline{r_i^{\{-i\}}} = \overline{r_i^{\{-i\}}} - \sum_{s \neq i}^{S} q_{is} \overline{r_s^{\{-i\}}}, \tag{1.4}$$

where the q_{is} are the scaling factors, and S is the number of total species in the community. To identify the processes that generate a rare-species advantage, we can substitute Eq.2.6 into Eq.2.7 and group like-terms. The invasion growth rate now becomes

$$\begin{aligned}
\overline{r_i^{\{-i\}}} \approx & \underbrace{\alpha_i^{(1)}(\overline{E_i} - E_i^*) + \frac{1}{2}\alpha_i^{(2)}\mathrm{Var}(E_i) - \left(\sum_{k=1}^{L} \phi_{ik}^{(1)} F_k^{*i}\right) - \sum_{s \neq i}^{S} q_{is}\left((\overline{E_s} - E_s^*) + \frac{1}{2}\alpha_s^{(2)}\mathrm{Var}(E_s) - \sum_{k=1}^{L} \phi_{sk}^{(1)} F_k^{*s}\right)}_{r_i' \text{: Density-independent effects}} \\
& + \underbrace{\left(\sum_{k=1}^{L} \phi_{ik}^{(1)} \overline{F_k^{\{-i\}}}\right) - \sum_{s \neq i}^{S} q_{is}\left(\sum_{k=1}^{L} \phi_{sk}^{(1)} \overline{F_k^{\{-i\}}}\right)}_{\Delta\rho_i \text{: Linear density-dependent effects}} \\
& + \underbrace{\frac{1}{2}\left[\left(\sum_{k=1}^{L}\sum_{m=1}^{L} \phi_{ikm}^{(2)} \mathrm{Cov}\left(F_k^{\{-i\}}, F_m^{\{-i\}}\right)\right) - \sum_{s \neq i}^{S} q_{is} \sum_{k=1}^{L}\sum_{m=1}^{L} \phi_{skm}^{(2)} \mathrm{Cov}\left(F_k^{\{-i\}}, F_m^{\{-i\}}\right)\right]}_{\Delta N_i \text{: Relative nonlinearity}} \\
& + \underbrace{\sum_{k=1}^{L} \zeta_{ik}^{(1)} \mathrm{Cov}\left(E_i, F_k^{\{-i\}}\right) - \sum_{s \neq i}^{S} q_{is} \sum_{k=1}^{L} \zeta_{sk}^{(1)} \mathrm{Cov}\left(E_s, F_k^{\{-i\}}\right)}_{\Delta I_i \text{ : The storage effect}}
\end{aligned} \tag{1.5}$$

The symbols under the brackets (r_i', $\Delta\rho_i$, ΔN_i, and ΔI) denote the coexistence mechanisms.

The interpretations of the coexistence mechanisms are as follows: *The density independent effects*, ΔE_i, is the degree to which all density-independent factors favor the invader. *The linear density-*

dependent effects, $\Delta\rho_i$, represents a rare-species advantage due to specialization on regulating factors (e.g., resources, natural enemies). *Relative nonlinearity*, ΔN_i, is a rare-species advantage due to specialization on variation in regulating factors. *The storage effect*, ΔI_i, is the rare-species advantage due to specialization on certain states of a variable environment. See Barabás et al. (2018) for a more thorough discussion of the coexistence mechanisms, their interpretations, and their connection to specific models.

Experts may note that our presentation of MCT differs subtly from that of previous research. First, our exposition above only accommodates models with temporal variation. There is an analogous version of MCT for models with spatial variation (Chesson, 2000a), which we do not present here for the sake of simplicity. Second, we write the per capita growth rate directly as a function of shared (across species) regulating factors, as opposed to a function of a species-specific competition parameter (as in Chesson, 1994; Barabás et al., 2018). Third, we do not change coordinates to the so-called *standard parameters*, which function to generate coexistence mechanisms that sum exactly to the invasion growth rate (Chesson, 2020); we exclude these *exact coexistence mechanisms* from our exposition for the sake of simplicity, but they are computed in the case study.

1.1.3.2 Scaling factors

The scaling factors were introduced by Chesson and Huntly (1997), and later integrated into Modern Coexistence Theory (MCT; Chesson, 1994). They were referred to only by symbols until Ellner et al. (2016) coined the term *scaling factors*. The scaling factors have been referred to as *comparison quotients* (Chesson, 2018) and have been denoted in different ways (Barabás et al., 2018; Chesson, 2020; Barabás and D'Andrea, 2020). It is worth recognizing that these superficially different versions of the scaling factors all serve the same fundamental goal: canceling the $\Delta\rho_i$ coexistence mechanism.

To define the scaling factors, we must first define the standard standard competition parameter:

$$\mathscr{C}_j(t) = g_j(E_j^*, \boldsymbol{F}). \tag{1.6}$$

The regulating factors $\boldsymbol{F}$ may have different meanings in different models (representing different species and/or communities); they may even have different units (e.g., abundance vs. biomass). By contrast, the standard competition parameter is always defined with the common currency of growth rates (or pseudo-rates in the case of discrete time), and can therefore be thought of as the main effect of competition on the average per capita growth rate.

The scaling factors are defined as

$$q_{is} = \frac{\partial \mathscr{C}_i^{\{-i\}}}{\partial \mathscr{C}_s^{\{-i\}}}, \tag{1.7}$$

evaluated at $\mathscr{C}_s = 0$. Note that the definition of the scaling factors presumes that the invader's $\mathscr{C}_i$ can be written as a function of the residents' $\mathscr{C}_s$ (assumption *a6* in Chesson, 1994). In Appendix 1.1.B, we show that the scaling factors are solely functions of species' sensitivities to regulating factors, $\phi_{jk}^{(1)}$ (see Eq.2.5), and further, that the scaling factors can be obtained by solving a system of linear equations. A solution does not exist if there are more limiting factors than resident species; in this case, the scaling factors cancel the linear density-dependent effects (i.e., $\Delta\rho_i = 0$). If the converse is true — the number of limiting factors is less than or equal to the number of resident species — then there are an infinite number of the solutions, and thus the scaling factors are not uniquely defined.

The purpose of the scaling factor is to eliminate the linear density-dependent effects, $\Delta\rho_i$. But why eliminate $\Delta\rho_i$? To our knowledge, the most explicit explanation comes from Chesson (2020, p. 3): "The idea is that the [invader–resident] comparison should eliminate common components of competition to highlight critical species differences." It is not clear why $\Delta\rho_i$ does not constitute a critical species difference, particularly since it encapsulates classical explanations for species coexistence: resource partitioning and natural-enemy partitioning. Perhaps we can arrive at a clearer justification of the scaling factors by studying papers in which the scaling factors played a crucial role.

Chesson and Huntly (1997) analyzed a model where per capita growth rates responded linearly to environmental fluctuations and a single regulating factor. The scaling factors eliminated $\Delta\rho_i$, and the linear responses precluded the fluctuation-dependent mechanisms, ΔN_i and ΔI_i. Thus, a species' average growth rate could be represented entirely by the density-independent effects, r_i'. One can show that a weighted sum of r_i' across species is equal to zero; if some species have a positive r_i', others necessarily have a negative r_i', so at least one species is destined for extinction. This result is a triumph of the scaling factors because it contradicted the idea that disturbances per se promote coexistence (Wiens, 1977; Huston, 1979; Strong Jr, 1983).

The scaling factors can also highlight the role of fluctuations in coexistence. If $\Delta\rho_i$ is cancelled, then not all species can coexist on r_i'. If species nonetheless coexist, then coexistence must be attributable to fluctuation-dependent mechanisms, ΔN_i and/or ΔI_i. Using this approach, Chesson (1994) showed that fluctuations are necessary for coexistence in the lottery model and the annual plant model. Crucially, in both of the aforementioned papers (i.e., Chesson and Huntly, 1997; and Chesson, 1994), the cancelling of $\Delta\rho_i$ is valuable because it tells us how species are *not* coexisting.

There are two auxiliary reasons for canceling $\Delta\rho_i$, one technical and one pragmatic. The technical small-

noise assumptions of MCT (Chesson, 1994) imply that the fluctuation-dependent mechanisms are small (i.e., $\mathcal{O}(\sigma^2)$, where σ is a small parameter), but imply nothing about $\Delta\rho_i$. Therefore, if $\Delta\rho_i$ is not eliminated, it can dominate the invader-resident comparison, rendering the original point of MCT (understanding the role environmental fluctuations) moot. Of course, this is no concern for empirical applications of MCT: environmental fluctuations are not small in the real world, and even if $\Delta\rho_i$ does dominate the invader–resident comparison, that in itself is scientifically interesting.

There is one pragmatic rationale for the scaling factors: they prevent us from having having to calculate the temporal averages of the regulating factors (which are inherent in $\Delta\rho$; Eq.1.5). This is mainly useful for theorists, since analytical expressions for $\overline{\boldsymbol{F}^{\{-i\}}}$ can be unobtainable or otherwise too complicated to be insightful. For empirical applications of MCT, one can simply evaluate $\overline{\boldsymbol{F}^{\{-i\}}}$ numerically. Barabás et al. (2018, p. 282) claim that eliminating $\Delta\rho_i$ can prevent us from having to explicitly model the dynamics of the regulating factors, since even though the variance and covariance terms in ΔN and ΔI depend on the regulating factors, "...these quantities can be calculated without a detailed knowledge of the dynamics of limiting factors (for an example, see Appendix S4)." We do not believe that this is true most of the time – Barabás et al.'s example relies on the unrealistic assumption that the value of the regulating factor only depends on the current environmental parameter, which in turn implies either 1) a time-scale separation where environmental change is much slower than the dynamics of regulating factors, or 2) a very particular model structure; e.g., in the two-species lottery model, the resident density is fixed at one, so competition effectively does not depend on adult density.

Given that the scaling factors are a seminal part of MCT, which itself is an all-purpose framework, it is easy to get the impression that the scaling factors are also all-purpose. Yet the historical record shows that the scaling factors have been used as a means to specific ends: expanding on the competitive exclusion principle, highlighting the role of fluctuation-dependent mechanisms, and simplifying mathematical formulas. More generally, the scaling factors are suited for deriving biological insights from the mathematical analysis of simple models. The original goal of MCT was to understand how fluctuations affect coexistence (Barabás et al., 2018, p. 288, Chesson, 2020, p. 6), and indeed, the scaling factors have proved valuable in pursuit of this goal.

There is growing interest in using MCT as a measurement tool; as a way to quantify the mechanisms of coexistence in real communities (e.g., Cáceres, 1997; Adler et al., 2006; Sears and Chesson, 2007; Descamps-Julien and Gonzalez, 2005; Angert et al., 2009; Usinowicz et al., 2012; Chesson et al., 2012; Chu and Adler, 2015; Usinowicz et al., 2017; Hallett et al., 2019; Armitage and Jones, 2019; Armitage and Jones, 2020; Zepeda and Martorell, 2019; Zepeda and Martorell, 2019; Towers et al., 2020; Ellner et al., 2016; Ellner et al., 2019). It is arguable, *a priori*, that the scaling factors do not serve this goal. We want to know the

degree to which classical explanations (i.e., resource and natural-enemy partitioning) promote coexistence, so we should not try to cancel $\Delta\rho_i$. Quite the opposite — to gain a more fine-grained understanding of coexistence, we typically expand $\Delta\rho_i$ into contributions from individual regulating factors.

1.1.3.3 The simple comparison

Ellner et al. (2019) suggested abandoning the scaling factors and redefining the coexistence mechanisms with a simple average over resident species. This schema, which we call *the simple comparison*, can be thought of as a special case of the generalized invasion growth rate partition:

$$\begin{aligned}
\overline{r}_i \approx & \underbrace{\left(\alpha_i^{(1)}(\overline{E_i} - E_i^*) + \frac{1}{2}\alpha_i^{(2)}\mathrm{Var}(E_i)\right) - \sum_{s\neq i}^{S} A_{is}\left((\overline{E_s} - E_s^*) + \frac{1}{2}\alpha_s^{(2)}\mathrm{Var}(E_s)\right)}_{\Delta E_i:\ \text{Density-independent effects}} \\
& + \underbrace{\left(\sum_{k=1}^{L}\phi_{ik}^{(1)}\left(\overline{F_k^{\{-i\}}} - F_k^{*i}\right)\right) - \sum_{s\neq i}^{S} A_{is}\left(\sum_{k=1}^{L}\phi_{sk}^{(1)}\left(\overline{F_k^{\{-i\}}} - F_k^{*s}\right)\right)}_{\Delta\rho_i:\ \text{Linear density-dependent effects}} \\
& + \underbrace{\frac{1}{2}\left[\left(\sum_{k=1}^{L}\sum_{m=1}^{L}\phi_{ikm}^{(2)}\mathrm{Cov}\left(F_k^{\{-i\}}, F_m^{\{-i\}}\right)\right) - \sum_{s\neq i}^{S} A_{is}\left(\sum_{k=1}^{L}\sum_{m=1}^{L}\phi_{skm}^{(2)}\mathrm{Cov}\left(F_k^{\{-i\}}, F_m^{\{-i\}}\right)\right)\right]}_{\Delta N_i:\ \text{Relative nonlinearity}} \\
& + \underbrace{\left(\sum_{k=1}^{L}\zeta_{ik}^{(1)}\mathrm{Cov}\left(E_i, F_k^{\{-i\}}\right)\right) - \sum_{s\neq i}^{S} A_{is}\left(\sum_{k=1}^{L}\zeta_{sk}^{(1)}\mathrm{Cov}\left(E_s, F_k^{\{-i\}}\right)\right)}_{\Delta I_i\ :\ \text{The storage effect}},
\end{aligned} \tag{1.8}$$

where A_{is} is the *generalized scaling factor*. Note that because $\Delta\rho_i$ does not need to be cancelled, there is no need to shunt $\boldsymbol{F}^{*j}$ terms from $\Delta\rho_i$ to the density-independent effects. Because the density-independent effects contains only environmental parameters, it is now denoted by ΔE_i. The linear density-dependent effects, $\Delta\rho_i$, can be expanded further into contributions from individual regulating factors. For instance, the degree to which species i specializes on regulating factor k is

$$\Delta\rho_{i,F_k} = \left(\phi_{ik}^{(1)}\left(\overline{F_k^{\{-i\}}} - F_k^{*i}\right)\right) - \sum_{s\neq i}^{S} A_{is}\left(\phi_{sk}^{(1)}\left(\overline{F_k^{\{-i\}}} - F_k^{*s}\right)\right). \tag{1.9}$$

If one so desires, similar expansions could be applied to the other consistence mechanisms.

The simple comparison is obtained by fixing the generalized scaling factor at

$$A_{is} = \frac{1}{S-1}, \tag{1.10}$$

such that the invader is compared the arithmetic mean of resident terms. Coexistence is understood as a rare-species advantage, which necessitates a comparison of low-density states and high-density states. The simple comparison ostensibly gives equal weight to the low-density state and the high-density state, while equally utilizing each resident. However, there is a sense in which the simple factors do not give equal weight to all residents. Consider a single resident that has the capacity to grow and decline at a rapid rate. Even though this resident's average growth rate is zero, the resident's grow rate components (i.e., the additive terms in Eq.2.6) will tend to be large in magnitude, and will therefore tend to dominate the invader–resident comparison. The simple comparison inappropriately emphasizes species with fast life-cycles.

1.1.3.4 Generation time scaling

We recommend scaling resident growth rates by ratios of generation times. To use this method, take the invasion growth rate partition (Eq.1.8) and plug-in the generalized scaling factors as

$$A_{is} = \frac{1}{S-1}\frac{T_s}{T_i}, \tag{1.11}$$

where T_j is the generation time of species j. Generation time scaling still gives equal weight to the low-density state and the high-density state (hence the factor $1/(S-1)$), but further decrements residents with short generation times. Because $1/T_j$ is a measure of population-dynamical speed, the generation time scaling can be thought of as converting the population-dynamical speed of the resident to that of the invader; the factor T_s is cancelled by the resident's speed (implicit in the resident's growth rate), leaving only the invader's speed, $1/T_i$.

But why do we need to correct for speed? The simple answer is that failing to correct for speed will cause species with fast population dynamics to dominate the invader–resident comparison. The more elaborate answer is that speed is a (mostly) density-independent factor that does not reflect the sort of specialization or ecological differentiation that we would like coexistence mechanisms to measure.

That is not to say that population-dynamical speed is irrelevant for coexistence. On the contrary, population speed can weaken relative nonlinearity by dampening variation in resource concentration (Hsu, 1980; Smith, 1981), or strengthen the storage effect by increasing population build-up when the environment is favorable (Li and Chesson, 2016). Population speed can even promote coexistence via $\Delta\rho$ in Lotka Volterra models (Song et al., 2020, Appendix B). Crucially, in all of these examples, the effects of speed on coexistence are mediated through some form of niche differences (speed *per se* cannot cause coexistence, as it is a density-independent property). The generation time scaling "corrects for population speed" in the sense that it level out the magnitudes of species' per capita growth rate components; it does not simulate a world in which

species have exactly the same speed.

While there is no single definition of generation time in structured population models (Caswell, 2001, Section 5.3), many definitions are equivalent when species have attained their limiting dynamics (Ellner, 2018). A good general-use definition of generation time is the weighted average of parent age across all births at one time, with weights equal to the reproductive value of offspring. This quantity can be calculated with a simple formula in deterministic structured population models (Eq. 12 in Bienvenu and Legendre, 2015) and can easily be calculated via simulation in more complex settings (e.g., individual-based, stochastic, and/or spatial models). Additionally, when the offspring state is independent of the parent state, and parent mortality is independent of age, the generation time is simply the mean age of individuals. Thus, in continuous-time models with per capita death rate δ, the distribution of lifespans is given by the exponential distribution with mean age $1/\delta$. Similarly, for discrete-time models with death probability δ, the distribution of lifespans is given by a geometric distribution with mean age $1/\delta$.

The generation time scaling aims to correct for intrinsic (i.e., density-independent) between-species differences in population-dynamical speed. If generation time is to be a proxy for population speed, we should treat it as an intrinsic, density-independent property. In many models, generation time does not depend on population density – the lottery model (Section 1.1.3.7) and case study #1 (Section 1.1.4) are two such examples. However, in models where the generation time varies with population density, one should calculate the generation time while fixing the environment and regulating factors at their equilibrium values, E_j^* and $\boldsymbol{F}^{*j}$. The resulting "intrinsic generation time" has the added virtues of a) being easier to calculate, since simple formulas for generation time in *deterministic* stage-structured models can now be applied (i.e., Eq. 12 in Bienvenu and Legendre, 2015); b) numerically coinciding for four different measures of generation time (Ellner, 2018; and c) requiring no additional modelling choices, since the equilibrium parameters must always be selected.

To calculate generation time, one must have distinct information about survival and fecundity. Unfortunately, some population models (particularly simple unstructured models) only include the aggregate effects of survival and fecundity. For example, the term $\left(-\sum_{j=1}^{S} \alpha_{ij} n_j(t)\right)$ in the competitive Lotka-Volterra model could represent the fact the birth rates decrease with population density or that death rates increase with population density (Allen, 2010, p. 125).

That being said, generation time can be estimated most of the time. There are standard methods for estimating survival and fecundity empirically, and many empirical applications of MCT employ mechanistic models from which generation times can be immediately extracted. Throughout all the empirical applications of MCT mentioned in Section 1.1.3.2 (last paragraph), generation time would be difficult to estimate for only two types of study organisms: phytoplankton (Ellner et al., 2019; Descamps-Julien and Gonzalez, 2005)

and duckweeds (Armitage and Jones, 2019). Both types of study organisms cannot be effectively aged and are hard to track.

When the generation time is difficult to estimate, there are several options, the efficacy of which should be judged on a case-by-case basis. 1) Make an assumption (or educated guess) about what terms in the per capita growth rate function represent survival and fecundity. For example, in the competition Lotka Volterra model with per capita growth rate $r_i(1-\sum_j \alpha_{ij} n_j(t)$, we might assume that r_i is the birth rate and $\sum_j \alpha_{ij} n_j(t)$ is the death rate. 2) Assume that generation time is approximately equal to the average adult lifespan, and obtain this statistic from one of several databases (e.g., De Magalhaes and Costa, 2009; Jones et al., 2009; Myhrvold et al., 2015) 3) Use β scaling (discussed in the next section) in lieu of the generation time scaling.

1.1.3.5 The β scaling method

Chesson (2018) has recently suggested scaling growth rates by sensitivity to competition. First, we define a species-specific competition parameter C_j, which is a function of the regulating factors: $C_j = \phi'(\boldsymbol{F})$. Naturally, the equilibrium level of competition is $C_j^* = \phi'(\boldsymbol{F}^{*j})$. Second, we re-parameterize the growth function such that the per capita growth rate is given by $g_j'(E_j, C_j)$. The sensitivity to competition can now be written as

$$\beta_j = \frac{\partial g_j'(E_j^*, C_j^*)}{\partial C_j}. \tag{1.12}$$

The β scaling method is defined by the generalized partition (Eq.1.8) and the generalized scaling factor,

$$A_{is} = \frac{1}{S-1} \frac{|\beta_i|}{|\beta_s|}. \tag{1.13}$$

The β scaling method and generation time scaling method share the exact same justification. Both methods attempt to correct for population-dynamical speed to prevent species with fast life cycles from dominating the invader–resident comparison. Based on the observation that $1/\beta_j$ is equal to generation time in the lottery model and the annual plant model, Chesson (2018) writes, "... the timescale that allows the clean comparisons ... is the timescale of a generation, or if not exactly that, longevity is a major factor in this timescale. Thus, “tortoise-hare” can become “perennial-annual” for plants."

Though β scaling and generation time scaling aim to solve the same problem — and sometimes give the same answers — there are several reasons for favoring generation time scaling. We list these reasons below and provide elaboration / examples in Appendix 1.1.D.

1. The sensitivity to competition, β_j, depends on how the competition parameter is defined. Two rea-

sonable choices of C_j lead to two different β_j's, and in turn, two different partitions of the invasion growth rate. In all fairness, the values of coexistence mechanisms always depend on subjective choices — definitions of the environmental parameters, regulating factors, and equilibrium parameters — but, the competition parameter introduce an additional level of subjectivity.

2. Some definitions of C_j lead to a $1/\beta_j$ that differs substantially from generation time. There is no reason to use the β_j scaling method in such cases, given that the sole justification of the β scaling (according to Chesson, 2018) is the connection between $1/\beta_j$ and generation time. In case study #2, Appendix 1.1.C, we show how a reasonable choice of C_j can lead to nonsensical values of coexistence mechanisms.

3. Sometimes, there is no reasonable definition of C_j, and thus no reasonable definition of β_j. In Appendix 1.1.D, we introduce a model with two environmental parameters (per species) and argue that there is no way to write the per capita growth rate as a function of both environment and competition parameters. Either the environmental parameters become latent (hidden within C_j), in which case the storage effect is subsumed by relative nonlinearity, or one defines two competition parameters, in which case there are two β_j's per species and no obvious way to combine them.

4. The sensitivity to competition is not well-defined in stochastic stage-structured models. In scalar populations, the sensitivity to competition is defined as a partial derivative of the function g'_j, which gives the per capita growth rate at a single point in time. In stochastic stage-structured models, there is no obvious analogue of the per capita growth rate at a single point in time, due to the systemic effects of temporal autocorrelation on the long-term average growth rate (Tuljapurkar, 1982; Caswell, 2001, Section 14.3.6.2). We suspect that β scaling faces similar problems in other kinds of complex models.

1.1.3.6 The invader–invader comparison

So far, we have been operating under the implicit assumption that coexistence mechanisms should be calculated as invader–resident comparisons. At first glance, this seems appropriate: Coexistence mechanisms are supposed to measure the importance of different explanations for coexistence, the concept of specialization/differentiation has played a central role in historical explanations of coexistence, and the invader–resident comparison putatively captures the notion of specialization/differentiation. However, upon further reflection, we may worry that the invader–resident comparison not only captures the rare-species advantage that results from specialization, but also that which results from intrinsic, density-independent differences between species.

The alternative to the invader–resident comparison is what we call the *invader–invader comparison*: a comparison of the high density and low density states of a single focal species. An invader–invader comparison holds species-specific features constant, thus isolating the effects of rarity. Using the *difference-making / but-for account of causation* (Moore, 2019), we can say that the invader–invader comparison gives the causal effects (on average per capita growth rates) of perturbing a species to low density, mediated through different variables (e.g., mean resource levels for $\Delta\rho_i$, resource variation for ΔN_i). Though the invader–invader comparison isolates the effects of rarity, it does not directly compare different species, and therefore, the resulting coexistence mechanisms do not always capture the notion of *specialization*; see the case study (Section 1.1.4) for a demonstration of this phenomenon.

The inventor of MCT, Peter Chesson, has previously alluded to the invader–invader comparison: "Often the mechanism is most easily understood in terms of how the conditions encountered by an individual species change between its resident and invader states." (Chesson, 2008), and "...within-species comparison is more reliable if appropriate within-species resident and invaders states can be prepared" (Chesson, 2013). To our knowledge, there are no published uses of the invader–invader comparison, which we define in the following partition of the invasion growth rate:

$$\begin{aligned}
\overline{r}_i \approx & \underbrace{\left(\sum_{k=1}^{L} \phi_{ik}^{(1)} \left(\overline{F_k^{\{-i\}}} - F_k^{*i}\right)\right) - \left(\sum_{k=1}^{L} \phi_{ik}^{(1)} \left(\overline{F_k} - F_k^{*i}\right)\right)}_{\Delta\rho_i\text{: Linear density-dependent effects}} \\
& + \underbrace{\frac{1}{2}\left[\left(\sum_{k=1}^{L}\sum_{m=1}^{L} \phi_{ikm}^{(2)} \mathrm{Cov}\left(F_k^{\{-i\}}, F_m^{\{-i\}}\right)\right) - \left(\sum_{k=1}^{L}\sum_{m=1}^{L} \phi_{ikm}^{(2)} \mathrm{Cov}(F_k, F_m)\right)\right]}_{\Delta N_i\text{: Relative nonlinearity}} \\
& + \underbrace{\left(\sum_{k=1}^{L} \zeta_{ik}^{(1)} \mathrm{Cov}\left(E_i, F_k^{\{-i\}}\right)\right) - \left(\sum_{k=1}^{L} \zeta_{ik}^{(1)} \mathrm{Cov}(E_s, F_k)\right)}_{\Delta I_i\text{: The storage effect}},
\end{aligned} \tag{1.14}$$

Note the absence of the superscript "$\{-i\}$" from the subtracted terms, which indicates that the reference state is a community where all species are at their typical densities. Also note that the density-independent effects, ΔE_i, have vanished.

Unfortunately, the invader–invader comparison lacks the generality of the invader–resident comparison. There may be no stable high-density state for the focal species, as is the case when the focal species has a negative invasion growth rate, or when the focal species becomes temporarily abundant only to become excluded later on (a phenomenon that has been dubbed *the resident strikes back*; Mylius and Diekmann, 2001; Geritz et al., 2002). In such cases, the invader–invader comparison does not exist, and thus cannot tell us how species are failing to coexist. When the invader–invader comparison does exist, it will not be unique

if there are multiple stable high-density states for the focal species.

1.1.3.7 The relationship between scaling factors, generation time scaling, and β scaling

In models with a single regulating factor, the scaling factors are

$$q_{is} = \frac{\phi_{i1}^{(1)}}{\phi_{s1}^{(1)}}. \tag{1.15}$$

The right-hand-side resembles both the generation time scaling quotient, T_s/T_i, and the β scaling quotient, $|\beta_i|/|\beta_s|$. As it turns out, all three of these quotients are identical in the lottery model and the annual plant model, two canonical models in MCT (Chesson, 1994, Section 5). In the lottery model of reef fish dynamics, the finite rate of increase can be written as

$$\lambda_j = \exp(E_j - C) + (1 - d_j), \tag{1.16}$$

where d_j is the death probability for an adult fish, E_j is the logarithm of per capita fecundity, and C is the logarithm of fish larvae per open territory. By noting that $\exp\big(E_j^* - C^*\big) = d_j$, and treating the competition parameter as a single regulating factor, one can show that $\phi_{j1}^{(1)} = \beta_j = -d_j$. As discussed in Section 1.1.3.4, the generation time in this context is simply the reciprocal of the death probability: $T_j = 1/d_j$. Now it becomes easy to see that all thee scaling methods multiply residents' rates by d_i/d_s.

The equivalence of scaling methods does much to explain the continued usage of scaling factors: the problems with scaling factors are not evident in the simple models that theoreticians tend to study. Scaling factors can become enormous (due to the inversion of a matrix with nearly dependent columns), but this problem is not evident if one studies models with a single regulating factor.

When theoreticians do study models with multiple regulating factors, they often envision species competing equally with all heterospecifics (e.g., Chesson, 1994; Chesson, 2000b), a scenario that has been referred to as *diffuse competition* (Stump, 2017). The simplifying structure of diffuse competition allows one to derive mathematical formulas in the S-species case, which is intractable in most cases. When the regulating factors are species' densities, species' sensitivities to regulating factors are defined by a matrix of competition coefficients with intraspecific competition c and interspecific competition x. In Appendix 1.1.E, we derive the exceedingly simple formula

$$q_{is} = \frac{x}{c + (S-2)x}, \tag{1.17}$$

which converges to the simple comparison for large S. Further, all residents are weighted equally, precluding a small set of species from dominating the invader–resident comparison. Again, we see that simple models

obscure substantial differences between scaling methods. Judgements about the utility of scaling methods for empirical applications of MCT should be based off complex models with multiple regulating factors and asymmetric niches.

1.1.4 Results

Here we test methods for calculating coexistence mechanisms in a model where the true reasons for coexistence are known. Modern Coexistence Theory (MCT) systematizes the analysis of models by breaking an arbitrarily complex growth rate function into simple polynomial terms, and therefore, is most useful when we don't know how species are coexisting. However, if MCT is to be a useful measurement tool, it ought to conform to expectations when we do know how species are coexisting.

Inspired by the Armstrong-McGehee model (1976; 1980), we examine a deterministic, continuous-time resource-consumer model where relative nonlinearity features as a crucial coexistence mechanisms. A stochastic stage-structured model of annual and perennial plants is analyzed in Appendix 1.1.C. All computations can be replicated using the Mathematica notebooks, `ArmMc_3Spp.nb` and `SE_3Spp.nb`, found at https://github.com/ejohnson6767/scaling_factors.

The dynamics of three consumers (densities denoted by N_1, N_2, and N_3) and two resources (densities denoted by R_1 and R_2) are described by the equations,

$$\begin{aligned}
\frac{dN_1}{dt} &= N_1 b_1 \left[c_{11}R_1 + c_{21}R_2 - d\right] \\
\frac{dN_2}{dt} &= N_2 b_2 \left[c_{12}R_1 + \frac{c_{22}R_2}{\eta + R_2} - d\right] \\
\frac{dN_3}{dt} &= N_3 b_3 \left[c_{13}R_1 + c_{23}R_2 - d\right] \\
\frac{dR_1}{dt} &= R_1 \left[r_1\left(1 - \frac{R_1}{K_1}\right) - c_{11}N_1 - c_{12}N_2 - c_{13}N_3\right] \\
\frac{dR_2}{dt} &= R_2 \left[r_2\left(1 - \frac{R_2}{K_2}\right) - c_{21}N_1 - \frac{c_{22}N_2}{\eta + R_2} - c_{23}N_3\right].
\end{aligned} \tag{1.18}$$

In the absence of consumers, both resources grow logistically with intrinsic growth rates r_j and carrying capacities K_j. Consumers share a mortality parameter, d, and have birth rates proportional to resource consumption. The maximum (per-consumer, per-resource) rate at which resource k is consumed by consumer j is given by c_{kj}. Consumers 1 and 3 have linear functional responses to resource densities. Consumer 2 has a linear response to resource 1, but has a type II functional response to resource 2 with a half-saturation constant η. Population-dynamical speed is denoted by b_j.

Individuals die at the rate $b_j d$, making the generation time ratio $T_s/T_i = b_i/b_s$. Intuitively, the competition parameter should be a decreasing function of resource consumption: the bracketed terms in the

consumer equations, excluding $-d$. Making the natural choice $C_1 = -\log(c_{11}R_1 + c_{21}R_2)$, and analogous choices for consumers 2 and 3, the sensitivities to competition become $\beta_j = -b_j d$. The β scaling ratios are thus $|\beta_i|/|\beta_s| = b_i/b_s$. The generation time scaling and β scaling are equivalent in this model, but give very different results in case study #2 (Appendix 1.1.C). The scaling factors are obtained by solving a system of linear equations (see Appendix 1.1.B).

We select parameter values so that consumer 1 specializes on resource 1, consumer 2 specializes on resource 2 and consumer 3 specializes on the variation in resource 2: $c_{11} = c_{22} = c_{23} = 1$, $c_{21} = c_{12} = c_{13} = 0.05$, $d_1 = d_2 = d_3 = 0.47$, $r_1 = r_2 = 1$, $K_1 = K_2 = 1.5$, $\eta = 0.5$. These parameter values produce two virtually independent subsystems: {consumer 1, resource 1} and {consumer 2, consumer 3, resource 2}, the latter of which is essentially the Armstrong-McGehee model. The regulating factors are simply the resource densities. The environmental parameter E_j is nonexistent, so ΔE_i and ΔI_i are necessarily zero.

Consumer 1 specializes on resource 1, and thus coexists via the linear density-dependent effects. Because consumer 2 and consumer 3 both heavily consume the same resource, one of these species must coexist via fluctuation-dependent mechanisms. Consumer 2 clearly coexists via linear density-dependent effects, because it is the superior competitor (compared to consumer 3) in the absence of fluctuations via Tilman's R^* rule (see Fig. 1.1). Consumer 3 clearly coexists via relative nonlinearity, because consumer 2's birth rate function is relatively concave down, meaning that resource fluctuations help consumer 3 relative to consumer 2.

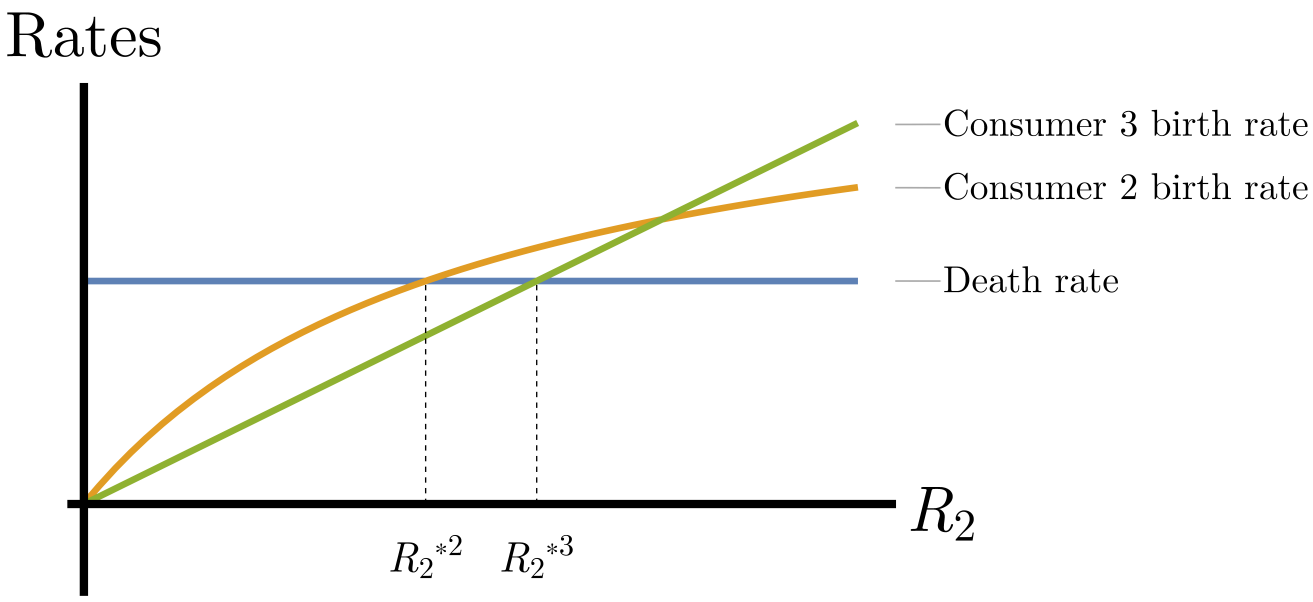

Figure 1.1: An opportunist-gleaner trade-off. Consumer 2 (the *gleaner*) excludes consumer 3 (the *opportunist*) in the absence of resource fluctuations (by Tilman's (1982) R^* rule: $R_2^* < R_3^*$), but consumer 2 is hurt more by resource fluctuations (by Jensen et al.'s (1906) inequality). Consumer 2 specializes on mean resource levels, whereas Consumer 3 specializes on resource variation. Consumer 1 is not shown.

Following the intuition in the previous paragraph, we predict that $\Delta\rho_1$, $\Delta\rho_2$, and ΔN_3 will be positive and large (relative to other coexistence mechanisms within each species, respectively). This is precisely what we see for both the simple comparison and generation time scaling (Table 1.1). By contrast, the scaling factors counterintuitively attribute the persistence of species 1 to relative nonlinearity (i.e., in Table 1.1, box A, ΔN_1 is large and positive). It is not so surprising that ΔN_1 is non-zero: after all, species 1 does have a nonlinear response to competition, relative to species 2. What is surprising is that ΔN_1 is so large that it almost entirely accounts for the positive invasion growth rate of species 1. Of course, it is unreasonable to think that $\Delta\rho_1$ would be large and positive when using the scaling factors (the whole point of the scaling factors is to cancel $\Delta\rho_i$), but one might reasonably think that r_1' would be large and positive, since both $\Delta\rho_1$ and r_1' represent fluctuation-independent forces.

The failure of the scaling factors method (i.e., the counterintuitively large ΔN_1) can be explained by the sheer magnitude of the scaling factors, which are $q_{12} \approx -84$ and $q_{13} \approx 64$. Because species 2 barely interacts with species 1, the growth rate components of species 2 must be heavily weighted in order to cancel $\Delta\rho_1$. Consider the analytical formula for one scaling factor, $q_{12} = (\phi_{12}^{(1)}\phi_{31}^{(1)} - \phi_{11}^{(1)}\phi_{32}^{(1)})/(\phi_{22}^{(1)}\phi_{31}^{(1)} - \phi_{21}^{(1)}\phi_{32}^{(1)})$. This formula demonstrates that the scaling factors can become large via division by a small number; ϕ_{31} and ϕ_{21} are small, so the denominator $\phi_{22}^{(1)}\phi_{31}^{(1)} - \phi_{21}^{(1)}\phi_{32}^{(1)}$ is small even though all species respond similarly to resources in total (i.e., $\phi_{11}^{(1)} + \phi_{21}^{(1)} + \phi_{31}^{(1)} \approx \phi_{12}^{(1)} + \phi_{22}^{(1)} + \phi_{32}^{(1)}$)

When species have similar population-dynamical speeds, the simple comparison and generation time scaling both give results that accord with intuition: $\Delta\rho_1$, $\Delta\rho_2$, and ΔN_3 are positive and large (relative to other coexistence mechanisms within each species). Strangely, the invader–invader comparison produces exactly the opposite of what we predicted for species 2 and 3: the coexistence mechanisms ΔN_2 and $\Delta\rho_3$ are large and positive (see box B and C in Table 1.1).

We make sense of the invader–invader coexistence mechanisms by recognizing that they do not directly compare species, and therefore do not always capture the notions of specialization or ecological differentiation. In our model, consumer 2 and consumer 3 exhibit an *opportunist-gleaner trade-off* (Fig. 1.1; Grover, 1997). When species 2 — the gleaner — becomes abundant, it increases resource variation by inducing cyclical resource-consumer dynamics. Because the gleaner has a concave-down per capita growth rate function, its high-density state suffers from the increased variation, resulting in $\Delta N_2 > 0$. When the opportunist — species 3 — is absent from the community, the gleaner produces a lower $\overline{F_2^{\{-3\}}}$ through nonlinear averaging. When the opportunist is at its high-density state, resource fluctuations becomes smaller, nonlinear averaging becomes weaker, and mean resource level rise, resulting in $\Delta\rho_3 > 0$.

To better understand the effects of population-dynamical speed on the coexistence mechanisms, we increase species 1's speed by setting $b_1 = 100$. Because species 1 attains an equilibrium with resource 1

and barely interacts with the subsystem {consumer 2, consumer 3, resource 2}, increasing the speed of species 1's population dynamics has little effect on population dynamics of the full three-species community, or any of the sub-communities (see simulated time series in the Mathematica notebook `ArmMc_3Spp.nb`. Nonetheless, Table 1.2 shows that increasing species 1's speed can complicate the interpretation of species 3's coexistence mechanisms. Species 3 specializes on resource variation relative to species 2, so ΔN_3 should be large; this is precisely what we see for the generation time scaling method. However, the simple comparison method gives us a large $\Delta\rho_{3,F_1}$ (Table 1.2, Box A), implying that species 3 persists by specializing on resource 1, despite the fact that species 3 barely consumes resource 1.

Because species 3 barely consumes resource 1, the mean level of resource 1 barely changes species 3 is perturbed to the invader state. However, there is a small persistent difference between $\overline{F_1^{\{-3\}}}$ and F_1^{*1}, not because of species 3's interaction with resource 1, but because the community is a nonlinear and non-equilibrium system (because of nonlinear averaging, it is not possible to select $\boldsymbol{F^{*1}} = \overline{\boldsymbol{F}^{\{-3\}}}$ and still satisfy the constraint $g_1(E_1^*, \boldsymbol{F^{*1}}) = 0$). The small difference between $\overline{F_1^{\{-3\}}}$ and F_1^{*1} gets amplified by species 1's extreme responsiveness to regulating factors (i.e., a large $\phi_{11}^{(1)}$), which is a natural consequence of species 1's fast population dynamics. The term $\phi_{11}^{(1)}\left(\overline{F_1} - F_1^{*1}\right)$, belonging to species 1, comes to dominate in the simple comparison method, resulting in a large $\Delta\rho_{3,F_1}$. The generation time scaling method successfully counteracts this phenomenon.

Table 1.1: Values of coexistence mechanisms when species have the same population-dynamical speed. Red boxes highlight the failures of various methods: the large and positive values indicate coexistence via mechanisms that are not actually helping species coexist. Coexistence mechanisms are calculated with the generalized partitioning framework of Ellner et al. (2019). The density-independent effects are denoted by r_i' (only for the scaling factor method) or ΔE_i. We display the linear effects of the two regulating factors and their aggregate effect: $\Delta\rho_i = \Delta\rho_{i,F_1} + \Delta\rho_{i,F_2}$.

Species $i =$	**Calculation method**	**Coexistence mechanisms**				
		r_i'or ΔE_i	$\Delta\rho_i$	$\Delta\rho_{i,F_1}$	$\Delta\rho_{i,F_2}$	ΔN_i
1	Scaling factors	-7.922	0	NA	NA	10.855 A
1	Simple comparison	0	0.957	0.962	-0.005	0.065
1	Generation time scaling	0	0.957	0.962	-0.005	0.065
1	β scaling	0	0.957	0.962	-0.005	0.065
1	Invader–invader comparison	0	1.010	1.013	-0.002	0.000
2	Scaling factors	0.094	0	NA	NA	0.000
2	Simple comparison	0	0.094	-0.000	0.094	0.000
2	Generation time scaling	0	0.094	-0.000	0.094	0.000
2	β scaling	0	0.094	-0.000	0.094	0.000
2	Invader–invader comparison	0	0.001	-0.000	0.001	0.117 B
3	Scaling factors	-0.124	0	NA	NA	0.228
3	Simple comparison	0	-0.013	0.001	-0.015	0.087
3	Generation time scaling	0	-0.013	0.001	-0.015	0.087
3	β scaling	0	-0.013	0.001	-0.015	0.087
3	Invader–invader comparison	0	0.056 C	-0.000	0.056	0.000

1.1.5 Discussion

If we can define coexistence mechanisms as measures of the importance of various explanations for coexistence, then they can be straightforwardly used to infer how species are coexisting in real communities (through the analysis of empirically-calibrated models). In this paper, we have discussed five definitions of coexistence mechanisms, each respectively based on *scaling factors, a simple comparison, generation time scaling, β scaling, and an invader–invader comparison.*

Scaling factors can be useful in theoretical research, but they are not recommended for the purpose of quantifying coexistence mechanisms in real communities. There are better alternative methods for computing coexistence mechanisms (namely the simple comparison, generation time scaling, and β scaling), each with strengths and weaknesses (Table 1.3). The simple comparison method is easy to compute and interpret, but may give unintuitive results when species have dissimilar generation times. Generation time scaling works well when species have dissimilar generation times, but is not always well-defined. The invader–invader comparison directly measures the causal effects of low density, but it does not always exist. When the invader–invader comparison does exist, it does not always quantify the notion of specialization/differentiation; this

Table 1.2: Values of coexistence mechanisms when species 1 has fast population dynamics ($b_1 = 100$).

Species $i =$	**Calculation method**	**Coexistence mechanisms**				
		r_i'or ΔE_i	$\Delta\rho_i$	$\Delta\rho_{i,F_1}$	$\Delta\rho_{i,F_2}$	ΔN_i
1	Scaling factors	-792.237	0	NA	NA	1085.440
1	Simple comparison	0	100.976	101.237	-0.261	0.065
1	Generation time scaling	0	95.742	96.223	-0.481	6.453
1	β scaling	0	95.742	96.223	-0.481	6.453
1	Invader–invader comparison	0	101.029	101.288	-0.259	0.000
2	Scaling factors	0.094	0	NA	NA	0.000
2	Simple comparison	0	0.094	-0.002	0.096	0.000
2	Generation time scaling	0	0.094	-0.000	0.094	0.000
2	β scaling	0	0.094	-0.000	0.094	0.000
2	Invader–invader comparison	0	-0.001	0.000	-0.001	0.117
3	Scaling factors	-0.124	0	NA	NA	0.234
3	Simple comparison	0	-0.013	0.138 A	-0.151	0.089
3	Generation time scaling	0	-0.013	0.001	-0.014	0.089
3	β scaling	0	-0.013	0.001	-0.014	0.089
3	Invader–invader comparison	0	0.055	-0.000	0.055	0.000

has lead to counterintuitive results in case study #1 (Section 1.1.4) and in a phytoplankton model (Steve Ellner, *personal communication*). Though we have substantial conceptual arguments in favor of generation time scaling, we have only compared methods in two case studies (Section 1.1.4 and Appendix 1.1.C).

We tentatively recommend the general use of generation time scaling. If generation time cannot be unambiguously extracted from a model, but the sensitivity to competition is well-defined, then β scaling should be used in lieu of the generation time scaling. If neither the generation time nor the sensitivity to competition is well-defined, then the simple comparison is recommended. Neither the scaling factors nor the invader–invader comparison should be used in empirical research.

In the end, the difference between the simple comparison and generation time scaling may be inconsequential: coexistence is most often studied in guilds of species that have similar generation times, because the putative coexistence of species with similar life histories is more surprising in light of the competitive exclusion principle (Gause, 1934; Levin, 1970). When there are small between-species differences in generation times, any inferential error that results from selecting the simple comparison over generation time scaling will likely be small, relative to the error which results from failing to account for parameter uncertainty (if one does not calculate coexistence mechanisms across either the joint posterior or bootstrap distribution of model parameters) and structural uncertainty (if one does not calculate coexistence mechanisms for several disparate models). It is important to keep in mind that there are many ways in which a MCT analysis can be provisional.

The simple comparison method captures the notion of specialization, but also captures intrinsic between-species differences like population-dynamical speed. The invader–invader comparison, on the other hand, isolates the effects of rarity, but does not necessarily capture the notion of specialization. We may think of generation time scaling as giving the best of both worlds: reducing between-species differences that are irrelevant to coexistence, but capturing the notion of specialization (by remaining within the paradigm of invader–resident comparisons). In fact, generation time scaling can be thought of as partially correcting for between-species differences in average fitness (Appendix 1.1.F).

We have criticized the scaling factors, the simple comparison, and the invader–invader comparison on the grounds that they can lead to counterintuitive conclusions about how species are coexisting. Our intuitions are rooted in a belief that coexistence mechanisms should measure explanations for coexistence, and that in turn, explanations for coexistence should involve specialization/differentiation that lead to systematic (i.e., across species) rare-species advantages. Historically, the notion of specialization has been central to explanations for coexistence. For example, the heuristic "...each species must consume proportionately more of the resource that more limits its growth" (Tilman, 1982, p. 96) contains the word "proportionately", which insinuates a cross-species comparison: demographic parameters from multiple species must be considered simultaneously. Indeed, this can be seen in either the mathematical (Tilman, 1982, p. 77), or the graphical (Chase and Leibold, 2003) versions of Tilman's coexistence theory.

Unfortunately, heady concepts like *specialization* or *population-dynamical speed* do not have formal definitions that apply generally (i.e., in an arbitrary model), meaning that generation time scaling cannot be justified with a single concise argument. Instead, we have evaluated methods through conceptual analysis and the probing of particular models. Though the two case studies support the usage of generation time scaling, it is the possible that they can be problematic in contexts that we have failed to imagine. MCT is powerful because it is a general framework: take an arbitrary model, select a few equilibrium parameters, and algorithmically partition the invasion growth rate. In a sense, calculating coexistence mechanisms is the easy part; the hard part is determining the meaning of the numbers that MCT spits out.

Table 1.3: Pros and cons of methods for calculating coexistence mechanisms

Method	Pros	Cons
Scaling factors		

		• Eliminates $\Delta\rho_i$ when there are more residents than regulating factors, showing that not all species can coexist via classical mechanisms • Converts the units of resident growth to that of invader growth; Useful if species are measured in different units • Ensures that all coexistence mechanisms are of the same magnitude under small-noise assumptions • In rare cases, eliminating $\Delta\rho_i$ can eliminate the need to explicitly model the dynamics of regulating factors	• Eliminates $\Delta\rho_i$ when there are more residents than regulating factors; prevents us from determining the degree to which species coexist via classical mechanisms • Modulates other coexistence mechanisms, sometimes leading to counterintuitive inferences about how species are coexisting • Are not uniquely determined when there are more regulating factors than resident species • Are not uniquely determined (even if there are less regulating factors than resident species) when the invader's $\mathscr{C}$ cannot be written as a function of the resident $\mathscr{C}$s (see Eq. 2 in Appendix 1.1.B) • Can be sensitive to small changes in inputs if species responses to regulating factors are nearly linearly dependent • In models with mutualism, can turn an invader–resident difference into an invader–resident sum; the interpretation of coexistence mechanisms as a rare-species advantage is lost
Simple comparison		• Solves all of the scaling factor cons • Easy to compute; works universally	• If some species have fast population dynamics, they will dominate the invader–resident comparison, leading to counterintuitive inferences about how species are coexisting
Generation time scaling			

	• Solves all of the scaling factor and simple comparison cons; puts species with different population-dynamical speeds on an equal footing	• If it is not clear what demographic parameters are associated with birth vs. death processes, then generation time is not well-defined • Has only been tested in two case studies
β scaling		
	• Solves all of the scaling factor and simple comparison cons; puts species with different population-dynamical speeds on an equal footing • Can sometimes succeed where generation time scaling fails — in simple, unstructured population models	• Reasonable definitions of the competition parameter can lead to different β_j's; results can be sensitive to subjective modelling choices • A reasonable competition parameter may not exist, even in simple models • Even when the competition parameter does exist, β_j is not well-defined in complex models, like stochastic stage-structured models or individual-based models
Invader–invader comparison		
	• Has a straightforward causal interpretation as the effects of perturbing a species to low density (mediated through mean regulating factors, variation in regulating factors, etc.) • Solves all of the scaling factor and simple comparison cons; puts species with different population-dynamical speeds on an equal footing	• Can't be computed if the focal species has a negative invasion growth rate or in the case of *the resident strikes back* • Can't always be interpreted in terms of specialization / differentiation • Can't be interpreted in terms of the invader out-performing the residents, which is the actual determinant of invasion success

Appendices

1.1.A Strategies for selecting equilibrium parameters

In the case of one regulating factor, the canonical way to select the equilibrium parameters is to set environmental noise to zero (thus creating a *deterministic skeleton*), set E_j^* as the now-fixed environmental parameter, and then solve for F^{*j} using the constraint $g_j(E_j^*, F^{*j}) = 0$ (see Chesson, 1994, Section 5). Alternatively, Barabás et al. (2018) suggests selecting $E_j^* = \overline{E_j}$ (without first eliminating environmental noise), and then solving for F^{*j}. In the case of multiple regulating factors, Chesson (2020) suggests selecting reasonable $\boldsymbol{F}^{*j}$ first, and then solving for E_j^*. For instance, one could simulate the full community dynamics (where all species are present), set the equilibrium regulating factors to their temporal averages, $\overline{\boldsymbol{F}}$, and then solve for E_j^* for each species. However, because the quality of the Taylor series approximation of the invasion growth rate depends on $\boldsymbol{F}^{*j}$ being close to $\overline{\boldsymbol{F}^{\{-i\}}}$ (the temporal averages of regulating factors in the community without invader i), this method could work poorly if putting a species in the invader state would substantially change the mean levels of the regulating factors.

It is worth noting that the values of coexistence mechanisms generally depend on one's definition of the E_j and $\boldsymbol{F}$, as well as the corresponding equilibrium parameters (Chesson, 1994; Barabás et al., 2018). Thus, one's inferences about how species are coexisting should not be based solely on the relative values of coexistence mechanisms, especially when comparisons are being made across species or communities with disparate models. Rather, one should use all available means (e.g., definitions of E_j and $\boldsymbol{F}$, model analysis, analogy with previously well-studied models) to understand what mechanical explanations for coexistence are entailed by particular instantiations of coexistence mechanisms.

1.1.B The mathematics of scaling factors

As stated in the main text, the scaling factors are defined as

$$q_{is} = \frac{\partial \mathscr{C}_i^{\{-i\}}}{\partial \mathscr{C}_s^{\{-i\}}}, \tag{1.19}$$

evaluated at $\mathscr{C}_s = 0$. Next, we make two assumptions (respectively Assumption *a6* and Eq.49 in Chesson, 1994). Assume that we can express the standard competition parameter of the invader as a function of the residents' standard competition parameters:

$$\mathscr{C}_i^{\{-i\}} = f\left(\mathscr{C}_1^{\{-i\}}, \ldots, \mathscr{C}_S^{\{-i\}}\right). \tag{1.20}$$

Further, assume that the standard competitive parameters can be written as a function of L competitive factors $(F_1, \ldots, F_L)^\intercal = \boldsymbol{F}$:

$$\mathscr{C}_j = \phi_j(F_1, \ldots, F_L) = \phi_j(\boldsymbol{F}). \tag{1.21}$$

The competitive factors can now be related to the scaling factors through the chain rule,

$$\frac{\partial \mathscr{C}_i^{\{-i\}}}{F_k} = \sum_{s \neq i}^{S} \frac{\partial \mathscr{C}_i^{\{-i\}}}{\partial \mathscr{C}_s^{\{-i\}}} \frac{\partial \mathscr{C}_s^{\{-i\}}}{F_k} \tag{1.22}$$

with all derivatives evaluated at $\mathscr{C}_s^{\{-i\}} = 0$. The partial derivatives of $\mathscr{C}_j^{\{-i\}}$ with respect to F_k are the first order coefficients of a Taylor series of ϕ_j expanded about $\boldsymbol{F} = \boldsymbol{F^{*j}}$, so we we may use the notation $\phi_{jk}^{(1)} = \partial \mathscr{C}_j / \partial F_k|_{F_k = F_k^{*j}} = \partial \mathscr{C}_j^{\{-i\}} / \partial F_k \Big|_{F_k = F_k^{*j}}$

Substituting $\phi_{jk}^{(1)}$ and the left-hand-side of Eq.1.19 into Eq.1.22, we get

$$\phi_{ik}^{(1)} = \sum_{s \neq i}^{S} q_{ir} \phi_{rk}^{(1)}. \tag{1.23}$$

With this one equation and $S - 1$ unknowns (the q_{ir}'s), Eq.1.23 is underdetermined. If we consider the equations of all L competitive factors simultaneously, we get the vector-matrix equation

$$\boldsymbol{\Phi}_{i*} = \boldsymbol{q_{i*}} \boldsymbol{\Phi}^{(-i)}. \tag{1.24}$$

Here, $\boldsymbol{\Phi}$ is a $(S \times L)$ matrix of species' sensitivities to competitive factors, with elements $\phi_{jk}^{(1)}$. The symbol $\boldsymbol{\Phi}_{i*}$ is the $(1 \times L)$ row vector of the invader's sensitivities to regulating factors; $\boldsymbol{q_{i*}}$ is the $(1 \times (S-1))$ row vector of scaling factors (the element q_{ii} is not included); and $\boldsymbol{\Phi}^{(-i)}$ is a $((S-1) \times L)$ matrix, obtained by removing the invader (i.e., the i-th row) from $\boldsymbol{\Phi}$.

Solving for $\boldsymbol{q_{i*}}$ involves multiplying both sides of Eq.1.24 by the inverse of $\boldsymbol{\Phi}^{(-i)}$. However, the invertible matrix theorem states that the matrix inverse only exists if $\boldsymbol{\Phi}^{(-i)}$ is square (i.e., $S - 1 = L$) and has linearly independent columns. What do we do when $\boldsymbol{\Phi}^{(-i)}$ is not square: when there are more residents than regulating factors, or more regulating factors than residents?

Chesson's (1994) solution is the *generalized inverse*. A generalized inverse of a matrix $\boldsymbol{A}$ is denoted as $\boldsymbol{A}^g$, and satisfies the equation $\boldsymbol{A}\boldsymbol{A}^g\boldsymbol{A} = \boldsymbol{A}$ (Ben-Israel and Greville, 2003). Our expression for the scaling factors now becomes

$$\boldsymbol{q_{i*}} = \boldsymbol{\Phi}_{i*} \left(\boldsymbol{\Phi}^{(-i)} \right)^{g}. \tag{1.25}$$

When $\boldsymbol{\Phi}^{(-i)}$ is square and has full rank, then the regular matrix inverse is the unique generalized inverse. When the linear system is underdetermined (i.e., $S-1 > L$, assuming $\boldsymbol{\Phi}^{(-i)}$ has full rank), then a generalized inverse produces an infinite number of solutions to Eq.1.24. According to Chesson (2020, p. 6) this non-uniqueness is a virtue: different choices of generalized inverses allow the user of MCT to ask different scientific questions.

When a solution is available, the resulting scaling factors (Eq.1.25) can be used to cancel the linear effects of density-dependence, i.e., $\Delta\rho_i$. The linear effects of density-dependence can be expressed in vector-matrix form:

$$\Delta\rho_i = \boldsymbol{\Phi}_{i*}\overline{\boldsymbol{F^{\{-i\}}}} - \boldsymbol{q_{i*}}\boldsymbol{\Phi}^{(-i)}\overline{\boldsymbol{F^{\{-i\}}}}. \tag{1.26}$$

Substituting in the right-hand-side of Eq.1.25, we get

$$\Delta\rho_i = \boldsymbol{\Phi}_{i*}\overline{\boldsymbol{F^{\{-i\}}}} - \boldsymbol{\Phi}_{i*} \left(\boldsymbol{\Phi}^{(-i)} \right)^{g} \boldsymbol{\Phi}^{(-i)}\overline{\boldsymbol{F^{\{-i\}}}}. \tag{1.27}$$

The matrix product $\left(\boldsymbol{\Phi}^{(-i)} \right)^{g} \boldsymbol{\Phi}^{(-i)}$ evaluates to the $(L \times L)$ identity matrix, and therefore, $\Delta\rho_i = 0$.

When the linear system in Eq.1.24 is overdetermined (i.e., $S - 1 < L$, assuming $\boldsymbol{\Phi}^{(-i)}$ has full rank), Eq.1.25 can still be used, but the resulting $\boldsymbol{q_{i*}}$ will not be a strict solution. Barabás et al. (2018) suggests cancelling a major regulating factor that has a particularly strong effect on per capita growth rates. In fact, one could cancel up to $(L - S + 1)$ such major regulating factors by computing the generalized inverse for a submatrix of $\boldsymbol{\Phi}^{(-i)}$ that contains only columns corresponding to the major regulating factors.

In this paper, we will argue against most uses of the scaling factors. However, if one still desires to use the scaling factors, we suggest using the Moore-Pensrose Pseudoinverse (denoted with a dagger: †) when the linear system in Eq.1.24 is underdetermined or overdetermined. Specifically, in the case of overdetermination, we suggest

$$\boldsymbol{q_{i*}} = \boldsymbol{\Phi}_{i*} \left(\boldsymbol{\Phi}^{(-i)} \right)^{\dagger}. \tag{1.28}$$

The pseudoinverse gives the optimal solution in the least-squares sense (Ben-Israel and Greville, 2003, p. 122), so while it may be impossible to cancel $\Delta\rho_i$, it may be possible to get close. In the case of underdetermination, we suggest

$$\boldsymbol{q_{i*}} = \boldsymbol{z} + (\boldsymbol{\Phi}_{i*} - \boldsymbol{z}\boldsymbol{\Phi}^{(-i)}) \left(\boldsymbol{\Phi}^{(-i)}\right)^{\dagger}, \tag{1.29}$$

where $\boldsymbol{z}$ is an $(1 \times (S-1))$ row vector where each element is equal to $1/(S-1)$. This formula comes from taking Eq.1.24, replacing $\boldsymbol{q_{i*}}$ with $\boldsymbol{x}+\boldsymbol{z}$, and attempting to solve for $\boldsymbol{x}$. The answer gives the minimum norm solution (Ben-Israel and Greville, 2003, p. 109) for $\boldsymbol{x}$, which means $\boldsymbol{q_{i*}} = \boldsymbol{x}+\boldsymbol{z}$ is close $\boldsymbol{z}$ in the least-squares sense. In other words, we eliminate $\Delta\rho_i$ while deviating a minimal amount from the simple average over residents.

1.1.C Case study #2: Coexistence via the storage effect in a annual–perennial plant model

General model description

Here, we examine a stochastic, stage-structure, discrete-time model of annual and perennial plants. The densities of seeds and germinants are denoted $X_j(t)$ and $N_j(t)$, respectively. At the beginning of the growing season, seeds germinate with probability G_j; the remaining seeds survive to the next year with probability s_j. Per germinant seed production fluctuates over time, but tends to decline with the density of germinant competitors. After new seeds join the seed bank, the germinants survive to the beginning of the next growing season with probability $\widetilde{s}_j$. Annual plants necessarily have $\widetilde{s}_j = 0$.

The equations for the three plants are

$$\begin{aligned} X_j(t+1) &= X_j(t)s_j(1-G_j) + \frac{(X_j(t)G_j + N_j(t))\exp(E_j(t))}{1+\alpha_{j1}(X_1(t)G_1+N_1(t))+\alpha_{j2}(X_2(t)G_2+N_2(t))+\alpha_{j3}(X_3(t)G_3+N_3(t))}, \\ N_j(t+1) &= (X_j(t)G_j + N_j(t))\,\widetilde{s}_j, \quad j=(1,2,3), \end{aligned} \tag{1.30}$$

where the α_{jk} are competition coefficients and $\exp(E_j(t))$ are the maximum fecundities. We assume that each species' maximum fecundity is temporally autocorrelated, which serves to generate the covariance between environment and competition that is needed for the storage effect (Li and Chesson, 2016, Schreiber, 2021). Through inter-generational population growth, a good environment for a resident generically leads to high competition in the future. However, a covariance between the future environment and future competition can only be established if the future environment is similar to the present environment, i.e., if the environment is autocorrelated.

The environmental parameters follow autoregressive order-1 dynamics,

$$\begin{aligned} E_j(t+1) &= \mu_j + \theta_j(E_j(t) - \mu_j) + \sigma_j\sqrt{1-\theta_j^2}, \quad j = (1,2,3), \\ (\epsilon_1(t), \epsilon_2(t), \epsilon_3(t))^\intercal &\sim MultivariateNormal(0, \boldsymbol{W}), \end{aligned} \tag{1.31}$$

with mean μ_j, autoregressive parameter θ_j, noise scale σ_j, and covariance matrix $\boldsymbol{W}$. The factor $\sqrt{1-\theta_j^2}$, when combined with the fact that the variances of ϵ_j are equal to one (i.e., $W_{jj} = 1$), ensures that the variance of the marginal asymptotic stationary distribution of $E_j(t)$ is always σ_j^2. This fact allows us to control the level of environmental noise while modulating the autoregressive parameters.

Quantities for the various scaling methods

The regulating factors $\boldsymbol{F}$ are the number of germinants of each species after the germination phase of the growing season, e.g., $F_1 = X_1(t)G_1 + N_1(t)$. The equilibrium regulating factors are found by fixing E_j at $E_j^* = \mu_j$, and then numerically finding the equilibrium where all species have positive seed and germinant densities. Then, the equilibrium population densities are used to calculate the equilibrium regulating factors, e.g., $F_1^* = X_1^* G_1 + N_1^*$. With the crucial parameters defined (E_j, E_j^*, $\boldsymbol{F}$, and $\boldsymbol{F}^{*j}$), we can now calculate the scaling factors.

In general, the scaling factors can't cancel $\Delta\rho_i$ when the number of residents is less than or equal to the number of regulating factors. Here, we ostensibly have 3 residents and 3 regulating factors, but when a species is placed in the invader state, one of the regulating factors vanishes and the scaling factors can be used to cancel $\Delta\rho_i$. Thus, when calculating the scaling factors, we invert the matrix of responses with the i-th row and i-th column removed (Chesson, 1994, p. 250), as opposed to only removing the row (as in Eq.1.25, Appendix 1.1.B).

To obtain the intrinsic generation time of species j, we first write the equations of population dynamics (Eq.1.30) in matrix-vector form, i.e., $\boldsymbol{Y}(t+1) = \boldsymbol{M}_j(t)\boldsymbol{Y}(t+1)$, where $\boldsymbol{M}_j(t)$ is the transition probability matrix and $\boldsymbol{Y} = (X, N)^\intercal$ is the state. Second, we write the transition probability matrix as the sum of a fecundity matrix $\widetilde{\boldsymbol{F}}_j$ and survival matrix $\widetilde{\boldsymbol{S}}_j$. The three focal matrixes are

$$\boldsymbol{M}_j(t) = \begin{bmatrix} s_j(1-G_j) + \frac{G_j \exp(E_j(t))}{1+\alpha_{j1}F_1(t)+\alpha_{j2}F_2(t)+\alpha_{j3}F_3(t)} & \frac{\exp(E_j(t))}{1+\alpha_{j1}F_1(t)+\alpha_{j2}F_2(t)+\alpha_{j3}F_3(t)} \\ G_j\widetilde{s}_j & \widetilde{s}_j \end{bmatrix}, \tag{1.32}$$

$$\widetilde{\boldsymbol{F}}_j(t) = \begin{bmatrix} \frac{G_j \exp(E_j(t))}{1+\alpha_{j1}F_1(t)+\alpha_{j2}F_2(t)+\alpha_{j3}F_3(t)} & \frac{\exp(E_j(t))}{1+\alpha_{j1}F_1(t)+\alpha_{j2}F_2(t)+\alpha_{j3}F_3(t)} \\ 0 & 0 \end{bmatrix}, \quad \text{and} \tag{1.33}$$

$$\widetilde{\boldsymbol{S}}_j(t) = \begin{bmatrix} s_j(1-G_j) & 0 \\ G_j\widetilde{s}_j & \widetilde{s}_j \end{bmatrix}. \tag{1.34}$$

The intrinsic generation time is given by the formula

$$T_j = \frac{v_j^\intercal w_j}{v_j^\intercal \widetilde{F}_j w_j}\Big|_{\substack{E_j=E^* \\ \boldsymbol{F}=\boldsymbol{F}^{*j}}}, \tag{1.35}$$

which is the same as Eq. 12 in Bienvenu and Legendre (2015) and Eq. 13 in Ellner (2018), except our formulation does not explicitly include the dominant eigenvalue (it is always one, because the population is at equilibrium). Here w_j is the stable age/stage distribution (the normalized right eigenvector of $\boldsymbol{M}_j$) and v_j contains the reproductive values (the normalized left eigenvector of $\boldsymbol{M}_j$). The vertical bar and symbols thereafter indicate that the quantity is evaluated at equilibrium.

Plugging the matrixes (Eq.1.32 and Eq.1.33) into Eq.1.35, substituting in the equilibrium parameters, and simplifying, we find that the intrinsic generation time is

$$T_j = \frac{1-(1-G_j)s_j\widetilde{s}_j}{(1-\widetilde{s}_j)(1-(1-G_j)s_j)}. \tag{1.36}$$

In the case of an annual species ($\widetilde{s}_j = 0$), the intrinsic generation time collapses to $T_j = 1/(1-(1-G_j)s_j)$. As expected, this is the average lifespan of a seed in the canonical annual plant model of Modern Coexistence Theory (Chesson, 1994, Section 5).

To use the β scaling method, we must define the sensitivity to competition. We use the formula

$$\beta_j = \frac{\partial \log(\lambda_{j,0})}{\partial C_j}\Big|_{\substack{E_j=E^* \\ C_j=C_j^*}}, \tag{1.37}$$

where $\lambda_{j,0}$ is the dominant eigenvalue of the species j's transition probability matrix, reparameterized in terms of E_j and C_j (as opposed to E_j and $\boldsymbol{F}$). While the expression above is the only obvious definition of β_j, it is (somewhat) conceptually unsatisfactory for reasons explained in Appendix 1.1.D (Reason # 4).

One of the major problems with β scaling is that the value of β_j can be sensitive to the definition of the competition parameter. In the context of annual–perennial model, there are two reasonable definitions of C_j. The first definition identifies competition as a linear combination of regulating factors: $C_j^{(1)} = \alpha_{j1}(X_1G_1 + N_1) + \alpha_{j2}(X_2G_2 + N_2) + \alpha_{j3}(X_3G_3 + N_3)$. The second definition identifies competition as the logarithm of the denominator in Eq.1.30: $C_j^{(2)} = \log\big(1 + \alpha_{j1}(X_1G_1 + N_1) + \alpha_{j2}(X_2G_2 + N_2) + \alpha_{j3}(X_3G_3 + N_3)\big)$. These two definitions (distinguished by superscripts "(1)" and "(2)") lead to two completely different sensitivities

to competition:

$$\beta_j^{(1)} = -\frac{e^{-\mu_j}(1-\widetilde{s}_j)^2(1-(1-G_j)s_j)^2}{G_j-(1-G_j)G_j s_j \widetilde{s}_j}, \quad \text{and} \quad \beta_j^{(2)} = -\frac{(1-\widetilde{s}_j)(1-(1-G_j)s_j)}{1-(1-G_j)s_j\widetilde{s}_j}. \tag{1.38}$$

It is easy to verify that $1/\left|\beta_j^{(2)}\right| = T_j$. Thus, the β scaling can give results that are equivalent to that of the generation time scaling, but only if the analyst intuits the "correct" definition of C_j. By contrast, the intrinsic generation time does not depend on how the model is parameterized (e.g., the definition of $\boldsymbol{F}$).

In certain parameter regimes, β scaling (with $\beta_j^{(1)}$) and generation time scaling can give similar results. That is, $1/\left|\beta_j^{(1)}\right| \approx T_j$. We found this to be the case when the germination and seed survival probabilities have moderate values (e.g., $G_j = s_j = 0.5$). However, in other parameter regimes, the two methods diverge greatly. Figure 1.2 shows how much a perennial resident is scaled when an equivalent annual is an invader. When the germination probability is low and seed survival is high, the generation time is relatively insensitive to the germinant survival probability. This makes sense — with these parameters, most of an individual's life is spent in the seed stage, regardless of the value of $\widetilde{s}_j$. The sensitivity to competition, on the other hand, grows quickly as $\widetilde{s}_j$ increases. We are unsure of the ecological interpretation of this pattern. Regardless, we will show that the extremely large values of $\left|\beta_s^{(1)}\right|/\left|\beta_i^{(1)}\right|$ can produce counterintuitive values of coexistence mechanisms.

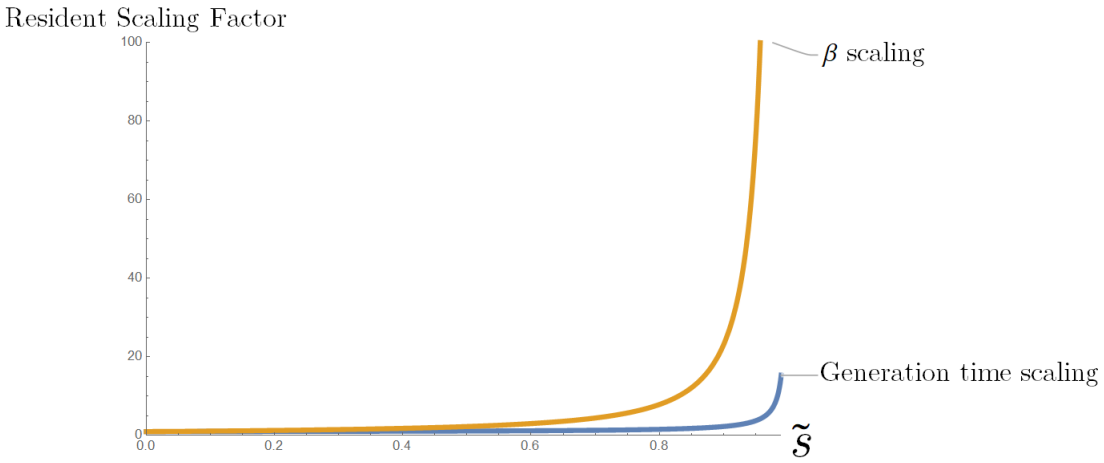

Figure 1.2: A comparison of scaling methods. The x-axis (limits $= [0, 0.99]$) depicts the germinant survival probability of the resident. The y-axis (limits $= [0, 100]$) depicts $\left|\beta_s^{(1)}\right|/\left|\beta_i^{(1)}\right|$ for the "β scaling" line and T_s/T_i for the "Generation time scaling" line. The invader is an annual (i.e., $\widetilde{s}_i = 0$). Both species share other parameters: $G_j = 0.1$, $s_j = 0.95$, $\mu_j = 4$.

Results

In every scenario, the competition coefficient matrix and noise covariance matrixes are respectively

$$\boldsymbol{\alpha} = \begin{bmatrix} 1 & 0.001 & 0.001 \\ 0.001 & 1 & 1.001 \\ 0.001 & 1.001 & 1 \end{bmatrix}, \quad \boldsymbol{W} = \begin{bmatrix} 1 & -0.49 & -0.49 \\ -0.49 & 1 & -0.49 \\ -0.49 & -0.49 & 1 \end{bmatrix}. \tag{1.39}$$

With competition structured in this way, species 1 is nearly-independent of species 2 and 3. In the absence of fluctuations, the either species 2 or 3 is competitively excluded depending on initial conditions; However, these *priority effects* may be overcome by the storage effect. For ease of interpretation, we will group ΔE_i and $\Delta\rho_i$ to represent all fluctuation-independent mechanisms. Intuition dictates that $\Delta E_i + \Delta\rho_1$ ($\Delta r_i'$ in the case of scaling factors), ΔI_2, and ΔI_3 will be positive and large (relative to other coexistence mechanisms within each species). In Scenario #1, we imagine that all species are long-lived perennial ($\widetilde{s}_j = 0.975$ for all j). All species are highly fecund, have long-lived seeds, small germination probabilities, and experience a temporally autocorrelated environment with moderate variance: $\mu_j = 4$, $s_j = 0.9$, $G_j = 0.1$, $\sigma_j = 1$, and $\theta_j = 0.9$ for all j. In this scenario, all methods agree with intuition (Table 1.4, the values of $\Delta E_1 + \Delta\rho_1$ in the box are large).

Scenario #2 is identical to Scenario #1 except for the fact that species 1 is now an annual (i.e., $s_1 = 0$). Here, the β scaling method (using $\beta_j^{(1)}$ from the previous section, Eq.1.38) fails spectacularly. Even though species 1 barely interacts with the other species and has roughly the same seed density as the perennials (germination is low and seed survival is high), the β scaling method indicates that species 1 is persisting because of the storage effect (Table 1.5, the value of ΔI_1 in the box is large, relative to other values in its row). All other methods agree with intuition, once again indicating that species 1 is persisting due to fluctuation-independent mechanisms.

The β_j method fails because it greatly up-weights the residents; when species 1 is the invader, the resident scaling factor is $|\beta_i|/|\beta_s| \approx 350$. We do not have a ecological explanation for why the perennials are so sensitive to competition in this parameter regime, but it is concerning that a reasonable definition of C_j can result in such unreasonable coexistence mechanisms.

1.1.D Extended discussion of β scaling

It is worth noting a few differences between the β scaling method and the method which was implied by Chesson (2018). First, Chesson uses the b_j instead of β_j (see Eq. 9 in Chesson, 2018). Second, Chesson defines the sensitivity to competition with a negative sign "baked in" (see Eq. 7 in Chesson, 2018), such

Table 1.4: Case study #2, Scenario #1: Coexistence mechanisms when all species are perennials. Species 2 and 3 behave symmetrically, so they have the same coexistence mechanisms. Model parameters are $\mu_j = 4$, $s_j = 0.9$, $G_j = 0.1$, $\sigma_j = 1$, $\theta_j = 0.9$, and $\widetilde{s}_j = 0.975$ for all j.

Species i = ...	**Calculation method**	**Coexistence mechanisms**		
		r_i' or $\Delta E_i + \Delta\rho_i$	ΔN_i	ΔI_i
1	Scaling factors	1.163	0.027	0.177
1	Simple comparison	1.163	0.027	0.177
1	Generation time scaling	1.163	0.027	0.177
1	β scaling	1.163	0.027	0.177
1	Invader-invader comparison	1.160	0.025	0.181
2 & 3	Scaling factors	-0.003	-0.002	0.008
2 & 3	Simple comparison	-0.003	-0.002	0.008
2 & 3	Generation time scaling	-0.003	-0.002	0.008
2 & 3	β scaling	-0.003	-0.002	0.008
2 & 3	Invader-invader comparison	-0.002	-0.000	0.006

that $beta_j$ is typically positive. We elect to use the absolute value, since Chesson's sign convention can return a negative β_i/β_r (when g_j' is an increasing function of the competition parameter C_j), thus ruining the interpretation of $|\beta_i|/|\beta_r|$ as converting between species' population dynamical speeds. Third, we scale the residents' average per capita growth rates, whereas Chesson (2018) divides all species' average per capita growth rates by their respective β_j's. Scaling the invader is supposed to ensure that no species dominates the *community-average coexistence mechanisms* (Chesson, 2003; Barabás et al., 2018). As we argue elsewhere (Johnson and Hastings, 2022), community-average coexistence mechanisms should be calculated by dividing species-level coexistence mechanisms by the absolute value of the focal species' invasion growth rate, not by sensitivity to competition.

Below we expand on the four reasons for favoring generation time scaling over β scaling.

1. The sensitivity to competition, β_j, depends on how the competition parameter is defined. Consider a model of two lake phytoplankton species competing for a single resource:

$$\begin{aligned} \frac{dN_j(t)}{dt} &= N_j(t)\left[e^{E_j(t)}\frac{w_j F(t)}{K_j + F(t)} - d\right] \quad j = 1, 2 \\ \frac{dF(t)}{dt} &= d(a - F(t)) - e^{E_1(t)}\frac{N_1(t)F(t)}{K_1 + F(t)} - e^{E_2(t)}\frac{N_2(t)F(t)}{K_2 + F(t)}. \end{aligned} \tag{1.40}$$

Table 1.5: Case study #2, Scenario #2: Coexistence mechanisms when species 2 & 3 are perennials and species 1 is an annual. Species 2 and 3 behave symmetrically, so they have the same coexistence mechanisms. Model parameters are $\mu_j = 4$, $s_j = 0.9$, $G_j = 0.1$, $\sigma_j = 1$, $\theta_j = 0.9$, for all j; $\widetilde{s}_2 = \widetilde{s}_3 = 0.975$, $\widetilde{s}_1 = 0$.

Species $i = \ldots$	**Calculation method**	**Coexistence mechanisms**		
		r_i' or $\Delta E_i + \Delta\rho_i$	ΔN_i	ΔI_i
1	Scaling factors	1.054	0.031	0.050
1	Simple comparison	1.020	0.003	0.112
1	Generation time scaling	1.018	0.002	0.115
1	β scaling	-0.488	-1.248	2.887
1	Invader-invader comparison	1.053	-0.053	0.134
2 & 3	Scaling factors	0.002	-0.046	0.048
2 & 3	Simple comparison	0.000	-0.004	0.008
2 & 3	Generation time scaling	0.000	-0.004	0.007
2 & 3	β scaling	0.000	0.001	0.002
2 & 3	Invader-invader comparison	-0.002	-0.000	0.006

Here, $N_j(t)$ is the phytoplankton density, $F(t)$ is the resource concentration, $e^{E_j(t)}$ is the temporally-fluctuating maximum uptake rate, w_j is the resource-to-phytoplankton conversion factor, K_j is the half-saturation constant, d is the dilution rate, and a is the resource supply. For a single resident, the equilibrium parameter is fixed at E_j^* and the corresponding equilibrium resource level is $dK_j/(w_j e^{E_j^*} - d)$.

If one selects competition as proportional to the handling time per unit resource, i.e. $C_j(t) = (K + F(t))/F(t)$, then the sensitivity to competition evaluates to $|\beta_j| = d^2/(w_j e^{E_j^*})$. If, on the other hand, one selects competition as the reciprocal of resource availability, i.e. $C_j = 1/F(t)$, then the sensitivity to competition evaluates to $|\beta_j| = (K_j w_j d^2 e^{E_j^*})/(d + K_j w_j e^{E_j^*})^2$. Two reasonable choices of C_j lead to two different β_j's, and in turn, two different partitions of the invasion growth rate.

2. Reasonable definitions of C_j can produce factors $1/\beta_j$ that differ substantially from the generation time. For an example, see case study #2 (Appendix 1.1.C)

3. Sometimes, there is no reasonable definition of C_j, and thus no reasonable definition of β_j. Consider a phytoplankton species (akin to that in Eq.1.40) which consumes two resources:

$$\frac{dN_j(t)}{dt} = N_j(t)\left[\left(\frac{e^{E_{j1}(t)}w_{j1}F_1(t)}{K_{j1}+F_1(t)} + \frac{e^{E_{j2}(t)}w_{j2}F_2(t)}{K_{j2}+F_2(t)}\right) - d\right]. \tag{1.41}$$

There is no way to write the per capita growth rate as a function of the two environmental parameters and a single competition parameter. It may be tempting to define the competition parameter as the reciprocal of the entire term in parentheses, but then the environmental parameters would be latent (hidden within C_j), and the piece of invasion growth rate attributable to the storage effect would be absorbed by relative nonlinearity. It may be tempting to define two separate competition parameters, but then there would be two β_j's with no obvious way to combine them (take the mean? the maximum?).

4. The sensitivity to competition is not well-defined in stochastic stage-structured models. The sensitivity to competition is defined as a partial derivative of the function g'_j, which gives the per capita growth rate at a single point in time (i.e., $dN_j(t)/dt$ or $\log(\lambda_j(t)) = \log(N_j(t+1)/N_j(t))$). A stage-structure model has at least two such per capita growth rates (one for each stage) and no obvious analogue of the overall per capita growth rate at single point in time. One candidate is the logarithm of the dominant lyapunov exponent of the transition probability matrix at a single point in time, denoted by $\log(\lambda_{j,0}(t))$.

   Unfortunately, $\lambda_0(t)$ not the current per capita growth rate, but rather the long-term average growth rate under the assumption that the elements of the transition probability matrix do not change. Further, the long-term average growth rate is not simply the temporal average of $\log(\lambda_{j,0}(t))$ (due to the systemic effect of temporal auto-correlations; see Tuljapurkar, 1982; Caswell, 2001, Section 14.3.6.2), thus making the measure $\log(\lambda_{j,0}(t))$ somewhat disanalogous to $\log(\lambda_j(t))$ in scalar population models. It is no great surprise that β_j is not well-defined in stochastic stage-structured models. Like the scaling factors, β scaling was designed to deliver theoretical insights (Chesson, 2000b; Chesson, 2018), not to quantify coexistence mechanisms in real communities.

1.1.E Scaling factors in the case of diffuse competition

Consider the S-species Lotka-Volterra model:

$$\frac{1}{n_j(t)}\frac{dn_j(t)}{dt} = k_j - \sum_{k=1}^{S}\alpha_{jk}n_k(t), \quad j = (1,\ldots,S). \tag{1.42}$$

In the case of diffuse competition where x is interspecific competition and c is intraspecific competition, the competition coefficients are

$$\alpha_{jk} = \begin{cases} c & \text{if } j = k \\ x & \text{if } j \neq k \end{cases}. \tag{1.43}$$

The regulating factors in this model are the species densities. The matrix of sensitivities to regulating factors is thus

$$\mathbf{\Phi} = \begin{bmatrix} c & x & \dots & x \\ x & c & \dots & x \\ \vdots & \vdots & \ddots & \vdots \\ x & x & \dots & c \end{bmatrix}. \tag{1.44}$$

When a species is placed in the invader state, one of the regulating factors vanishes. Therefore, we invert the matrix of responses with the i-th row and i-th column removed. This matrix, which we will still call $\mathbf{\Phi^{\{-i\}}}$, is a square $(S-1) \times (S-1)$ matrix. Note that this is a slight abuse of notation, since in Appendix 1.1.B, $\mathbf{\Phi^{\{-i\}}}$ represents a matrix where only the invader's *row* has been removed.

To invert $\mathbf{\Phi^{\{-i\}}}$, we first decompose it:

$$\mathbf{\Phi^{\{-i\}}} = A + uv^\intercal, \tag{1.45}$$

where $A = \begin{bmatrix} c-x & 0 & \dots & 0 \\ 0 & c-x & \dots & 0 \\ \vdots & \vdots & \ddots & \vdots \\ 0 & 0 & \dots & c-x \end{bmatrix}$, $u = \begin{bmatrix} x \\ \vdots \\ x \end{bmatrix}$, and $v^\intercal = \begin{bmatrix} 1 \dots 1 \end{bmatrix}$.

The variables A, u, and v all have $S-1$ rows. Now we can use the Sherman-Morrison formula for the matrix inverse, which states that

$$\mathbf{\Phi^{\{-i\}}} = (A + uv^\intercal)^{-1} = A^{-1} - \frac{A^{-1}uv^\intercal A^{-1}}{1 + v^\intercal A^{-1} u}. \tag{1.46}$$

Combined with the well-known fact that the inverse of a diagonal matrix is the matrix of the reciprocals of diagonal elements, we find that $\left(\mathbf{\Phi^{\{-i\}}}\right)^{-1}$ is a symmetric matrix with diagonal elements equal to $\frac{x}{(c-x)(c+x(S-2)}$, and off-diagonal elements equal to $\frac{1}{c-x} - \frac{x}{(c-x)(c+x(S-2)}$.

Since $\mathbf{\Phi^{\{-i\}}}$ is invertible, the solution for the scaling factors, Eq.1.25, becomes

$$\boldsymbol{q_{i*}} = \mathbf{\Phi}_{i*} \left(\mathbf{\Phi}^{(-i)}\right)^{-1}. \tag{1.47}$$

Performing this computation with $\mathbf{\Phi}_{i*} = \begin{bmatrix} x \dots x \end{bmatrix}$, a row vector with $S-1$ elements, we get

$$q_{is} = \frac{x}{c + (S-2)x}. \tag{1.48}$$

1.1.F Generation time scaling corrects for *average fitness differences*

One side of Modern Coexistence Theory (MCT) is concerned with partitioning the invasion growth rate into coexistence mechanisms like relative nonlinearity, the storage effect, etc. There is an entirely different side of MCT, which is concerted with explaining the coexistence in terms of equalizing mechanisms and stabilizing mechanisms (Chesson, 1990; Chesson, 2000b; Chesson, 2018). *Equalizing mechanisms* weaken competitive differences between species, whereas *stabilizing mechanisms* strengthen niche differences. The important insight here is that different kinds of between-species differences can have different effects on coexistence.

The equalizing vs. stabilizing paradigm only applies to two-species models with Lotka-Volterra-like dynamics (There is a multi-species theory, but the mathematical objects are different; Song et al., 2019). Consider the following parameterization of the Lotka-Volterra Model:

$$\frac{1}{N_j}\frac{dN_j}{dt} = b_j\left(1 - \sum_{k=1}^{2}\alpha_{jk}N_k\right). \tag{1.49}$$

The conditions for coexistence are described by the relation

$$\rho < \frac{\kappa_1}{\kappa_2} < \frac{1}{\rho}, \tag{1.50}$$

where ρ is the *niche overlap* and κ_1/κ_2 is the *average fitness ratio*. They are defined as

$$\rho = \sqrt{\frac{b_1\alpha_{12}b_2\alpha_{21}}{b_1\alpha_{11}b_2\alpha_{22}}}, \quad \text{and} \tag{1.51}$$

$$\frac{\kappa_1}{\kappa_2} = \frac{b_2}{b_1}\sqrt{\frac{\alpha_{21}\alpha_{22}}{\alpha_{11}\alpha_{12}}}. \tag{1.52}$$

The reciprocal of the average fitness ratio, κ_2/κ_1 includes the ratio of generation times, b_1/b_2. Crucially, the speed parameters, b_j, cancel out in the niche overlap, but not the average fitness difference. Therefore, if one accepts that κ_j can be rightfully called the average fitness of species j (justification in Chesson, 2018; counterpoint in Barabás et al., 2018), then it is reasonable to think of the action of generation time scaling as virtually reducing average fitness differences between species. Even though the average fitness ratio and the ratio of generation times are not identical, dividing by the fitness ratio and ratio of generation times will

have largely the same effect if species have different dynamical speeds, but similar competitive effects. This supports our claim in the main text (*Discussion*) that generation time scaling is most useful when species have dissimilar population-dynamical speeds.

Data availability statement

All computations can be replicated using the Mathematica notebooks, `ArmMc_3Spp.nb` and `SE_3Spp.nb`, found at https://github.com/ejohnson6767/scaling_factors.

References

Adler, P. B., HilleRisLambers, J., Kyriakidis, P. C., Guan, Q., & Levine, J. M. (2006). Climate variability has a stabilizing effect on the coexistence of prairie grasses. *Proceedings of the National Academy of Sciences*, *103*(34), 12793–12798.

Allen, L. J. (2010). *An introduction to stochastic processes with applications to biology* (2nd ed.). CRC press.

Angert, A. L., Huxman, T. E., Chesson, P., & Venable, D. L. (2009). Functional tradeoffs determine species coexistence via the storage effect. *Proceedings of the National Academy of Sciences*, *106*(28), 11641–11645.

Armitage, D. W., & Jones, S. E. (2019). Negative frequency-dependent growth underlies the stable coexistence of two cosmopolitan aquatic plants. *Ecology*, *100*(5), e02657.

Armitage, D. W., & Jones, S. E. (2020). Coexistence barriers confine the poleward range of a globally distributed plant. *Ecology Letters*, *23*(12), 1838–1848.

Armstrong, R. A., & McGehee, R. (1976). Coexistence of species competing for shared resources. *Theoretical Population Biology*, *9*(3), 317–328.

Armstrong, R. A., & McGehee, R. (1980). Competitive exclusion. *The American Naturalist*, *115*(2), 151–170.

Barabás, G., & D'Andrea, R. (2020). Chesson's coexistence theory: Reply. *Ecology*, *101*(11).

Barabás, G., D'Andrea, R., & Stump, S. M. (2018). Chesson's coexistence theory. *Ecological Monographs*, *88*(3), 277–303.

Ben-Israel, A., & Greville, T. N. (2003). *Generalized inverses: Theory and applications* (2nd ed.). Springer.

Bienvenu, F., & Legendre, S. (2015). A new approach to the generation time in matrix population models. *The American Naturalist*, *185*(6), 834–843.

Cáceres, C. E. (1997). Temporal variation, dormancy, and coexistence: A field test of the storage effect. *Proceedings of the National Academy of Sciences*, *94*(17), 9171–9175.

Caswell, H. (2001). *Matrix population models: Construction, analysis, and interpretation* (2nd ed.). Sinauer Associates.

Chase, J. M., & Leibold, M. A. (2003). *Ecological niches: Linking classical and contemporary approaches*. University of Chicago Press.

Chesson, P. (1990). Macarthur's consumer-resource model. *Theoretical Population Biology*, *37*(1), 26–38.

Chesson, P. (1994). Multispecies competition in variable environments. *Theoretical Population Biology*, *45*(3), 227–276.

Chesson, P. (2000a). General theory of competitive coexistence in spatially-varying environments. *Theoretical Population Biology*, *58*(3), 211–237.

Chesson, P. (2000b). Mechanisms of maintenance of species diversity. *Annual review of Ecology and Systematics*, *31*(1), 343–366.

Chesson, P. (2003). Quantifying and testing coexistence mechanisms arising from recruitment fluctuations. *Theoretical Population Biology*, *64*(3), 345–357.

Chesson, P. (2008). Quantifying and testing species coexistence mechanisms. In *Unity in diversity: Reflections on ecology after the legacy of Ramon Margalef* (pp. 119–164). Fundacion BBVA Bilbao.

Chesson, P. (2013). Species competition and predation. In *Ecological systems* (pp. 223–256). Springer.

Chesson, P. (2018). Updates on mechanisms of maintenance of species diversity. *Journal of ecology*, *106*(5), 1773–1794.

Chesson, P. (2020). Chesson's coexistence theory: Comment. *Ecology*, *101*(11), e02851.

Chesson, P., & Huntly, N. (1997). The roles of harsh and fluctuating conditions in the dynamics of ecological communities. *The American Naturalist*, *150*(5), 519–553.

Chesson, P., Huntly, N. J., Roxburgh, S. H., Pantastico-Caldas, M., & Facelli, J. M. (2012). The storage effect: Definition and tests in two plant communities. In *Temporal dynamics and ecological process* (pp. 11–40). Cambridge University Press.

Chu, C., & Adler, P. B. (2015). Large niche differences emerge at the recruitment stage to stabilize grassland coexistence. *Ecological Monographs*, *85*(3), 373–392.

De Magalhaes, J., & Costa, J. (2009). A database of vertebrate longevity records and their relation to other life-history traits. *Journal of evolutionary biology*, *22*(8), 1770–1774.

Descamps-Julien, B., & Gonzalez, A. (2005). Stable coexistence in a fluctuating environment: An experimental demonstration. *Ecology*, *86*(10), 2815–2824.

Ellner, S. P. (2018). Generation time in structured populations. *The American Naturalist*, *192*(1), 105–110.

Ellner, S. P., Snyder, R. E., & Adler, P. B. (2016). How to quantify the temporal storage effect using simulations instead of math. *Ecology letters*, *19*(11), 1333–1342.

Ellner, S. P., Snyder, R. E., Adler, P. B., & Hooker, G. (2019). An expanded modern coexistence theory for empirical applications. *Ecology letters*, *22*(1), 3–18.

Gause, G. F. (1934). *The struggle for existence*. Williams & Wilkins.

Geritz, S. A., Gyllenberg, M., Jacobs, F. J., & Parvinen, K. (2002). Invasion dynamics and attractor inheritance. *Journal of mathematical biology*, *44*(6), 548–560.

Grover, J. P. (1997). *Resource competition*. Springer.

Hallett, L. M., Shoemaker, L. G., White, C. T., & Suding, K. N. (2019). Rainfall variability maintains grass-forb species coexistence. *Ecology Letters*, *22*(10), 1658–1667.

Hsu, S.-B. (1980). A competition model for a seasonally fluctuating nutrient. *Journal of Mathematical Biology*, *9*(2), 115–132.

Huston, M. (1979). A general hypothesis of species diversity. *The American Naturalist*, *113*(1), 81–101.

Jensen, J. L. W. V., et al. (1906). Sur les fonctions convexes et les inégalités entre les valeurs moyennes. *Acta Mathematica*, *30*, 175–193.

Johnson, E. C., & Hastings, A. (2022). Resolving conceptual issues in modern coexistence theory. *arXiv preprint arXiv:2201.07926*.

Jones, K. E., Bielby, J., Cardillo, M., Fritz, S. A., O'Dell, J., Orme, C. D. L., Safi, K., Sechrest, W., Boakes, E. H., Carbone, C., et al. (2009). Pantheria: A species-level database of life history, ecology, and geography of extant and recently extinct mammals: Ecological archives e090-184. *Ecology*, *90*(9), 2648–2648.

Levin, S. A. (1970). Community equilibria and stability, and an extension of the competitive exclusion principle. *The American Naturalist*, *104*(939), 413–423.

Li, L., & Chesson, P. (2016). The effects of dynamical rates on species coexistence in a variable environment: The paradox of the plankton revisited. *The American Naturalist*, *188*(2), E46–E58.

Moore, M. (2019). Causation in the law. In E. N. Zalta (Ed.), *The Stanford encyclopedia of philosophy* (Winter 2019). Metaphysics Research Lab, Stanford University.

Myhrvold, N. P., Baldridge, E., Chan, B., Sivam, D., Freeman, D. L., & Ernest, S. M. (2015). An amniote life-history database to perform comparative analyses with birds, mammals, and reptiles: Ecological archives e096-269. *Ecology*, *96*(11), 3109–3109.

Mylius, S. D., & Diekmann, O. (2001). The resident strikes back: Invader-induced switching of resident attractor. *Journal of Theoretical Biology*, *211*(4), 297–311.

Schreiber, S. J. (2021). Positively and negatively autocorrelated environmental fluctuations have opposing effects on species coexistence. *The American Naturalist*, *197*(4), 000–000.

Sears, A. L., & Chesson, P. (2007). New methods for quantifying the spatial storage effect: An illustration with desert annuals. *Ecology*, *88*(9), 2240–2247.

Smith, H. L. (1981). Competitive coexistence in an oscillating chemostat. *SIAM Journal on Applied Mathematics*, *40*(3), 498–522.

Snyder, R. E., Borer, E. T., & Chesson, P. (2005). Examining the relative importance of spatial and nonspatial coexistence mechanisms. *The American Naturalist*, *166*(4), E75–E94.

Song, C., Barabás, G., & Saavedra, S. (2019). On the consequences of the interdependence of stabilizing and equalizing mechanisms. *The American Naturalist*, *194*(5), 627–639.

Song, C., Rohr, R. P., Vasseur, D., & Saavedra, S. (2020). Disentangling the effects of external perturbations on coexistence and priority effects. *Journal of Ecology*, *108*(4), 1677–1689.

Strong Jr, D. R. (1983). Natural variability and the manifold mechanisms of ecological communities. *The American Naturalist*, *122*(5), 636–660.

Stump, S. M. (2017). Multispecies coexistence without diffuse competition; or, why phylogenetic signal and trait clustering weaken coexistence. *The American Naturalist*, *190*(2), 213–228.

Tilman, D. (1982). *Resource competition and community structure*. Princeton University Press.

Towers, I. R., Bowler, C. H., Mayfield, M. M., & Dwyer, J. M. (2020). Requirements for the spatial storage effect are weakly evident for common species in natural annual plant assemblages. *Ecology*, *101*(12), e03185.

Tuljapurkar, S. D. (1982). Population dynamics in variable environments. iii. evolutionary dynamics of r-selection. *Theoretical Population Biology*, *21*(1), 141–165.

Usinowicz, J., Chang-Yang, C.-H., Chen, Y.-Y., Clark, J. S., Fletcher, C., Garwood, N. C., Hao, Z., Johnstone, J., Lin, Y., Metz, M. R., Masaki, T., Nakashizuka, T., Sun, I.-F., Valencia, R., Wang, Y., Zimmerman, J. K., Ives, A. R., & Wright, S. J. (2017). Temporal coexistence mechanisms contribute to the latitudinal gradient in forest diversity. *Nature*, *550*(7674), 105–108.

Usinowicz, J., Wright, S. J., & Ives, A. R. (2012). Coexistence in tropical forests through asynchronous variation in annual seed production. *Ecology*, *93*(9), 2073–2084.

Wiens, J. A. (1977). On competition and variable environments: Populations may experience" ecological crunches" in variable climates, nullifying the assumptions of competition theory and limiting the usefulness of short-term studies of population patterns. *American Scientist*, *65*(5), 590–597.

Zepeda, V., & Martorell, C. (2019). Fluctuation-independent niche differentiation and relative non-linearity drive coexistence in a species-rich grassland. *Ecology*, *100*(8), e02726.

1.2 Coexistence in spatiotemporally fluctuating environments

1.2.1 Abstract

Ecologists have put forward many explanations for coexistence, but these are only *partial explanations*; nature is complex, so it is reasonable to assume that in any given ecological community, multiple mechanisms of coexistence are operating at the same time. Here, we present a methodology for quantifying the relative importance of different explanations for coexistence, based on an extension of *Modern Coexistence Theory*. Current versions of Modern Coexistence Theory only allow for the analysis of communities that are affected by spatial *or* temporal environmental variation, but not both. We show how to analyze communities with spatiotemporal fluctuations, how to parse the importance of spatial variation and temporal variation, and how to measure everything with either mathematical expressions or simulation experiments. Our extension of Modern Coexistence Theory shows that many more species can coexist than originally thought. More importantly, it allows empiricists to use realistic models and more data to better infer the mechanisms of coexistence in real communities. ta to better infer the mechanisms of coexistence in real communities.

Table 1.6: The symbols and terminology of Spatiotemporal Modern Coexistence Theory (MCT).

	Description
MCT-specific terminology	
invader	a rare species; for mathematical convenience, the per capita growth rate of this species is approximated by perturbing population density to zero.
resident	a common species, more precisely understood as a species at its typical abundances
invasion growth rate	the long-term average of the per capita growth rate of an invader
partition	a scheme for breaking up an invasion growth rate into a sum of component parts
coexistence mechanism	a class of explanations for coexistence; corresponds to a component of the invasion growth rate partition of Spatiotemporal MCT
space-time decomposition	a type of partition which parses the effects of spatial and temporal variation on the invasion growth rate
invader–resident comparison	a comparison between an invader and the resident species; measures a rare-species advantage
generation time quotient	scales resident growth rates, hypothetically converting the population-dynamical speeds of resident species to that of the invader; corrects for average fitness differences in the invader–resident comparison; replaces the *scaling factors*, also known as *comparison quotients*, from previous versions of MCT
Variable	
x	a location in space
t	a point in time
j	species index (subscript)

$n_j(x,t)$	the population density of species j at patch x and time t.
$\nu_j(x,t)$	relative density, calculated as local population density divided by the spatial average of population density, i.e., $n_j(x,t)/\mathbb{E}_x[n_j]$
λ_j(x,t)	the local finite rate of increase. In non-spatial models, λ_j is defined as $n_j(x,t+1)/n_j(x,t)$. However, in spatial models, λ_j is defined as $n'_j(x,t)/n_j(x,t)$, where $n'_j(x,t)$ is the population size after the local growth phase, but before the dispersal phase.
$\widetilde{\lambda}_j(t)$	the metapopulation finite rate of increase, defined as a density-weighted average of λ_j over patches: $\widetilde{\lambda}_j = \mathbb{E}_x[(n_j/\mathbb{E}_x[n_j])\lambda_j]$
$\mathbb{E}_t\left[\log\left(\widetilde{\lambda}_j\right)\right]$	The long-term average per capita growth rate; for resident species, this is zero by definition; for invader, this is the invasion growth rate
$E_j(x,t)$	the environmental parameter, more generally understood as the effects of density-independent factors
$C_j(x,t)$	the competition parameter, more generally understood as the effects of density-dependent factors
g_j	a function that gives the local finite rate of increase: $\lambda_j(x,t) = g_j(E_j(x,t), C_j(x,t))$
E_j^*	the equilibrium environmental parameter, defined so that $g_j(E_j^*, C_j^*) = 1$
C_j^*	the equilibrium competition parameter, defined so that $g_j(E_j^*, C_j^*) = 1$
σ	the scale of environmental fluctuations: $E_j(x,t) - E_j^* = \mathcal{O}(\sigma)$; it is sometimes the case that σ controls the size of fluctuations in n_j, E_j, and C_j, see Appendix 1.2.B.2
S	the total number of species in the community; $S-1$ is the number of residents
GT_j	the generation time of species j, evaluated at equilibrium; the quantity $1/GT_j$ is a measure of the *speed* of population dynamics — the intrinsic capacity to grow or decline quickly;
$\frac{GT_r}{GT_i}$	generation time quotient; effectively converts the population-dynamical speed of resident r to that of the invader i
$\overline{\mathscr{E}_j}$	the main effect of density-independent factors on the average per capita growth rate, defined as $\mathbb{E}_t\left[\log\left(\mathbb{E}_x\left[g_j(E_j, C_j^*)\right]\right)\right]$
$\overline{\mathscr{C}_j}$	the main effect of density-dependent on the average per capita growth rate, defined as $\mathbb{E}_t\left[\log\left(\mathbb{E}_x\left[g_j(E_j^*, C_j)\right]\right)\right]$

$\overline{\mathscr{I}_j}$	the interaction effect of density-dependent and density-independent factors on the average per capita growth rate, defined as $\mathbb{E}_t[\log(\mathbb{E}_x[g_j(E_j, C_j)])] - \overline{\mathscr{E}_j} - \overline{\mathscr{C}_j}$
$\overline{\mathscr{K}_j}$	the main effect of allowing relative density to vary on the average per capita growth rate, defined as $\mathbb{E}_t[\log(\mathbb{E}_x[\nu_j g_j(E_j, C_j)])] - \mathbb{E}_t[\log(\mathbb{E}_x[g_j(E_j, C_j)])]$

Coexistence mechanisms

ΔE_i	Density-independent effects; the degree to which density-independent factors favor the invader
$\Delta \rho_i$	Linear density-dependent effects; specialization on resources and/or natural enemies
ΔN_i	Relative nonlinearity; specialization on the spatiotemporal variance of resources and/or natural enemies
ΔI_i	The storage effect; specialization on different states of a spatiotemporally varying environment
$\Delta \kappa_i$	Fitness-density covariance; the differential ability of rare species to end up in locations with high ecological fitness

Taylor series coefficients

$\alpha_j^{(1)}$	the linear effects of fluctuations in E_j, defined as $\frac{\partial g_j}{\partial E_j}\Big\vert_{\substack{E_j=E_j^* \\ C_j=C_j^*}} = \frac{\partial g_j(E_j^*, C_j^*)}{\partial E_j}$
$\alpha_j^{(2)}$	the nonlinear effects of of fluctuations in E_j, defined as $\frac{\partial^2 g_j(E_j^*, C_j^*)}{\partial E_j^2}$
$\beta_j^{(1)}$	the linear effects of fluctuations in C_j, defined as $\frac{\partial g_j(E_j^*, C_j^*)}{\partial C_j}$
$\beta_j^{(2)}$	the nonlinear effects of fluctuations in C_j, defined as $\frac{\partial^2 g_j(E_j^*, C_j^*)}{\partial C_j^2}$
$\zeta_j^{(1)}$	the non-additive (i.e., interaction) effects of fluctuations in E_j and C_j, defined as $\zeta_j = \frac{\partial^2 g_j(E_j^*, C_j^*)}{\partial E_j \partial C_j}$

Superscripts and subscripts

Subscripts

j	index of an arbitrary species
i	index of the invader
r	index of a resident
x	indicates that a summary statistic (e.g., mean, covariance, variance) is calculated by summing across space
t	indicates that a summary statistic (e.g., mean, covariance, variance) is calculated by summing across time
A	denotes the effect of average conditions in the space-time decomposition
S	denotes the main effect of spatial variation in the space-time decomposition
T	denotes the main effect of temporal variation in the space-time decomposition
R	denotes the interaction effect of spatial and temporal variation in the space-time decomposition

Superscripts

(e)	denotes exact coexistence mechanisms, or intermediate products in the calculation of exact coexistence mechanisms
#	indicates that the elements of a vector or matrix have been shuffled (sampled randomly without replacement)

Operators

$\mathbb{E}_{x,t}[\cdot]$	The spatiotemporal *sample* arithmetic mean; for a variable Z that varies over K patches and T time points, $\mathbb{E}_x[Z] = (1/K)\sum_{x=1}^{K} Z(x,t)$, $\mathbb{E}_t[Z] = (1/T)\sum_{t=1}^{T} Z(x,t)$, and $\mathbb{E}_{x,t}[Z] = (1/(TK))\sum_{t=1}^{T}\sum_{x=1}^{K} Z(x,t)$
$\mathrm{Var}_{x,t}(\cdot)$	The spatiotemporal *sample* variance; for a variable Z that varies over K patches and T time points,

	$\mathrm{Var}_x(Z) = (1/K)\sum_{x=1}^{K}(Z(x,t) - \mathbb{E}_x[Z])^2$,
	$\mathrm{Var}_t(Z) = (1/T)\sum_{t=1}^{T}(Z(x,t) - \mathbb{E}_t[Z])^2$, and
	$\mathrm{Var}_{x,t}(Z) = (1/(TK))\sum_{t=1}^{T}\sum_{x=1}^{K}(Z(x,t) - \mathbb{E}_{x,t}[Z])^2$
$\mathrm{Cov}_{x,t}(\cdot,\cdot)$	The spatiotemporal *sample* covariance; for variables W and Z that vary over K patches and T time points,
	$\mathrm{Cov}_x(W,Z) = (1/K)\sum_{x=1}^{K}(W(x,t) - \mathbb{E}_x[W])(Z(x,t) - \mathbb{E}_x[Z])$,
	$\mathrm{Cov}_t(W,Z) = (1/T)\sum_{t=1}^{T}(W(x,t) - \mathbb{E}_t[W])(Z(x,t) - \mathbb{E}_t[Z])$, and
	$\mathrm{Cov}_{x,t}(W,Z) = (1/(TK))\sum_{t=1}^{T}\sum_{x=1}^{K}(W(x,t) - \mathbb{E}_{x,t}[W])(Z(x,t) - \mathbb{E}_{x,t}[Z])$

1.2.2 Introduction

Modern Coexistence Theory (MCT) is a framework for understanding ecological coexistence (Chesson, 1994; Chesson, 2000; see Barabás et al., 2018 for a recent review). MCT has two main strengths. First, MCT gives us the relative importance of different explanations for coexistence, and thus tells us *how* species are coexisting, not simply whether they *are* coexisting. Second, MCT is *general* because it is a framework for analyzing arbitrary models of population dynamics (which could represent all kinds of different communities). This feature of MCT stands in contrast to several big theories in community ecology — such as neutral theory, maximum entropy, and metacommunity theory — in which highly constrained models are used to make inferences about many communities. MCT has been successfully used to derive theoretical insights (e.g., Chesson and Huntly, 1997; Stump and Chesson, 2015; Li and Chesson, 2016; Snyder and Chesson, 2003; Chesson, 2008; Kuang and Chesson, 2010; Schreiber, 2021), and to infer the mechanisms of coexistence in real communities (Cáceres, 1997; Adler et al., 2006; Angert et al., 2009; Sears and Chesson, 2007; Usinowicz et al., 2012; Descamps-Julien and Gonzalez, 2005; Chu and Adler, 2015; Usinowicz et al., 2017; Ignace et al., 2018; Towers et al., 2020).

Despite MCT's successes, there are a handful of problems that limit its applicability. One such problem is that currently, MCT can be used to analyze models where the environment fluctuates over space or time, but not both. **Here, we extend Modern Coexistence Theory (MCT) to show how models with spatiotemporal fluctuations can be analyzed. Further, we show how to parse the importance of spatial fluctuations and temporal fluctuations, and how to measure everything with mathematics or simulations**. While a couple papers (Chesson, 1985; Snyder et al., 2005; Snyder, 2008) have examined the effects of spatiotemporal fluctuations in particular models, our approach permits the analysis of a broad variety of models and is thus targeted towards empirical applications.

MCT is based on *invasion growth rates*, the average per capita growth rates of species that have been perturbed to low density. However, the appropriate average is not trivial to compute in spatiotemporal models. A simple arithmetic average over space and time is not appropriate, due to a fundamental difference in how populations grow over space and time: with respect to the geometric mean of the finite rate of increase (the quantity predictive of persistence; Lewontin and Cohen, 1969; Dempster, 1955; Stearns, 2000; Metz et al., 1992), contributions from populations across space are additive, but contributions from populations across time are multiplicative. Therefore, the appropriate spatiotemporal averaging involves a density-weighted spatial average, followed by a temporal average on the log-scale.

The ability to analyze models with spatiotemporal fluctuations helps us better understand coexistence in real ecological communities: MCT necessarily interfaces with the real world through empirically-calibrated

models, and good representations of real communities will undoubtedly involve spatiotemporal variation. But the addition of spatiotemporal fluctuations is not realism for realism's sake: failure to include spatiotemporal fluctuations will typically lead to underestimates of fluctuation-dependent coexistence mechanisms, which could lead to poor downstream inferences about the nature of coexistence and macroecological patterns that entail coexistence (e.g., metacommunity structure, species abundance distributions). Further, our extension of MCT permits a more fine-grained quantification of coexistence mechanism. With Spatiotemporal MCT, one can compare the relative importance of spatial variation, temporal variation, and classical coexistence mechanisms (e.g., resource partitioning); one can partition individual coexistence mechanisms — like the *storage effect* — into its spatial and temporal constituents.

The ability to analyze models with spatiotemporal fluctuations can also lead to novel theoretical insights. For instance, we show that 1) temporal variation can promote the storage effect in the lottery model, even in the case of non-overlapping generations (Section 1.2.5), 2) that it is (nearly) impossible for the competitive exclusion principle to hold true in the presence of spatiotemporal fluctuations (Section 1.2.6), and 3) the inclusion of spatiotemporal fluctuations exactly doubles the maximum number of species that can coexist due to fluctuation-dependent coexistence mechanisms (Section 1.2.6).

1.2.3 Spatiotemporal coexistence mechanisms

1.2.3.1 Overview

At the coarsest level of description, Modern Coexistence Theory (MCT) has two steps: "decompose and compare" (Ellner et al., 2019). First, *decompose* the average per capita growth rate of each species into terms that correspond to conceptually distinct processes (e.g., growth that can be attributed to resource consumption). Second, *compare* the like-terms of rare species (termed *invaders*) and common species (termed *residents*) in order to discover which processes tend to help rare species. These invader–resident comparisons, called *coexistence mechanisms*, correspond to classes of explanations for coexistence. The sum of coexistence mechanisms is the *invasion growth rate*, the long-term average per capita growth rate of a species that has been perturbed to near-zero density.

How do invasion growth rates and coexistence mechanisms relate to coexistence? The main idea is that invasion growth rates measure the tendency to recover from rarity, so a set of S species can be said to coexist if each species has a positive invasion growth rate in the sub-community of $S-1$ resident species. This is known as the *mutual invasibility criterion* for coexistence (Turelli, 1978; Chesson, 2000; Chesson and Ellner, 1989; Grainger, Levine, et al., 2019).

In truth, the relationship between invasion growth rates and coexistence is not so simple. The mutual

invasibility criterion fails when the elimination of one species causes knock-on extinctions, such that the $S-1$ residents cannot coexist. For the mutual invasibility criterion to work, we must either assume that all $S-1$ residents can coexist (Case, 2000), or limit ourselves to two-species competitive communities (Ellner, 1989). When the mutual invasibility criterion fails, one can still use invasion growth rates as inputs to the Hofbauer criterion for coexistence (Hofbauer, 1981; Benaïm and Schreiber, 2019, Eq.3.4), a sufficient condition for a type of global stability called *permanence* or *uniform persistence* (Schreiber, 2000; Garay and Hofbauer, 2003; Schreiber et al., 2011; Roth and Schreiber, 2014). But this criterion potentially combines invasion growth rates in many sub-communities (with $S-n$ residents, for $n=1,2,\ldots,S$), so it is unclear to how to average over sub-communities to obtain species-level coexistence mechanisms or community-average coexistence mechanisms (as in Chesson, 2003, Eq.16).

Invasion growth rates are used in the mutual invasibility criterion and the Hofbauer criterion, both of which test for *global stability*. However, global stability can sometimes be too strong a notion of coexistence: under a certain set of scenarios (e.g., Allee effects, obligate mutualisms, and intransitive competition) negative invasion growth rates can erroneously indicate a failure to coexistence, since all species would be able to coexist if simultaneously introduced at higher densities. We leave all of these issues to future research; thus, we temporarily use these concepts heuristically: larger coexistence mechanisms $\rightarrow$ larger invasion growth rate $\rightarrow$ stronger coexistence. We deliberately avoid models with obligate mutualisms and Allee effects; if placing a species in the invader state causes knock-on extinctions, we forge onward, measuring coexistence mechanisms with the reduced number of residents.

In this paper, we will define two types of *coexistence mechanisms*. The first is *small-noise coexistence mechanisms*, which closely approximate the invasion growth rate when environmental fluctuations are small. The second type is *exact coexistence mechanisms*, which always sum exactly to the invasion growth rate. Small-noise coexistence mechanisms are calculated with Taylor series expansions (i.e., a linearization of population dynamics about an equilibrium), whereas exact coexistence mechanisms are calculated with simulation data (an approach pioneered by Ellner et al. (2016, 2019). To be clear, small-noise coexistence mechanisms do not assume that environmental fluctuations are unimportant or that the fluctuation-independent mechanisms drive coexistence. *Small-noise* refers to a technical assumption that environmental fluctuations are small relative to other parameters in a model of population growth. This assumption, (when paired some additional assumptions; Appendix 1.2.B.2) allows us to derive analytical expressions for the coexistence mechanisms.

There has been recent debate about how exactly coexistence mechanisms should be defined (Barabás et al., 2018; Chesson, 2020; and Barabás and D'Andrea, 2020), with Chesson claiming that true coexistence mechanisms are exact (Chesson, 2020, Eq. 9) contradicting previous work (Chesson, 1994, Eq. 22). Some

expositions of MCT mix-and-match both types of coexistence mechanisms (e.g., Chesson, 1994, Eq. 19–22), adding to the confusion. We present the two types of coexistence mechanisms separately, partially for clarity, but primarily because they have distinct pros and cons.

Even though small-noise coexistence mechanisms only approximate the invasion growth rate, there are situations in which small-noise coexistence mechanisms are preferred. For one, the small-noise approximations can be calculated quickly, which is important in empirical applications where coexistence mechanisms are calculated for many draws from a posterior or bootstrap distribution of model parameters. Secondly, small-noise coexistence mechanisms sometimes permit analytical expressions (for a worked example, see Section 1.2.5), whereas the exact coexistence mechanisms almost never do. Finally, the small-noise coexistence mechanisms could correspond more closely to our verbal/textual explanations for coexistence, and thus could be more interpretable. On the other hand, the primary advantage of the exact coexistence mechanisms is that they sum exactly to the invasion growth rate. We will derive both the small-noise coexistence mechanisms (Section 1.2.3.2) and the exact coexistence mechanisms (Section 1.2.3.3), but we leave it to the reader to determine which is more relevant to their work.

Our exposition focuses on discrete-time models with spatial structure but without age/stage structure. In Appendix 1.2.E, we discuss generalizations of Spatiotemporal MCT to different classes of models, including continuous-time models and age/stage-structured models. For the time being, community dynamics are governed by a system of difference equations,

$$n_j(x,t+1) = n_j(x,t)\ \lambda_j(x,t) + c_j(x,t) - e_j(x,t) \qquad j = (1,2,...,S), \tag{1.53}$$

where $n_j(x,t)$ is the local density of species j, λ_j is the local finite rate of increase, x is a discrete patch in space, t is a discrete point in time, and S is the number of species in the community. The terms c_j and e_j represent immigration and emmigration respectively, in units of population density. We require that the sum of c_j and e_j across space (i.e., net dispersal) vanishes (Appendix 1.2.B.3), which occurs generically when either 1) the system is *closed* (i.e., no individuals can enter or leave the system of patches), or 2) that the system of patches is representative of a larger metacommunity, such that it receives roughly as many immigrants as it loses emigrants.

A few notes on notation are necessary. For convenience, we will often write out random variables without the explicit dependence on space and time; for example, we will write λ_j instead of $\lambda_j(x,t)$. We use the operator $\mathbb{E}[Z]$ to denote average of some random variable Z, with subscripts to denote whether the average is being taken across space, time, or both. For example, in a system with K patches that has been observed for T time-steps, $\mathbb{E}_x[Z] = (1/K)\sum_{x=1}^{K} Z(x,t)$, $\mathbb{E}_t[Z] = (1/T)\sum_{t=1}^{T} Z(x,t)$, and $\mathbb{E}_{x,t}[Z] =$

$(1/(TK))\sum_{t=1}^{T}\sum_{x=1}^{K} Z(x,t)$. We use the operators $\mathrm{Var}_{x,t}(.)$ and $\mathrm{Cov}_{x,t}(.,.)$ in a similar fashion, to the denote the sample variance and sample covariance respectively.

Our use of the expectation operator is unorthodox: it usually denotes the average across an infinite number of instantiations of the stochastic population process at one point in time, not the temporal average of one instantiation. However, the sample average is asymptotically equivalent to the expectation if the stochastic process is stationary and ergodic; see Section 1.2.4). Additionally, $\mathbb{E}_{x,t}[.]$ is visually similar to $\mathrm{Var}_{x,t}(.)$ and $\mathrm{Cov}_{x,t}(.,.)$, whereas the subscripts "x,t" are located incongruously in more conventional notation for the mean, e.g., $\langle Z\rangle_{x,t}$, $\overline{Z}^{\{x,t\}}$.

The *local finite rate of increase* is defined as $\lambda_j = n'_j(x,t+1)/n_j(x,t)$, where $n'_j(x,t+1)$ is the population density after a bout of local population growth, but before the dispersal phase. The *metapopulation finite rate of increase*, $\widetilde{\lambda}_j = \mathbb{E}_x[(n_j/\mathbb{E}_x[n_j])\lambda_j]$, is the density-weighted spatial average of λ_j. The *average growth rate* rate, $\mathbb{E}_t\left[\log\left(\widetilde{\lambda}_j\right)\right]$, is the quantity whose sign is predictive of long-term growth (Schreiber et al., 2011). The average growth rate of the invader is called the *invasion growth rate*. The subscript i references an invader species, the subscript r references a resident species, and the subscript j references a generic species whose status as a resident or invader is impertinent.

1.2.3.2 Small-noise coexistence mechanisms

A full derivation of small-noise spatiotemporal coexistence mechanisms is provided in Appendix 1.2.A. Here, we summarize the main steps:

1. The local finite rate of increase is expressed as a function of an environmental parameter E_j, and a competition parameter C_j: $\lambda_j(x,t) = g_j(E_j(x,t), C_j(x,t))$.

   The environmental parameter E_j has also been referred to as "the environmentally-dependent parameter", "the environmental response", or simply, "the environment". It is more generally defined as some parameter that depends on spatiotemporally fluctuating density-independent factors (e.g., the germination probability of a seed, which depends on precipitation). Similarly, the competition parameter C_j, also known as "competition", is more generally defined as some parameter that depends on density-dependent factors. As such, C_j may represent resource competition, apparent competition, or even mutualism. The competition parameter can often be expressed as function of multiple regulating factors (see Appendix 1.2.E.3), such as resources, refugia, competitors' densities, and predators.

2. The local finite rate of increase is approximated with a second-order Taylor series expansion of g_j about the *equilibrium parameters*, E_j^* and C_j^*, constants which are specified by the user of MCT but must satisfy the constraint $g_j(E_j^*, C_j^*) = 1$. The resulting second-order polynomial will lead to an accurate

approximation of the invasion growth rate, but only if some assumptions about the magnitude of environmental fluctuations are met (see Appendix 1.2.B.2). To help satisfy these assumptions, it is important to select the equilibrium parameters so that they are close to their spatiotemporal means, $\mathbb{E}_{x,t}[E_j]$ and $\mathbb{E}_{x,t}[C_j]$, respectively.

3. The appropriate spatial and temporal averaging is applied in order to express average growth rates entirely in terms of moments of local growth, λ_j, and relative density, $\nu_j = n_j/\mathbb{E}_x[n_j]$:

$$\mathbb{E}_t\Big[\log\Big(\widetilde{\lambda}_j\Big)\Big] \approx \mathbb{E}_{x,t}[\lambda_j] + \mathbb{E}_t[\mathrm{Cov}_x(\nu, \lambda_j)] - 1 - \frac{1}{2}\mathrm{Var}_t(\mathbb{E}_t[\lambda_j]) \tag{1.54}$$

4. The Taylor series approximation of λ_j (see step 2) is substituted into the expression for the average growth rate (Eq.1.54), resulting in a long expression for species j's average growth rate:

$$\begin{aligned}\mathbb{E}_t\Big[\log\Big(\widetilde{\lambda}_j\Big)\Big]\Big|_{\substack{C_j=C_j^* \\ E_j=E_j^*}} \approx\ & \alpha_j^{(1)}\mathbb{E}_{x,t}\big[(E_j - E_j^*)\big] + \beta_j^{(1)}\mathbb{E}_{x,t}\big[(C_j - C_j^*)\big] \\ & + \frac{1}{2}\alpha_j^{(2)}\mathrm{Var}_{x,t}(E_j) + \frac{1}{2}\beta_j^{(2)}\mathrm{Var}_{x,t}(C_j) + \zeta_j\mathrm{Cov}_{x,t}(E_j, C_j) \\ & + \mathbb{E}_t\Big[\mathrm{Cov}_x\Big(\nu_j, \alpha_j^{(1)}(E_j - E_j^*) + \beta_j^{(1)}(C_j - C_j^*)\Big)\Big] \\ & - \frac{1}{2}{\alpha_j^{(1)}}^2\mathrm{Var}_t(\mathbb{E}_x[E_j]) - \frac{1}{2}{\beta_j^{(1)}}^2\mathrm{Var}_t(\mathbb{E}_x[E_j]) - \alpha_j^{(1)}\beta_j^{(1)}\mathrm{Cov}_t(\mathbb{E}_x[E_j], \mathbb{E}_x[C_j]),\end{aligned} \tag{1.55}$$

where the coefficients of the Taylor series,

$$\alpha_j^{(1)} = \frac{\partial g_j(E_j^*, C_j^*)}{\partial E_j}, \quad \beta_j^{(1)} = \frac{\partial g_j(E_j^*, C_j^*)}{\partial C_j}, \quad \alpha_j^{(2)} = \frac{\partial^2 g_j(E_j^*, C_j^*)}{\partial E_j^2}, \quad \beta_j^{(2)} = \frac{\partial^2 g_j(E_j^*, C_j^*)}{\partial {C_j,}^2}, \quad \zeta_j = \frac{\partial^2 g_j(E_j^*, C_j^*)}{\partial E_j \partial C_j}, \tag{1.56}$$

are all evaluated at user-specified equilibrium values $E_j = E_j^*$ and $C_j = C_j^*$, as implied by the notation.

The additive terms in the above equation (Eq.1.55), which we may call *growth rate components*, can be conceptualized as distinct processes. For example, the second term $\beta_j^{(1)}\mathbb{E}_{x,t}\big[(C_j - C_j^*)\big]$ is the effect of the mean level of competition on the average growth rate.

5. The invader is compared to the residents. Because coexistence is about a *rare-species advantage*, we do not care so much about the invader's growth rate components, but rather their magnitude relative to the corresponding components of residents. Since every resident species cannot grow or decline on

average (i.e., $\mathbb{E}_t\left[\log\left(\widetilde{\lambda}_r\right)\right] = 0$) we may subtract a linear combination of the $S-1$ resident species from the invasion growth rate

$$\mathbb{E}_t\left[\log\left(\widetilde{\lambda}_i\right)\right] = \mathbb{E}_t\left[\log\left(\widetilde{\lambda}_i\right)\right] - \frac{1}{S-1}\sum_{r\neq i}^{S}\frac{GT_r}{GT_i}\mathbb{E}_t\left[\log\left(\widetilde{\lambda}_r\right)\right], \tag{1.57}$$

without any distortion of the invasion growth rate. The weighting by $1/(S-1)$ assumes that all $S-1$ species can coexist; if perturbing a species to the invader state causes knock-on extinctions, then we only average over extant residents. The coefficients GT_r/GT_i are quotients of species' generation times and function to hypothetically convert the population-dynamical speed of the residents to that of the invader (Johnson and Hastings, 2022a). They will be discussed further in a few paragraphs. The long decomposition of the average growth rate (Eq.1.55) can be substituted into the above equation (Eq.1.57), and like-terms can be grouped such that the invasion growth rate is expressed as a sum of invader–resident comparisons. These comparisons are the *coexistence mechanisms*.

Formulas for small-noise coexistence mechanisms

The invasion growth rate

$$\mathbb{E}_t\left[\log\left(\widetilde{\lambda}_i\right)\right] \approx \Delta E_i + \Delta\rho_i + \Delta \mathrm{N}_i + \Delta \mathrm{I}_i + \Delta\kappa_i \tag{1.58}$$

Density-independent effects

$$\begin{aligned}\Delta E_i = &\left[\alpha_i^{(1)}\mathbb{E}_{x,t}[E_i - E_i^*] + \frac{1}{2}\alpha_i^{(2)}\mathrm{Var}_{x,t}(E_i) - \frac{1}{2}\alpha_i^{(1)^2}\mathrm{Var}_t(\mathbb{E}_x[E_i])\right] \\ &- \frac{1}{S-1}\sum_{r\neq i}^{S}\frac{GT_r}{GT_i}\left[\alpha_r^{(1)}\mathbb{E}_{x,t}[E_r - E_r^*] + \frac{1}{2}\alpha_r^{(2)}\mathrm{Var}_{x,t}(E_r) - \frac{1}{2}\alpha_r^{(1)^2}\mathrm{Var}_t(\mathbb{E}_x[E_r])\right]\end{aligned} \tag{1.59}$$

Linear density-dependent effects

$$\Delta\rho_i = \beta_i^{(1)}\mathbb{E}_{x,t}[C_i - C_i^*] - \frac{1}{S-1}\sum_{r\neq i}^{S}\frac{GT_r}{GT_i}\beta_r^{(1)}\mathbb{E}_{x,t}[C_r - C_r^*] \tag{1.60}$$

Relative nonlinearity

$$\Delta N_i = \frac{1}{2}\left[\beta_i^{(2)}\mathrm{Var}_{x,t}(C_i) - {\beta_i^{(1)}}^2\mathrm{Var}_t(\mathbb{E}_x[C_i])\right] - \frac{1}{S-1}\sum_{r\neq i}^{S}\frac{GT_r}{GT_i}\left[\beta_r^{(2)}\mathrm{Var}_{x,t}(C_r) - {\beta_r^{(1)}}^2\mathrm{Var}_t(\mathbb{E}_x[C_r])\right] \quad (1.61)$$

The storage effect

$$\Delta I_i = \left[\zeta_i\mathrm{Cov}_{x,t}(E_i, C_i) - \alpha_i^{(1)}\beta_i^{(1)}\mathrm{Cov}_t(\mathbb{E}_x[E_i], \mathbb{E}_x[C_i])\right] - \frac{1}{S-1}\sum_{r\neq i}^{S}\frac{GT_r}{GT_i}\left[\zeta_r\mathrm{Cov}_{x,t}(E_r, C_r) - \alpha_r^{(1)}\beta_r^{(1)}\mathrm{Cov}_t(\mathbb{E}_x[E_r], \mathbb{E}_x[C_r])\right] \quad (1.62)$$

Fitness-density covariance

$$\Delta\kappa_i = \mathbb{E}_t\left[\mathrm{Cov}_x\left(\nu_i, \alpha_i^{(1)}E_i + \beta_i^{(1)}C_i\right)\right] - \frac{1}{S-1}\sum_{r\neq i}^{S}\frac{GT_r}{GT_i}\mathbb{E}_t\left[\mathrm{Cov}_x\left(\nu_r, \alpha_r^{(1)}E_r + \beta_r^{(1)}C_r\right)\right] \quad (1.63)$$

The density-independent effects (ΔE_i) is the degree to which all density-independent factors favor the invader. The linear density-dependent effects ($\Delta\rho_i$) represents a rare-species advantage due to specialization on regulating factors (i.e., resources and/or natural enemies). Relative nonlinearity (ΔN_i) is a rare-species advantage due to specialization on variation in regulating factors. The storage effect (ΔI_i) is the rare-species advantage due to specialization on certain states of a variable environment. Fitness-density covariance ($\Delta\kappa$) is the differential ability of a rare species' individuals to end up in locations where they have high fitness. Note that "coexistence mechanism" is a misnomer when it comes to ΔE_i, since ΔE_i can only support a single species in the absence of all other mechanisms. See Barabás et al. (2018) for a more thorough discussion of the canonical coexistence mechanisms and their interpretations.

Experts in coexistence theory may notice several differences between spatiotemporal MCT and previous versions of MCT (i.e., Chesson, 1994, Chesson, 2000; Barabás et al., 2018), aside from the inclusion of spatiotemporal fluctuations. First, we keep the equilibrium competition parameters, C_j^*, as part of $\Delta\rho_i$, whereas previous versions of MCT shunted the C_j^* to the density-independent effects, which are then denoted by r_i' (see Barabás et al., 2018, Eq.19). Second, we scale resident growth rates by a quotient of generation times, whereas previous versions of MCT scaled resident growth rates by the so-called *scaling factors*. Both

the shunting of C_j^* and the scaling factors have a very specific function: to cancel $\Delta\rho_i$. As we have argued elsewhere (Johnson and Hastings, 2022a), cancelling $\Delta\rho_i$ can be useful in the context of theoretical research, but is not recommended for "measuring coexistence" (i.e., using MCT to infer the mechanisms of coexistence in real communities). In the myopic quest to cancel $\Delta\rho_i$, the scaling factors can dramatically modulate the values of other coexistence mechanisms, potentially leading to incorrect inferences about coexistence.

Retaining the C_j^* terms in $\Delta\rho_i$ helps with the interpretability of $\Delta\rho_i$: the term $\alpha_j^{(1)}(\mathbb{E}_{x,t}[C_j] - C_j^*)$ can be interpreted as the effect (on per capita growth rates) of the average deviation from equilibrium competition, whereas $\alpha_j^{(1)}\mathbb{E}_{x,t}[C_j]$ has no clear meaning. That being said, it will sometimes make sense to present the sum of $\Delta\rho_i$ and ΔE_i, the total contribution of fluctuation-independent forces (e.g., Johnson and Hastings, 2022a, *SI Table 1–2*; Ellner et al., 2019, *Table 2*, "Fluctuation-free growth rate").

To ensure that species with fast life-cycles do not dominate the invader–resident comparison, we multiply each residents' average growth rate by a quotient of generation times, GT_r/GT_i. Because $1/GT_j$ is a measure of population-dynamical speed, the scaling quotients can be thought of as converting the speed of resident dynamics to that of the invader: the reciprocal of resident speed, GT_r, is canceled by the speed implicit in the resident's average growth rate, leaving only the invader's speed, $1/GT_i$. When the species under consideration do not have dramatically different generation times, it is often reasonable (and in some models, considerably simpler) to fix $GT_r/GT_i = 1$ for all i and r. This approach, dubbed *the simple comparison* by Johnson and Hastings (2022a), was originally performed by Ellner et al. (2016, 2019), who also retained $\Delta\rho_i$ (using different notation).

There is no single definition of generation time, but many definitions are quantitatively equivalent in a stable population (Ellner, 2018). Thus, to minimize arbitrariness, we fix model parameters at their equilibrium values and operationalize generation time as the weighted average of parent age across all births at one time, with weights equal to the reproductive value of offspring. This quantity can be calculated with a simple formula in structured population models (Bienvenu and Legendre, 2015, Eq. 12; Ellner, 2018, Eq. 13), or via simulation in more complex models. In simple models where individuals are identical (i.e., there is no variation in reproductive values) and reproduction is independent of parent age, the generation time is simply the average age of adults; if then mortality occurs at a density-independent rate δ, the distribution of adult age is given by a geometric distribution (or exponential distribution in continuous-time models) with mean $1/\delta$.

1.2.3.3 Exact coexistence mechanisms

The sum of small-noise coexistence mechanisms merely approximates the invasion growth rate (Eq.1.58). The approximation will be good if environmental fluctuations are small (see Appendix 1.2.B.2 for all assumptions),

but in empirically-calibrated models there is no guarantee that the small-noise assumptions will be met. An alternative approach is to define a set of coexistence mechanisms that sum exactly to the invasion growth rate. We call these *exact coexistence mechanisms* and demarcate them with the superscript "(e)", e.g., the exact relative nonlinearity is $\Delta N_i^{(e)}$.

The average growth rate of species j can be broken into two terms:

$$\mathbb{E}_t\Big[\log\Big(\widetilde{\lambda}_j\Big)\Big] = \underbrace{\mathbb{E}_t[\log(\mathbb{E}_x[\lambda_j])]}_{①} + \underbrace{\mathbb{E}_t\Big[\log\Big(\widetilde{\lambda}_j\Big)\Big] - \mathbb{E}_t[\log(\mathbb{E}_x[\lambda_j])]}_{②}. \tag{1.64}$$

Term ① captures the appropriate spatiotemporal average of fitness. Term ② captures the effects of variation in relative density, which can be seen either by noting that $\mathbb{E}_t\Big[\log\Big(\widetilde{\lambda}_j\Big)\Big] = \mathbb{E}_t[\log(\mathbb{E}_x[\lambda_j])]$ when fitness-density covariance is zero (Eq.1.54), or that the second term will approximate $\mathbb{E}_t[\mathrm{Cov}_x(\nu_j, \lambda_j)]$ when the small-noise assumptions (Appendix 1.2.B.2) are met.

Term ① can be further decomposed with the following schema:

$$\mathbb{E}_t[\log(\mathbb{E}_x[\lambda_j])] = \overline{\mathscr{E}_j} + \overline{\mathscr{C}_j} + \overline{\mathscr{I}_j} \tag{1.65}$$

$$\overline{\mathscr{E}_j} = \mathbb{E}_t\big[\log\big(\mathbb{E}_x\big[g_j(E_j, C_j^*)\big]\big)\big] \tag{1.66}$$

$$\overline{\mathscr{C}_j} = \mathbb{E}_t\big[\log\big(\mathbb{E}_x\big[g_j(E_j^*, C_j)\big]\big)\big] \tag{1.67}$$

$$\overline{\mathscr{I}_j} = \mathbb{E}_t[\log(\mathbb{E}_x[g_j(E_j, C_j)])] - \big(\overline{\mathscr{E}_j} + \overline{\mathscr{C}_j}\big) \tag{1.68}$$

The term $\overline{\mathscr{E}_j}$ is the main effect of the environment on the average growth rate, $\overline{\mathscr{C}_j}$ is the main effect of competition, and $\overline{\mathscr{I}_j}$ is the effect of interactions between environment and competition, in analogy with a two-way ANOVA. These new terms are analogous to the temporal or spatial means of the *standard parameters*, quantities that played an important role in previous iterations of MCT (e.g. Chesson, 1994, Eq. 8–9; Chesson, 2000, Eq. 28–29). However, they are not equivalent, despite sharing the same notation.

Term ② can be re-expressed as

$$\log\Big(\widetilde{\lambda}_j\Big) - \mathbb{E}_t[\log(\mathbb{E}_x[\lambda_j])] = \overline{\mathscr{K}_j}, \tag{1.69}$$

$$\overline{\mathscr{K}}_j = \mathbb{E}_t[\log(\mathbb{E}_x[\nu_j g_j(E_j, C_j)])] - \mathbb{E}_t[\log(\mathbb{E}_x[g_j(E_j, C_j)])]\,, \tag{1.70}$$

where $\overline{\mathscr{K}}_j$ is the main effect of allowing relative density, $\nu_j = n_j/\mathbb{E}_x[n_j]$, to vary across space.

The intermediate quantities — $\overline{\mathscr{E}_j}$, $\overline{\mathscr{C}_j}$, $\overline{\mathscr{I}_j}$, and $\overline{\mathscr{K}_j}$ — can be computed generically using simulation

data. Simply run a simulation of a model while archiving a record of the E_j's, C_j's and ν_j's; specify the equilibrium parameters E_j^* and C_j^*; and plug everything into the above equations.

To preempt a point of potential confusion, we emphasize that simulation data is never *created* while holding E_j or C_j at their equilibrium values. To compute $\overline{\mathscr{C}_j}$, one must evaluate g_j function while holding the environment at E_j^* and allowing C_j to vary; but we still use the C_j that we would have obtained had we not held the environment at E_j^*. To obtain these unadulterated C_j, we first run a business-as-usual simulation whilst recording E_j and C_j.

To calculate the exact coexistence mechanisms, our new quantities ($\overline{\mathscr{E}_j}$, $\overline{\mathscr{C}_j}$, and $\overline{\mathscr{I}_j}$) are used in the invader–resident comparison (Eq.1.57) in lieu of the appropriately averaged Taylor series terms (i.e., the additive terms in Eq.1.55).

Formulas for exact coexistence mechanisms

The invasion growth rate

$$\mathbb{E}_t\Big[\log\Big(\widetilde{\lambda}_i\Big)\Big] = \Delta E_i{}^{(e)} + \Delta\rho_i{}^{(e)} + \Delta \mathrm{N}_i{}^{(e)} + \Delta \mathrm{I}_i{}^{(e)} + \Delta\kappa_i{}^{(e)}, \tag{1.71}$$

Density-independent effects

$$\Delta E_i{}^{(e)} = \overline{\mathscr{E}_i} - \frac{1}{S-1}\sum_{r\neq i}^{S}\frac{GT_r}{GT_i}\overline{\mathscr{E}_r} \tag{1.72}$$

$$\overline{\mathscr{E}}_j = \mathbb{E}_t\big[\log\big(\mathbb{E}_x\big[g_j(E_j, C_j^*)\big]\big)\big] \tag{1.73}$$

Linear density-dependent effects

$$\Delta\rho_i{}^{(e)} = \log(g_i(E_i^*, \mathbb{E}_{x,t}[C_i])) - \frac{1}{S-1}\sum_{r\neq i}^{S}\frac{GT_r}{GT_i}\log(g_r(E_r^*, \mathbb{E}_{x,t}[C_r])) \tag{1.74}$$

Relative nonlinearity

$$\Delta N_i{}^{(e)} = \left[\overline{\mathscr{C}_i} - \frac{1}{S-1}\sum_{r\neq i}^{S}\frac{GT_r}{GT_i}\overline{\mathscr{C}_r}\right] - \Delta\rho_i{}^{(e)} \tag{1.75}$$

$$\overline{\mathscr{C}}_j = \mathbb{E}_t\big[\log\big(\mathbb{E}_x\big[g_j(E_j^*, C_j)\big]\big)\big] \tag{1.76}$$

The storage effect

$$\Delta I_i^{(e)} = \overline{\mathscr{I}_i} - \frac{1}{S-1}\sum_{r\neq i}^{S}\frac{GT_r}{GT_i}\overline{\mathscr{I}_r} \tag{1.77}$$

$$\overline{\mathscr{I}_j} = \mathbb{E}_t[\log(\mathbb{E}_x[g_j(E_j, C_j)])] - \big(\overline{\mathscr{E}_j} + \overline{\mathscr{C}_j}\big) \tag{1.78}$$

Fitness-density covariance

$$\Delta\kappa_i^{(e)} = \overline{\mathscr{K}_i} - \frac{1}{S-1}\sum_{r\neq i}^{S}\frac{GT_r}{GT_i}\overline{\mathscr{K}_r} \tag{1.79}$$

$$\begin{aligned}\overline{\mathscr{K}}_j =& \mathbb{E}_t[\log(\mathbb{E}_x[\nu_j\ g_j(E_j, C_j)])] - \mathbb{E}_t[\log(\mathbb{E}_x[g_j(E_j, C_j)])] \\ & \mathbb{E}_t[\log(\mathbb{E}_x[\nu_j\ g_j(E_j, C_j)])] - \big(\overline{\mathscr{E}_j} + \overline{\mathscr{C}_j} + \overline{\mathscr{I}_j}\big)\end{aligned} \tag{1.80}$$

1.2.3.4 The space-time decomposition of small-noise coexistence mechanisms

Ideally, we would like to take any coexistence mechanism that relies on spatiotemporal variation, and perform a *space-time decomposition* to generate four additive components: the contribution of average E_j and C_j, the contribution of spatial variation, the contribution of temporal variation, and the contribution of the interaction between spatial and temporal variation. For example, we would like to write the density-independent effects as $\Delta E_i = \Delta E_{i,A} + \Delta E_{i,S} + \Delta E_{i,T} + \Delta E_{i,R}$, with the subscripts A, S, T, and R respectively corresponding to the average component, the space component, the time component, and the space-time interaction. The letter R was chosen because the space-time interaction is calculated as a $\underline{R}$emainder (Eq.1.84), and because the letter I is already used in ΔI_i and $\overline{\mathscr{I}_i}$.

Before decomposing entire coexistence mechanisms, we will decompose $\mathrm{Var}_{x,t}(E_j)$, a building block of

the ΔE_i coexistence mechanism. The space-time decomposition of $\text{Var}_{x,t}(E_j)$ is

$$\text{Var}_{x,t}(E_j) = S_j + T_j + R_j \tag{1.81}$$

$$\begin{aligned} S_j =& \text{Var}_x(\mathbb{E}_t[E_j]) && (1.82)\\ T_j =& \text{Var}_t(\mathbb{E}_x[E_j]) && (1.83)\\ R_j =& \text{Var}_{x,t}(E_j) - (S_j + T_j) && (1.84)\\ =& \mathbb{E}_x[\text{Var}_t(E_j)] - \text{Var}_t(\mathbb{E}_x[E_j])\\ =& \mathbb{E}_t[\text{Var}_x(E_j)] - \text{Var}_x(\mathbb{E}_t[E_j])\,. \end{aligned}$$

The last two expressions for R_j are obtained using the law of total variance. A close examination confirms our space-time decomposition satisfies some minimal requirements: $S_j = 0$ when there is no spatial variation in E_j, $T_j = 0$ when there is no temporal variation, and $R_j = 0$ when there is either no spatial or temporal variation.

The components of the space-time decomposition of $\text{Var}_{x,t}(E_j)$ can be thought of as differences between hypothetical worlds in which spatial and/or temporal variation has been turned on or off. For example, the space term, S_j, is the difference between the variance of E_j in a world where temporal variation has been turned off (by setting $E_j(x,t)$ to $\mathbb{E}_t[E_j]$, leaving only spatial variation), and the variance of E_j in a reference world where both spatial and temporal variation have turned off (which is necessarily zero). Adding only spatial variation to the reference state of "no variation" gives the main effect of spatial variation. The interaction effect of spatial and temporal variation is the marginal effect of turning on both spatial and temporal variation; it is the extent to which the combination of spatial and temporal variation exceeds the sum of its parts, which is why the interaction term (Eq.1.84) involves subtracting both main effects.

Our talk of "hypothetical worlds" and "turning off variation" may give our space-time decomposition a speciously *ad hoc* aura. However, it is ordinary scientific practice to measure *the causal effect of X* as the marginal effect of X is relation to some reference state (VanderWeele, 2015); think of a clinical trial where the effect of drug X is the difference in health outcomes between the control and treatment groups. In Appendix 1.2.C, we justify our space-time decomposition by 1) showing that the results it gives in a toy model accords with intuition, and 2) using the philosophical literature to show that our decomposition results in terms that can be interpreted as the *causal effects* of spatial and temporal variation.

In Eq.1.81–1.84, we defined the space-time decomposition of $\text{Var}_{x,t}(E_j)$. The other variance/covariance terms featured in the small-noise coexistence mechanisms (i.e., $\text{Var}_{x,t}(C_j)$ and $\text{Cov}_{x,t}(E_j, C_j)$) can be de-

composed in analogous fashion, by turning on/off E_j and C_j in tandem. To obtain the space-time decomposition of the small-noise coexistence mechanisms, we propagate the small-noise decompositions of $\text{Var}_{x,t}(E_j)$, $\text{Var}_{x,t}(C_j)$, and $\text{Cov}_{x,t}(E_j, C_j)$ though the expressions for the small-noise coexistence mechanisms (Eq.2.14–1.63). For example, since variance in E_j is the purview of the density-independent effects (ΔE_i), and because the space-component of $\text{Var}_{x,t}(E_j)$ is $\text{Var}_x(\mathbb{E}_t[E])$, it follows that all terms involving $\text{Var}_x(\mathbb{E}_t[E])$ will belong to $\Delta E_{i,S}$, the space-component of the density-independent effects.

How should the space-time components of coexistence mechanisms be interpreted? In the abstract, they are the causal effects of spatial or temporal variation (or their interaction) on particular coexistence mechanisms. For example, the space-component of the storage effect, $\Delta I_{i,S}$, is the rare-species advantage that results from species specializing on persistent spatial heterogeneity. Because models without temporal variation will generate a $\Delta I_{i,S}$ that is quantitatively identical to the *spatial storage effect* of Chesson's (2000) spatial coexistence theory, we may call $\Delta I_{i,S}$ the spatial storage effect, with the notable caveat that $\Delta I_{i,S}$ does not capture *all* the effects of spatial variation ($\Delta I_{i,R}$ also depends on spatial variation). The space-time components may have more precise ecological interpretations — beyond "the causal effects of spatial (temporal) variation on X coexistence mechanism" — but these will depend on the idiosyncrasies of particular models.

All averages over space and time are shunted into the "Average" components of the space-time time decomposition, denoted with the subscript A. Note that relative nonlinearity (ΔN_i) has no average component because the average effect of C_j is captured in the linear density-dependent effects ($\Delta \rho_i$). Also note that the average component of the storage effect ($\Delta I_{i,A}$) equals zero, since the covariance between two constants is always zero.

Formulas for space-time decomposition of small-noise coexistence mechanisms

Density-independent effects

$$\Delta E_i = \Delta E_{i,A} + \Delta E_{i,S} + \Delta E_{i,T} + \Delta E_{i,R} \tag{1.85}$$

$$\Delta E_{i,A} = \alpha_i^{(1)} \mathbb{E}_{x,t}[E_i - E_i^*] - \frac{1}{S-1} \sum_{r \neq i}^{S} \frac{GT_r}{GT_i} \alpha_r^{(1)} \mathbb{E}_{x,t}[E_r - E_r^*] \tag{1.86}$$

$$\Delta E_{i,S} = \frac{1}{2} \alpha_i^{(2)} \mathrm{Var}_x(\mathbb{E}_t[E_i]) - \frac{1}{S-1} \sum_{r \neq i}^{S} \frac{GT_r}{GT_i} \frac{1}{2} \alpha_r^{(2)} \mathrm{Var}_x(\mathbb{E}_t[E_r]) \tag{1.87}$$

$$\Delta E_{i,T} = \frac{1}{2} \left(\alpha_i^{(2)} - \alpha_i^{(1)^2} \right) \mathrm{Var}_t(\mathbb{E}_x[E_i]) - \frac{1}{S-1} \sum_{r \neq i}^{S} \frac{GT_r}{GT_i} \frac{1}{2} \left(\alpha_r^{(2)} - \alpha_r^{(1)^2} \right) \mathrm{Var}_t(\mathbb{E}_x[E_r]) \tag{1.88}$$

$$\begin{aligned} \Delta E_{i,R} &= \frac{1}{2} \alpha_i^{(2)} \Big[\mathbb{E}_t[\mathrm{Var}_x(E_i)] - \mathrm{Var}_x(\mathbb{E}_t[E_i]) \Big] \\ &\quad - \frac{1}{S-1} \sum_{r \neq i}^{S} \frac{GT_r}{GT_i} \frac{1}{2} \alpha_r^{(2)} \Big[\mathbb{E}_t[\mathrm{Var}_x(E_r)] - \mathrm{Var}_x(\mathbb{E}_t[E_r]) \Big] \\ &= \frac{1}{2} \alpha_i^{(2)} \Big[\mathbb{E}_x[\mathrm{Var}_t(E_i)] - \mathrm{Var}_t(\mathbb{E}_x[E_i]) \Big] \\ &\quad - \frac{1}{S-1} \sum_{r \neq i}^{S} \frac{GT_r}{GT_i} \frac{1}{2} \alpha_r^{(2)} \Big[\mathbb{E}_x[\mathrm{Var}_t(E_r)] - \mathrm{Var}_t(\mathbb{E}_x[E_r]) \Big] \end{aligned} \tag{1.89}$$

Linear density-dependent effects

$$\Delta \rho_i = \beta_i^{(1)} \mathbb{E}_{x,t}[C_i - C_i^*] - \frac{1}{S-1} \sum_{r \neq i}^{S} \frac{GT_r}{GT_i} \beta_r^{(1)} \mathbb{E}_{x,t}[C_r - C_r^*] \tag{1.90}$$

Relative nonlinearity

$$\Delta N_i = \Delta N_{i,S} + \Delta N_{i,T} + \Delta N_{i,R}, \tag{1.91}$$

$$\Delta N_{i,S} = \frac{1}{2}\beta_i^{(2)}\mathrm{Var}_x(\mathbb{E}_t[C_i]) - \frac{1}{S-1}\sum_{r\neq i}^{S}\frac{GT_r}{GT_i}\frac{1}{2}\beta_r^{(2)}\mathrm{Var}_x(\mathbb{E}_t[C_r]) \tag{1.92}$$

$$\Delta N_{i,T} = \frac{1}{2}\left(\beta_i^{(2)} - {\beta_i^{(1)}}^2\right)\mathrm{Var}_t(\mathbb{E}_x[C_i]) - \frac{1}{S-1}\sum_{r\neq i}^{S}\frac{GT_r}{GT_i}\frac{1}{2}\left(\beta_r^{(2)} - {\beta_r^{(1)}}^2\right)\mathrm{Var}_t(\mathbb{E}_x[C_r]) \tag{1.93}$$

$$\begin{aligned}\Delta N_{i,R} &= \frac{1}{2}\beta_i^{(2)}\Big[\mathbb{E}_t[\mathrm{Var}_x(C_i)] - \mathrm{Var}_x(\mathbb{E}_t[C_i])\Big] \\ &\quad - \frac{1}{S-1}\sum_{r\neq i}^{S}\frac{GT_r}{GT_i}\frac{1}{2}\beta_r^{(2)}\Big[\mathbb{E}_t[\mathrm{Var}_x(C_r)] - \mathrm{Var}_x(\mathbb{E}_t[C_r])\Big] \\ &= \frac{1}{2}\beta_i^{(2)}\Big[\mathbb{E}_x[\mathrm{Var}_t(C_i)] - \mathrm{Var}_t(\mathbb{E}_x[C_i])\Big] \\ &\quad - \frac{1}{S-1}\sum_{r\neq i}^{S}\frac{GT_r}{GT_i}\frac{1}{2}\beta_r^{(2)}\Big[\mathbb{E}_x[\mathrm{Var}_t(C_r)] - \mathrm{Var}_t(\mathbb{E}_x[C_r])\Big]\end{aligned} \tag{1.94}$$

The storage effect

$$\Delta I_i = \Delta I_{i,A} + \Delta I_{i,S} + \Delta I_{i,T} + \Delta I_{i,R} \tag{1.95}$$

$$\Delta I_{i,A} = 0 \tag{1.96}$$

$$\Delta I_{i,S} = \zeta_i\mathrm{Cov}_x(\mathbb{E}_t[E_i], \mathbb{E}_t[C_i]) - \frac{1}{S-1}\sum_{r\neq i}^{S}\frac{GT_r}{GT_i}\zeta_r\mathrm{Cov}_x(\mathbb{E}_t[E_r], \mathbb{E}_t[C_r]) \tag{1.97}$$

$$\begin{aligned}\Delta I_{i,T} &= \left(\zeta_i - \alpha_i^{(1)}\beta_i^{(1)}\right)\mathrm{Cov}_t(\mathbb{E}_x[E_i], \mathbb{E}_x[C_i]) \\ &\quad - \frac{1}{S-1}\sum_{r\neq i}^{S}\frac{GT_r}{GT_i}\left(\zeta_r - \alpha_r^{(1)}\beta_r^{(1)}\right)\mathrm{Cov}_t(\mathbb{E}_x[E_r], \mathbb{E}_x[C_r])\end{aligned} \tag{1.98}$$

$$\begin{aligned}\Delta I_{i,R} &= \Big[\zeta_i\left(\mathbb{E}_t[\mathrm{Cov}_x(E_i, C_i)] - \mathrm{Cov}_x(\mathbb{E}_t[E_i], \mathbb{E}_t[C_i])\right)\Big] \\ &\quad - \frac{1}{S-1}\sum_{r\neq i}^{S}\frac{GT_r}{GT_i}\Big[\zeta_r\left(\mathbb{E}_t[\mathrm{Cov}_x(E_r, C_r)] - \mathrm{Cov}_x(\mathbb{E}_t[E_r], \mathbb{E}_t[C_r])\right)\Big] \\ &= \Big[\zeta_i\left(\mathbb{E}_x[\mathrm{Cov}_t(E_i, C_i)] - \mathrm{Cov}_t(\mathbb{E}_x[E_i], \mathbb{E}_x[C_i])\right)\Big] \\ &\quad - \frac{1}{S-1}\sum_{r\neq i}^{S}\frac{GT_r}{GT_i}\Big[\zeta_r\left(\mathbb{E}_x[\mathrm{Cov}_t(E_r, C_r)] - \mathrm{Cov}_t(\mathbb{E}_x[E_r], \mathbb{E}_x[C_r])\right)\Big]\end{aligned} \tag{1.99}$$

Fitness-density covariance

$$\Delta\kappa_i = \Delta\kappa_{i,A} + \Delta\kappa_{i,S} + \Delta\kappa_{i,T} + \Delta\kappa_{i,R} \tag{1.100}$$

$$\Delta\kappa_{i,A} = 0 \tag{1.101}$$

$$\Delta\kappa_{i,S} = \mathrm{Cov}_x\Big(\mathbb{E}_t[\nu_i], \alpha_i^{(1)}\mathbb{E}_t[E_i] + \beta_i^{(1)}\mathbb{E}_t[C_i]\Big) \tag{1.102}$$
$$- \frac{1}{S-1}\sum_{r\neq i}^{S}\frac{GT_r}{GT_i}\mathrm{Cov}_x\Big(\mathbb{E}_t[\nu_r], \alpha_r^{(1)}\mathbb{E}_t[E_r] + \beta_r^{(1)}\mathbb{E}_t[C_r]\Big)$$

$$\Delta\kappa_{i,T} = 0 \tag{1.103}$$

$$\Delta\kappa_{i,R} = \mathbb{E}_t\Big[\mathrm{Cov}_x\Big(\nu_i, \alpha_i^{(1)}E_i + \beta_i^{(1)}C_i\Big)\Big] - \mathrm{Cov}_x\Big(\mathbb{E}_t[\nu_i], \alpha_i^{(1)}\mathbb{E}_t[E_i] + \beta_i^{(1)}\mathbb{E}_t[C_i]\Big) \tag{1.104}$$
$$- \frac{1}{S-1}\sum_{r\neq i}^{S}\frac{GT_r}{GT_i}\Bigg(\mathbb{E}_t\Big[\mathrm{Cov}_x\Big(\nu_r, \alpha_r^{(1)}E_r + \beta_r^{(1)}C_r\Big)\Big]$$
$$- \mathrm{Cov}_x\Big(\mathbb{E}_t[\nu_r], \alpha_r^{(1)}\mathbb{E}_t[E_r] + \beta_r^{(1)}\mathbb{E}_t[C_r]\Big)\Bigg)$$
$$= \mathbb{E}_x\Big[\mathrm{Cov}_t\Big(\nu_i, \alpha_i^{(1)}E_i + \beta_i^{(1)}C_i\Big)\Big] - \mathrm{Cov}_t\Big(\mathbb{E}_x[\nu_i], \alpha_i^{(1)}\mathbb{E}_x[E_i] + \beta_i^{(1)}\mathbb{E}_x[C_i]\Big)$$
$$- \frac{1}{S-1}\sum_{r\neq i}^{S}\frac{GT_r}{GT_i}\Bigg(\mathbb{E}_x\Big[\mathrm{Cov}_t\Big(\nu_r, \alpha_r^{(1)}E_r + \beta_r^{(1)}C_r\Big)\Big]$$
$$- \mathrm{Cov}_t\Big(\mathbb{E}_x[\nu_r], \alpha_r^{(1)}\mathbb{E}_x[E_r] + \beta_r^{(1)}\mathbb{E}_x[C_r]\Big)\Bigg)$$

1.2.3.5 The space-time decomposition of exact coexistence mechanisms

In this section, we will describe how the space-time decomposition of the exact coexistence mechanisms can be computed using data from simulations. Our exposition is focused on the storage effect because it is the most difficult exact coexistence mechanism to quantify.

Ellner et al. (2016) showed how simulations could be used to calculate the exact temporal storage in a model with only temporal variation. Their procedure can be naturally extended to models with spatiotemporal variation:

1. Simulate the model. For each species, record a matrix of $E_j(x,t)$'s and a matrix of $C_j(x,t)$'s with each row corresponding to a location in space, and each column corresponding to a point in time. Call these matrices E_j and C_j.

2. For each species, shuffle the elements of E_j. That is, fill in a matrix with equivalent dimensions by randomly sampling without replacement from the flattened E_j. Call this new matrix $E_j^{\#}$. Shuffling (i.e.,

randomly sampling without replacement, or permuting) destroys the covariance between environment and competition (as well as any higher order mixed moments) that is integral to the storage effect.

3. For each species, estimate the interaction effect as $\overline{\mathscr{I}_j} = \mathbb{E}_t\left[\log(\mathbb{E}_x[g_j(E_j, C_j)])\right] - \mathbb{E}_t\left[\log\left(\mathbb{E}_x\left[g_j(E_j^{\#}, C_j)\right]\right)\right]$. Note here that we are averaging finite rates of increase across patches instead of individuals. This ensures that our estimate of $\Delta I_i^{(e)}$ does not include any bit of growth rate that can be attributed to the fitness-density covariance, $\Delta\kappa_i$.

4. Calculate the exact storage effect as $\Delta I_i^{(e)} = \overline{\mathscr{I}_i} - \sum_{r\neq i}^{S} \frac{GT_r}{GT_i}\overline{\mathscr{I}_r}$.

Ellner et al.'s (2016) critical idea — shuffling an archive of environmental parameters — can also be utilized to calculate the space-time decomposition of the exact storage effect. To illustrate, we will discuss how one may calculate the space component of the precursor to the exact storage effect: $\mathscr{I}_{j,S}$. To measure the causal effect of spatial covariation, we must compare a hypothetical world with only spatial variation to a (reference) hypothetical world with only spatial variation and no EC covariation. We obtain the hypothetical world with only spatial variation by squashing temporal variation, i.e., by setting $E_j(x,t)$ to $\mathbb{E}_t[E_j]$ and setting $C_j(x,t)$ to $\mathbb{E}_t\left[C_j\right]$. This produces the growth rate $\log(\mathbb{E}_x[g_j(\mathbb{E}_t[E_j]\,, \mathbb{E}_t[C_j])])$. We obtain the hypothetical world with no temporal variation and no spatial covariation by squashing temporal variation just as we did before, and then shuffling the vector of $\mathbb{E}_t[E_j]$. This produces the growth rate $\log\left(\mathbb{E}_x\left[g_j(\mathbb{E}_t[E_j]^{\#}\,, \mathbb{E}_t[C_j])\right]\right)$. The effects of spatial covariation (and higher order mixed moments) on species j's average growth rate is simply the difference between the growth rates corresponding to the two hypothetical worlds. Put into symbols, we say that $\overline{\mathscr{I}}_{j,S} = \log(\mathbb{E}_x[g_j(\mathbb{E}_t[E_j]\,, \mathbb{E}_t[C_j])]) - \log\left(\mathbb{E}_x\left[g_j(\mathbb{E}_t[E_j]^{\#}\,, \mathbb{E}_t[C_j])\right]\right)$.

Instead of writing out steps for quantifying every space-time component of every exact coexistence mechanism, we will provide formulas that indicate how simulated data are to be used. Of notable importance to the storage effect is the previously introduced shuffle operator, denoted by the superscript #, which indicates that the elements of a matrix or vector are to be shuffled, i.e., randomly sampled without replacement.

Note that $\overline{\mathscr{I}}_{j,A}$, the precursor to the "Average" component of the storage effect, is not necessarily zero (as it was in the analogous small-noise expression) though it should be small in the limit of small-noise. Unlike $\overline{\mathscr{E}}_{j,A}$ and $\overline{\mathscr{C}}_{j,A}$, which could reasonably be called the effect of the average environment and average competition (respectively), $\overline{\mathscr{I}}_{j,A}$ has no good interpretation — it is the effect of setting the environment and competition parameters to their spatiotemporal averages, which is simply a textual reiteration of the mathematical definition.

Formulas for space-time decomposition of exact coexistence mechanisms

Density-independent effects

$$\Delta E_i{}^{(e)} = \Delta E_{i,A}{}^{(e)} + \Delta E_{i,S}{}^{(e)} + \Delta E_{i,T}{}^{(e)} + \Delta E_{i,R}{}^{(e)} \tag{1.105}$$

$$\Delta E_{i,A}{}^{(e)} = \overline{\mathscr{E}}_{i,A} - \frac{1}{S-1}\sum_{r\neq i}^{S}\frac{GT_r}{GT_i}\overline{\mathscr{E}}_{r,A} \tag{1.106}$$

$$\Delta E_{i,S}{}^{(e)} = \overline{\mathscr{E}}_{i,S} - \frac{1}{S-1}\sum_{r\neq i}^{S}\frac{GT_r}{GT_i}\overline{\mathscr{E}}_{r,S} \tag{1.107}$$

$$\Delta E_{i,T}{}^{(e)} = \overline{\mathscr{E}}_{i,T} - \frac{1}{S-1}\sum_{r\neq i}^{S}\frac{GT_r}{GT_i}\overline{\mathscr{E}}_{r,T} \tag{1.108}$$

$$\Delta E_{i,R}{}^{(e)} = \overline{\mathscr{E}}_{i,R} - \frac{1}{S-1}\sum_{r\neq i}^{S}\frac{GT_r}{GT_i}\overline{\mathscr{E}}_{r,R} \tag{1.109}$$

$$\overline{\mathscr{E}}_j = \mathbb{E}_t\big[\log\big(\mathbb{E}_x\big[g_j(E_j, C_j^*)\big]\big)\big] \tag{1.110}$$

$$\overline{\mathscr{E}}_{j,A} = \log\big(g_j(\mathbb{E}_{x,t}[E_j], C_j^*)\big) \tag{1.111}$$

$$\overline{\mathscr{E}}_{j,S} = \log\big(\mathbb{E}_x\big[g_j(\mathbb{E}_t[E_j], C_j^*)\big]\big) - \overline{\mathscr{E}}_{j,A} \tag{1.112}$$

$$\overline{\mathscr{E}}_{j,T} = \mathbb{E}_t\big[\log\big(g_j(\mathbb{E}_x[E_j], C_j^*)\big)\big] - \overline{\mathscr{E}}_{j,A} \tag{1.113}$$

$$\overline{\mathscr{E}}_{j,R} = \overline{\mathscr{E}}_j - \big(\overline{\mathscr{E}}_{j,A} + \overline{\mathscr{E}}_{j,S} + \overline{\mathscr{E}}_{j,T}\big) \tag{1.114}$$

Linear density-dependent effects

$$\Delta\rho_i{}^{(e)} = \overline{\mathscr{C}}_{i,A} - \frac{1}{S-1}\sum_{r\neq i}^{S}\frac{GT_r}{GT_i}\overline{\mathscr{C}}_{r,A} \tag{1.115}$$

$$\overline{\mathscr{C}}_{j,A} = \log(g_i(E_i^*, \mathbb{E}_{x,t}[C_i])) \tag{1.116}$$

Relative nonlinearity

$$\Delta N_i{}^{(e)} = \Delta N_{i,S}{}^{(e)} + \Delta N_{i,T}{}^{(e)} + \Delta N_{i,R}{}^{(e)}, \tag{1.117}$$

$$\Delta N_{i,S}{}^{(e)} = \overline{\mathscr{C}}_{i,S} - \frac{1}{S-1}\sum_{r\neq i}^{S}\frac{GT_r}{GT_i}\overline{\mathscr{C}}_{r,S} \tag{1.118}$$

$$\Delta N_{i,T}{}^{(e)} = \overline{\mathscr{C}}_{i,T} - \frac{1}{S-1}\sum_{r\neq i}^{S}\frac{GT_r}{GT_i}\overline{\mathscr{C}}_{r,T} \tag{1.119}$$

$$\Delta N_{i,R}{}^{(e)} = \overline{\mathscr{C}}_{i,R} - \frac{1}{S-1}\sum_{r\neq i}^{S}\frac{GT_r}{GT_i}\overline{\mathscr{C}}_{r,R} \tag{1.120}$$

$$\overline{\mathscr{C}}_{j} = \mathbb{E}_t\big[\log\big(\mathbb{E}_x\big[g_j(E_j^*, C_j)\big]\big)\big] \tag{1.121}$$

$$\overline{\mathscr{C}}_{j,A} = \log\big(g_j(E_j^*, \mathbb{E}_{x,t}[C_j])\big) \tag{1.122}$$

$$\overline{\mathscr{C}}_{j,S} = \log\big(\mathbb{E}_x\big[g_j(E_j^*, \mathbb{E}_t[C_j])\big]\big) - \overline{\mathscr{C}}_{j,A} \tag{1.123}$$

$$\overline{\mathscr{C}}_{j,T} = \mathbb{E}_t\big[\log\big(g_j(E_j^*, \mathbb{E}_x[C_j])\big)\big] - \overline{\mathscr{C}}_{j,A} \tag{1.124}$$

$$\overline{\mathscr{C}}_{j,R} = \overline{\mathscr{C}}_{j} - \big(\overline{\mathscr{C}}_{j,A} + \overline{\mathscr{C}}_{j,S} + \overline{\mathscr{C}}_{j,T}\big) \tag{1.125}$$

The storage effect

$$\Delta I_i{}^{(e)} = \Delta I_{i,A}{}^{(e)} + \Delta I_{i,S}{}^{(e)} + \Delta I_{i,T}{}^{(e)} + \Delta I_{i,R}{}^{(e)}, \tag{1.126}$$

$$\Delta I_{i,A}{}^{(e)} = \overline{\mathscr{I}}_{i,A} - \frac{1}{S-1}\sum_{r\neq i}^{S}\frac{GT_r}{GT_i}\overline{\mathscr{I}}_{r,A} \tag{1.127}$$

$$\Delta I_{i,S}{}^{(e)} = \overline{\mathscr{I}}_{i,S} - \frac{1}{S-1}\sum_{r\neq i}^{S}\frac{GT_r}{GT_i}\overline{\mathscr{I}}_{r,S} \tag{1.128}$$

$$\Delta I_{i,T}{}^{(e)} = \overline{\mathscr{I}}_{i,T} - \frac{1}{S-1}\sum_{r\neq i}^{S}\frac{GT_r}{GT_i}\overline{\mathscr{I}}_{r,T} \tag{1.129}$$

$$\Delta I_{i,R}{}^{(e)} = \overline{\mathscr{I}}_{i,R} - \frac{1}{S-1}\sum_{r\neq i}^{S}\frac{GT_r}{GT_i}\overline{\mathscr{I}}_{r,R} \tag{1.130}$$

$$\overline{\mathscr{I}}_j = \mathbb{E}_t[\log(\mathbb{E}_x[g_j(E_j, C_j)])] - \left(\overline{\mathscr{E}}_j + \overline{\mathscr{C}}_j\right) \tag{1.131}$$

$$\approx \mathbb{E}_t[\log(\mathbb{E}_x[g_j(E_j, C_j)])] - \mathbb{E}_t\Big[\log\Big(\mathbb{E}_x\Big[g_j(E_j^{\#}, C_j)\Big]\Big)\Big] \tag{1.132}$$

$$\overline{\mathscr{I}}_{j,A} = \log(g_j(\mathbb{E}_{x,t}[E_j], \mathbb{E}_{x,t}[C_j])) - \left(\overline{\mathscr{E}}_{j,A} + \overline{\mathscr{C}}_{j,A}\right) \tag{1.133}$$

$$\overline{\mathscr{I}}_{j,S} = \log(\mathbb{E}_x[g_j(\mathbb{E}_t[E_j], \mathbb{E}_t[C_j])]) - \log\Big(\mathbb{E}_x\Big[g_j(\mathbb{E}_t[E_j]^{\#}, \mathbb{E}_t[C_j])\Big]\Big) \tag{1.134}$$

$$\overline{\mathscr{I}}_{j,T} = \mathbb{E}_t[\log(g_j(\mathbb{E}_x[E_j], \mathbb{E}_x[C_j]))] - \mathbb{E}_t\Big[\log\Big(g_j(\mathbb{E}_x[E_j]^{\#}, \mathbb{E}_x[C_j])\Big)\Big] \tag{1.135}$$

$$\overline{\mathscr{I}}_{j,R} = \overline{\mathscr{I}}_j - \left(\overline{\mathscr{I}}_{j,A} + \overline{\mathscr{I}}_{j,S} + \overline{\mathscr{I}}_{j,T}\right) \tag{1.136}$$

Fitness-density covariance

$$\Delta\kappa_i{}^{(e)} = \Delta\kappa_{i,A}{}^{(e)} + \Delta\kappa_{i,S}{}^{(e)} + \Delta\kappa_{i,T}{}^{(e)} + \Delta\kappa_{i,R}{}^{(e)}, \tag{1.137}$$

$$\Delta\kappa_{i,A}{}^{(e)} = \overline{\mathscr{K}}_{i,A} - \frac{1}{S-1}\sum_{r\neq i}^{S}\frac{GT_r}{GT_i}\overline{\mathscr{K}}_{r,A} = 0 \tag{1.138}$$

$$\Delta\kappa_{i,S}{}^{(e)} = \overline{\mathscr{K}}_{i,S} - \frac{1}{S-1}\sum_{r\neq i}^{S}\frac{GT_r}{GT_i}\overline{\mathscr{K}}_{r,S} \tag{1.139}$$

$$\Delta\kappa_{i,T}{}^{(e)} = \overline{\mathscr{K}}_{i,T} - \frac{1}{S-1}\sum_{r\neq i}^{S}\frac{GT_r}{GT_i}\overline{\mathscr{K}}_{r,T} = 0 \tag{1.140}$$

$$\Delta\kappa_{i,R}{}^{(e)} = \overline{\mathscr{K}}_{i,R} - \frac{1}{S-1}\sum_{r\neq i}^{S}\frac{GT_r}{GT_i}\overline{\mathscr{K}}_{r,R} \tag{1.141}$$

$$\overline{\mathscr{K}}_j = \mathbb{E}_t[\log(\mathbb{E}_x[\nu_j\ g_j(E_j, C_j)])] - \mathbb{E}_t[\log(\mathbb{E}_x[g_j(E_j, C_j)])] \tag{1.142}$$

$$\overline{\mathscr{K}}_{j,A} = 0 \tag{1.143}$$

$$\overline{\mathscr{K}}_{j,S} = \log(\mathbb{E}_x[\mathbb{E}_t[\nu_j]\, g_j(\mathbb{E}_t[E_j], \mathbb{E}_t[C_j])]) - \log(\mathbb{E}_x[g_j(\mathbb{E}_t[E_j], \mathbb{E}_t[C_j])]) \tag{1.144}$$

$$\overline{\mathscr{K}}_{j,T} = 0 \tag{1.145}$$

$$\overline{\mathscr{K}}_{j,R} = \overline{\mathscr{K}}_j - \left(\overline{\mathscr{K}}_{j,A} + \overline{\mathscr{K}}_{j,S} + \overline{\mathscr{K}}_{j,T}\right) \tag{1.146}$$

1.2.4 Computational tricks for measuring invasion growth rates

We have given formulas for computing coexistence mechanisms, but the components of the those formulas (E_j and C_j) must be measured in a specific context. Specifically, the invasion growth rate and coexistence mechanisms must be measured in the context where 1) the invader's environment (which includes the resident species) has attained its limiting dynamics, and 2) the invader has attained its quasi-steady spatial distribution.

Here, "the invader's environment" does not refer to the environmental parameter E_i, but rather all variables that influence the invader's per capita growth rate (e.g., resident densities, resources, temperature). Previous expositions of MCT required that the invader's environment be an ergodic stationary stochastic process (Chesson, 1994, p. 236). This assumption is convenient because ergodicity implies that initial conditions are irrelevant, and stationarity allows the long-term average (inherent in the invasion growth rate) to be replaced with the expectation over the stationary distribution of the state of the invader's environment; as we will see, there are several well-established tricks for calculating stationary distributions. However, requiring a stationary distribution excludes any models where parameters change over time, including models with seasonality and models that track weather patterns. Instead, we only a require that the invader's environment has a unique, asymptotic, time-average distribution (Glynn and Sigman, 1998). This requirement technically excludes models with unidirectional environmental change, but we discuss several work-arounds in Section 1.2.6.

In many ecological models, the time-average distribution of invader's environment is a *stationary distribution* (Nisbet and C., 1982). In homogeneous (i.e., time-invariant) Markov chain models with a finite number of states, the stationary distribution can be computed as the dominant eigenvector of the *transition probability matrix* or the *generator matrix* (the terminology changes depending on whether the model is in discrete time or continuous time; Allen, 2010, p. 67). When the state space is the natural numbers (i.e., there are a countable but infinite number of states), one may approximate the stationary distribution as the dominant eigenvector of a truncated transition probability matrix (or generator matrix) where rows and columns corresponding to states of improbably high abundance have been removed (e.g., Allen, 2010, p. 107). Alternatively, one may obtain an approximate stationary distribution using the Wentzel–Kramers–Brillouin (WKB) approximation (Assaf and Meerson, 2010; Pande and Shnerb, 2020). For models that take the form of stochastic differential equations, the stationary distribution can be obtained by solving a second order differential equation (Karlin and Taylor, 1981, ch. 15.3). Alternatively, one may obtain an approximate stationary distribution by finding the minimum action of a path integral (Chow and Buice, 2015; Kamenev et al., 2008). However, because the volume of state space (of joint abundances/densities) increases exponentially

with the number of species, the computation time for all the aforementioned methods scales exponentially with the number of species under consideration.

For models with many species, or models where the notion of *stationarity* is not appropriate, one may have to take a brute-force approach: simulate a model forward in time, recording the frequency distribution of different states after a sufficiently long burn-in period. To determine the length of the burn-in period, one may simply "eye-ball" a time series plot, perhaps selecting 2 $\times$ the time it takes for the residents to attain typical densities. When one must obtain the time-average distribution for many different parameter combinations, the "eye-ball" approach becomes impractical. Instead, one can employ heuristic tests for determining the length of the burn-in period (for examples, see Caswell and Etter, 1993; Hiebeler and Millett, 2011).

MCT assumes that all populations have infinite population sizes; otherwise, the invader could go extinct before it experiences a representative collection of environmental states, in which case the invasion growth rate would depend on the initial conditions of the invader's environment. Because the resident species can also go extinct in finite-population models, the concept of the stationary distribution can be replaced with the quasi-stationary distribution (QSD): the distribution of resident densities conditioned on non-extinction. In single-resident birth-death models, there is iterative numerical procedure for finding the quasi-stationary distribution (Nisbet and C., 1982, p. 183–184). Unlike the stationary distribution, the QSD cannot be computed with naive simulation. The problem is that a simulation must run for a long time in order for the frequency distribution to converge, but the longer the simulation, the more likely extinction is. One solution is the Fleming-Voit method (Ferrari and Maric, 2007; Blanchet et al., 2016), where a number of simulations are run in parallel so that extinct simulations can be restarted with initial conditions equal to the state of one of the other simulations. A similar method restarts extinct simulations by drawing randomly from an archive of past states (Groisman and Jonckheere, 2012).

To avoid simulations, one may *approximate* the QSD by analyzing an auxiliary model. This auxiliary model is exactly like the original model, except either 1) each transition from a non-zero state to the zero state (i.e., extinction), has probability equal to zero (Pielou, 1969, p. 27; Allen, 2010, p. 127), or 2) one individual is immortal for all time (Weiss and Dishon, 1971; Norden, 1982). The stationary distribution of the auxiliary model (computed using the methods in the previous paragraphs) is an approximation of the quasi-stationary distribution of the original model. The auxiliary model #1 leads to better results for populations with long mean extinction times, whereas the auxiliary model #2 leads to better results for populations with short mean extinction times (Nåsell, 2001; Kryscio and Lefévre, 1989).

A unique challenge in spatiotemporal models (with either infinite or finite populations) is determining the *quasi-steady spatial distribution* of the invader, not to be confused with the previously discussed quasi-

stationary distribution of resident densities. To accurately measure the invasion growth rate, one must inoculate the invader and then wait until it has attained its natural spatial distribution, which we might technically define as a second-order stationary and isotropic process (Cressie, 2015). However, the longer one waits for the invader to attain this distribution, the larger the invader population becomes (assuming a positive invasion growth rate and barring stochastic extinction), leading to inaccurate measurements of the invasion growth rate. One hopes that the dynamics of spatial correlations operate on a much faster timescale than the dynamics of total density, such that a quasi-steady spatial distribution of invader density is attained long before the total density changes too much. The requisite time-scale separation can be verified by plotting spatial correlations against total density (as in Le Galliard et al., 2003, Fig. 7). Analytical expressions for the quasi-steady distribution are only available in simple spatially implicit models (see Appendix 1.2.D for a worked example) or in simple spatially explicit models with the help of *pair approximation* (Ferrière and Galliard, 2001).

In more complex models, simulation experiments are needed to compute the quasi-steady spatial distribution of the invader. After virtually inoculating the invader species and waiting through a sufficiently long burn-in period, one can begin measuring the invasion growth rate. If the regional invader population density exceeds a user-specified ceiling (i.e., the invader becomes common), then the simulation can be restarted. Indeed, this general strategy can be used to compute other kinds of quasi-steady distributions, such as the invader's stable-age distribution. In finite population models, the invader may go extinct. To circumvent this problem, one may apply the previously discussed Fleming-Voit method (Ferrari and Maric, 2007; Blanchet et al., 2016).

1.2.5 Example: the spatiotemporal lottery model

To give readers a sense of how Spatiotemporal MCT may be used in practice, we analyze the lottery model (Chesson and Warner, 1981; Chesson, 1994) with spatiotemporal fluctuations. The lottery model is one of the simplest models that features fluctuation-dependent coexistence mechanisms, and has thus become a canonical model in theoretical ecology. We derive analytical expressions for the special case of two species with similar demographic parameters (Eq.1.151–Eq.1.166). Additionally, we compute exact coexistence mechanisms in a three-species system with dissimilar parameters (Fig. 1.3).

Imagine several fish species inhabiting territories on a coral reef. During each time-step, an individual of species j produces $\xi_j(x,t)$ larvae; per capita larval production fluctuates over space and time. The remaining life history is very simple. Adult fish die with the density-independent probability δ_j. Within a single patch, the larvae inherit the empty territories with a per-larva recruitment probability equal to the number of empty

sites, divided by the total number of larvae. The remaining larvae perish. Note that "empty territories" and "total larvae" here are patch-specific quantities; so far, we have only described local population dynamics. The uniform per-larva probability of recruitment explains the lottery model's name (Sale, 1977).

If there are S species, the local dynamics of the lottery model can be encoded in a S-dimensional difference equation:

$$\lambda_j(x,t) = \overbrace{1-\delta_j}^{\text{survival prob.}} + \overbrace{\xi_j(x,t)}^{\text{per capita fecundity}} \left[\frac{\overbrace{\sum_{j\neq i}^{S} \delta_j n_j(x,t)}^{\text{open territories}}}{\underbrace{\sum_{j\neq i}^{S} \xi_j(x,t) n_j(x,t)}_{\text{total larvae}}} \right], \tag{1.147}$$

Selecting $E_j = \log(\xi_j)$ and $C = \log\left(\frac{\sum_{j\neq i}^{S} \xi_j n_j}{\sum_{j\neq i}^{S} \delta_j n_j}\right)$, the local finite rate of increase takes the simple form,

$$g_j(E_j(x,t), C_j(x,t)) = 1 - \delta_j + \exp\{E_j(x,t) - C(x,t)\}. \tag{1.148}$$

Both species share the same equilibrium competition parameter, $C^* = \frac{1}{S}\sum_{i=1}^{S} \mathbb{E}_{x,t}[C_i]$, which is the average competition experienced by the invader, averaged over all species acting as the invader. This equilibrium competition parameter fixes the species-specific equilibrium environmental parameter at $E_j^* = \log(\delta_j) + C^*$. With the equilibrium parameters in hand, we can now compute the Taylor series coefficients for the small-noise coexistence mechanisms: we find that $\alpha_j^{(1)} = \delta_j$, $\beta_j^{(1)} = -\delta_j$, $\alpha_j^{(2)} = \delta_j$, $\beta_j^{(2)} = \delta_j$, $\zeta_j = -\delta_j$. The generation time quotients (see Section 1.2.3.2) are $GT_r/GT_i = \delta_i/\delta_r$.

In the second segment of each time-step, after local growth occurs, a fraction of individuals, q_j, are retained at site x while the $1-q_j$ fraction of dispersing individuals are distributed evenly across all K patches. This particular form of dispersal dynamics, which we may call *local retention with global dispersal*, is easy to simulate and is analytically tractable. The full dynamics of species j can now be written as

$$n_j(x,t+1) = q_j n_j(x,t) g_j(E_j(x,t), C_j(x,t)) + \frac{1-q_j}{K}\sum_{s=1}^{K} n_j(s,t) g_j(E_j(s,t), C_j(s,t)). \tag{1.149}$$

Finally, we must describe the structure of environmental variation. The environmental parameter, $E_j(x,t)$, is the sum of a patch effect $a(x)$, a time effect $b(t)$, and their interaction, which is scaled by the interaction coefficient θ_j:

$$E_j(x,t) = a_j(x) + b_j(t) + \theta_j a_j(x) b_j(t) \tag{1.150}$$

For simplicity, $a_j(x)$ and $b_j(t)$ are independently drawn from normal distributions with standard deviations $\sigma_j^{(x)}$ and $\sigma_j^{(t)}$, respectively. There is no autocorrelation, but there are cross-species correlations: the correlation between $a_j(x)$ and $a_k(x)$ is $\phi_{jk}^{(x)}$, and the correlation between $b_j(t)$ and $b_k(t)$ is $\phi_{jk}^{(t)}$. Under the small-noise assumptions of MCT, the term $\theta_j a_j(x) b_j(t)$ will become negligibly small when squared, and thus the space-time interaction component of the space-time decomposition will be zero. For purely illustrative purposes, we will assume that $\theta_j = \mathcal{O}(\sigma^{-1})$, as this allows us to obtain a non-zero interaction component while still keeping the simple form of Eq.1.150.

We now analyze a particularly simple case of the spatiotemporal lottery model in which two species are similar in many respects. Each species has equal death probabilities δ, equal spatial variances ${\sigma^{(t)}}^2$, equal temporal variances ${\sigma^{(t)}}^2$, equal space-time interaction coefficients θ, and equal retention fractions, q. The two species only differ in how they respond to the environment (i.e., $\phi^{(x)} < 1$, and $\phi^{(t)} < 1$).

Various tricks can be used to simplify the expressions for the small-noise coexistence mechanisms. In order to calculate the variance and covariance terms inherent the in small-noise coexistence mechanisms, the competition parameter can be expressed in terms of the environmental parameter, by 1) Taylor-series expanding competition with respect to the E_j and n_j, 2) substituting the expansions into the covariance terms and truncating at first order in accordance with the small-noise assumptions, 3) recognizing that $\text{Cov}\,(E_j, n_j) = 0$ due to the absence of spatial or temporal autocorrelation, and 4) recognizing that $\text{Var}\,(n_r) = 0$ in the case of two species, since n_r is fixed at 1. To compute fitness-density covariance, $\Delta\kappa$, we must first calculate the quasi-steady spatial distribution of the invader (see Section 1.2.4). In Appendix 1.2.D, we derive an approximation of this distribution using perturbation theory, recursion, and the geometric series.

Small-noise coexistence mechanisms in the spatiotemporal lottery model: two symmetric species with diffuse competition

Density-independent effects

$$\Delta E_i = 0 \tag{1.151}$$

$$\Delta E_{i,A} = 0 \tag{1.152}$$

$$\Delta E_{i,S} = 0 \tag{1.153}$$

$$\Delta E_{i,T} = 0 \tag{1.154}$$

$$\Delta Ei, R = 0 \tag{1.155}$$

Linear density-dependent effects

$$\Delta\rho_i = 0 \tag{1.156}$$

Relative nonlinearity

$$\Delta N_i = 0 \tag{1.157}$$

$$\Delta N_{i,S} = 0 \tag{1.158}$$

$$\Delta N_{i,T} = 0 \tag{1.159}$$

$$\Delta N_{i,R} = 0 \tag{1.160}$$

The storage effect

$$\Delta I_i = \delta_i \left[{\sigma^{(x)}}^2 \left(1 - \phi_{ir}^{(x)}\right) + {\sigma^{(t)}}^2 \left[\left(\delta_i - 1\right) \phi_{ir}^{(x)} - \left(\delta_r - 1\right) \right] + \theta^2 {\sigma^{(x)}}^2 {\sigma^{(t)}}^2 \left(1 - \phi_{ir}^{(x)} \phi_{ir}^{(t)}\right) \right] \tag{1.161}$$

$$\Delta I_{i,A} = 0 \tag{1.162}$$

$$\Delta I_{i,S} = \delta {\sigma^{(x)}}^2 \left(1 - \phi_{ir}^{(x)}\right) \tag{1.163}$$

$$\Delta I_{i,T} = \delta \left(1 - \delta\right) {\sigma^{(t)}}^2 \left(1 - \phi_{ir}^{(t)}\right) \tag{1.164}$$

$$\Delta I_{i,R} = \delta \theta^2 {\sigma^{(x)}}^2 {\sigma^{(t)}}^2 \left(1 - \phi_{ir}^{(x)} \phi_{ir}^{(t)}\right) \tag{1.165}$$

Fitness-density covariance

$$\Delta\kappa_i = \frac{2q\delta^2 {\sigma^{(x)}}^2}{1 - q} \left[\theta^2 {\sigma^{(t)}}^2 \left(1 - \phi_{ir}^{(x)} \phi_{ir}^{(t)}\right) + \left(1 - \phi_{ir}^{(x)}\right) \right] \tag{1.166}$$

$$\Delta\kappa_{i,A} = 0 \tag{1.167}$$

$$\Delta\kappa_{i,S} = \frac{2q}{1-q}\left(\delta\sigma^{(x)}\right)^2\left(1-\phi_{ir}^{(x)}\right) \tag{1.168}$$

$$\Delta\kappa_{i,T} = 0 \tag{1.169}$$

$$\Delta\kappa_{i,R} = \frac{2q}{1-q}\left(\delta\theta\sigma^{(x)}\sigma^{(t)}\right)^2\left(1-\phi_{ir}^{(x)}\phi_{ir}^{(t)}\right) \tag{1.170}$$

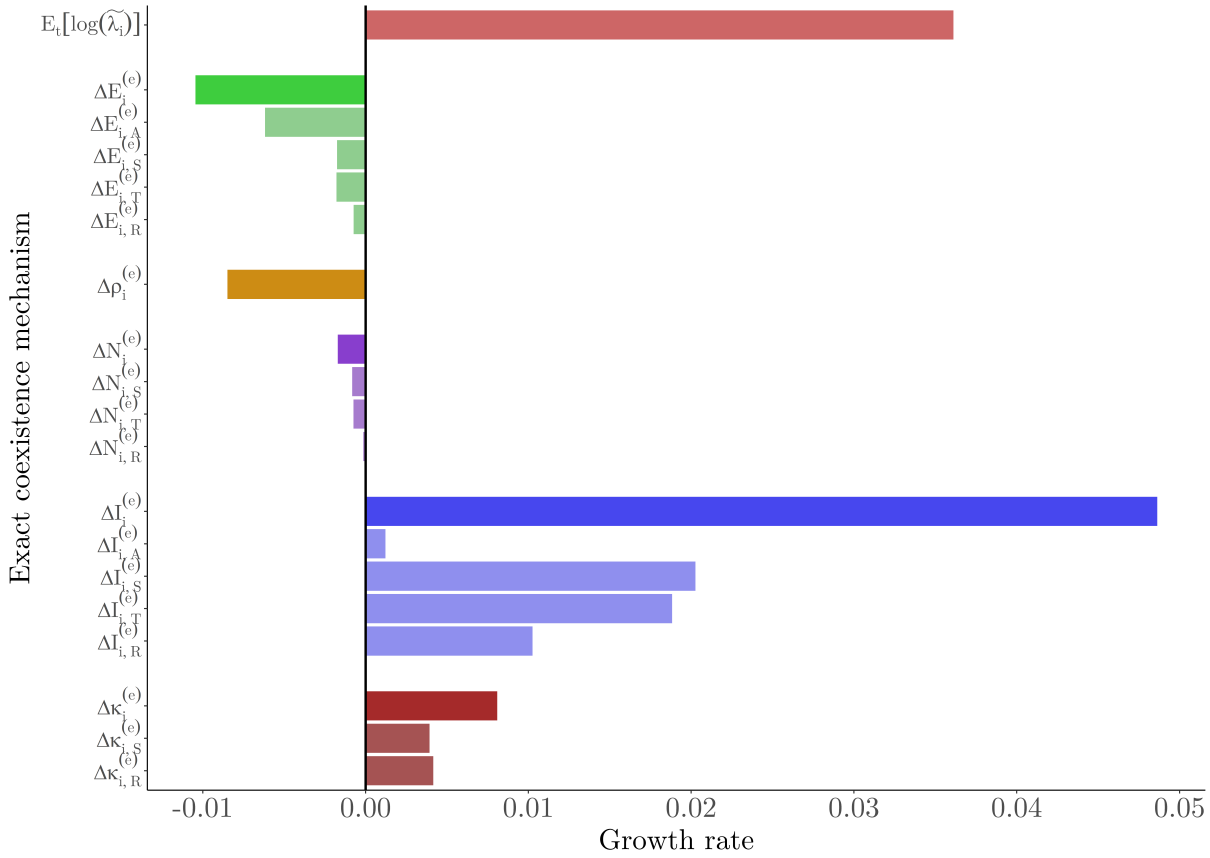

Figure 1.3: Values of exact coexistence mechanisms in the spatiotemporal lottery model with 3 species. The mechanisms are color coded, with the components of the space-time decomposition taking a lighter hue. Coexistence can be attributed to the storage effect and fitness-density covariance. Parameter values and code can be found in `lottery_model_example.R` at https://github.com/ejohnson6767/spatiotemporal_coexistence.

We first use the small-noise coexistence mechanisms above to look at edge cases where there is no spatial or temporal variation. When there is no spatial variation (i.e., $\sigma^{(x)} = 0$), the lottery model analyzed in this section collapses to the temporal lottery model of Chesson (1994). The entire invasion growth rate is $\delta(1-\delta)\left(\sigma^{(t)}\right)^2(1-\phi^{(t)})$, which transparently shows that stable coexistence is not possible if species'

responses to the environment are perfectly correlated (i.e., if $\phi^{(t)} = 1$), or if generations are non-overlapping (i.e., if $\delta = 1$). This latter result speaks to the storage effect's namesake: coexistence "... relies on such buffering effects of persistent stages..." (Chesson, 2003).

When there is no temporal variation and we assume no local retention (i.e., $\sigma^{(t)} = 0$ and $q = 0$), our lottery model collapses to the spatial lottery model of Chesson (2000). In this case, the invasion growth rate is $\delta \left(\sigma^{(x)}\right)^2 \left(1 - \phi^{(x)}\right)$, which demonstrates that the spatial storage effect can promote coexistence in the face of non-overlapping generations.

Finally, we consider the spatiotemporal lottery model. The invasion growth rate, minus fitness-density covariance and any space-time interaction terms is $\Delta I_{i,T} + \Delta I_{i,S} = \delta {\sigma^{(t)}}^2 (1 - \delta) \left(1 - \phi^{(t)}\right) + \delta {\sigma^{(x)}}^2 \left(1 - \phi^{(x)}\right)$, the sum of invasion growth rates in the purely-temporal-variation case and the only-spatial-variation case. This quantity shows us that while spatial and temporal variation both tend to promote coexistence, they do not do so symmetrically. Specifically, compared to spatial variation, temporal variation is discounted by a factor of $(1 - \delta)$. This discrepancy can be explained by the tendency of temporal variation to decrease the geometric mean of λ_j (Lewontin and Cohen, 1969).

Next, consider the sum of all space-time interaction terms from the space-time decomposition, which is equal to $\delta\theta^2(1 - \phi^{(x)}\phi^{(t)}) \left(\sigma^{(x)}\sigma^{(t)}\right)^2$. Both this quantity and the small-noise fitness density covariance (Eq.1.166) reveal that even when generations are overlapping and responses to time-effects are perfectly correlated across species (i.e., $\phi^{(t)} = 1$), temporal variation can still promote coexistence by effectively amplifying species-specific responses to spatial variation, with strength according to the interaction coefficient θ. Note, however, that this result is a consequence of the assumption that the interaction between spatial and temporal variation, θ, is large (to counteract the fact that $\sigma^{(x)}\sigma^{(t)}$ is very small). Also note that when both species respond identically to patch effect and time effects, the space-time interaction terms disappear, confirming the perennial fact that niche differences are required for stable coexistence.

When we consider the general case of multiple residents and asymmetric demographic parameters, the small-noise coexistence mechanisms become more complicated. However, plotting the exact coexistence mechanisms (Fig. 1.3) corroborates the idea that coexistence in the lottery model is achieved via the storage effect and fitness-density covariance. In empirical applications of MCT, *Coefficient plots* (such as Fig. 1.3) should always include error bars representing parameter uncertainty, and potentially model uncertainty, propagated through to the level of coexistence mechanisms.

Here we have examined the space-time decomposition of coexistence mechanisms. In general, there are many ways to partition the invasion growth rate, each potentially leading to ecological insights. One may wish to aggregate terms in various ways, e.g., all space terms, all terms containing partial derivatives of C (i.e., both $\Delta\rho_i$ and ΔN_i). Conversely, the invasion growth rate partition can be made even more fine-grained.

Ellner et al. (2019) decomposed ΔE_i into multiple terms, and partitioned the invasion growth rates with respect to trait values (as opposed to E and C). In many models, the competition parameter C_j can be expressed as a function of multiple regulating factors (see Appendix 1.2.E.3), so naturally, $\Delta\rho_i$, ΔN_i, and ΔI_i can be broken down further into terms which measure the contributions of individual (or subsets of) regulating factors.

1.2.6 Discussion

In this paper, we have shown how the invasion growth rate can be partitioned so as to isolate the effects of spatial variation and temporal variation. With this new capability, one can determine whether species are coexisting because of spatial heterogeneity, temporally changing environmental conditions, or both. Further, one can break-down individual coexistence mechanisms (such as the storage effect) into contributions from spatial and temporal variation, e.g., the spatial storage effect and the temporal storage effect can be extracted from a complex model with spatiotemporal variation.

In addition to the partitioning of spatiotemporal variation, the framework presented here contains several improvements on previous iterations of Modern Coexistence Theory (MCT). 1) Resident growth rates are scaled by quotients of generation times, as opposed to the conventional but infamously confusing scaling factors (see Section 1.2.3.2; Johnson and Hastings, 2022a). 2) Coexistence mechanisms based on small-noise approximations are clearly delineated from exact coexistence mechanisms (Section 1.2.3.1). 3) Both small-noise and exact coexistence mechanisms can be extracted from a diversity of model types, including discrete-time models, continuous-time models (including Stochastic Differential Equations), models with multiple regulating factors, and structured population models (Appendix 1.2.E). We have presented canonical coexistence mechanisms (e.g., the storage effect), but more exotic coexistence mechanisms can be derived with a generalized partition (following Ellner et al., 2019); replace the arguments of the growth function g_j with any number of variables, and apply the logic of Section 1.2.3.

Spatiotemporal MCT allows for the analysis of more realistic models, which naturally lead to better inferences regarding mechanisms of coexistence in real communities. Although generating realistic models requires immense amounts of system-specific knowledge, data collection, and statistical expertise, all of this hard work can be thought of as a safeguard against bad inferences. When simplistic statistical approaches are used to understand community structure, the data are often overdetermined by theory. For example, left skew in a species abundance distributions could indicate neutral population dynamics (Hubbell, 2001); or temporal autocorrelation in sampling (McGill, 2003); or an excess of transient species (Magurran and Henderson, 2003); or a sequential stick-breaking model (Nee et al., 1991); or a log-normal distribution paired with a

zero-sum constraint (Pueyo, 2006). Randomization-based null models for detecting interspecific competition can implicitly exclude or include the effects of competition (Connor and Simberloff, 1979, Diamond and Gilpin, 1982). A saturating curve on a plot of regional vs. local species richness could indicate environmental filtering (Cornell and Lawton, 1992) or dispersal limitation (Fox et al., 2000).

While data is always overdetermined by theory to some extent (Duhem, 1954), the problem can be abated by MCT's *model-based* approach and a few *best practices*. First, one ought to use large and flexible models. As Leonard Savage used to say, all models should be "as big as a house" (qtd in Draper, 1995). Big models tend to be less biased and implicitly capture structural uncertainty in the form of parameter uncertainty (Draper, 1995). As a statistical example of this phenomenon, consider a student t-distribution, which interpolates between a Gaussian distribution and a Cauchy distribution depending on the *degrees of freedom* parameter. An ecological example is MacArthur's resource-consumer model (MacArthur, 1970; Chesson, 1990), which interpolates between an explicit resource-consumer model and the Lotka Volterra model depending on the speed of resource dynamics. Simple template models (like the annual plant model; Law and Watkinson, 1987; Chesson, 1994, Section 5; Godoy and Levine, 2014) can be made complex through the process of *continuous, iterative model expansion* (Box, 1980; Draper, 1995; Gelman et al., 2020; Gelman et al., 2020).

When dealing with complex models, there is a legitimate fear of *overfitting* (Hastie et al., 2009, Ch. 7). However, overfitting can be addressed by *regularization*, the general term for penalizing model complexity in the parameter-tuning process (Gelman and Vehtari, 2021), as opposed to penalizing complexity in the model selection process (using AIC, cross-validation, etc.). Regularization can be enforced via model-fitting algorithms (such as the LASSO, ridge-regression, or least-angle regression; Hastie et al., 2009, Ch. 3), prior distributions in the Bayesian context (see horseshoe priors for sparsity-inducing regularization; Carvalho et al., 2009), and hierarchical model structures (Gelman and Hill, 2006). Hierarchical model structures are the obvious way of reducing estimation variance for large matrixes of competition coefficients (S species $\rightarrow$ S^2 competition coefficients!); alternatively, the number of parameters can be reduced by grouping species based on phylogeny, ecological function, or traits (Martyn et al., 2021). It is worth noting that overfitting can be largely avoided simply by using a Bayesian model-fitting framework: MCMC methods explore the typical set (the volume where the posterior density is close to its expected value; Gelman et al., 2020), *not* the posterior mode, and are therefore unlikely to sample parameter values with spuriously high likelihoods.

Another modelling *best practice* is to propagate uncertainty in model parameters through to the level of coexistence mechanisms, which can be generically accomplished by sampling from bootstrap or posterior distributions of model parameters. To our knowledge, only one empirical application of MCT (Ellner et al., 2016, Section SI.8) has performed this crucial step. Without uncertainty propagation, it is difficult to say

whether estimates of coexistence mechanisms reflect reality or sampling error.

MCT assumes that the statistical properties of the environment (e.g., the mean level and variance) do not change in a directional manner (i.e., a unique time-averaged distribution of the invader's environment exists; Section 1.2.4), an assumption that is certainly false in many cases. However, MCT can still be used when unidirectional environmental change is considerably slower than demographic change (Fig. 1.4). For example, temperate lake phytoplankton can invade on the time-scale of years, but are appreciably affected by climate change on the time-scale of decades (Izmest'eva et al., 2011). Therefore, it may be reasonable to not incorporate climate change projections into one's model of phytoplankton dynamics, with the understanding that the validity of one's inferences regarding coexistence only extends so far into the future.

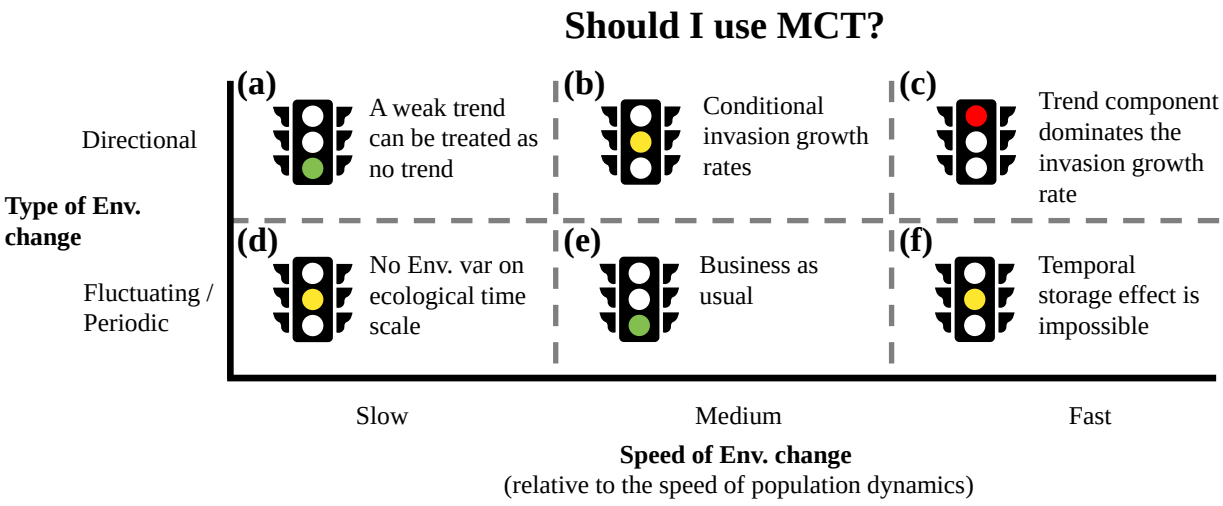

Figure 1.4: How the utility of MCT changes with the type and speed of environmental change. *Red* indicates that MCT is a not a suitable tool; *yellow* indicates that some coexistence mechanisms are automatically absent, or that MCT can be used with caveats; *green* indicates that MCT can be used without worry. **a)** When environmental change is directional but slow, one can estimate invasion growth rates by treating the current statistical characteristics of the environment (e.g., the mean, variance) as constant. **b)** When environmental change is directional and appreciable, quasi invasion growth rates can be calculated, but they are conditional on initial conditions and the time period over which growth rates are averaged. **c)** Invasion growth rates are dominated by the trend component of the environment; coexistence mechanisms do not matter. **d)** When environmental change is slow relative to the speed of population dynamics, the environment is effectively constant on ecological time-scales; the temporal storage effect and environment-induced temporal relative nonlinearity will be zero, but MCT can still be used to quantify spatial coexistence mechanisms, temporal relative nonlinearity via endogenous population cycles (*sensu* Armstrong and McGehee, 1976; Armstrong and McGehee, 1980), and to partition the linear density-dependent effects (Appendix 1.2.E.3). **e)** There are no problems applying MCT in this regime. **f)** When the environment fluctuates too quickly, there is not enough time for population buildup to occur during favorable periods, thus enervating the high intraspecific competition felt by common species; in the limit of a fast environment, the temporal storage effect is zero (Li and Chesson, 2016).

When the time scales of demographic change and directional environmental change are commensurate, it is still possible to use MCT. Invasion growth rates can be calculated under projected environmental change, but their values will depend on the initial conditions and the length of the period over which growth rates are averaged. While this subjectivity is undesirable, there are reasonable methods for dealing with it. One could select the initial conditions to be time-dependent equilibrium parameters, the most recent observation, or a range of recent observations (in which case marginalizing invasion growth rates would be necessary). The dependence of invasion growth rates on the time-frame of measurement cannot be circumvented, but it can be acknowledged by plotting a temporal moving-average of growth rates (i.e., a *local* invasion growth rate) and subsequent coexistence mechanisms across time.

When environmental change is much slower than demographic change, the infinite population assumption of MCT (Section 1.2.4) breaks-down: in theory, long periods of unfavorable conditions can be offset by sufficiently favorable conditions; in reality, long periods of unfavorable conditions lead to extinction. In the limit of strong environmental autocorrelation, the environment is effectively fixed its initial conditions (Kamenev et al., 2008) and competitive exclusion occurs in the absence of other coexistence-promoting mechanisms. Regardless of the relative speed of environmental change, one ought to be wary of calculating invasion growth rates over long time-scales. Even though the invasion growth rate of a tree species may converge after 500,000 years — perhaps after the effects of anthropogenic climate change have been attenuated by several Milankovitch cycles — our models of contemporary population dynamics will certainly be poor representations of the far future.

A few basic insights emerge from Spatiotemporal Modern Coexistence Theory (MCT). The inclusion of spatiotemporal fluctuations (as opposed to only spatial or only temporal fluctuations) exactly doubles the maximum number of species that the fluctuation-dependent coexistence mechanisms can support (Table 1.7). The reason is laid bare in the space-time decomposition of the small-noise coexistence mechanisms (Eq.1.85–Eq.1.104): species may specialize on either spatial variation *or* temporal variation. It is worth noting that this result depends on the veracity of the small-noise assumptions (Appendix 1.2.B.2); even more species could potentially coexist by specializing on higher-order moments (Zicarelli, 1975; Levins, 1979), such as the spatial skew of resource concentrations.

Table 1.7: The maximum number of species that can coexist via various coexistence mechanisms, in a system with L discrete resources, M discrete environmental states, and K discrete patches. In the column headings, *spatial variation* and *temporal variation* refer to variation in the environment, regulating factors, and relative density. The entries in this table were derived as follows: only one species will have the largest ΔE, and in the absence of other influences on the per capita growth rates, this species' relative frequency will approach 1 over time. The entries for $\Delta\rho$ simply express the competitive exclusion principle. The entries for ΔN follow from recognizing that the covariances between regulating factors can be treated as honorary regulating factors, and then by applying the competitive exclusion principle. The entries for ΔI are derived in the same way, and are an obvious extrapolation of the work by Miller and Klausmeier, 2017. The entries for $\Delta\kappa$ come from Appendix 1.2.F. It is well known that many species can coexist if patches have different resource supply points (Levin, 1974; Tilman, 1982; Chase and Leibold, 2003); this manifests as the $M \times L$ term in the entries for $\Delta\kappa$, where M is the number of distinct resource supply points. We have not formally analyzed the case where fitness-density covariance is caused by aggregating behavior (such as swarming or schooling) or preferential dispersal (Barabás et al., 2018, Appendix S5), but we imagine that behaviors or patch preferences can be treated as density-independent variables, and therefore, that the table entries for $\Delta\kappa$ are still accurate.

Coexistence mechanisms	Models with neither spatial nor temporal variation	Models with only spatial variation	Models with only temporal variation	Models with spatiotemporal variation
ΔE: Density-independent effects	1	1	1	1
$\Delta\rho$: Linear, density-dependent effects	L	L	L	L
ΔN: Relative nonlinearity	0	$(L(L-1))/2$	$(L(L-1))/2$	$L(L-1)$
ΔI: Storage effect	0	LM	LM	$2LM$
$\Delta\kappa$: Fitness-density covariance	0	$LM + (L(L-1))/2$	0	$LM + (L(L-1))/2$

Table 1.7 reveals that with even a modest number of regulating factors and environmental states, there are more than enough ways for species to coexist. This highlights the importance of actually measuring coexistence mechanisms in real communities. Table 1.7 also shows the enormous potential of the fluctuation-dependent coexistence mechanisms, relative to classical explanations for coexistence (i.e., $\Delta\rho_i$). While this may be interesting, it is not likely to drive diversity patterns in the real world. For one, it has been argued that regulating factors are plentiful if you look hard enough (Levin, 1970; Haigh and Smith, 1972; Abrams, 1988). Second, biodiversity is affected by many forces, including structural stability (Gyllenberg and Meszéna, 2005), evolutionary / developmental / physiological constraints on extreme forms of specialization, and extinction–speciation balance.

Spatiotemporal MCT also strengthens an *a priori* refutation of the *competitive exclusion principle*, the idea that no more than L species can coexist on L regulating factors). The competitive exclusion principle

was originally based on equilibrium theory (Volterra, 1926, Lotka, 1932, Gause, 1934), but the principle still applies in fluctuating environments when there are no fluctuation-dependent coexistence mechanisms (Hening and Nguyen, 2020; Barabás et al., 2018, p.295). Of course, for this to occur, there must be linear responses to regulating factors (this precludes relative nonlinearity) and no interaction effect between environment and competition (this precludes the storage effect). Spatiotemporal MCT shows that species' responses to regulating factors cannot simultaneously be linear with respect to fluctuations on the natural scale (i.e., $\frac{\partial^2 g_j(E_j^*,C_j^*)}{\partial C_j^2} = \beta_j^{(2)} = 0$), which is necessary for spatial averaging, and linear with respect to fluctuations on the log-scale (i.e., $\frac{\partial^2 \log\left(g_j(E_j^*,C_j^*)\right)}{\partial C_j^2} = \beta_j^{(2)} - \beta_j^{(1)^2} = 0$), which is necessary for temporal averaging. This shows that the competitive exclusion principle is unlikely to have real-world relevance.

The competitive exclusion principle has been challenged from many angles: it is trivial (Cole, 1960; Ayala, 1969), tautological (Gilbert et al., 1952), relies on the false assumption of a stable equilibrium (Armstrong and McGehee, 1980), has stymied the development of a broader research program (Simha et al., 2022), and is irrelevant on ecologically relevant time scales, since similar species can co-occur for a long time (Hurtt and Pacala, 1995). Nevertheless, the competitive exclusion principle and its interrogative forms — the paradox of the plankton a.k.a. the diversity paradox (Hutchinson, 1961) — are frequently used to motivate coexistence research (Simha et al., 2022, supplement 1), probably because authors need to cite *something* other than their personal interest in biodiversity. The competitive exclusion principle does deserve to be recognized, not for making believable predictions, but for its role in the dialectical narrative of coexistence research.

The Hegelian dialectic is a model of history in which a *thesis* is met with an *antithesis*, and the conflict itself produces *synthesis*. In our current context, the thesis is the presumption of competitive exclusion, an idea that started with Darwin and was formalized with the competitive exclusion principle. Charles Darwin, not knowing the genetic basis for inheritance, believed that evolution necessitated fierce competition; otherwise, favorable mutations would be blended with the wild-type until the population was phenotypically uniform (Lewens, 2010). Indeed, Darwin (1859, p. 322) writes "We need not marvel at extinction; if we must marvel, let it be at our own presumption in imagining for a moment that we understand the many complex contingencies on which the existence of each species depends."

It is plausible that Darwin's emphasis on competition and exclusion was influenced not only by the faulty of theory of blending inheritance, but also by the upper-class milieu of 1800s England — Darwin was a member of the Whig party during the era of the New Poor Law and was predominantly influenced by the work of the eugenicist Thomas Malthus, consequently endorsing the extermination (via disease, famine, economic deprivation) of colonized people in the name of creative destruction, all the while detesting explicit genocide (Moore and Desmond, 1991). The presumption of competitive exclusion evolved into the competitive exclu-

sion principle, though the exact reason for the principle's prominence is unclear. Explanations include the attention of few superstar authors (namely Robert MacArthur and G.E. Hutchinson, see Schoener, 1982), the naturalization of capitalist ideology (Simha et al., 2022), and the fact that mutualism — the conceptual reciprocal of competition — does not play nice with the tools of theoretical ecology (May, 1981, p. 95).

The antithesis of competitive exclusion emerged from the discovery of fluctuation-dependent mechanisms (Armstrong and McGehee, 1976; Chesson and Warner, 1981), the realization that spatial and temporal variances could be treated as regulating factors (Levins, 1979), and formulae suggesting that an arbitrary number of species could coexist on a single resource (e.g., Chesson, 1994, Eq. 81). The focal question flipped from "Why are there so many species?" to "Why are there so few species?". These two questions, laid side-by-side, reveal the absurdity of trying to make strong quantitative predictions without an underlying model. Depending on one's theoretical commitments, biodiversity can be bounded in whatever way one chooses; recall that the bounds in Table 1.7 depend on the small-noise assumptions (Section 1.2.B.2) and the assumption that both resources and environmental states are fundamentally discrete. The conflict between the thesis and antithesis suggests the synthesis: the question "Why is the number of species that which we observe?" By serving as a methodology for measuring coexistence, Spatiotemporal MCT is poised to help answer this question.

Although we have extended MCT to more complex models, there remain a number of problems with MCT (see Section 1.2.3.1). But we should not be surprised nor disheartened that such problems exist: MCT was invented to explain the role of environmental variation in coexistence (Barabás et al., 2018, p. 288, Chesson, 2020, p. 6), not to be a measurement tool. There has been a recent surge of interest in the interpretation and application of MCT (Ellner et al., 2016; Ellner et al., 2019; Grainger, Letten, et al., 2019; Song et al., 2020; Pande et al., 2020; Ellner et al., 2020; Barabás et al., 2018; Chesson, 2020; and Barabás and D'Andrea, 2020; Johnson and Hastings, 2022a; Johnson and Hastings, 2022b), but more work needs to be done.

Appendices

1.2.A Deriving small-noise coexistence mechanisms

The derivation of spatiotemporal coexistence mechanisms can be broken into four parts. In part 1, the local finite rate of increase is expressed in a common format: a polynomial of E_j and C_j. This requires re-writing model of population dynamics as in terms of E_j and C_j (Appendix 1.2.B), assuming that environmental fluctuations are small (Appendix 1.2.B.2), and applying a Taylor series expansion (Appendix 1.2.B.1). In part 2, the appropriate spatial (Appendix 1.2.B.3) and temporal (Appendix 1.2.B.4) averaging is applied in order to express the invasion growth rate in terms of local finite rates of increase. In part 3, The approximations derived in parts 1 and 2 are combined to create a long expression for each species' average growth rate (Appendix 1.2.B.5). In part 4, the small-noise coexistence mechanisms are finally produced (formulas presented in the main text) by comparing the invader to the residents.

Why does our exposition feature discrete-time populations dynamics? For one, the connection with data-based modelling of real communities is more transparent, since data is collected at discrete points in time, and as a consequence, ecologists primarily fit discrete-time models. Secondly, the expressions for the small-noise coexistence mechanisms in the case of discrete-time are identical to those in case of continuous-time when environmental stochasticity is proportional to white noise (Appendix 1.2.E.1).

A brief technical note: throughout the paper, we use the notation E_j as shorthand for $E_j(x,t)$; it is *not* the case that E_j is a random variable and that $E_j(x,t)$ is a realization of said random variable, as the notation seems to imply. As Chesson (2000) points out, the notation can be made more precise by adding the seed number/ sample path as an additional argument, such that $E_j(x,t,\omega)$ is a realization of the random variable $E_j(x,t)$. Throughout this paper, when we apply the expectation operator (or covariance or variance operators), we sum over space and/or time while fixing the sample path ω.

1.2.B Population growth as a function of the environment and competition

The local finite rate of increase, λ_j, is given by the function $g_j(E_j, C_j)$, where E_j represents the effects of density-independent factors and C_j represents the effects of density-dependent factors (also known as regulating factors or limiting factors).

The parameter E_j has many names: the *environmentally-dependent parameter*, the *response to the environment*, the *environmental parameter*, or the *environment*. It is typically a demographic parameter that depends on the abiotic environment, such as per capita fecundity or the probability of seed germination, hence the terminology *response to the environment*. But E_j may also be a literal environmental variable, such as annual precipitation, degree days, or soil type. It is important to keep in mind that E_j need not

represent the effects of the abiotic environment, since not all density-independent factors are part of the abiotic environment (e.g., mortality from a generalist predator), and not all density-dependent factors are biotic (e.g., refugia, soil nutrients).

The parameter C_j is often called the *competition parameter*, or simply *competition*. Concrete examples of the competition parameter are the number of juvenile fish competing per open territory in the lottery model, or a linear combination of population densities, as in the competitive Lotka-Volterra model. The focus on competition reflects MCT's intellectual origin (and more generally, ecology's bias towards competition; Mittelbach, 2019, p. 164) but the density-dependent C_j can just as easily represent predation pressure (Kuang and Chesson, 2010; Chesson and Kuang, 2010; Stump and Chesson, 2015; Stump and Chesson, 2017) or mutualistic benefits (Stump et al., 2018).

We note that in some papers (e.g., (Chesson, 1994; Chesson, 2018; Ellner et al., 2016), $C_j^{\{-i\}}$ or $C_{j\setminus i}$ is used to denote the competition parameter of species j when species i is absent. We use C_j to denote the same, since we are always considering a community in which one species is the invader.

1.2.B.1 Decomposing the finite rate of increase: the quadratic approximation

We will decompose $g_j(E_j, C_j)$ via a second-order Taylor series expansion. First though, we must select *equilibrium values* of the environment and competition to expand about. These values, denoted E_j^* and C_j^*, must be selected so that $g_j(E_j^*, C_j^*) = 1$, a constraint that functions to eliminate the zeroth-order Taylor series coefficient (see Eq.2.4).

In general, there is no unique choice of E_j^* and C_j^*, though as Chesson (1994) notes, fixing one parameter will determine the other. That being said, not all choices are equally appropriate. In particular, for every term in the Taylor series expansion to be the same order of magnitude – and thus of commensurate importance – we must simultaneously select E_j^* to be close to $\mathbb{E}_{x,t}[E_j]$, and C_j^* to be close to $\mathbb{E}_{x,t}[C_j]$ (the reasoning will be explained in the following section, 1.2.B.2).

There is a canonical method for selecting E_j^* and C_j^*: virtually eliminate environmental noise, select E_j^* as the environmental parameter in the resulting *deterministic skeleton*, and then select C_j^* based on the constraint $g_j(E_j^*, C_j^*) = 1$. In models with multiple regulating factors (see Appendix 1.2.E.3), there are an infinite number of ways to select equilibrium parameters — there are many unknowns and just one constraint ($g_j(E_j^*, C_j^*) = 1$) — but there are several reasonable strategies (see Johnson and Hastings, 2022a, Section 2.1).

With the appropriate selection of the equilibrium parameters, we expand the local finite rate of increase

with a second-order Taylor Series about E_j^* and C_j^*:

$$\begin{aligned} g_j(E_j, C_j) \approx 1 + \alpha_j^{(1)}(E_j - E_j^*) + \beta_j^{(1)}(C_j - C_j^*) \\ + \frac{1}{2}\alpha_j^{(2)}(E_j - E_j^*)^2 + \frac{1}{2}\beta_j^{(2)}(C_j - C_j^*)^2 + \zeta_j(E_j - E_j^*)(C_j - C_j^*). \end{aligned} \tag{1.171}$$

The coefficients of the Taylor series are

$$\alpha_j^{(1)} = \frac{\partial g_{j(E_j^*, C_j^*)}}{\partial E_j}, \quad \beta_j^{(1)} = \frac{\partial g_{j(E_j^*, C_j^*)}}{\partial C_j}, \quad \alpha_j^{(2)} = \frac{\partial^2 g_{j(E_j^*, C_j^*)}}{\partial E_j^2}, \quad \beta_j^{(2)} = \frac{\partial^2 g_{j(E_j^*, C_j^*)}}{\partial C_j,^2} \quad \zeta_j = \frac{\partial^2 g_{j(E_j^*, C_j^*)}}{\partial E_j \partial C_j}. \tag{1.172}$$

1.2.B.2 Small-noise assumptions

In order for the second-order Taylor series expansion (the r.h.s. of Eq.2.4) to be a good approximation of $g_j(E_j, C_j)$, we must make some assumptions about the magnitude of environmental fluctuations. First, we assume that the environmental parameter E_j fluctuates about E_j^* in a small finite range, and that the size of this range in controlled by a small parameter σ. Here, we use the conventional "big-oh" notation to denote an upper bound on magnitude of fluctuations:

$$E_j - E_j^* = \mathcal{O}(\sigma). \tag{1.173}$$

This means that $\left|E_j - E_j^*\right| < k\sigma$, with some constant k as $\sigma \to 0$. Our next assumption states that environmental fluctuations are even smaller when averaged across space and time:

$$\mathbb{E}_{x,t}[E_j] - E_j^* = \mathcal{O}(\sigma^2). \tag{1.174}$$

The justification of the above assumption is either 1) that positive and negative fluctuations cancel out, or 2) that large fluctuations (which set the magnitude of $E_j - E_j^*$) are overpowered by many smaller fluctuations. Functionally, the assumption ensures that the effects of spatiotemporal averages are on the same order of magnitude as the effects of spatiotemporal variance; note that Eq.1.173 and Eq.1.174 imply that $\mathrm{Var}_{x,t}(E) = \mathcal{O}(\sigma^2)$.

To help make sense of the above assumptions, consider an environmental parameter $E_j(x,t) = a(x) + b(t)$. Both the patch effect $a(x)$ and time effect $b(t)$ independently take the value $+\sigma$ or $-\sigma$ with probability $= 0.5$. By construction, the first assumption, Eq.1.173, is met. If we then select $E_j^* = 0$, the relevant bounds are $\left|E_j - E_j^*\right| \leq 2\sigma$, $\left|\mathbb{E}_t[E_j] - E_j^*\right| \leq \sigma$, and $\left|\mathbb{E}_t[E_j] - E_j^*\right| \leq \sigma$. Here we see that spatial and temporal averages of environmental fluctuations are on the same order of magnitude as the raw fluctuations, $E_j - E_j^*$. Furthermore,

we see that $\mathbb{E}_{x,t}[E_j] - E_j^* = 0$, which neatly demonstrates that the spatiotemporal average of fluctuations is exceedingly small (Eq.1.174).

In order for environment and competition to have commensurate effects on per capita growth rates, we must assume analogous bounds for for the competition parameter ($C_j - C_j^* = \mathcal{O}(\sigma)$ and $\mathbb{E}_{x,t}[C_j] - C_j^* = \mathcal{O}(\sigma^2)$) and for relative density ($\nu_j - 1 = \mathcal{O}(\sigma)$ and $\mathbb{E}_{x,t}[\nu_j] - 1 = \mathcal{O}(\sigma^2)$). In some situations, these bounds are not pure assumptions, but rather the result of some conditions. Heavily paraphrased, the conditions are 1) that species have a shared competition parameter (Chesson, 1994, p. 268) or have very similar competition parameters (Chesson, 1994, p. 270, second equation), 2) that competition is a function of population densities and environmental responses (Chesson, 1994, p. 269); 3) that competition does not amplify itself over time (Chesson, 1994, p. 269)); and 4) that "... any increase in local density due to dispersal cannot increase competition any more than $\mathcal{O}(\sigma)$ above the maximum competition applicable if there were no dispersal." (Chesson, 2000, p. 234). Additionally, if there are more residents than regulating factors, then the scaling factors can be used to cancel the $\Delta\rho_i$ coexistence mechanisms, and concerns about bounding C_j are moot. For all the details, see Appendix 2 of Chesson (1994) and Appendix 3 of Chesson (2000).

The small-noise assumptions serve two primary purposes. First, they allow us to truncate the Taylor series (Eq.2.4) at second order, thus limiting the number of coexistence mechanisms that we might simultaneously consider. Second, the small-noise assumptions allow us to use the *small-noise approximation* for dynamical systems (Gardiner, 1985), resulting in simple stochastic models that permit analytical expressions for important quantities, e.g., the covariance between environment and competition (See Schreiber, 2021 for an example).

When the small-noise assumptions (and the auxiliary conditions above) are not met, one can proceed with two risks. First, the small-noise coexistence mechanisms may not sum approximately to the invasion growth rate; they will "miss" important processes that promote or hinder coexistence. Second, the exact coexistence mechanisms may capture unknown processes that involve large environmental fluctuations, thus making the exact coexistence mechanism less interpretable.

The small-noise assumptions above require large fluctuations to be impossible, not just improbable. Restricting fluctuations to a finite range ensures that growth rates will not be dominated by low-probability, high-impact events. The gain in internal validity comes at the cost of external validity: it is often reasonable to model the environmental response by a random variable with support on the positive real numbers. For example, recruitment in some marine animals appears to follow lognormal distributions (Hennemuth et al., 1980; Ripley and Caswell, 2006). However, the exact coexistence mechanisms circumvent the finite range assumption entirely, as long as we exclude from consideration the unlikely scenario where the distributions of E_j and C_j are so fat-tailed that spatial, temporal, or spatiotemporal averages of E_j and C_j do not exist.

Given the plethora of assumptions implicit in any ecological model, a violation of the finite range assumption is just one of many ways in which the results of an MCT analysis are provisional.

1.2.B.3 Spatial averaging and fitness-density covariance

Next, we will derive a decomposition of the metapopulation finite rate of increase, $\widetilde{\lambda}_j(t)$. Consider a community with K distinct patches. The metapopulation finite rate of increase can be calculated as simple average of each individual's finite rate of increase, or equivalently, a weighted average of each patch's finite rate of increase, with weights equal to the relative density of the population in that patch. To see the logic of the latter scheme, first note that

$$\widetilde{\lambda}_j(t) = \frac{\sum_{x=1}^{K} n_j(x,t+1)}{\sum_{x=1}^{K} n_j(x,t)} = \frac{\sum_{x=1}^{K} n_j(x,t+1)}{K\ \mathbb{E}_x[n_j(t)]}. \tag{1.175}$$

Using the local dynamics (Eq.1.53) to substitute for $n_j(x,t+1)$, we find that

$$\widetilde{\lambda}_j(t) = \frac{1}{K\ \mathbb{E}_x[n_j(t)]} \sum_{x=1}^{K} \left(n_j(x,t)\ g_j(E_j(x,t), C_j(x,t))\right) + \frac{1}{K\ \mathbb{E}_x[n_j(t)]} \sum_{x=1}^{K} \left(c_j(x,t) - e_j(x,t)\right). \tag{1.176}$$

To simplify the above expression, we would like second additive term (the spatial sum of net dispersal) to vanish. This can be accomplished by assuming either 1) that the system is closed, i.e., no individuals can enter or leave the system of patches, or 2) that the community receives roughly as many immigrants as it loses emigrants. Scenario 1 is likely to be approximately true for communities that span entire ecosystems, or for communities with very specific habitat requirements (e.g., Californian plants endemic to serpentine soils; Harrison et al., 2006). In either case, there is no immigration into the metacommunity, and emmigration out of the metacommunity results in mortality that can be treated as part of the local dynamics of marginal patches. Scenario 2 is likely to be approximately true when the habitat surrounding the focal area is similar enough to the habitat within the focal area, such that immigration and emigration are balanced over the margin of the focal area. The focal area (which itself is not closed) is representative of a larger metacommunity which is effectively closed.

Assuming that dispersal is negligible at the spatial scale of the metapopulation, dropping the notation for explicit time-dependence, and rearranging terms, Eq.1.176 simplifies significantly,

$$\widetilde{\lambda}_j = \mathbb{E}_x\left[\frac{n_j}{\mathbb{E}_x[n_j]} g_j(E_j, C_j)\right], \tag{1.177}$$

thus revealing that the metapopulation finite rate of increase is a density-weighted average of local finite rates of increase. $\widetilde{\lambda}_j$ can be decomposed further with the law of total covariance:

$$\begin{aligned}\widetilde{\lambda}_j &= \mathbb{E}_x\left[\frac{n_j}{\mathbb{E}_x[n_j]}\right]\mathbb{E}_x[g_j(E_j,C_j)] + \mathrm{Cov}_x\left(\frac{n_j}{\mathbb{E}_x[n_j]}, g_j(E_j,C_j)\right)\\ &= \mathbb{E}_x[g_j(E_j,C_j)] + \mathrm{Cov}_x(\nu_j, g_j(E_j,C_j))\end{aligned} \tag{1.178}$$

where ν_j is the *relative density* of species j, defined precisely as $\nu_j(x,t) = \frac{n_j(x,t)}{\mathbb{E}_x[n_j(t)]}$.

The first term in Eq.1.178 is the spatial average of local per capita growth rates. The second term is the covariance between relative-density and growth rates, which captures the ability of species j to end up in locations where it has high fitness (though the mechanism of this ability is completely unspecified). This term is the precursor to *fitness-density covariance*.

1.2.B.4 Temporal averaging

The quantity which is predictive of persistence is not $\mathbb{E}_t\left[\widetilde{\lambda}_k\right]$, but rather $\mathbb{E}_t\left[\log\widetilde{\lambda}_j\right]$. The logarithmic transformation converts a product of $\widetilde{\lambda}_j$ into a sum of $\log\left(\widetilde{\lambda}_j\right)$, which facilitates the application of an arithmetic average.

Conditions on the magnitude of fluctuations in E_j, C_j, and ν_j (Appendix 1.2.B.2) can be used to show that $\widetilde{\lambda}_j = 1 + \mathcal{O}(\sigma)$ and $\mathbb{E}_t\left[\widetilde{\lambda}_j\right] = 1 + \mathcal{O}(\sigma^2)$. The logarithm can now be decomposed with a Taylor series expansion

$$\log\left(\widetilde{\lambda}_j\right)\Big|_{\widetilde{\lambda}_j=1} \approx \widetilde{\lambda}_j - 1 - \frac{1}{2}\left(\widetilde{\lambda}_j - 1\right)^2. \tag{1.179}$$

Utilizing the fact that $\mathbb{E}_t\left[\left(\widetilde{\lambda}_j - 1\right)^2\right] = \mathrm{Var}_t\left(\widetilde{\lambda}_j\right) + \mathcal{O}(\sigma^4)$, we take the average over time to obtain the average growth rate:

$$\mathbb{E}_t\left[\log\left(\widetilde{\lambda}_j\right)\right] \approx \mathbb{E}_t\left[\widetilde{\lambda}_j\right] - 1 - \frac{1}{2}\mathrm{Var}_t\left(\widetilde{\lambda}_j\right). \tag{1.180}$$

Plugging the decomposition of $\widetilde{\lambda}_j$ (Eq.1.178) into equation Eq.1.180, we find that the invasion growth rate can be approximated entirely by moments of λ_j and ν_j.

$$\mathbb{E}_t\left[\log\left(\widetilde{\lambda}_j\right)\right] \approx \mathbb{E}_{x,t}[\lambda_j] + \mathbb{E}_t[\mathrm{Cov}_x(\nu_j(t),\lambda_j)] - 1 - \frac{1}{2}\mathrm{Var}_t(\mathbb{E}_t[\lambda_j]). \tag{1.181}$$

1.2.B.5 Putting it all together: A decomposition of the average growth rate

The Taylor series decomposition of $g_j(E_k, C_j)$ (Eq.2.4) can be plugged into Eq.1.181, producing a fine-grained partition of species j's average growth rate

$$\begin{aligned}\mathbb{E}_t\Big[\log\Big(\widetilde{\lambda}_j\Big)\Big]\Big|_{\substack{C_j=C_j^* \\ E_j=E_j^*}} \approx\ & \alpha_j^{(1)}\mathbb{E}_{x,t}\big[(E_j - E_j^*)\big] + \beta_j^{(1)}\mathbb{E}_{x,t}\big[(C_j - C_j^*)\big] \\ & + \frac{1}{2}\alpha_j^{(2)}\mathrm{Var}_{x,t}(E_j) + \frac{1}{2}\beta_j^{(2)}\mathrm{Var}_{x,t}(C_j) + \zeta_j\mathrm{Cov}_{x,t}(E_j, C_j) \\ & + \mathbb{E}_t\Big[\mathrm{Cov}_x\Big(\nu_j, \alpha_j^{(1)}(E_j - E_j^*) + \beta_j^{(1)}(C_j - C_j^*)\Big)\Big] \\ & - \frac{1}{2}\alpha_j^{(1)^2}\mathrm{Var}_t(\mathbb{E}_x[E_j]) - \frac{1}{2}\beta_j^{(1)^2}\mathrm{Var}_t(\mathbb{E}_x[E_j]) - \alpha_j^{(1)}\beta_j^{(1)}\mathrm{Cov}_t(\mathbb{E}_x[E_j]\,, \mathbb{E}_x[C_j])\,.\end{aligned} \tag{1.182}$$

The additive terms in Eq.1.182, can be thought of as a components of the average growth rate, each of which captures some "effect" on population growth. The components are not generally independent, which correctly implies that the subsequent coexistence mechanisms are not generally independent (Song et al., 2020; Kuang and Chesson, 2010; Yuan and Chesson, 2015). For instance, in the spatiotemporal lottery model (Section 1.2.5 in the main text), the mortality parameter modulates all coexistence mechanisms. However, growth rate components may be conceptualized as distinct processes, just as ecology and evolution are interdependent but conceptually distinct.

Note that the term $\mathbb{E}_{x,t}\left[(E_j - E_j^*)(C_j - C_j^*)\right]$ has been replaced with $\mathrm{Cov}_{x,t}\left(E_j, C_j\right)$, since $\mathrm{Cov}_{x,t}\left(E_j, C_j\right) = \mathbb{E}_{x,t}\left[(E_j - E_j^*)(C_j - C_j^*)\right] + \mathcal{O}(\sigma^3)$ via the small-noise assumptions. Analogous replacements have been made for other variance and covariance terms in Eq.1.182. These replacements are not a necessary part of MCT, but they do make the mathematical expressions shorter and more comprehensible.

1.2.C Justification of the space-time decomposition

To isolate the effects of spatial and temporal variation, we first define a reference state where both spatial and temporal variation are turned off; then, we separately turn on spatial (temporal) variation, and identify the difference as the main effect of spatial (temporal) variation. Put in such colloquial terms, this procedure may appear *ad hoc* at first glance. However, we show that this procedure agrees with intuition in a simple example (Appendix 1.2.C.1), and is concordant with philosophical accounts of causation (Appendix 1.2.C.2).

1.2.C.1 A toy model with only spatially or only temporally varying abiotic factors

Here we analyze the edge case where the environmental response E_j is a function of abiotic factors that individually vary over only space or time. This case is simple enough that we can describe our intuitions

regarding what a space-time decomposition should do: the space component should only include the effects of the spatially varying abiotic factors, and the time component should only include the effects of the temporally varying abiotic factors.

To be more concrete, consider two abiotic factors, W and Y. The factor W only varies over space (i.e., at a particular location, W does not vary from year-to-year) and Y only varies over time (i.e., at a single point in time, all locations have the same value of Y). Select the equilibrium values of the abiotic resources, W^* and Y^*, so that $E_j^* = f_j(W^*, Y^*)$, where f_j is a function that maps abiotic factors to species j's environmental response. The small-noise assumptions of MCT imply that $W - W^* = \mathcal{O}(\sigma)$, $Y - Y^* = \mathcal{O}(\sigma)$, $\mathbb{E}_{x,t}[W - W^*] = \mathbb{E}_x[W - W^*] = \mathcal{O}(\sigma^2)$, and $\mathbb{E}_{x,t}[Y - Y^*] = \mathbb{E}_t[Y - Y^*] = \mathcal{O}(\sigma^2)$. Using this information, we can derive expressions for the space-time decomposition of $\mathrm{Var}_{x,t}(E_j)$. Applying a Taylor series of f_j about W^* and Y^*, plugging the resulting expression into the space-time decomposition equations (Eq.1.82–Eq.1.84), and utilizing the fact that the variance of a constant equals zero (e.g., $\mathrm{Var}_t(W) = 0$), we find that

$$S_j = \left[\frac{\partial f_j(W^*, Y^*)}{\partial W}\right]^2 \mathrm{Var}_x(W) + \mathcal{O}(\sigma^3) \tag{1.183}$$

$$T_j = \left[\frac{\partial f_j(W^*, Y^*)}{\partial Y}\right]^2 \mathrm{Var}_t(Y) + \mathcal{O}(\sigma^3), \quad \text{and} \tag{1.184}$$

$$R_j = \left[\frac{\partial^2 f_j(W^*, Y^*)}{\partial W \partial Y}\right]^2 \mathrm{Var}_x(W)\,\mathrm{Var}_t(Y) + \mathcal{O}(\sigma^5). \tag{1.185}$$

The Taylor series coefficients show that S_j captures the main effect of the spatially varying abiotic factor, T_j captures the main effect of the temporally varying abiotic factor, and that R_j captures the interaction effect between the two abiotic factors. This model is exceedingly simple, but it is the first line of evidence that our space-time decomposition behaves as desired.

1.2.C.2 The space-time decomposition measures causation

Counterfactual theories of causation posit that causation can be explained in terms of counterfactual dependency (Hume, 1748, Section *XII*; Mill, 1856 , Lewis, 1973, Pearl and Mackenzie, 2018). To say "A caused B", is to say "if A had not occurred, then B would not have occurred". To operationalize causation, we may calculate differences (with respect to some outcome of interest) between possible worlds, where the possible worlds are similar in every relevant way except for some focal causal factor. The comparison of possible worlds is crucial, which is why the counterfactual account of causation is sometimes called the difference-making account of causation. Lewis (1973) explains "We think of a cause as something that makes

a difference, and the difference it makes must be a difference from what would have happened without it."

The exposition above makes our challenge clear: to justify our space-time decomposition on the grounds that it captures causation, we must 1) describe S_j, T_j, and R_j (see Eq.1.82–Eq.1.84) in terms of differences between possible worlds, as has been done in the main text (Section 1.2.3.3) and 2) argue that the possible worlds in question are close in some relevant sense, following Lewis's (1979) guideline that possible worlds "...maximize the spatiotemporal region thorough-out which perfect match of particular fact prevails". By using spatial (temporal) averaging to squash spatial (temporal) variation, we are doing just that: the sequence of spatial averages $A(t) = \mathbb{E}_x[E_j]$ minimizes the squared error $\sum_{x,t} \left(E_j(x,t) - A(t)\right)^2$, under the constraints that there is no spatial variation, and that spatial variation must be squashed using only information from the E_j's within each individual time-step.

1.2.D Deriving the small-noise fitness-density covariance for the spatiotemporal lottery model

Like all coexistence mechanisms, the fitness-density covariance coexistence mechanisms is $\mathcal{O}(\sigma^2)$, which implies that the leading-order approximation for the covariance will involve $\mathcal{O}(\sigma)$ approximations of $\nu_j(t)$ and $\lambda_j(t)$. To this end, we take a perturbative approach, expanding both parameters in powers of σ, $\nu_j(x,t) = \nu_{j,0}(x,t) + \sigma\nu_{j,1}(x,t) + ...$; and $\lambda_j(x,t) = \lambda_{j,0}(x,t) + \sigma\lambda_{j,1}(x,t) + ...$

Matching like-terms in the perturbative expansion and the Taylor series expansion of λ_j (Eq.2.4), we find that $\lambda_{j,0}(x,t) = 1$ and $\sigma\lambda_{j,1}(x,t) = \alpha_j^{(1)}(E_j(x,t) - E_j^*) + \beta_j^{(1)}(C_j(x,t) - C_j^*)$. The solution $\lambda_{j,0}(x,t) = 1$ implies that $\nu_{j,0}(x,t) = 1$. Noting the constancy of the zeroth-order solutions, the covariance can now be approximated as

$$\begin{aligned} \mathrm{Cov}_x(v_j(t), \lambda_j(t)) &= \mathrm{Cov}_x(v_{j,0}(t) + \sigma v_{j,1}(t) + ..., \lambda_{j,0}(t) + \sigma\lambda_{j,1}(t) + ...) \\ &\approx \mathrm{Cov}_x(\sigma v_{j,1}(t), \sigma\lambda_{j,1}(t))\,. \end{aligned} \tag{1.186}$$

We now seek to simplify by expressing $v_{j,1}(x,t)$ in terms of the environmental parameter. Dividing both sides of the population map (Eq.1.149) by $\mathbb{E}_x[n_j(t)]$ gives the relative-density map.

$$\nu_j(x,t+1) = q_j\nu_j(x,t)\frac{\lambda_j(x,t)}{\widetilde{\lambda}_j(t)} + 1 - q_j. \tag{1.187}$$

The small-noise assumptions (Appendix 1.2.B.2) allow us to make the substitution, $\widetilde{\lambda}_j(x,t) = 1 + \mathcal{O}(\sigma)$, which simplifies the relative density map to

$$\nu_j(x,t+1) = q_j\nu_j(x,t)\lambda_j(x,t) + 1 - q_j. \tag{1.188}$$

We now expand v_j in powers of σ and match terms of order σ.

$$\mathcal{O}(\sigma): \qquad \nu_{j,1}(x,t+1) = q_j\nu_{j,1}(x,t) + q_j\lambda_{j,1}(x,t). \tag{1.189}$$

Substituting the above expression into the covariance produces

$$\begin{aligned}
\mathrm{Cov}_x(v_j(t),\lambda_j(t)) \approx& \mathrm{Cov}_x(\sigma v_{j,1}(t),\sigma\lambda_{j,1}(t)) \\
=&\sigma^2\mathrm{Cov}_x(qv_{j,1}(t-1)+\lambda_j(t-1),\lambda_{j,1}(t)) \\
=&\sigma^2\mathrm{Cov}_x\big(q^2v_{j,1}(t-2)+q\lambda_{j,1}(t-2)+\lambda_{j,1}(t-1),\lambda_{j,1}(t)\big) \\
&\vdots \\
=&\sigma^2\sum_{i=1}^{\infty} q^i\mathrm{Cov}_x(\lambda_{j,1}(t-i),\lambda_{j,1}(t))\,.
\end{aligned} \tag{1.190}$$

Substituting $\alpha_j^{(1)}(E_j(x,t)-E_j^*)+\beta_j^{(1)}(C_j(x,t)-C_j^*)+\mathcal{O}(\sigma^2)$ for $\sigma\lambda_{j,1}$, we get

$$\begin{aligned}
\mathrm{Cov}_x(v_i(t),\lambda_i(t)) \approx \sum_{s=1}^{\infty} q^s\mathrm{Cov}_x\big(&\alpha_i^{(1)}(E_i(x,t-s)-E_i^*)+\beta_i^{(1)}(C_i(x,t-s)-C_i^*), \\
&\alpha_i^{(1)}(E_i(x,t)-E_i^*)+\beta_i^{(1)}(C_i(x,t)-C_i^*)\big).
\end{aligned} \tag{1.191}$$

Next, we express the invader's competition parameter fluctuation in terms of the resident's environmental response. In the two-species lottery model of Section 1.2.5, $C_i(x,t)-C_i^* = E_r(x,t)-E_r^*+\mathcal{O}(\sigma^2)$. The covariance expression is now

$$\begin{aligned}
\mathrm{Cov}_x(v_i(t),\lambda_i(t)) \approx \sum_{s=1}^{\infty} q^s\mathrm{Cov}_x\big(&\alpha_i^{(1)}(E_i(x,t-s)-E_i^*)+\beta_i^{(1)}(E_r(x,t-s)-E_r^*), \\
&\alpha_i^{(1)}(E_i(x,t)-E_i^*)+\beta_i^{(1)}(E_r(x,t)-E_r^*)\big).
\end{aligned} \tag{1.192}$$

Finally, we write the environmental fluctuations in terms of patch and time effects (Eq.1.150), evaluate the above expression using the geometric series and the symbols introduced in the Section 1.2.5 (e.g., $\mathrm{Cov}_x(a_i,a_r) = \phi_{ir}^{(x)}\sigma_i^{(x)}\sigma_r^{(x)}$), and take the average across time:

$$\mathbb{E}_t[\mathrm{Cov}_x(v_i,\lambda_i)] \approx \frac{q}{1-q}\Big[\alpha_i^{(1)^2}\sigma_i^{(x)^2} + \beta_i^{(1)^2}\sigma_r^{(x)^2} + 2\alpha_i^{(1)}\beta_i^{(1)}\phi_{ir}^{(x)}\sigma_i^{(x)}\sigma_r^{(x)} + \alpha_i^{(1)^2}\theta_i^2\sigma_i^{(x)^2}\sigma_i^{(t)^2} + \beta_i^{(1)^2}\theta_r^2\sigma_r^{(x)^2}\sigma_r^{(t)^2} + 2\alpha_i^{(1)}\beta_i^{(1)}\theta_i\theta_r\phi_{ir}^{(x)}\phi_{ir}^{(t)}\sigma_i^{(x)}\sigma_i^{(t)}\sigma_r^{(x)}\sigma_r^{(t)}\Big]. \tag{1.193}$$

In the lottery model, there are always more larvae produced than are necessary to compensate for adult mortality. If there is only one resident, its local density will be exactly 1 everywhere after the local growth phase. Since global dispersal with local retention acts symmetrically on all patches, the resident's density will still be 1 everywhere after the dispersal phase. Therefore, the resident's covariance term is zero, and the fitness density covariance coexistence mechanism is simply the expression above, Eq.1.193; i.e., $\Delta\kappa_i = \mathbb{E}_t\left[\mathrm{Cov}_x(v_i,\lambda_i)\right]$. When symmetries in demographic parameters are taken into consideration, Eq.1.193 reduces to the result in the main text, Eq.1.166.

1.2.E Generalization of MCT to different classes of models

In the main text (Section 1.2.3), we presented formulas for coexistence mechanisms in models with discrete-time dynamics and no age/stage-structure . With slight modification, these same formulas can be used to calculate coexistence mechanisms in other classes of models.

In continuous-time models, g_j represents the local per capita growth rate, $dn_j(t)/dt$ (as opposed to the finite rate of increase in the discrete-time case). In models with multiple regulating factors, the C_j argument is replaced with an arbitrary number of arguments representing regulating factors, and finer-grained fluctuation-dependent coexistence mechanisms are computed by allowing one or two of these factors to vary while holding the rest constant. In structured population models the function g_j represents the finite rate of increase of the sum of states, i.e., $\|n(t+1)\|/\|n(t)\|$, where $\|n(t)\|$ is the sum (or integral) of population densities across all traits/ages/stages.

1.2.E.1 Stochastic Differential Equations (SDEs)

A Stochastic Differential Equation (SDE) is a continuous-time process in which stochastic perturbations occur at an infinitesimal time-scale. Ecological SDES are usually not physically motivated, and can often be viewed as approximations to stochastic difference equations as the length of the time step shrinks to zero (Turelli, 1977). Such approximations are useful because they permit analytical results (e.g., the stationary distribution of population densities in Hatfield and Chesson, 1989).

A univariate, non-spatial SDE can be written as

$$dn(t) = n(t)\left[a(n(t))dt + b(n(t))dW(t)\right], \tag{1.194}$$

where $a(n(t))$ is the *infinitesimal per capita mean* and $b(n(t))$ is the *infinitesimal per capita scale*. These two quantities are respectively defined as the expectation and variance of per capita population growth, conditioned on $n(t)$, in the limit of small time steps; or in symbols,

$$a(n) = \lim_{\Delta t \to 0} \frac{\mathbb{E}[n(t+\Delta t)] - n(t)}{n(t)\Delta t}, \quad \text{and} \tag{1.195}$$

$$b(n) = \lim_{\Delta t \to 0} \sqrt{\frac{\mathrm{Var}(n(t+\Delta t) - n(t))}{n(t)\Delta t}}. \tag{1.196}$$

To solve the SDE, we use Itô's lemma to perform a change of variables. Itô's lemma (Karlin and Taylor, 1981, p. 347–348) states that for an arbitrary SDE,

$$dX(t) = A(X,t)dt + B(X,t)dW(t), \tag{1.197}$$

the SDE for the transformation $f(X,t)$ is

$$df = \left[\frac{\partial f}{\partial t} + A(X,t)\frac{\partial f}{\partial x} + \frac{B(X,t)^2}{2}\frac{\partial^2 f}{\partial x^2}\right]dt + B(X,t)\frac{\partial f}{\partial x}dW(t). \tag{1.198}$$

We define the transformation $f(n,t) = \log(n(t))$. The SDE is

$$df = \left[a(n(t)) - \frac{b(n(t))^2}{2}\right]dt + b(n(t))dW(t), \tag{1.199}$$

which reveals that the tendency for population density to increase/decrease is given by the sign of $\lim_{t\to\infty} \int_0^t a(n(s)) - \frac{b(n(s))^2}{2} ds$. For resident species, $\mathbb{E}_t\left[a(n) - \frac{b(n)^2}{2}\right] = 0$. In SDEs, the quantity $a(n) - \frac{b(n)^2}{2}$ plays the same role that the logged finite rate of increase plays in discrete time models. The discounting of the expected per capita growth rate by half of the variance should be reminiscent of Eq.1.180.

For illustrative purposes, we have thus far looked at a univariate, non-spatial SDE. To make the general SDE notation more congruent with the formalism of spatiotemporal MCT, we first define the local per capita growth rate, r_j, as the output of the function g_j:

$$r_j := g_j(E_j, C_j) = a_j(C_j) + b_j(C_j)(E_j - E_j^*). \tag{1.200}$$

The model has been parameterized so that $\mathrm{Var}(E_j(x,t))$ (the variance of $E_j(x,t)$ across sample paths)

is not proportional to the time step. For example, consider the Lotka Volterra model with spatiotemporal environmental noise

$$n_j'(x,t+dt) - n_j(x,t) = \left(1 - \sum_{k=1}^{S} \alpha_{jk} n_k(x,t)\right) dt + \epsilon_j(x) dt + \sigma_j dW_j(t), \tag{1.201}$$

where $\epsilon_j(x)$ is the effect of location x on environmental noise, σ_j is the scale of temporal environmental fluctuations, and $n_j'(x,t)$ is the population density after the local population growth phase, but before the dispersal phase. Here, the competition parameter is $C_j(x,t) = \sum_{k=1}^{S} \alpha_{jk} n_k(x,t)$ by convention (Chesson, 1994, Section 5). The environmental parameter is $E_j(x,t) = \epsilon_j(x) + \sigma_j dW_j(t)/\sqrt{dt}$; because $\mathbb{E}[dW] = dt$ (Karlin and Taylor, 1981, p.347), division by $\sqrt{dt}$ ensures that variances of E_j will not be proportional to the time step. With E_j and C_j defined in this way, we have $\mathrm{Var}(E_j(x,t)) = \sigma_j^2$ and $g_j(E_j, C_j) = (1 - C_j) + E_j$.

Following the logic of Section 1.2.B.3, the metapopulation per capita growth rate is

$$\widetilde{r}_j = \mathbb{E}_x[r] + \mathrm{Cov}_x(\nu_j, r_j)\,, \tag{1.202}$$

To approximate the average per capita growth rate, we approximate $\mathbb{E}_t[\widetilde{r_j}]$ and $\mathrm{Var}_t(\widetilde{r_j})$ with Taylor series of g_j about E_j and C_j; and truncate using the small-noise assumptions (Appendix 1.2.B.2). The result is

$$\begin{aligned}\left(\mathbb{E}_t[\widetilde{r_j}] - \frac{\mathrm{Var}_t(\widetilde{r_j})}{2}\right) \approx\ & \alpha_j^{(1)} \mathbb{E}_{x,t}\big[(E_j - E_j^*)\big] + \beta_j^{(1)} \mathbb{E}_{x,t}\big[(C_j - C_j^*)\big] \\ & + \frac{1}{2}\alpha_j^{(2)} \mathrm{Var}_{x,t}(E_j) + \frac{1}{2}\beta_j^{(2)} \mathrm{Var}_{x,t}(C_j) + \zeta_j \mathrm{Cov}_{x,t}(E_j, C_j) \\ & + \mathbb{E}_t\Big[\mathrm{Cov}_x\Big(\nu_j, \alpha_j^{(1)}(E_j - E_j^*) + \beta_j^{(1)}(C_j - C_j^*)\Big)\Big] \\ & - \frac{1}{2}{\alpha_j^{(1)}}^2 \mathrm{Var}_t(\mathbb{E}_x[E_j]) - \frac{1}{2}{\beta_j^{(1)}}^2 \mathrm{Var}_t(\mathbb{E}_x[E_j]) - \alpha_j^{(1)}\beta_j^{(1)} \mathrm{Cov}_t(\mathbb{E}_x[E_j]\,, \mathbb{E}_x[C_j])\,,\end{aligned} \tag{1.203}$$

which is nearly identical to the corresponding discrete-time approximation (Eq.1.182), the only difference being that the function $g_j(E_j, C_j)$ generates the per capita growth rate as opposed to the finite rate of increase, such that the Taylor series coefficients have different meanings. Because of the correspondence between the continuous-time and discrete-time approximations of the average growth rate, equations from the main text (Eq.2.14–Eq.1.63 & Eq.1.85–Eq.1.104) can be used to calculate the small-noise coexistence mechanisms for SDE models, again with the caveat that the Taylor series coefficients may have different meanings.

The derivation of exact coexistence mechanisms follows Section 1.2.3.3 from the main text, except that $r_j - \frac{(r_j - \mathbb{E}_t[r_j])^2}{2}$ is used in place of $\log(\lambda)$.

Formulas for exact coexistence mechanisms in SDE models

The invasion growth rate

$$\left(\mathbb{E}_t[\widetilde{r_i}] - \frac{\mathrm{Var}_t(\widetilde{r_i})}{2}\right) = \Delta {E_i}^{(e)} + \Delta {\rho_i}^{(e)} + \Delta {\mathrm{N}_i}^{(e)} + \Delta {\mathrm{I}_i}^{(e)} + \Delta {\kappa_i}^{(e)}, \tag{1.204}$$

Density-independent effects

$$\Delta {E_i}^{(e)} = \overline{\mathscr{E}_i} - \frac{1}{S-1}\sum_{r\neq i}^{S} \frac{GT_r}{GT_i}\overline{\mathscr{E}_r} \tag{1.205}$$

$$\overline{\mathscr{E}}_j = \mathbb{E}_t\left[\mathbb{E}_x\big[g_j(E_j, C_j^*)\big] - \frac{\big(\mathbb{E}_x\big[g_j(E_j, C_j^*)\big] - \mathbb{E}_{x,t}\big[g_j(E_j, C_j^*)\big]\big)^2}{2}\right] \tag{1.206}$$

Linear density-dependent effects

$$\Delta {\rho_i}^{(e)} = g_i(E_i^*, \mathbb{E}_{x,t}[C_i]) - \frac{1}{S-1}\sum_{r\neq i}^{S} \frac{GT_r}{GT_i} g_r(E_r^*, \mathbb{E}_{x,t}[C_r]) \tag{1.207}$$

Relative nonlinearity

$$\Delta {N_i}^{(e)} = \left[\overline{\mathscr{C}_i} - \frac{1}{S-1}\sum_{r\neq i}^{S} \frac{GT_r}{GT_i}\overline{\mathscr{C}_r}\right] - \Delta {\rho_i}^{(e)} \tag{1.208}$$

$$\overline{\mathscr{C}}_j = \mathbb{E}_t\left[\mathbb{E}_x\big[g_j(E_j^*, C_j)\big] - \frac{\big(\mathbb{E}_x\big[g_j(E_j^*, C_j)\big] - \mathbb{E}_{x,t}\big[g_j(E_j^*, C_j)\big]\big)^2}{2}\right] \tag{1.209}$$

The storage effect

$$\Delta {I_i}^{(e)} = \overline{\mathscr{I}_i} - \frac{1}{S-1}\sum_{r\neq i}^{S} \frac{GT_r}{GT_i}\overline{\mathscr{I}_r} \tag{1.210}$$

$$\overline{\mathscr{I}_j} = \mathbb{E}_t\left[\mathbb{E}_x[g_j(E_j, C_j)] - \frac{\left(\mathbb{E}_x[g_j(E_j, C_j)] - \mathbb{E}_{x,t}[g_j(E_j, C_j)]\right)^2}{2}\right] - \left(\overline{\mathscr{E}_j} + \overline{\mathscr{C}_j}\right) \tag{1.211}$$

Fitness-density covariance

$$\Delta\kappa_i{}^{(e)} = \overline{\mathscr{K}_i} - \frac{1}{S-1}\sum_{r\neq i}^{S}\frac{GT_r}{GT_i}\overline{\mathscr{K}_r} \tag{1.212}$$

$$\overline{\mathscr{K}}_j = \mathbb{E}_t\left[\mathbb{E}_x[\nu_j\ g_j(E_j, C_j)] - \frac{\left(\mathbb{E}_x[\nu_j\ g_j(E_j, C_j)] - \mathbb{E}_t[\mathbb{E}_x[\nu_j\ g_j(E_j, C_j)]]\right)^2}{2}\right] \tag{1.213}$$

$$- \mathbb{E}_t\left[\mathbb{E}_x[g_j(E_j, C_j)] - \frac{\left(\mathbb{E}_x[g_j(E_j, C_j)] - \mathbb{E}_{x,t}\left[g_j(E_j, C_j^*)\right]\right)^2}{2}\right]$$

$$= \mathbb{E}_t\left[\mathbb{E}_x[\nu_j\ g_j(E_j, C_j)] - \frac{\left(\mathbb{E}_x[\nu_j\ g_j(E_j, C_j)] - \mathbb{E}_t[\mathbb{E}_x[\nu_j\ g_j(E_j, C_j)]]\right)^2}{2}\right] - \left(\overline{\mathscr{E}_j} + \overline{\mathscr{C}_j} + \overline{\mathscr{I}_j}\right) \tag{1.214}$$

1.2.E.2 Continuous-time models (non-SDEs)

When the dynamics of population density are not governed by SDEs (even when E_j or C_j are governed by SDEs, as in Li and Chesson, 2016) a simple arithmetic average over space and time gives the correct average growth rate. With the function g_j generating the per capita growth rate, dn_j/dt, the average growth rate can be approximated as

$$\begin{aligned}\mathbb{E}_t[\widetilde{r_j}] \approx\ & \alpha_j^{(1)}\mathbb{E}_{x,t}\left[(E_j - E_j^*)\right] + \beta_j^{(1)}\mathbb{E}_{x,t}\left[(C_j - C_j^*)\right] \\ & + \frac{1}{2}\alpha_j^{(2)}\mathrm{Var}_{x,t}(E_j) + \frac{1}{2}\beta_j^{(2)}\mathrm{Var}_{x,t}(C_j) + \zeta_j\mathrm{Cov}_{x,t}(E_j, C_j) \\ & + \mathbb{E}_t\Big[\mathrm{Cov}_x\Big(\nu_j, \alpha_j^{(1)}(E_j - E_j^*) + \beta_j^{(1)}(C_j - C_j^*)\Big)\Big].\end{aligned} \tag{1.215}$$

Here, there is no discounting for temporal variation, so spatial and temporal variation are treated symmetrically (with the exception of fitness density covariance). The small-noise and exact coexistence mechanisms are as follows:

Formulas for small-noise coexistence mechanisms in (non-SDE) continuous-time models

The invasion growth rate

$$\mathbb{E}_t[\widetilde{r}_i] \approx \Delta E_i + \Delta\rho_i + \Delta \mathrm{N}_i + \Delta \mathrm{I}_i + \Delta\kappa_i \tag{1.216}$$

Density-independent effects

$$\begin{aligned}\Delta E_i = &\left[\alpha_i^{(1)}\mathbb{E}_{x,t}[E_i - E_i^*] + \frac{1}{2}\alpha_i^{(2)}\mathrm{Var}_{x,t}(E_i)\right] \\ &- \frac{1}{S-1}\sum_{r\neq i}^{S}\frac{GT_r}{GT_i}\left[\alpha_r^{(1)}\mathbb{E}_{x,t}[E_r - E_r^*] + \frac{1}{2}\alpha_r^{(2)}\mathrm{Var}_{x,t}(E_r)\right]\end{aligned} \tag{1.217}$$

Linear density-dependent effects

$$\Delta\rho_i = \beta_i^{(1)}\mathbb{E}_{x,t}[C_i - C_i^*] - \frac{1}{S-1}\sum_{r\neq i}^{S}\frac{GT_r}{GT_i}\beta_r^{(1)}\mathbb{E}_{x,t}[C_r - C_r^*] \tag{1.218}$$

Relative nonlinearity

$$\Delta N_i = \frac{1}{2}\beta_i^{(2)}\mathrm{Var}_{x,t}(C_i) - \frac{1}{S-1}\sum_{r\neq i}^{S}\frac{GT_r}{GT_i}\frac{1}{2}\beta_r^{(2)}\mathrm{Var}_{x,t}(C_r) \tag{1.219}$$

The storage effect

$$\Delta I_i = \zeta_i\mathrm{Cov}_{x,t}(E_i, C_i) - \frac{1}{S-1}\sum_{r\neq i}^{S}\frac{GT_r}{GT_i}\zeta_r\mathrm{Cov}_{x,t}(E_r, C_r) \tag{1.220}$$

Fitness-density covariance

$$\Delta\kappa_i = \mathbb{E}_t\Big[\mathrm{Cov}_x\Big(\nu_i, \alpha_i^{(1)}E_i + \beta_i^{(1)}C_i\Big)\Big] - \frac{1}{S-1}\sum_{r\neq i}^{S}\frac{GT_r}{GT_i}\mathbb{E}_t\Big[\mathrm{Cov}_x\Big(\nu_r, \alpha_r^{(1)}E_r + \beta_r^{(1)}C_r\Big)\Big] \tag{1.221}$$

Formulas for exact coexistence mechanisms in (non-SDE) continuous-time models

The invasion growth rate

$$\mathbb{E}_t[\widetilde{r_i}] = \Delta {E_i}^{(e)} + \Delta {\rho_i}^{(e)} + \Delta {\mathrm{N}_i}^{(e)} + \Delta {\mathrm{I}_i}^{(e)} + \Delta {\kappa_i}^{(e)}, \tag{1.222}$$

Density-independent effects

$$\Delta {E_i}^{(e)} = \overline{\mathscr{E}_i} - \frac{1}{S-1}\sum_{r\neq i}^{S} \frac{GT_r}{GT_i}\overline{\mathscr{E}_r} \tag{1.223}$$

$$\overline{\mathscr{E}}_j = \mathbb{E}_{x,t}\big[g_j(E_j, C_j^*)\big] \tag{1.224}$$

Linear density-dependent effects

$$\Delta {\rho_i}^{(e)} = g_i(E_i^*, \mathbb{E}_{x,t}[C_i]) - \frac{1}{S-1}\sum_{r\neq i}^{S} \frac{GT_r}{GT_i} g_r(E_r^*, \mathbb{E}_{x,t}[C_r]) \tag{1.225}$$

Relative nonlinearity

$$\Delta {N_i}^{(e)} = \left[\overline{\mathscr{C}_i} - \frac{1}{S-1}\sum_{r\neq i}^{S} \frac{GT_r}{GT_i}\overline{\mathscr{C}_r}\right] - \Delta {\rho_i}^{(e)} \tag{1.226}$$

$$\overline{\mathscr{C}}_j = \mathbb{E}_{x,t}\big[g_j(E_j^*, C_j)\big] \tag{1.227}$$

The storage effect

$$\Delta {I_i}^{(e)} = \overline{\mathscr{I}_i} - \frac{1}{S-1}\sum_{r\neq i}^{S} \frac{GT_r}{GT_i}\overline{\mathscr{I}_r} \tag{1.228}$$

$$\overline{\mathscr{I}_j} = \mathbb{E}_{x,t}[g_j(E_j, C_j)] - \big(\overline{\mathscr{E}_j} + \overline{\mathscr{C}_j}\big) \tag{1.229}$$

Fitness-density covariance

$$\Delta\kappa_i{}^{(e)} = \overline{\mathscr{K}_i} - \frac{1}{S-1}\sum_{r\neq i}^{S}\frac{GT_r}{GT_i}\overline{\mathscr{K}_r} \tag{1.230}$$

$$\overline{\mathscr{K}}_j = \mathbb{E}_{x,t}[\nu_j\ g_j(E_j, C_j)] - \mathbb{E}_{x,t}[g_j(E_j, C_j)] \tag{1.231}$$

$$\mathbb{E}_{x,t}[\nu_j\ g_j(E_j, C_j)] - \left(\overline{\mathscr{E}_j} + \overline{\mathscr{C}_j} + \overline{\mathscr{I}_j}\right) \tag{1.232}$$

1.2.E.3 Multiple regulating factors

In the spatiotemporal lottery model, competition is a function of just one regulating factor: open reef territories. In more realistic models, we may want to cast competition as function of L regulating factors, $\boldsymbol{F} = (F_1, F_2, ..., F_L)$, which may be species densities, refugia, resources, natural enemies:

$$C_j = \phi_j(\boldsymbol{F}). \tag{1.233}$$

In previous work (e.g., Barabás et al., 2018; Chesson, 2020), the finite rate of increase is directly expanded with respect to the regulating factors. We will expand the competition-generating function ϕ_j with respect to the regulating factors, and then substitute the expansion for C_j within the mathematical expressions for small-noise coexistence mechanisms. Our approach makes the formulas slightly longer (unlike previous theory, the coefficients $\beta_j^{(1)}$ and $\beta_j^{(2)}$ are not absorbed into $\phi_{jk}^{(1)}$ and $\phi_{jkl}^{(2)}$, the Taylor series coefficients of ϕ_j), but in substituting $\phi_j(\boldsymbol{F})$ for C_j, we demonstrate that the case of multiple regulating factors is not different from what is presented in the main text. Note however that in some models, the only reasonable choice for the competition parameter results in $C_j = \lambda_j$, such that $\beta_j^{(1)} = \beta_j^{(2)} = 1$.

Formulas for small-noise coexistence mechanisms which explicitly use the regulating factors can be obtained by taking the formulas for small-noise coexistence mechanisms in the main text (Eq.2.14–Eq.1.63), substituting in the Taylor series expansion of ϕ_j in place of C_j, and truncating using the small-noise assumptions. To Taylor-expand ϕ_j, one must select equilibrium values $\boldsymbol{F^{*j}}$ such that $C_j^* = \phi_j(\boldsymbol{F}^{*j})$. This task may be guided by the conditions $F_k - F_k^{*j} = \mathcal{O}(\sigma)$ and $\mathbb{E}_{x,t}[F_k] - F_k^{*j} = \mathcal{O}(\sigma^2)$, which are implied by the small-noise assumptions (Appendix 1.2.B.2). Note that the equilibrium levels of the regulating factors can be species-specific (hence the superscript "j"). There is no best way to select the equilibrium parameters, but various strategies are discussed briefly by Johnson and Hastings, 2022a, Appendix 1. The Taylor series

coefficients are denoted $\phi^{(1)}_{jk} = \frac{\partial \phi_j(\boldsymbol{F^{*j}})}{\partial F_k}$ and $\phi^{(2)}_{jkl} = \frac{\partial^2 \phi_j(\boldsymbol{F^{*j}})}{\partial F_k \partial F_l}$.

Formulas for small-noise coexistence mechanisms: multiple regulating factors

The invasion growth rate

$$\mathbb{E}_t\Big[\log\Big(\widetilde{\lambda}_i\Big)\Big] \approx \Delta E_i + \Delta\rho_i + \Delta \mathrm{N}_i + \Delta \mathrm{I}_i + \Delta\kappa_i, \tag{1.234}$$

Density-independent effects

$$\begin{aligned}\Delta E_i = &\left[\alpha_i^{(1)}\mathbb{E}_{x,t}[(E_i - E_i^*)] + \frac{1}{2}\alpha_i^{(2)}\mathrm{Var}_{x,t}(E_i) - \frac{1}{2}{\alpha_i^{(1)}}^2\mathrm{Var}_t(\mathbb{E}_x[E_i])\right] \\ &- \frac{1}{S-1}\sum_{r\neq i}^{S}\frac{GT_r}{GT_i}\left[\alpha_r^{(1)}\mathbb{E}_{x,t}[(E_r - E_r^*)] + \frac{1}{2}\alpha_r^{(2)}\mathrm{Var}_{x,t}(E_r) - \frac{1}{2}{\alpha_r^{(1)}}^2\mathrm{Var}_t(\mathbb{E}_x[E_r])\right]\end{aligned} \tag{1.235}$$

Linear density-dependent effects

$$\Delta\rho_i = \left[\sum_{k=1}^{L}\beta_i^{(1)}\phi_{ik}^{(1)}\mathbb{E}_{x,t}\big[F_k - F_k^{*i}\big]\right] - \frac{1}{S-1}\sum_{r\neq i}^{S}\frac{GT_r}{GT_i}\left[\sum_{k=1}^{L}\beta_r^{(1)}\phi_{rk}^{(1)}\mathbb{E}_{x,t}[F_k - F_k^{*r}]\right] \tag{1.236}$$

Relative nonlinearity

$$\begin{aligned}\Delta \mathrm{N}_i = &\frac{1}{2}\left[\sum_{k=1}^{L}\sum_{l=1}^{L}\Big(\beta_i^{(2)}\phi_{ikl}^{(2)}\mathrm{Cov}_{x,t}(F_k,F_l) - {\beta_i^{(1)}}^2\phi_{ik}^{(1)}\phi_{il}^{(1)}\mathrm{Cov}_t(\mathbb{E}_x[F_k],\mathbb{E}_x[F_l])\Big)\right] \\ &- \frac{1}{S-1}\sum_{r\neq i}^{S}\frac{GT_r}{GT_i}\frac{1}{2}\left[\sum_{k=1}^{L}\sum_{l=1}^{L}\Big(\beta_r^{(2)}\phi_{rkl}^{(2)}\mathrm{Cov}_{x,t}(F_k,F_l) - {\beta_r^{(1)}}^2\phi_{rk}^{(1)}\phi_{rl}^{(1)}\mathrm{Cov}_t(\mathbb{E}_x[F_k],\mathbb{E}_x[F_l])\Big)\right]\end{aligned} \tag{1.237}$$

The storage effect

$$\begin{aligned}\Delta \mathrm{I}_i = &\left[\sum_{k=1}^{L}\Big(\zeta_i\phi_{ik}^{(1)}\mathrm{Cov}_{x,t}(E_i,F_k) - \alpha_i^{(1)}\beta_i^{(1)}\phi_{ik}^{(1)}\mathrm{Cov}_t(\mathbb{E}_x[E_i],\mathbb{E}_x[F_k])\Big)\right] \\ &- \frac{1}{S-1}\sum_{r\neq i}^{S}\frac{GT_r}{GT_i}\left[\sum_{k=1}^{L}\Big(\zeta_r\phi_{rk}^{(1)}\mathrm{Cov}_{x,t}(E_r,F_k) - \alpha_r^{(1)}\beta_r^{(1)}\phi_{rk}^{(1)}\mathrm{Cov}_t(\mathbb{E}_x[E_r],\mathbb{E}_x[F_k])\Big)\right]\end{aligned} \tag{1.238}$$

Fitness-density covariance

$$\Delta\kappa_i = \left[\sum_{k=1}^{L} \mathbb{E}_t\Big[\mathrm{Cov}_x\Big(\nu_i, \alpha_i^{(1)} E_i + \beta_i^{(1)}\phi_{ik}^{(1)} F_k\Big)\Big]\right] - \frac{1}{S-1}\sum_{r\neq i}^{S}\frac{GT_r}{GT_i}\left[\sum_{k=1}^{L}\mathbb{E}_t\Big[\mathrm{Cov}_x\Big(\nu_r, \alpha_r^{(1)} E_r + \beta_r^{(1)}\phi_{rk}^{(1)} F_k\Big)\Big]\right] \tag{1.239}$$

The regulating factors have additive effects on the coexistence mechanisms, thus allowing the contribution of subsets of regulating factors to be extracted. We will demonstrate how this partitioning would work, using examples with a single regulating factor, F_k.

The contribution of regulating factor F_k to the linear density-dependent effects, i.e., species i's degree of specialization on F_k:

$$\beta_i^{(1)}\phi_{ik}^{(1)}\mathbb{E}_{x,t}\big[F_k - F_k^{*i}\big] - \frac{1}{S-1}\sum_{r\neq i}^{S}\frac{GT_r}{GT_i}\beta_r^{(1)}\phi_{rk}^{(1)}\mathbb{E}_{x,t}[F_k - F_k^{*r}]\,.$$

The contribution of regulating factor F_k to the storage effect:

$$\Big[\zeta_i\phi_{ik}^{(1)}\mathrm{Cov}_{x,t}(E_i, F_k) - \alpha_i^{(1)}\beta_i^{(1)}\phi_{ik}^{(1)}\mathrm{Cov}_t(\mathbb{E}_x[E_i]\,, \mathbb{E}_x[F_k])\Big] - \frac{1}{S-1}\sum_{r\neq i}^{S}\frac{GT_r}{GT_i}\Big[\zeta_r\phi_{rk}^{(1)}\mathrm{Cov}_{x,t}(E_r, F_k) - \alpha_r^{(1)}\beta_r^{(1)}\phi_{rk}^{(1)}\mathrm{Cov}_t(\mathbb{E}_x[E_r]\,, \mathbb{E}_x[F_k])\Big]$$

It should also be straightforward to derive the space-time decompositions of the small-noise coexistence mechanisms. For example, the contribution of F_k to the time component of the storage effect is

$$\Big(\zeta_i\phi_{ik}^{(1)} - \alpha_i^{(1)}\beta_i^{(1)}\phi_{ik}^{(1)}\Big)\,\mathrm{Cov}_t(\mathbb{E}_x[E_i]\,, \mathbb{E}_x[F_k]) - \frac{1}{S-1}\sum_{r\neq i}^{S}\frac{GT_r}{GT_i}\Big(\zeta_r\phi_{rk}^{(1)} - \alpha_r^{(1)}\beta_r^{(1)}\phi_{rk}^{(1)}\Big)\,\mathrm{Cov}_t(\mathbb{E}_x[E_r]\,, \mathbb{E}_x[F_k])\,. \tag{1.240}$$

The contribution of regulating factor F_k to relative nonlinearity Arguably, there are several ways to partition relative nonlinearity further with respect to individual regulating factors.

1. The contribution of F_k's variance to relative nonlinearity, or equivalently, the degree of specialization on the variance in F_k:

$$\begin{aligned}
&\frac{1}{2}\left[\beta_i^{(2)}\phi_{ikk}^{(2)}\mathrm{Var}_{x,t}(F_k) - {\beta_i^{(1)}}^2\phi_{ik}^{(1)}\phi_{ik}^{(1)}\mathrm{Var}_t(\mathbb{E}_x[F_k])\right] \\
&-\frac{1}{S-1}\sum_{r\neq i}^{S}\frac{GT_r}{GT_i}\frac{1}{2}\left[\beta_r^{(2)}\phi_{rkk}^{(2)}\mathrm{Var}_{x,t}(F_k) - {\beta_r^{(1)}}^2\phi_{rk}^{(1)}\phi_{rk}^{(1)}\mathrm{Var}_t(\mathbb{E}_x[F_k])\right]
\end{aligned} \tag{1.241}$$

2. The contribution of covariance between F_k and F_l $(k \neq l)$ on relative nonlinearity, or equivalently, the degree of specialization on the covariance between F_k and F_l:

$$\begin{aligned}
&\left[\beta_i^{(2)}\phi_{ikl}^{(2)}\mathrm{Cov}_{x,t}(F_k,F_l) - {\beta_i^{(1)}}^2\phi_{ik}^{(1)}\phi_{il}^{(1)}\mathrm{Cov}_t(\mathbb{E}_x[F_k],\mathbb{E}_x[F_l])\right] \\
&-\frac{1}{S-1}\sum_{r\neq i}^{S}\frac{GT_r}{GT_i}\left[\beta_r^{(2)}\phi_{rkl}^{(2)}\mathrm{Cov}_{x,t}(F_k,F_l) - {\beta_r^{(1)}}^2\phi_{rk}^{(1)}\phi_{rl}^{(1)}\mathrm{Cov}_t(\mathbb{E}_x[F_k],\mathbb{E}_x[F_l])\right]
\end{aligned} \tag{1.242}$$

3. The total contribution of F_k to relative nonlinearity, including the contribution of the variance of F_k, and the contribution of covariances between F_k and other regulating factors:

$$\begin{aligned}
&\left[\frac{1}{2}\left(\beta_i^{(2)}\phi_{ikk}^{(2)}\mathrm{Var}_{x,t}(F_k) - {\beta_i^{(1)}}^2\phi_{ik}^{(1)}\phi_{ik}^{(1)}\mathrm{Var}_t(\mathbb{E}_x[F_k])\right)\right] \\
&-\left[\frac{1}{S-1}\sum_{r\neq i}^{S}\frac{GT_r}{GT_i}\frac{1}{2}\left(\beta_r^{(2)}\phi_{rkk}^{(2)}\mathrm{Var}_{x,t}(F_k) - {\beta_r^{(1)}}^2\phi_{rk}^{(1)}\phi_{rk}^{(1)}\mathrm{Var}_t(\mathbb{E}_x[F_k])\right)\right] \\
&+\left[\sum_{l\neq k}^{L}\left(\beta_i^{(2)}\phi_{ikl}^{(2)}\mathrm{Cov}_{x,t}(F_k,F_l) - {\beta_i^{(1)}}^2\phi_{ik}^{(1)}\phi_{il}^{(1)}\mathrm{Cov}_t(\mathbb{E}_x[F_k],\mathbb{E}_x[F_l])\right)\right] \\
&-\left[\frac{1}{S-1}\sum_{r\neq i}^{S}\frac{GT_r}{GT_i}\left[\sum_{l\neq k}^{L}\left(\beta_r^{(2)}\phi_{rkl}^{(2)}\mathrm{Cov}_{x,t}(F_k,F_l) - {\beta_r^{(1)}}^2\phi_{rk}^{(1)}\phi_{rl}^{(1)}\mathrm{Cov}_t(\mathbb{E}_x[F_k],\mathbb{E}_x[F_l])\right)\right]\right]
\end{aligned} \tag{1.243}$$

The exact coexistence mechanisms can be obtained by following the directions implied by the formulas in the main text (Eq.1.72–Eq.1.80). For example, the formula for ${\Delta\rho_i}^{(e)}$ (Eq.1.74) directs the user to set C_j to $\mathbb{E}_{x,t}[C_j]$; because $C_j = \phi_j(\boldsymbol{F})$, one would set $\phi_j(\boldsymbol{F})$ to $\mathbb{E}_{x,t}[\phi_j(\boldsymbol{F})]$.

However, to partition the coexistence mechanisms further into contributions from individual regulating factors, we need a slightly different approach: fix all regulating factors at $\boldsymbol{F^{*J}}$ and then modify the regulating factors one at a time. For example, when partitioning ${\Delta\rho_i}^{(e)}$, we set $\phi_j(F_1,\ldots,F_L)$ to $\phi_j(F_1^{*j},\ldots,\mathbb{E}_{x,t}[F_k],\ldots,F_L^{*j})$, one regulating factor at at a time, and then sum the L resulting pieces of invasion growth rate to approximate ${\Delta\rho_i}^{(e)}$. Unless ϕ_j is a linear function of the regulating factors, the aforementioned procedure will not exactly equal ${\Delta\rho_i}^{(e)}$ as defined in the main text (Section 1.2.3.3). This is discussed further below.

To define these exact coexistence mechanisms in a reasonable amount of page-space, new notation is

required. Let $\left\{\boldsymbol{v}^{-\{k\}}, a\right\}$ be a vector $\boldsymbol{v}$ where the k-th element has been replaced with a. Similarly, let $\left\{\boldsymbol{v}^{-\{k,l\}}, a, b\right\}$ be a vector $\boldsymbol{v}$ where the k-th element has been replaced with a, and the l-th element has been replaced by b. The notation introduced here allows us to express ideas such as holding all elements of $\boldsymbol{F}$ at their equilibrium values, except for F_k, which is held at its spatiotemporal average: $\left\{\boldsymbol{F^*}^{-\{k\}}, \mathbb{E}_{x,t}[F_k]\right\}$. The following formulas look complicated, but they express the simple idea, pioneered by Ellner et al. (2016, 2019), that coexistence mechanisms can be measured as the marginal effects of allowing some parameters to vary while holding the rest constant.

Formulas for exact coexistence mechanisms: multiple regulating factors

The invasion growth rate

$$\mathbb{E}_t\left[\log\left(\widetilde{\lambda}_i\right)\right] = \Delta {E_i}^{(e)} + \Delta {\rho_i}^{(e)} + \Delta {\mathrm{N}_i}^{(e)} + \Delta {\mathrm{I}_i}^{(e)} + \Delta {\kappa_i}^{(e)} + \Delta \epsilon_i, \tag{1.244}$$

Density-independent effects

$$\Delta {E_i}^{(e)} = \overline{\mathscr{E}_i} - \frac{1}{S-1}\sum_{r\neq i}^{S}\frac{GT_r}{GT_i}\overline{\mathscr{E}_r} \tag{1.245}$$

$$\overline{\mathscr{E}}_j = \mathbb{E}_t\left[\log\left(\mathbb{E}_x\left[g_j(E_j, \phi_j(\boldsymbol{F^{*j}})\right]\right)\right] \tag{1.246}$$

Linear density-dependent effects

$$\Delta {\rho_i}^{(e)} = \sum_{k=1}^{L}\Bigg[\log\left(g_i\left(E_i^*, \phi_i\left(\left\{\boldsymbol{F^{*i}}^{-\{k\}}, \mathbb{E}_{x,t}[F_k]\right\}\right)\right)\right) \tag{1.247}$$

$$- \frac{1}{S-1}\sum_{r\neq i}^{S}\frac{GT_r}{GT_i}\log\left(g_r\left(E_r^*, \phi_r\left(\left\{\boldsymbol{F^{*r}}^{-\{k\}}, \mathbb{E}_{x,t}[F_k]\right\}\right)\right)\right)\Bigg] \tag{1.248}$$

Relative nonlinearity

$$\Delta {N_i}^{(e)} = \left[\overline{\mathscr{C}_i} - \frac{1}{S-1}\sum_{r\neq i}^{S}\frac{GT_r}{GT_i}\overline{\mathscr{C}_r}\right] - \Delta {\rho_i}^{(e)} \tag{1.249}$$

$$\overline{\mathscr{C}}_j = \sum_{k=1}^{L}\sum_{l=1}^{k}\mathbb{E}_t\Big[\log\Big(\mathbb{E}_x\Big[g_j\left(E_j^*, \phi_j\left(\left\{\boldsymbol{F}^{*\boldsymbol{j}-\{k,l\}}, F_k, F_l\right\}\right)\right)\Big]\Big)\Big] \tag{1.250}$$

The storage effect

$$\Delta I_i{}^{(e)} = \overline{\mathscr{I}_i} - \frac{1}{S-1}\sum_{r\neq i}^{S}\frac{GT_r}{GT_i}\overline{\mathscr{I}_r} \tag{1.251}$$

$$\overline{\mathscr{I}_j} = \left[\sum_{k=1}^{L}\mathbb{E}_t\Big[\log\Big(\mathbb{E}_x\Big[g_j\left(E_j, \phi_j\left(\left\{\boldsymbol{F}^{*\boldsymbol{j}-\{k\}}, F_k\right\}\right)\right)\Big]\Big)\Big]\right] - \left(\overline{\mathscr{E}_j} + \overline{\mathscr{C}_j}\right) \tag{1.252}$$

Fitness-density covariance

$$\Delta\kappa_i{}^{(e)} = \overline{\mathscr{K}_i} - \frac{1}{S-1}\sum_{r\neq i}^{S}\frac{GT_r}{GT_i}\overline{\mathscr{K}_r} \tag{1.253}$$

$$\overline{\mathscr{K}}_j = \sum_{k=1}^{L}\mathbb{E}_t\Big[\log\Big(\mathbb{E}_x\Big[v_j\ g_j\left(E_j, \phi_j\left(\left\{\boldsymbol{F}^{*\boldsymbol{j}-\{k\}}, F_k\right\}\right)\right)\Big]\Big)\Big] \tag{1.254}$$

$$- \mathbb{E}_t\Big[\log\Big(\mathbb{E}_x\Big[g_j\left(E_j, \phi_j\left(\left\{\boldsymbol{F}^{*\boldsymbol{j}-\{k\}}, F_k\right\}\right)\right)\Big]\Big)\Big] \tag{1.255}$$

Remainder

$$\Delta\epsilon_i = \epsilon_i - \frac{1}{S-1}\sum_{r\neq i}^{S}\frac{GT_r}{GT_i}\epsilon_r \tag{1.256}$$

$$\epsilon_j = \mathbb{E}_t[\log(\mathbb{E}_x[v_j\ g_j(E_j, \phi_j(\boldsymbol{F})])] - \left(\overline{\mathscr{E}_j} + \overline{\mathscr{C}_j} + \overline{\mathscr{I}_j} + \overline{\mathscr{K}_j}\right) \tag{1.257}$$

The exact coexistence mechanisms here are different from those presented in the main text (Section 1.2.3.3: Eq.1.72–Eq.1.80), due to the fact that the competition parameter is generically a nonlinear function of the regulating factors, i.e., $\mathbb{E}_{x,t}\left[\phi_j(\boldsymbol{F})\right] \neq \sum_{k=1}^{L}\phi_j\left(\left\{\boldsymbol{F}^{*\boldsymbol{j}-\{k\}}, \mathbb{E}_{x,t}[F_k]\right\}\right)$. Normally, the precursor to the

exact fitness-density covariance, $\overline{\mathscr{K}}_j$, is defined as a deviation from the average growth rate. Above, we have defined $\overline{\mathscr{K}}_j$ differently — as deviations summed across regulating factors — and captured the remainder of the average growth rate with ϵ_j. The benefit of defining exact coexistence mechanisms in this way is that all canonical coexistence mechanisms can be partitioned into contributions from subsets of regulating factors.

1.2.E.4 Structured population models

In structured population models, the average per capita growth rate is replaced with the concept of the dominant lyapunov exponent (also known as the *stochastic growth rate*; Caswell, 2001, Section 14.3.3). Small-noise approximations of the stochastic growth rate tend to be complicated (Tuljapurkar, 1982), so we do not pursue them here.

The exact coexistence mechanisms can be computed using the formulas in the main text (Section 1.2.3.3: Eq.1.72–Eq.1.80) with one modification. Because the distribution of future population density is determined by $\sum_{t=0}^{\infty} \log\left(\|\boldsymbol{n'_j}(x,t+1)\|/\|\boldsymbol{n_j}(x,t)\|\right)$ (Tuljapurkar and Orzack, 1980), the function $g_j(E_j, C_j)$ now is taken to generate $\|\boldsymbol{n'_j}(x,t+1)\|/\|\boldsymbol{n_j}(x,t)\|$. Here, $\boldsymbol{n'_j}(x,t)$ is the vector of population densities corresponding to each age or stage class at location x and time t; $\boldsymbol{n'_j}(x,t+1)$ contains the population densities after the growth phase, but before the dispersal phase; and the operator $\|.\|$ computes the sum across of all elements in a vector. In models with continuous population structure (e.g., an integral projection models with size-dependent demographic rates), the population density becomes a function of continuous variables (e.g., $n_j(x,t,z)$, where z is body size), and $\|.\|$ computes the integral across said variables.

1.2.F The maximum number of species that can coexist via fitness density covariance

When there is no temporal variation, Eq.1.191 in Appendix 1.2.D reduces to

$$\begin{aligned}\mathbb{E}_t[\mathrm{Cov}_x(v_j,\lambda_j)] &\approx \frac{q}{1-q}\mathrm{Var}_x\left(\alpha_j^{(1)}(E_j(x)-E_j^*)+\beta_j^{(1)}(C_r(x)-C_r^*)\right)\\ &\approx \frac{q}{1-q}\left[{\alpha_j^{(1)}}^2\mathrm{Var}_x(E_j)+2\alpha_j^{(1)}\beta_j^{(1)}\mathrm{Cov}_x(E_j,C_j)+{\beta_j^{(1)}}^2\mathrm{Var}_x(C_j)\right].\end{aligned} \tag{1.258}$$

The competition parameter C_j can be expanded as a function of L regulating factors (see Appendix 1.2.E.3): $C_j = \phi_j(\boldsymbol{F})$, where $\boldsymbol{F} = (F_1, F_2, ..., F_L)$. The environment parameter can be expressed a vector of M discrete states: $E_j \in \boldsymbol{E'}$, where $\boldsymbol{E'} = (E'_1, E'_2, ..., E'_M)$. Then, there are $M \times L$ "effective regulating factors" with the form $\mathrm{Cov}_x(E'_m, F_k)$; and $L(L-1)/2$ "effective regulating factors" with the form $\mathrm{Cov}_x(F_k, F_l)$. This result shows that fitness density covariance can potentially support a large number of species.

Acknowledgements

We would like to thank Simon Stump, Sebastian Schreiber, and Oscar Godoy for discussions; and Logan Brissette for copy editing. This research is supported in part by NSF Grant DMS – 1817124 Metacommunity Dynamics: Integrating Local Dynamics, Stochasticity and Connectivity.

Data availability statement

The pertinent file `lottery_model_example.R` is available at https://github.com/ejohnson6767/spatiotemporal_coexistence.

References

Abrams, P. A. (1988). How should resources be counted? *Theoretical Population Biology*, *33*(2), 226–242.

Adler, P. B., HilleRisLambers, J., Kyriakidis, P. C., Guan, Q., & Levine, J. M. (2006). Climate variability has a stabilizing effect on the coexistence of prairie grasses. *Proceedings of the National Academy of Sciences*, *103*(34), 12793–12798.

Allen, L. J. (2010). *An introduction to stochastic processes with applications to biology* (2nd ed.). CRC press.

Angert, A. L., Huxman, T. E., Chesson, P., & Venable, D. L. (2009). Functional tradeoffs determine species coexistence via the storage effect. *Proceedings of the National Academy of Sciences*, *106*(28), 11641–11645.

Armstrong, R. A., & McGehee, R. (1976). Coexistence of species competing for shared resources. *Theoretical Population Biology*, *9*(3), 317–328.

Armstrong, R. A., & McGehee, R. (1980). Competitive exclusion. *The American Naturalist*, *115*(2), 151–170.

Assaf, M., & Meerson, B. (2010). Extinction of metastable stochastic populations. *Physical Review E*, *81*(2).

Ayala, F. J. (1969). Experimental invalidation of the principle of competitive exclusion. *Nature*, *224*(5224), 1076–1079.

Barabás, G., & D'Andrea, R. (2020). Chesson's coexistence theory: Reply. *Ecology*, *101*(11).

Barabás, G., D'Andrea, R., & Stump, S. M. (2018). Chesson's coexistence theory. *Ecological Monographs*, *88*(3), 277–303.

Benaïm, M., & Schreiber, S. J. (2019). Persistence and extinction for stochastic ecological models with internal and external variables. *Journal of mathematical biology*, *79*(1), 393–431.

Bienvenu, F., & Legendre, S. (2015). A new approach to the generation time in matrix population models. *The American Naturalist*, *185*(6), 834–843.

Blanchet, J., Glynn, P., & Zheng, S. (2016). Analysis of a stochastic approximation algorithm for computing quasi-stationary distributions. *Advances in Applied Probability*, *48*(3), 792–811.

Box, G. E. (1980). Sampling and bayes' inference in scientific modelling and robustness. *Journal of the Royal Statistical Society: Series A (General)*, *143*(4), 383–404.

Cáceres, C. E. (1997). Temporal variation, dormancy, and coexistence: A field test of the storage effect. *Proceedings of the National Academy of Sciences*, *94*(17), 9171–9175.

Carvalho, C. M., Polson, N. G., & Scott, J. G. (2009). Handling sparsity via the horseshoe. *Artificial Intelligence and Statistics*, 73–80.

Case, T. (2000). *An Illustrated Guide to Theoretical Ecology* (1st ed.). Oxford University Press.

Caswell, H. (2001). *Matrix population models: Construction, analysis, and interpretation* (2nd ed.). Sinauer Associates.

Caswell, H., & Etter, R. J. (1993). Ecological interactions in patchy environments: From patch-occupancy models to cellular automata. In *Patch dynamics* (pp. 93–109). Springer.

Chase, J. M., & Leibold, M. A. (2003). *Ecological niches: Linking classical and contemporary approaches*. University of Chicago Press.

Chesson, P. L., & Ellner, S. (1989). Invasibility and stochastic boundedness in monotonic competition models. *Journal of Mathematical Biology*, *27*(2), 117–138.

Chesson, P. (1990). Macarthur's consumer-resource model. *Theoretical Population Biology*, *37*(1), 26–38.

Chesson, P. (1994). Multispecies competition in variable environments. *Theoretical Population Biology*, *45*(3), 227–276.

Chesson, P. (2000). General theory of competitive coexistence in spatially-varying environments. *Theoretical Population Biology*, *58*(3), 211–237.

Chesson, P. (2003). Quantifying and testing coexistence mechanisms arising from recruitment fluctuations. *Theoretical Population Biology*, *64*(3), 345–357.

Chesson, P. (2008). Quantifying and testing species coexistence mechanisms. In *Unity in diversity: Reflections on ecology after the legacy of Ramon Margalef* (pp. 119–164). Fundacion BBVA Bilbao.

Chesson, P. (2018). Updates on mechanisms of maintenance of species diversity. *Journal of ecology*, *106*(5), 1773–1794.

Chesson, P. (2020). Chesson's coexistence theory: Comment. *Ecology*, *101*(11), e02851.

Chesson, P., & Huntly, N. (1997). The roles of harsh and fluctuating conditions in the dynamics of ecological communities. *The American Naturalist*, *150*(5), 519–553.

Chesson, P., & Kuang, J. J. (2010). The storage effect due to frequency-dependent predation in multispecies plant communities. *Theoretical Population Biology*, *78*(2), 148–164.

Chesson, P. L. (1985). Coexistence of competitors in spatially and temporally varying environments: A look at the combined effects of different sorts of variability. *Theoretical Population Biology*, *28*(3), 263–287.

Chesson, P. L., & Warner, R. R. (1981). Environmental variability promotes coexistence in lottery competitive systems. *The American Naturalist*, *117*(6), 923–943.

Chow, C. C., & Buice, M. A. (2015). Path integral methods for stochastic differential equations. *Journal of Mathematical Neuroscience*, *5*(1).

Chu, C., & Adler, P. B. (2015). Large niche differences emerge at the recruitment stage to stabilize grassland coexistence. *Ecological Monographs*, *85*(3), 373–392.

Cole, L. C. (1960). Competitive exclusion. *Science*, *132*(3423), 348–349.

Connor, E. F., & Simberloff, D. (1979). The Assembly of Species Communities: Chance or Competition? *Ecology*, *60*(6), 1132.

Cornell, H. V., & Lawton, J. H. (1992). Species Interactions, Local and Regional Processes, and Limits to the Richness of Ecological Communities: A Theoretical Perspective. *The Journal of Animal Ecology*, *61*(1), 1.

Cressie, N. (2015). *Statistics for spatial data*. John Wiley & Sons.

Darwin, C. M. A. (1859). *On the origins of species* (1st ed.). John Murray.

Dempster, E. R. (1955). Maintenance of genetic heterogeneity. *Cold Spring Harbor symposia on quantitative biology*, *20*.

Descamps-Julien, B., & Gonzalez, A. (2005). Stable coexistence in a fluctuating environment: An experimental demonstration. *Ecology*, *86*(10), 2815–2824.

Diamond, J. M., & Gilpin, M. E. (1982). Examination of the "null" model of connor and simberloff for species co-occurrences on Islands. *Oecologia*, *52*(1), 64–74.

Draper, D. (1995). Assessment and propagation of model uncertainty. *Journal of the Royal Statistical Society: Series B (Methodological)*, *57*(1), 45–70.

Duhem, P. M. M. (1954). *The aim and structure of physical theory*. Princeton University Press.

Ellner, S. (1989). Convergence to stationary distributions in two-species stochastic competition models. *Journal of Mathematical Biology*, *27*(4), 451–462.

Ellner, S. P. (2018). Generation time in structured populations. *The American Naturalist*, *192*(1), 105–110.

Ellner, S. P., Snyder, R. E., & Adler, P. B. (2016). How to quantify the temporal storage effect using simulations instead of math. *Ecology letters*, *19*(11), 1333–1342.

Ellner, S. P., Snyder, R. E., Adler, P. B., & Hooker, G. (2019). An expanded modern coexistence theory for empirical applications. *Ecology letters*, *22*(1), 3–18.

Ellner, S. P., Snyder, R. E., Adler, P. B., Hooker, G., & Schreiber, S. J. (2020). Technical Comment on Pande et al. (2020): Why invasion analysis is important for understanding coexistence. *Ecology Letters*, *23*(11), 1721–1724.

Ferrari, P., & Maric, N. (2007). Quasi stationary distributions and fleming-viot processes in countable spaces. *Electronic Journal of Probability*, *12*, 684–702.

Ferrière, R., & Galliard, J.-F. L. (2001). Invasion fitness and adaptive dynamics in spatial population models. *International Institute for Applied Systems Analysis Interim Report IR-01-043, September 2001.*

Fox, J. W., McGrady-Steed, J., & Petchey, O. L. (2000). Testing for local species saturation with nonindependent regional species pools. *Ecology Letters*, *3*(3), 198–206.

Garay, B. M., & Hofbauer, J. (2003). Robust permanence for ecological differential equations, minimax, and discretizations. *SIAM Journal on Mathematical Analysis*, *34*(5), 1007–1039.

Gardiner, C. W. (1985). *Handbook of stochastic methods* (Vol. 3). Springer.

Gause, G. F. (1934). *The struggle for existence.* Williams & Wilkins.

Gelman, A., & Hill, J. (2006). *Data analysis using regression and multilevel/hierarchical models.* Cambridge university press.

Gelman, A., & Vehtari, A. (2021). What are the most important statistical ideas of the past 50 years? *Journal of the American Statistical Association*, (just-accepted), 1–29.

Gelman, A., Vehtari, A., Simpson, D., Margossian, C. C., Carpenter, B., Yao, Y., Kennedy, L., Gabry, J., Bürkner, P.-C., & Modrák, M. (2020). Bayesian workflow. *arXiv preprint arXiv:2011.01808.*

Gilbert, O., Reynoldson, T., & Hobart, J. (1952). Gause's hypothesis: An examination. *Journal of Animal Ecology*, *21*(2), 310–312.

Glynn, P., & Sigman, K. (1998). Independent sampling of a stochastic process. *Stochastic processes and their applications*, *74*(2), 151–164.

Godoy, O., & Levine, J. M. (2014). Phenology effects on invasion success: Insights from coupling field experiments to coexistence theory. *Ecology*, *95*(3), 726–736.

Grainger, T. N., Letten, A. D., Gilbert, B., & Fukami, T. (2019). Applying modern coexistence theory to priority effects. *Proceedings of the National Academy of Sciences of the United States of America*, *116*(13), 6205–6210.

Grainger, T. N., Levine, J. M., & Gilbert, B. (2019). The Invasion Criterion: A Common Currency for Ecological Research. *Trends in Ecology and Evolution*, *34*(10), 925–935.

Groisman, P., & Jonckheere, M. (2012). Simulation of quasi-stationary distributions on countable spaces. *arXiv preprint arXiv:1206.6712.*

Gyllenberg, M., & Meszéna, G. (2005). On the impossibility of coexistence of infinitely many strategies. *Journal of Mathematical Biology*, *50*(2), 133–160.

Haigh, J., & Smith, J. M. (1972). Can there be more predators than prey? *Theoretical Population Biology*, *3*(3), 290–299.

Harrison, S., Safford, H. D., Grace, J. B., Viers, J. H., & Davies, K. F. (2006). Regional and local species richness in an insular environment: Serpentine plants in California. *Ecological Monographs*, *76*(1), 41–56.

Hastie, T., Tibshirani, R., & Friedman, J. (2009). *The elements of statistical learning: Data mining, inference, and prediction* (2nd ed.). Springer.

Hatfield, J. S., & Chesson, P. L. (1989). Diffusion analysis and stationary distribution of the two-species lottery competition model. *Theoretical Population Biology*, *36*(3), 251–266.

Hening, A., & Nguyen, D. H. (2020). The competitive exclusion principle in stochastic environments. *Journal of mathematical biology*, *80*(5), 1323–1351.

Hennemuth, R. C., Palmer, J. E., & Brown, B. E. (1980). A Statistical Description of Recruitment in Eighteen Selected Fish Stocks. *Journal of Northwest Atlantic Fishery Science*, *1*, 101–111.

Hiebeler, D. E., & Millett, N. E. (2011). Pair and triplet approximation of a spatial lattice population model with multiscale dispersal using markov chains for estimating spatial autocorrelation. *Journal of theoretical biology*, *279*(1), 74–82.

Hofbauer, J. (1981). A general cooperation theorem for hypercycles. *Monatshefte für Mathematik*, *91*(3), 233–240.

Hubbell, S. P. (2001). *The unified neutral theory of biodiversity and biogeography*. Princeton University Press.

Hume, D. (1748). *An enquiry concerning human understanding*.

Hurtt, G. C., & Pacala, S. W. (1995). The consequences of recruitment limitation: Reconciling chance, history and competitive differences between plants. *Journal of theoretical biology*, *176*(1), 1–12.

Hutchinson, G. E. (1961). The paradox of the plankton. *The American Naturalist*, *95*(882), 137–145.

Ignace, D. D., Huntly, N., & Chesson, P. (2018). The role of climate in the dynamics of annual plants in a chihuahuan desert ecosystem. *Evolutionary Ecology Research*, *19*(3), 279–297.

Izmest'eva, L., Silow, E., & Litchman, E. (2011). Long-term dynamics of lake baikal pelagic phytoplankton under climate change. *Inland Water Biology*, *4*(3), 301–307.

Johnson, E. C., & Hastings, A. (2022a). Methods for calculating coexistence mechanisms: Beyond scaling factors. *Oikos*.

Johnson, E. C., & Hastings, A. (2022b). Towards a heuristic understanding of the storage effect. *Ecology Letters*.

Kamenev, A., Meerson, B., & Shklovskii, B. (2008). How colored environmental noise affects population extinction. *Physical Review Letters*, *101*(26), 268103.

Karlin, S., & Taylor, H. E. (1981). *A second course in stochastic processes* (1st ed.). Academic Press.

Kryscio, R. J., & Lefévre, C. (1989). On the extinction of the sis stochastic logistic epidemic. *Journal of Applied Probability*, 685–694.

Kuang, J. J., & Chesson, P. (2010). Interacting coexistence mechanisms in annual plant communities: Frequency-dependent predation and the storage effect. *Theoretical Population Biology*, *77*(1), 56–70.

Law, R., & Watkinson, A. (1987). Response-surface analysis of two-species competition: An experiment on phleum arenarium and vulpia fasciculata. *The Journal of Ecology*, 871–886.

Le Galliard, J.-F., Ferrière, R., & Dieckmann, U. (2003). The adaptive dynamics of altruism in spatially heterogeneous populations. *Evolution*, *57*(1), 1–17.

Levin, S. A. (1970). Community equilibria and stability, and an extension of the competitive exclusion principle. *The American Naturalist*, *104*(939), 413–423.

Levin, S. A. (1974). Dispersion and population interactions. *The American Naturalist*, *108*(960), 207–228.

Levins, R. (1979). Coexistence in a variable environment. *The American Naturalist*, *114*(6), 765–783.

Lewens, T. (2010). Natural selection then and now. *Biological Reviews*, *85*(4), 829–835.

Lewis, D. (1973). Counterfactuals and comparative possibility. In *Ifs* (pp. 57–85). Springer.

Lewis, D. (1979). Counterfactual Dependence and Time's Arrow. *Noûs*, *13*(4), 455.

Lewontin, R. C., & Cohen, D. (1969). On population growth in a randomly varying environment. *Proceedings of the National Academy of Sciences of the United States of America*, *62*(4), 1056–1060.

Li, L., & Chesson, P. (2016). The effects of dynamical rates on species coexistence in a variable environment: The paradox of the plankton revisited. *The American Naturalist*, *188*(2), E46–E58.

Lotka, A. J. (1932). The growth of mixed populations: Two species competing for a common food supply. *Journal of the Washington Academy of Sciences*, *22*(16-17), 461–469.

MacArthur, R. (1970). Species packing and competitive equilibrium for many species. *Theoretical Population Biology*, *1*(1), 1–11.

Magurran, A. E., & Henderson, P. A. (2003). Explaining the excess of rare species in natural species abundance distributions. *Nature*, *422*(6933), 714–716.

Martyn, T. E., Stouffer, D. B., Godoy, O., Bartomeus, I., Pastore, A. I., & Mayfield, M. M. (2021). Identifying "useful" fitness models: Balancing the benefits of added complexity with realistic data requirements in models of individual plant fitness. *The American Naturalist*, *197*(4), 415–433.

May, R. (1981). Models for two interacting populations. In R. May (Ed.), *Theoretical ecology: Principles and applications*. Sinauer Associates.

McGill, B. J. (2003). Does mother nature really prefer rare species or are log-left-skewed sads a sampling artefact? *Ecology Letters*, *6*(8), 766–773.

Metz, J., Nisbet, R., & Geritz, S. (1992). How should we define 'fitness' for general ecological scenarios? *Trends in Ecology & Evolution*, *7*(6), 198–202.

Mill, J. S. (1856). *A system of logic, ratiocinative and inductive: 1* (Vol. 1). Parker.

Miller, E. T., & Klausmeier, C. A. (2017). Evolutionary stability of coexistence due to the storage effect in a two-season model. *Theoretical Ecology*, *10*(1), 91–103.

Mittelbach, G. G. (2019). *Community ecology* (2nd ed.). Oxford University Press.

Moore, J., & Desmond, A. (1991). *Darwin: The life of a tormented evolutionist*. W. W. Norton & Company.

Nåsell, I. (2001). Extinction and quasi-stationarity in the verhulst logistic model. *Journal of Theoretical Biology*, *211*(1), 11–27.

Nee, S., Harvey, P. H., & May, R. M. (1991). Lifting the veil on abundance patterns. *Proceedings of the Royal Society of London. Series B: Biological Sciences*, *243*(1307), 161–163.

Nisbet, R. M., & C., G. W. S. (1982). *Modelling fluctuating populations* (1st ed.). Wiley.

Norden, R. (1982). On the distribution of the time to extinction in the stochastic logistic population model. *Advances in Applied Probability*, 687–708.

Pande, J., Fung, T., Chisholm, R., & Shnerb, N. M. (2020). Mean growth rate when rare is not a reliable metric for persistence of species. *Ecology letters*, *23*(2), 274–282.

Pande, J., & Shnerb, N. M. (2020). Taming the diffusion approximation through a controlling-factor wkb method. *Physical Review E*, *102*(6), 062410.

Pearl, J., & Mackenzie, D. (2018). *The book of why: The new science of cause and effect*. Basic Books.

Pielou, E. C. (1969). *An introduction to mathematical ecology*. Wiley-Interscience.

Pueyo, S. (2006). Diversity: Between neutrality and structure. *Oikos*, *112*(2), 392–405.

Ripley, B. J., & Caswell, H. (2006). Recruitment variability and stochastic population growth of the soft-shell clam, Mya arenaria. *Ecological Modelling*, *193*(3-4), 517–530.

Roth, G., & Schreiber, S. J. (2014). Persistence in fluctuating environments for interacting structured populations. *Journal of Mathematical Biology*, *69*(5), 1267–1317.

Sale, P. F. (1977). Maintenance of High Diversity in Coral Reef Fish Communities. *The American Naturalist*, *111*(978), 337–359.

Schoener, T. W. (1982). The controversy over interspecific competition: Despite spirited criticism, competition continues to occupy a major domain in ecological thought. *American Scientist*, *70*(6), 586–595.

Schreiber, S. J. (2000). Criteria for Cr robust permanence. *Journal of Differential Equations*, *162*(2), 400–426.

Schreiber, S. J. (2021). Positively and negatively autocorrelated environmental fluctuations have opposing effects on species coexistence. *The American Naturalist*, *197*(4), 000–000.

Schreiber, S. J., Benaïm, M., & Atchadé, K. A. (2011). Persistence in fluctuating environments. *Journal of Mathematical Biology*, *62*(5), 655–683.

Sears, A. L. W., & Chesson, P. (2007). New Methods for Quantifying the Spatial Storage Effect: an Illustration With Desert Annuals. *Ecology*, *88*(9), 2240–2247.

Simha, A., Pardo-De la Hoz, C. J., & Carley, L. N. (2022). Moving beyond the "diversity paradox": The limitations of competition-based frameworks in understanding species diversity. *The American Naturalist*, *200*(1), 000–000.

Snyder, R. E. (2008). When does environmental variation most influence species coexistence? *Theoretical Ecology*, *1*(3), 129–139.

Snyder, R. E., Borer, E. T., & Chesson, P. (2005). Examining the relative importance of spatial and nonspatial coexistence mechanisms. *The American Naturalist*, *166*(4), E75–E94.

Snyder, R. E., & Chesson, P. (2003). Local dispersal can facilitate coexistence in the presence of permanent spatial heterogeneity. *Ecology letters*, *6*(4), 301–309.

Song, C., Von Ahn, S., Rohr, R. P., & Saavedra, S. (2020). Towards a Probabilistic Understanding About the Context-Dependency of Species Interactions. *Trends in Ecology and Evolution*, *35*(5), 384–396.

Stearns, S. C. (2000). *Daniel Bernoulli (1738): evolution and economics under risk* (tech. rep. No. 3).

Stump, S. M., & Chesson, P. (2015). Distance-responsive predation is not necessary for the janzen–connell hypothesis. *Theoretical Population Biology*, *106*, 60–70.

Stump, S. M., & Chesson, P. (2017). How optimally foraging predators promote prey coexistence in a variable environment. *Theoretical Population Biology*, *114*, 40–58.

Stump, S. M., Johnson, E. C., Sun, Z., & Klausmeier, C. A. (2018). How spatial structure and neighbor uncertainty promote mutualists and weaken black queen effects. *Journal of theoretical biology*, *446*, 33–60.

Tilman, D. (1982). *Resource competition and community structure*. Princeton University Press.

Towers, I. R., Bowler, C. H., Mayfield, M. M., & Dwyer, J. M. (2020). Requirements for the spatial storage effect are weakly evident for common species in natural annual plant assemblages. *Ecology*, *101*(12), e03185.

Tuljapurkar, S., & Orzack, S. H. (1980). Population dynamics in variable environments i. long-run growth rates and extinction. *Theoretical Population Biology*, *18*(3), 314–342.

Tuljapurkar, S. D. (1982). Population dynamics in variable environments. iii. evolutionary dynamics of r-selection. *Theoretical Population Biology*, *21*(1), 141–165.

Turelli, M. (1977). Random environments and stochastic calculus. *Theoretical population biology*, *12*(2), 140–178.

Turelli, M. (1978). Does environmental variability limit niche overlap? *Proceedings of the National Academy of Sciences*, *75*(10), 5085–5089.

Usinowicz, J., Chang-Yang, C. H., Chen, Y. Y., Clark, J. S., Fletcher, C., Garwood, N. C., Hao, Z., Johnstone, J., Lin, Y., Metz, M. R., Masaki, T., Nakashizuka, T., Sun, I. F., Valencia, R., Wang, Y., Zimmerman, J. K., Ives, A. R., & Wright, S. J. (2017). Temporal coexistence mechanisms contribute to the latitudinal gradient in forest diversity. *Nature*, *550*(7674), 105–108.

Usinowicz, J., Wright, S. J., & Ives, A. R. (2012). Coexistence in tropical forests through asynchronous variation in annual seed production. *Ecology*, *93*(9), 2073–2084.

VanderWeele, T. (2015). *Explanation in causal inference: Methods for mediation and interaction*. Oxford University Press.

Volterra, V. (1926). Variations and fluctuations of the number of individuals in animal species living together. *Animal Ecology*, 409–448.

Weiss, G. H., & Dishon, M. (1971). On the asymptotic behavior of the stochastic and deterministic models of an epidemic. *Mathematical Biosciences*, *11*(3-4), 261–265.

Yuan, C., & Chesson, P. (2015). The relative importance of relative nonlinearity and the storage effect in the lottery model. *Theoretical population biology*, *105*, 39–52.

Zicarelli, J. D. (1975). *Mathematical analysis of a population model with several predators on a single prey*. University of Minnesota.

Chapter 2

Interpreting coexistence mechanisms

Chapter Contents

2.1 Towards a heuristic understanding of the storage effect

2.1.1 Abstract

The storage effect is a general explanation for coexistence in a variable environment. Unfortunately, the storage effect is poorly understood, in part because the generality of the storage effect precludes an interpretation that is simultaneously simple, intuitive, and correct. Here, we explicate the storage effect by dividing one of its key conditions —- covariance between environment and competition — into two pieces, namely that there must be a strong causal relationship between environment and competition, and that the effects of the environment do not change too quickly. This finer-grained definition can explain a number of previous results, including 1) that the storage effect promotes annual plant coexistence when the germination rate fluctuates, but not when the seed yield fluctuates, 2) that the storage effect is more likely to be induced by resource competition than apparent competition, and 3) why the storage effect arises readily in models with either stage structure or environmental autocorrelation. Additionally, our expanded definition suggests two novel mechanisms by which the temporal storage effect can arise — transgenerational plasticity and causal chains of environmental variables —- thus suggesting that the storage effect is a more common phenomenon than previously thought.

2.1.2 Introduction

The storage effect is a general explanation for how species can stably coexist by specializing on different environmental states. A favorable environment for one species leads to a productive period that drives high intraspecific competition. A variable environment thus allows species to "take turns" having productive periods, such that intraspecific competition is (on average, across species and time / space) greater than interspecific competition. A temporally-varying environment can generate a *temporal storage effect* (Chesson, 1994; often simply called the storage effect) and a spatially heterogeneous environment can generate the *spatial storage effect* (Chesson, 2000a).

The temporal storage effect can be illustrated by the lottery model of coral reef fishes (depicted in Fig. 2.1; equations provided in Appendix 2.1.I). A good environment manifests as high per capita fecundity. For the abundant red species, a good environment leads to high competition, i.e., many fish larvae per empty territory. For the rare blue species, a good environment does not lead to high competition: the red fish has low per capita fecundity, and although the blue fish has high per capita fecundity, there are few adults to begin with. The positive effects of a good environment are undermined by the high competition that it brings about; because this phenomenon disproportionately hurts common species and helps rare species, population abundances are stabilized and coexistence is attained.

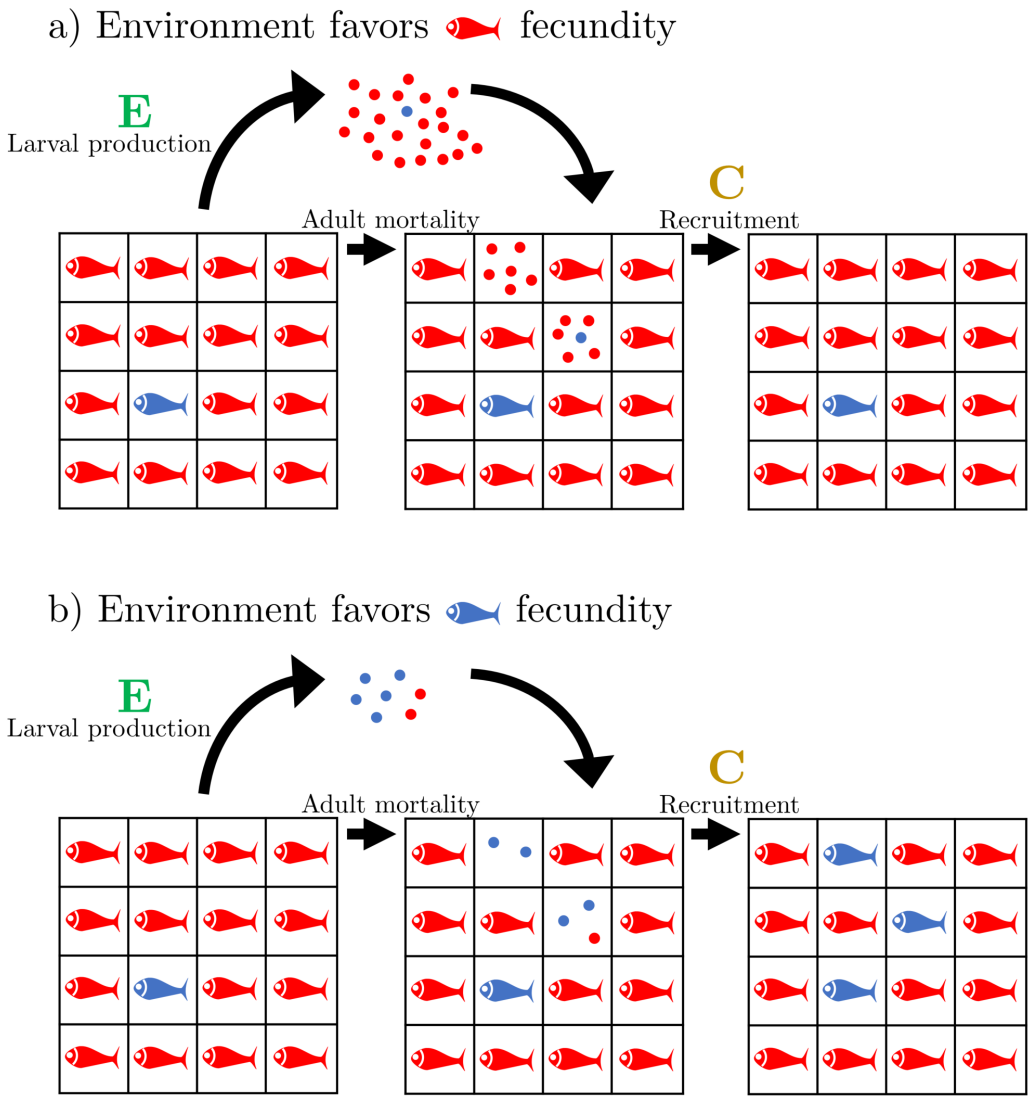

Figure 2.1: An illustration of the storage effect in the lottery model. **Panel a)**: For the common red species, a good environment (high per capita larval production) is undermined by the competition (total larvae per empty site) that it brings about. **Panel b)**: The blue species recovers from rarity because a good environment does not lead to high competition.

The storage effect is one of the most important concepts in community ecology. It subverted the ecology milieu of the 1970s, which focused on coexistence via resource partitioning and often regarded environmental stochasticity as a malignant force, both for individual species' persistence (Lewontin and Cohen, 1969) and for multi-species coexistence (May, 1974; but see Levins, 1979 & Huston, 1979 for the opposite perspective). Further, the storage effect subverted a tradition of thought going back to Darwin, who thought competitive

exclusion was the status quo of nature (see Lewens, 2010 for the reasons why), and therefore, that coexistence was the oddity worth explaining: "We need not marvel at extinction; if we must marvel, let it be at our own presumption in imagining for a moment that we understand the many complex contingencies on which the existence of each species depends" (Darwin, 1859, p. 322).

Darwin's presumption of competitive exclusion was formalized by the *competitive exclusion principle* (Volterra, 1926, Lotka, 1932, Gause, 1934; Levin, 1970) and later brought into focus by Hutchinson's (1961) *paradox of the plankton*, which asked how dozens of lake phytoplankton species could coexist on a handful of limiting nutrients. By showing that an arbitrary number of species can coexist on a single resource (e.g., Chesson, 1994, Eq. 81), the storage effect flipped the question of "Why are there so many species?" to "Why is the number of species that which we observe?" To this end, the storage effect and other coexistence mechanisms have been measured in a number of real ecological communities (Cáceres, 1997; Venable et al., 1993; Pake and Venable, 1995; Pake and Venable, 1996; Adler et al., 2006; Sears and Chesson, 2007; Descamps-Julien and Gonzalez, 2005; Facelli et al., 2005; Angert et al., 2009; Adler et al., 2010; Usinowicz et al., 2012; Chesson et al., 2012; Chu and Adler, 2015; Usinowicz et al., 2017; Ignace et al., 2018; Hallett et al., 2019; Armitage and Jones, 2019; Armitage and Jones, 2020; Zepeda and Martorell, 2019; Zepeda and Martorell, 2019; Holt and Chesson, 2014; Ellner et al., 2016; Ellner et al., 2019).

Unfortunately, the storage effect is difficult to understand in its entirety. The problem is that the storage effect is a general phenomenon that can look very different in different models, thus making it difficult to relate the storage effect to a small set of ecological constructs. Take for instance the two seminal models of the storage effect: the lottery model and the annual plant model (Chesson, 1994, Section 5). In the lottery model, coexistence is only possible if there are long-lived adult fish, i.e., if there are overlapping generations. In the structurally-similar annual plant model (seeds play the role of adult fish, germinants play the role of fish larvae), coexistence is only possible if there is a persistent seed-bank. Generalizing from these two models, one may be tempted to claim that the storage effect occurs when species have a robust life stage that can "wait it out" for a good year. However, this interpretation turns out to be imprecise, since multiple models (e.g., Abrams, 1984; Loreau, 1989; Li and Chesson, 2016; Schreiber, 2021) have shown that stage-structure and overlapping generations are neither necessary nor sufficient for the storage effect.

Perhaps a universal ecological interpretation of the storage effect is too ambitious. Instead, we can gain insight by studying the *ingredient-list definition of the storage effect*: a list of abstract conditions that *tend* to lead to a systematically positive storage effect, i.e., a storage effect that helps most species recover from rarity. The ingredients are neither necessary nor sufficient for a positive storage effect (see Appendix 2.1.A); rather, the ingredient list is a tool that can be used (in conjunction with examples) to understand how the storage effect promotes coexistence. Here, we attempt to explicate the storage effect by expanding on a

single ingredient: the covariance between environment and competition. This paper is not meant to be a comprehensive overview of the storage effect, as this has been done elsewhere (Chesson et al., 2003, Snyder, 2012; Barabás et al., 2018).

The ingredient-list definition states that the storage effect depends on

1. species-specific responses to the environment,
2. a non-zero interaction effect of environment and competition on per capita growth rates (also known as *non-additivity*), and
3. covariance between environment and competition (*EC covariance*).

To some extent, the ingredient list definition recapitulates the mathematical definition of the storage effect (derived in Appendix 2.1.A). When ecologists talk colloquially about a storage effect, they are typically talking about a positive (i.e., coexistence-promoting) storage effect that is mediated through competition. However, apparent competition can mediate the storage effect, sometimes called "the storage effect due to predation" (Kuang and Chesson, 2010; Chesson and Kuang, 2010; Stump and Chesson, 2017). The storage effect tends to be positive when the interaction effect is negative and *EC* covariance is positive (as is the case in almost all models of the storage effect), or when the interaction effect is positive and the *EC* covariance is negative (Schreiber, 2021). When the converse is true, the storage effect tends to be negative (i.e., coexistence-hindering), which can generate a stochastic priority effect (Chesson, 1988; Schreiber, 2021) in the absence of other coexistence-promoting mechanisms.

The function of ingredient 1 is rather obvious: species-specific responses to the environment is a form of niche differentiation, which has long been recognized as critical for coexistence (Grinnell, 1904). Classically, "niche differentiation" refers to differences in resource consumption (Tilman, 1982), the affinities of natural enemies (Holt, 1977), or social/behavioral differences (Chesson, 1991). The storage effect is unique in that coexistence is achieved through environmental niche differences.

Ingredient 2, an interaction effect between environment and competition, is akin to an interaction effect in a multiple regression where the response variable is the per capita growth rate, and the predictor variables are the environment and competition parameters. The interaction effect speaks to a *synergy* between environment and competition: it is nor merely the case that a good environment leads to high competition and that high competition is bad for population growth; a negative interaction effect means that the simultaneous occurrence of a good environment and high competition is extra-bad. Put another way, a negative (positive) interaction effect occurs when species are less (more) sensitive to competition in the face of a poor environment.

The well-known *competitive exclusion principle* (Gause, 1934; Levin, 1970) states that no more than L species can coexist on L regulating factors (e.g., resources, natural enemies). The interaction effect breaks this theoretical limit to coexistence by combining environment and competition into a large number of *effective regulating factors*. The species-specific environmental responses explain the preponderance of these factors, whereas competition provides the density-dependence inherent in a regulating factor (environmental niche differentiation alone is incapable of promoting coexistence; Chesson and Huntly, 1997).

However, this is all very abstract. What causes an interaction effect in particular ecological systems? In the seminal models of coexistence theory (the lottery model and the annual plant model; Chesson, 1994, Section 5) a robust life-stage / overlapping generations generates a negative interaction effect, also known as *buffering* (Chesson et al., 2004; Snyder, 2012) — the survivability of a life-stage that is insensitive to both environment and competition protects against the double-whammy of a poor environment and high competition (Chesson and Huntly, 1988). In models where a robust life-stage is insensitive to competition but not the environment (e.g., adult fish or seed survival fluctuates; Chesson, 1988; Schreiber, 2021), we observe a positive interaction effect.

In other models, an interaction effect results from other types of population structure, whether it be dormancy (Cáceres, 1997; Ellner, 1987), phenotypic variation (Chesson, 2000b), or spatial population structure (Chesson, 2000a). However, an interaction effect can arise in the absence of population structure, simply due to the multiplicative form of a per capita growth rate function (Li and Chesson, 2016; Letten et al., 2018; Ellner et al., 2019). It is also worth noting that in the population genetic version of the storage effect, an interaction effect can result from heterozygosity (Dempster, 1955; Haldane and Jayakar, 1963), sex-linked alleles (Reinhold, 2000), epistasis (Gulisija et al., 2016), and maternal effects (Yamamichi and Hoso, 2017). There are many ways for an interaction effect to occur. At least for the moment, it is not possible to give a general interpretation of the interaction effect in terms of a small set of life-history characteristics, like dormancy, robust life stages, etc.

The final ingredient, covariation between environment and competition, is the focus of this paper. Covariation is typically used as statistical measure of linear association, so at first glance it may be unclear how the covariance arises from underlying population dynamics. To make ingredient 3 more comprehensible, we split it into two sub-ingredients: 3A) a strong causal relationship between environment and competition (i.e., a good environment leads to high competition, or conversely, a bad environment leads to low competition), and 3B) that the environment does not change too quickly. This expanded list can be levied to understand a number of theoretical results and to intuit novel contexts in which the storage effect can arise.

2.1.3 Expanding the ingredient-list definition of the storage effect

The ingredient-list definition of the storage effect can be expanded as follows:

3. Covariance between environment and competition.

    3A. A strong causal relationship between environment and competition, and

    3B. the environment does not change too quickly.

Before proceeding, we must note that the terms "environment" and "competition" are used loosely. While the environment E can represent abiotic variables per se, most often E is identified as a demographic parameter that depends on fluctuating density-dependent factors (e.g., germination probability depends on precipitation). For this reason, E is often called the environmental response or the environmentally-dependent parameter. Competition C can be generally understood as the effects of regulating factors, which may include species' densities, resources, refugia, territories, natural enemies, etc.

The first sub-ingredient, 3A — a strong causal relationship between environment E and competition C — establishes the *potentiality* of a covariance between E and C. If fluctuations in E cause fluctuations in C, then it is not hard to imagine that E will tend "go along with" C (though ingredient 3B is also essential). For example, increased temperatures can increase resource uptake rates, thus decreasing resource availability. More generally, a favorable environment leads to higher population densities, which leads to fewer resources, less space, or more predators on a per capita basis.

Given the well-known dictum "correlation does not imply causation", it may seem strange that ingredient 3A invokes the philosophically vexed concept of causation. Our hope is that the evocative ingredient 3A (as opposed to the inoffensive "E affects C") emphasizes that the covariance is not just a summary statistic, but a consequence of dynamic relationships between variables. In Appendix 2.1.B, we argue that while it is technically possible to obtain a positive EC covariance without causation between E and C, cases of the storage effect are always undergirded by a causal relationship between environment and competition at some level (i.e., for some definitions of E and C).

The second sub-ingredient, 3B — the environment does not change too quickly — is more difficult to understand. Per capita growth rates depend on the current values of E and C. However, since the environment causally affects the level of competition, and causes precede their effects, the only guaranteed statistical relationship is that between the current value of C and the past value of E. Figure 2.2 illustrates this idea: one causal arrow (and thus one unit of time) is required for the environment to directly affect growth rates, whereas two causal arrows (and thus two units of time) are required for the effects of the environment on the growth rate to be mediated through competition. For a non-zero covariance between the

current environment and competition, it is essential that the effects of the environment are carried forward through time, such that the effect of a past environment is brought into contact with the competition that it caused. In terms of the framework known as Modern Coexistence Theory (Chesson, 1994; Barabás et al., 2018) with E^* and C^* representing equilibrium levels of environment and competition respectively, per capita growth rates depend on the term $(E(t) - E^*)(C(t) - C^*)$ (see Appendix 2.1.A), whereas a causal relationship between E and C only ensures a statistical relationship between $(E(s) - E^*)$ and $(C(t) - C^*)$, for some $s < t$.

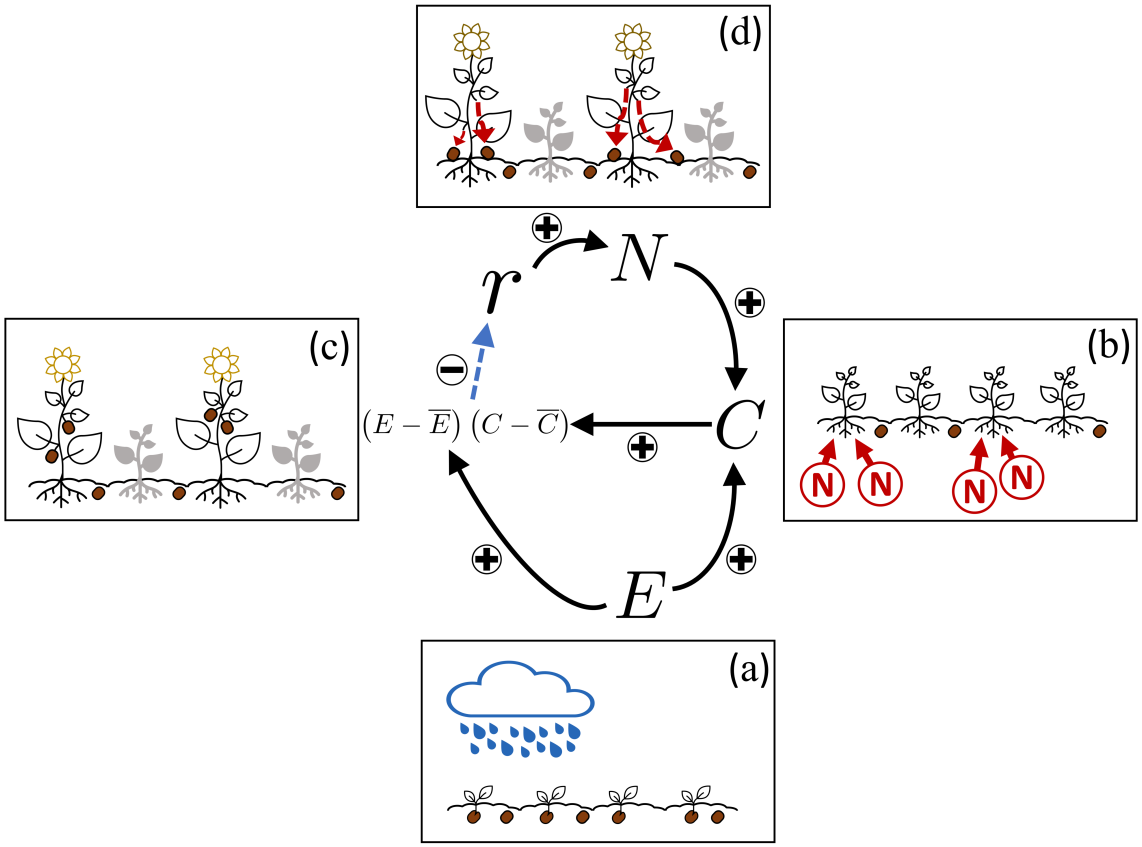

Figure 2.2: A causal diagram shows how the EC covariance arises generally, with panels showing how the EC covariance arises in the annual plant model. The black arrows show the direction of causation, e.g., increased population density N causes increased competition C. The blue dashed arrow indicate a set-subset relationship: the per capita growth rate r is a function of the effective regulating factor $\left(E_j - \overline{E}_j\right)\left(C - \overline{C}\right)$ (which becomes $\mathrm{Cov}(E, C)$ when averaged over time). The negative sign indicates the negative EC interaction effect typical of competition models. The environment E has a direct effect on r. However, it takes some time (i.e., two causal arrows) for the indirect effects of E on r to be mediated through C. Therefore, for E to covary with C, there must be some mechanism for carrying the effects of the environment through time. In the annual plant model, this mechanism is the germinant life stage. **Panel a)** Precipitation causes a high probability of germination. **Panel b)** The germinants compete for a limited supply of soil nitrogen. **Panel c)** A good environment (i.e., high germination probability) is undermined by the high competition that it brings about, manifesting as few seeds per capita (grey plants are dead germinants). **Panel d)** The seeds disperse and join the seed bank (off-season seed mortality not shown).

Ingredient 3 is the most surprising and contingent aspect of the storage effect. By contrast, it seems

natural for species to have idiosyncratic responses to the environment, thus satisfying ingredient 1: even if species are subjected to strong convergent evolution or environmental filtering, we would still expect some systematic difference between species due to evolutionary transient dynamics, development constraints, etc. It also seems natural for species to experience an interaction effect between environment and competition (thus satisfying ingredient 2), seeing as how the alternative — additivity — takes a very specific form in scalar populations: $\lambda = n(t+1)/n(t) = \exp\{\alpha E + \beta_j C + c\}$, where α, β, and c are constants. Chesson (1994) writes "There are so many ways in which nonadditivity can arise that it seems doubtful that any real populations could be additive, although approximate additivity could be common". But there is no guarantee that nature will simultaneously satisfy ingredients 3A and 3B, which together require that the environment not change before its causal effects on competition are felt.

To back up our verbal argument, we analyze a general model and find that the covariance between environment and competition is an increasing function of $T_E/T_{E\to C}$, where T_E is the timescale of environmental autocorrelation, and $T_{E\to C}$ is the time scale on which the environment affects competition. The time scale T_E is a measure of ingredient 3B, and $1/T_{E\to C}$ is a measure of ingredient 3A, with a stronger causal relationship between environment and competition corresponding to a smaller $T_{E\to C}$. Our result is insensitive to model details, including the structure of growth rate equations, whether the model is discrete-time or continuous-time, whether environmental variation is stochastic or seasonal, and whether or not resource-consumer dynamics are explicitly modelled. Full details are given in the Appendices 2.1.C–2.1.H, but here we present a instructive subset of our analysis.

Consider a general model that describes the dynamics of a single species with population density $N(t)$ and environmental parameter $E(t)$:

$$\begin{aligned} N(t+\Delta t) &= N(t) + F(N(t), E(t))\Delta t \\ E(t+\Delta t) &= E(t) + G(E(t))\,\Delta t + \sigma\sqrt{\Delta t}\,\eta(t). \end{aligned} \tag{2.1}$$

Here, F is the deterministic growth rate function of the population, G is the deterministic change function of the environmental parameter, σ is the scale of stochastic perturbations, t is time, Δt is the length of a time step, and $\eta(t)$ is a draw from the standard normal distribution.

Because the growth rate functions F and G are arbitrary, Eq.2.1 describes a large number of models. These models can be linearized about their equilbria, thus allowing the for a universal mathematical treatment of idiosyncratic population dynamics. In Appendix 2.1.C, we show that the covariance between

environment and competition is

$$\mathrm{Cov}(E,C) = \frac{(T_E\sigma)^2}{2\,T_{E\to C}\,(1 - T_E\,F_N)}, \tag{2.2}$$

where F_N is defined as the partial derivative of F evaluated at equilibrium, i.e., $F_N = \frac{\partial F(N,E)}{\partial N}\Big|_{\substack{N=N^* \\ E=E^*}}$. Stronger population regulation corresponds to a more negative F_N. The time scale of environmental change, T_E, is the reciprocal of the return rate of the environment: $T_E = -1/G_E$, where G_E is defined analogously to F_N. The other time scale parameter, $T_{E\to C}$, is the reciprocal of the rate at which the environment affects competition (note that time scales are always defined as the reciprocals of rates; Hastings, 2010). The EC covariance always increases with T_E and always decreases with $T_{E\to C}$, thus suggesting the following heuristic:

$$\mathrm{Cov}(E,C) \text{ is an increasing function of } \frac{T_E}{T_{E\to C}}.$$

In other words, a large covariance between environment and competition requires that the environment changes more slowly than the time it takes the environment to appreciably affect competition. A large covariance, in turn, corresponds to a more potent storage effect. The fraction $T_E/T_{E\to C}$ also helps to clarify ingredients 3A and 3B, which employ the frustratingly vague words "strong" and "quickly"; now we see that the environment must not change too quickly, *relative* to the strength of the causal relationship between environment and competition.

When species have environment niche differences but are otherwise equivalent, the storage effect (denoted ΔI) can be written as

$$\Delta I = -\,\zeta(1-\rho)\frac{(T_E\sigma)^2}{2\,T_{E\to C}\,(1 - T_E\,F_N)\,}, \tag{2.3}$$

which mathematically recapitulates the expanded ingredient-list definition of the storage effect. Ingredient 1 (species-specific responses to the environment) is captured by $1-\rho$, where ρ is the correlation between species' environmental responses. Ingredient 2 (the interaction effect between environment and competition) is captured by ζ_j. In models where the storage effect is mediated through resource competition, ζ is typically negative, so $-\zeta > 0$. Ingredient 3A (a strong causal relationship between environment and competition) is by captured by $1/T_{E\to C}$: a stronger causal relationship between E and C corresponds to to a faster rate at which the environment affects competition, and in turn, a smaller $T_{E\to C}$. Finally, ingredient 3B (the environment does not change too quickly) is captured by T_E.

2.1.4 Discussion

The interplay between ingredients 3A and 3B can explain several interesting results regarding the storage effect. Kuang and Chesson (2009) analyzed a model in which two species had one shared resource and one shared predator. Resource competition generated a storage effect, whereas the shared predator did not. Ingredients 3A and 3B explain why. The time scale of environmental change is a single time step, but the time it takes for the environment to affect predator density is two time steps: one time step for the environment to affect prey density, and one time step for prey density to affect predator density. By the time that competition (which includes all regulating factors, including predators) has responded to the environment, the environment has changed (i.e., $T_E/T_{E\to C}$ is small). In contrast, a predator-mediated storage effect may arise if predators respond quickly to prey density, as is the case with prey-switching behavior (Kuang and Chesson, 2010; Chesson and Kuang, 2010) or satiation due to a type 2 functional responses (Stump and Chesson, 2017). Here, it takes a single time step for prey density to react to the environment, and predator behavior tracks prey density instantaneously. The environment affects competition at a much faster rate (i.e., $T_{E\to C}$ is small, so $T_E/T_{E\to C}$ is large).

Another interesting result is that in the annual plant model, (Chesson, 1994) the storage effect arises when germination probability fluctuates, but not when the seed yield fluctuates. Both germination probability or per germinant seed yield (the two environmental parameters under consideration) have causal effects on competition. Increased per germinant yield increases the density of seeds, which increases the number of subsequent germinants, which then increases the level of competition for soil nutrients. Increased germination leads to an increased number of germinants, which also increases the level of competition. However, note the difference in the length of the two causal pathways: the germination probability affects competition in the current time step ($T_{E\to C}$ is small), whereas the yield affects competition in the next time step ($T_{E\to C}$ is large); by then, the environment has changed and the covariance between environment and competition evaporates.

The storage effect's namesake originates from the canonical lottery and annual plant models (see Chesson, 1994, Section 5), where a robust life stage is necessary for coexistence. In these models, the storage effect can support all species if years of good recruitment are "stored" in long-lived adult fish or in a dormant seed bank, as a non-zero survival parameter is necessary for a non-zero interaction effect between environment and competition (ingredient 2). However, such EC interaction effects arise readily without any need for stage structure, whenever per capita growth rates take a multiplicative functional form. For example, in a simple phytoplankton model (Appendix 2.1.H), the environmental parameter is related to the maximum resource uptake rate, and competition is inversely related to resource concentrations, so the product of

uptake rate $\times$ *resource concentration* in the phytoplankton's per capita growth rate function leads to an EC interaction effect. Clearly, a robust life stage is not required, which explains why sophisticated expositions of the storage effect regard "storage" as a metaphor (for periods of positive population growth that are not cancelled by periods of negative growth; Chesson, 1994), or replace it entirely with the notion of *buffering* (i.e., protection against the double whammy of an unfavorable environment and high competition; Chesson et al., 2004; Snyder, 2012).

The storage effect arises in temporally autocorrelated environments (Loreau, 1989; Loreau, 1992; Li and Chesson, 2016; Schreiber, 2021; Appendix 2.1.H), because the environment doesn't change too quickly, i.e., ingredient 3B is satisfied. But recall that "the environment" can refer to any model parameter that depends on fluctuating density-independent factors. From this broad perspective on what constitutes the environment, it becomes clear that an autocorrelated abiotic variable *per se* is not required. Rather, ingredient 3B can be satisfied by any mechanism that carries the effects of the abiotic environment through time.

The metaphor of environmental autocorrelation suggests an alternative meaning of "storage" — any mechanism that carries the effects of the environment through time, thus satisfying ingredient 3B. Autocorrelated environments perform this novel notion of storage in the sense that the current environment is predictive of the future environment. In the lottery model of coral reef fish dynamics, the abiotic environment affects per capita fecundity, which affects the number of fish larvae. The environment is thus "stored" in the larvae, which may drift offshore for months before returning to the reef and competing for territory. Similarly, in the annual plant model, the abiotic environment affects the probability of seed germination, and is thus "stored" in the number of germinants. Note that in the lottery model and annual plant model, the classical notion of storage is about generating an interaction effect (ingredient 2) via the long-lived life stage: adult fish or seeds. The novel notion of storage (i.e., carrying the effects of the environment through time) is about generating a covariance (ingredient 3) through the comparatively short-lived life stage: fish larvae or germinants.

To date, all models of the temporal storage effect feature either temporal autocorrelation or stage-structure, although both features are sometimes implicit. In the lottery model and annual plant model, the stage-structure is hidden by the fact that both juvenile and adult dynamics can fit into a single equation (per species). In Abrams's (1984) model, environmental fluctuations are speciously temporally uncorrelated, but there is an assumed time scale separation between environmental change and resource dynamics such that $T_E/T_{E\to C}$ is automatically large. Abrams (1984) writes "resources are assumed to attain new steady state densities rapidly after an environmental change which results in altered consumption rates", implying that the environment is autocorrelated on the short time scale of resource dynamics. Once one accepts that a function of stage-structure and temporal autocorrelation is satisfying ingredient 3B, it becomes readily

apparent that the storage effect can arise in other situations. Here, we present two novel mechanisms that may mediate the storage effect: transgenerational plasticity and causal chains of environmental variables.

We contend that non-adaptive transgenerational plasticity (TGP; Bell and Hellmann, 2019) can carry the effects of the environment forward through time, therefore satisfying ingredient 3B. A subset of TGP is *maternal effects*, classically envisioned as the provisioning of nutrients and resources into seeds or eggs. A nesting bird facing a favorable environment (e.g., a particular pattern of rainfall produces a large number of preferred seeds) accumulates muscle mass and fat reserves, which allows the bird to produce larger clutches with higher egg quality (Price, 1998). The "head-start" that the offspring receive make it more likely that they will survive and reproduce in following years, even if the following years' environments are comparatively poor. In this example, we see that a good environment in one year will lead to modified demographic rates in subsequent years — it is *as if* the environment is autocorrelated. Note that what we are proposing here is different from the model of Yamamichi and Hoso (2017), where maternal effects produces a negative interaction effect and diploidy leads to the EC covariance.

Non-adaptive TGP tends to carry-over the favorable effects of a good environment (or conversely, the deleterious effects of a poor environment), while adaptive TGP (Herman and Sultan, 2011) tends to buffer against the sustained impact of a poor environment. For example, if a drought-stressed plant passes its developmental drought-response (e.g., a deeper root system and earlier flowering time; Herman and Sultan, 2016; Galloway and Burgess, 2009) to its offspring, and the offspring also face drought conditions, then the offspring will perform better than they would have otherwise (if they had come from well-watered progenitors). Adaptive TGP does not reduce temporal autocorrelation, but rather reduces the overall variance in the environmental parameter. Of course, plasticity of any sort is only expected to evolve in spatially and temporally autocorrelated environment (Lachmann and Jablonka, 1996; Stomp et al., 2008; Colicchio and Herman, 2020), so we would expect that the storage effect would reflect the balance between the coexistence-promoting effects of autocorrelation and the coexistence-hindering effects of adaptive TGP.

Additionally, we contend that causal chains of environmental responses can satisfy ingredient 3B (Fig 2.3). Consider a community of annual plants. High precipitation in year 1 causes a high germination probability in year 1, and thus a large number of germinants in year 2. Simultaneously, high precipitation in year 1 causes a high abundance of fly pollinators in year 2, which causes a high per germinant seed yield in year 2. Thus, there is a covariance between an environmental response (i.e., per germinant seed yield) and competition (i.e., the density of germinant competitors), even if the abiotic environment (precipitation) and species' environmental responses (germination probability and per germinant yield) are temporally uncorrelated.

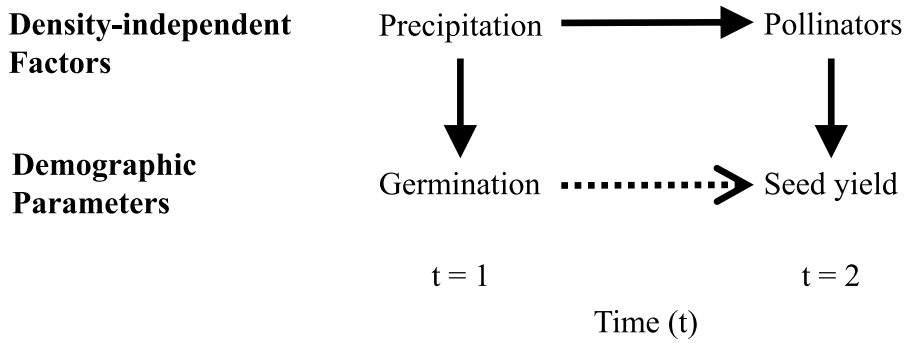

Figure 2.3: The covariance between environment and competition can be generated by causal chains of environmental variables. Solid arrows denote direct causal relationships. The dotted arrow denotes an indirect relationship. The causal relationship between the exogenous density-independent factors — precipitation and pollinators — prevents the effects of the environment from changing too quickly, thus satisfying ingredient 3B. The demographic parameters are correlated because both are causally affected by precipitation on different time-lags.

The previous example can be explained in two ways, depending on how one understands "the environment". In Modern Coexistence Theory, it is conventional for the environment to be a demographic parameter that depends on fluctuating density-independent factors. If we take this perspective, then it is clear that there is not a causal relationship between the environmental parameters (germination and yield). Rather, there is an indirect relationship that is a consequence of both parameters ultimately being caused by precipitation, but with different time-lags (Fig 2.3). If on the other hand, we identify the environment as exogenous density-independent factors, then ingredient 3B is generated by a causal chain of environmental variables, wherein precipitation causes increases in the pollinator population (recall that density-independent factors may be biotic).

Ingredient 3B also explains the putative potency of the spatial storage effect, which "...seems to be inevitable under realistic scenarios" (Chesson, 2000a). In models with permanent spatial heterogeneity, the local environment does not change over time, thus automatically satisfying ingredient 3B. This is not to say that environmental heterogeneity guarantees an environmental-competition covariance. It must also be the case that populations can build up in good environments, thus satisfying ingredient 3A. There are at least four scenarios that can generate a causal relationship between the local environment and local competition. 1) Either survival or fecundity varies over space, and not all individuals disperse after every time step; there is some *local retention* (*sensu* Chesson, 2000a). 2) Either survival or fecundity varies over space, and all individuals do disperse, but the spatial scale of environmental variation is larger than the scale of

dispersal (Snyder and Chesson, 2003; Snyder and Chesson, 2004). Note the similarity with scenario 2 — if an individual disperses but finds itself in an similar context, it is as if it never left. 3) Survival varies over space, and although there may be widespread dispersal, there are immobile individuals that survive between time steps (Muko and Iwasa, 2000; Snyder and Chesson, 2003). 4) Either survival or fecundity varies over space, and all individuals disperse, but the environment affects competition on a short, within-generation time scale (as opposed to an inter-generational time scale). For example, consider an annual plant model with global dispersal in every time step (e.g., intermittent flooding redistributes seeds) and spatially-varying germination probabilities. Within each time step, high germination probabilities lead to high competition between germinants; ingredient 3A is satisfied despite the fact that seed banks do not build-up in favorable locations.

It is interesting to note that the primary contingency for the temporal storage effect is ingredient 3B (will the effects of the environment be carried through time?) whereas the contingency for the spatial storage effect is 3A (will individuals stick around, such that the local environment has a causal relationship with local competition?). In both the lottery model and the annual plant model, there is no interaction effect (ingredient 2) when the survival probability varies across space (i.e., when scenario 3 in the previous paragraph is attained). Note: an analogous claim cannot be made about the temporal storage effect, due to the fact that temporal and spatial coexistence mechanisms are calculated differently (Chesson, 2000a, p. 218). While spatial variation in survival does not engender a storage effect in these simple models, the variation in population density that results from differential population buildup can engender a *fitness-density covariance* (see Muko and Iwasa, 2000 for an example), a spatial coexistence mechanism that often (but not always) goes along with the spatial storage effect. A discussion of the relationship between fitness-density covariance and the spatial storage effect is outside the scope of this paper, but see Chesson (2000a, 2012), Chesson et al. (2003), and Barabás et al. (2018) for more details.

The most thorough empirical test of the spatial storage effect found near-zero EC covariances in a community of herbaceous woodland plants (Towers et al., 2020). The authors provide several reasons for the absence of covariance, but ingredient 3A suggests an additional reason. It is possible that the average dispersal distance of the plants is much greater than the grain size of environmental variation, such that populations cannot build up in favorable environments. Herbaceous plants can disperse passively up to 2–3 meters (Harper, 1977; Vittoz and Engler, 2007; or much more via animal-based dispersal or flooding), and previous research has shown that nutrient supplies can vary significantly across a meter (Tilman, 1982, p. 100; Bogunovic et al., 2014), so this explanation for a weak spatial storage effect, while speculative, is not out of the question.

Though temporal autocorrelation is positively related to the temporal storage effect, it does not invariably

promote coexistence. Temporal autocorrelation in the environment increases the magnitude and duration of deviations from equilibrium population densities, which is related to the probability of stochastic extinction. In the limit of strong autocorrelation, the environment is effectively constant (Kamenev et al., 2008), leading to competitive exclusion in the absence of fluctuation-independent coexistence mechanisms. Thus, we expect a hump-shaped, uni-modal relationship between temporal environmental autocorrelation and the mean coexistence times of species, reflecting the balance between opposing forces of the storage effect and the intensity of perturbations (Adler and Drake, 2008; Pande et al., 2020).

Recent work has shown that the mean persistence time decreases monotonically with temporal autocorrelation in the lottery model (Danino et al., 2018; Meyer and Shnerb, 2018). However, this result is not a general feature of the storage effect in temporally autocorrelated environments, but rather a reflection of the lottery model's particular assumptions. The lottery model assumes that the number of total individuals (in the entire community) is equal to a fixed number of reef territories, and that there are always enough larvae to fill empty territories. Due to these assumptions, a sole resident species will have a constant density of adult fish, thus precluding a build-up of population density during extended periods of good conditions. On an between-year time scale, a good environment does not lead to high competition (as we discuss later, ingredient 3A will nonetheless be satisfied on the within-year time scale). However, the assumption of a constant community capacity is not realistic: even among territorial coral reef fishes, Thibaut et al. (2012) found substantial fluctuations in total abundance.

The storage effect in the lottery model is brought about by processes that occur *within* a year — processes obscured by the fact that the lottery model equations only track changes *between* years. For example, the lottery model generates a storage effect when the environmental parameter E is uncorrelated between years (Chesson, 1994); while this result may appear to be a violation of ingredient 3B, the environment is autocorrelated on the within-year time scale. On this faster time scale, the adult fish spawn, larvae drift offshore, adult fish die, larvae return to the reef, and larvae are recruited into empty territories. If the environmental parameter E is identified as the density of larvae per capita (recall that E can be defined as any fluctuating density-independent parameter), then E is effectively constant from the end of the spawning period to the beginning of the recruitment period (i.e., T_E is large). Competition — here operationalized as larvae per open site at the time of recruitment — is affected by E within a time step (i.e., $T_{E\to C}$ is small), and so $T_E/T_{E\to C}$ is large. The lottery model is analyzed further in Appendix 2.1.I.

It is interesting that the (mathematically) simplest models seem to obscure our heuristic explanation of the storage effect. In the two canonical models of the storage effect (the lottery model and the annual plant model) the competition parameter C can be expressed as a function of E (say, $C(t) = \widetilde{C}(E(t))$). Then, C can be approximated with a Taylor series, leading to the strikingly simple approximation $\mathrm{Cov}(E, C) =$

$\widetilde{C}_E \mathrm{Var}(E)$, where $\widetilde{C}_E$ is the first-order Taylor series coefficient. However, competition is emphatically not a function of the contemporaneous environment, but rather a function of contemporaneous density-dependent factors like resource availability, predator density, etc. The claim that competition is function of the environment is an indication of a hidden time scale: the current level of competition is affected by the past environment (mediated through density-dependent factors), but this dynamic relationship occurs within a time step and is not explicitly modelled. If E only changes between time steps, then this model structure enforces a time scale separation where $T_E \gg T_{E \to C}$.

In this paper, we have attempted to provide a better heuristic explanation of the storage effect by showing how an EC covariance is likely to arise. Our analysis shows how seemingly disparate models are actually similar. For example, a juvenile life stage (e.g., fish larvae in the lottery model), environmental autocorrelation, and permanent spatial heterogeneity all serve the same function: carrying the effects of the environment forward through time, to bring it into contact with the competition that it caused. Future research should focus on further explicating ingredient 2, an interaction effect between environment and competition. The interaction arises from a variety of mechanisms in a variety of models (see the Introduction), and it is unclear what ties these mechanisms together. A recent demonstration of this messiness comes from Schreiber (2021), who analyzed simple model in which fluctuating survival drives a positive interaction effect, but fluctuating fecundity drives a negative interaction effect. The storage effect would be much more understandable and predictable if one could know the sign of an interaction effect based only on a verbal description of an ecological system, not a mathematical analysis or analogy with previously studied classes of models.

Appendices

Throughout the Appendices, tedious and lengthy calculations (e.g., matrix inverses) are performed with the software *Mathematica*. See the supplementary files `SI_calculations.nb` and `SI_calculations.pdf` at https://github.com/ejohnson6767/storage_effect_heuristic, or Figshare, https://doi.org/10.6084/m9.figshare.20399253.v1.

2.1.A The Storage Effect

The mathematical definition of the storage effect is a product of *Modern Coexistence Theory* (Chesson, 1994; Chesson, 2000a; Barabás et al., 2018), a framework for partitioning invasion growth rates into *coexistence mechanisms*: terms that correspond to different explanations for coexistence. Here, we provide a derivation of the mathematical definition of the storage effect, partly for completeness, and partly because our definition deviates slightly from previous definitions (we will comment on these differences later).

1. **Choose an invader**. Modern Coexistence Theory is based on *invasion analysis*, the practice of checking (mathematically or computationally) whether species can recover from rarity. One species (*the invader*, subscript i) is perturbed to zero density, thus simulating a low-density scenario. The remaining species (*the residents*, subscript r) are left at their typical densities, and are given time to attain their limiting dynamics in the absence of the invader.

   The long term average per capita growth rate of the invader is the *invasion growth rate*, and the sign of the invasion growth rate determines whether the invader recovers in the medium-term (Schreiber et al., 2011; Pande et al., 2020). In the long-term, a phenomenon known as "the resident strikes back" is possible (Mylius and Diekmann, 2001; Geritz et al., 2002).

2. **Write the per capita growth rates in terms of the environmental and competition**. Write the per capita growth rate of species j as a function g_j of the environmental parameter $E_j(t)$ and the competition parameter $C_j(t)$, i.e., $dn_j(t)/(n_j(t)dt) = g_j(E_j(t), C_j(t))$. Note that both $E_j(t)$ and $C_j(t)$ may be species-specific. In discrete-time models, the effective per capita growth rate is the logged *finite rate of increase*, i.e., $\log(\lambda_j(t)) = g_j(E_j(t), C_j(t))$, where $\lambda_j(t) = n_j(t+1)/n_j(t)$. An extension of Modern Coexistence Theory for structured populations is provided by Ellner et al. (2019).

3. **Expand growth rates in the neighborhood of E_j^* and C_j^***. Select equilibrium values of the environment and competition, E_j^* and C_j^*, such that $g_j(E_j^*, C_j^*) = 0$. The canonical way to find the equilibrium parameters is set some noise parameter to zero, which should fix E^*; then, the constraint $g_j(E_j^*, C_j^*) = 0$ can be used to solve for C_j^*.

We perform a second-order Taylor series expansion of $g_j(E_j(t), C_j(t))$ about E_j^* and C_j^*, resulting in

$$\begin{aligned} g_j(E_j(t), C_j(t)) \approx \alpha_j^{(1)}(E_j(t) - E_j^*) + \beta_j^{(1)}(C_j(t) - C_j^*) \\ + \frac{1}{2}\alpha_j^{(2)}(E_j(t) - E_j^*)^2 + \frac{1}{2}\beta_j^{(2)}(C_j(t) - C_j^*)^2 + \zeta_j(E_j(t) - E_j^*)(C_j(t) - C_j^*), \end{aligned} \tag{2.4}$$

where the Taylor series coefficients are

$$\begin{aligned} \alpha_j^{(1)} &= \frac{\partial g_j}{\partial E_j}\Big|_{\substack{E_j=E_j^* \\ C_j=C_j^*}}, \quad \beta_j^{(1)} = \frac{\partial g_j}{\partial C_j}\Big|_{\substack{E_j=E_j^* \\ C_j=C_j^*}}, \\ \alpha_j^{(2)} &= \frac{\partial^2 g_j}{\partial E_j^2}\Big|_{\substack{E_j=E_j^* \\ C_j=C_j^*}}, \quad \beta_j^{(2)} = \frac{\partial^2 g_j}{\partial C_j^2}\Big|_{\substack{E_j=E_j^* \\ C_j=C_j^*}}, \quad \zeta_j = \frac{\partial^2 g}{\partial E_j \partial C_j}\Big|_{\substack{E_j=E_j^* \\ C_j=C_j^*}}. \end{aligned} \tag{2.5}$$

4. **Time-averaging**. Temporal averages are denoted with "bars", e.g., the temporal average of $E_j(t)$ is $\overline{E_j}$. From Eq.2.4, we find that

$$\begin{aligned} \overline{g_j(E_j, C_j)} \approx \alpha_j^{(1)}(\overline{E_j} - E_j^*) + \beta_j^{(1)}(\overline{C_j} - C_j^*) \\ + \frac{1}{2}\alpha_j^{(2)}\mathrm{Var}(E_j) + \frac{1}{2}\beta_j^{(2)}\mathrm{Var}(C_j) + \zeta_j \mathrm{Cov}(E_j, C_j)\,. \end{aligned} \tag{2.6}$$

The above expression depends on small-noise assumptions, specifically that the magnitude of environmental fluctuations (i.e., $\left|E_j(t) - E_j^*\right|$) is small, and that the average environmental fluctuation (i.e., $\left|\overline{E_j} - E_j^*\right|$) is even smaller (see Chesson, 1994 for details). These assumptions ensure the accuracy of the Taylor series and allow us to replace $\overline{(E_j - E_j^*)(C_j - C_j^*)}$ with $\mathrm{Cov}(E_j, C_j)$.

5. **Invader–resident comparisons**

The long-term average growth rate of each resident must be zero (otherwise residents would go extinct or explode to infinity), allowing us to write the seemingly trivial equation,

$$\overline{g_i(E_i, C_i)} = \overline{g_i(E_i, C_i)} - \sum_{r \neq i}^{S} q_{ir}\, \overline{g_r(E_r, C_r)}, \tag{2.7}$$

which will later facilitate a comparison between the invader and the residents. The q_{ir} are called *scaling factors* (Barabás et al., 2018), also known as comparison quotients (Chesson, 2020). The original definition, provided by Chesson (1994), is equivalent to $q_{ir} = \frac{\beta_i^{(1)}}{\beta_r^{(1)}}\frac{\partial C_i}{\partial C_r}$ with the partical derivative evaluated at the equilibrium values of environment and competition. When all species have a shared competition parameter (i.e., $C_j = C$), this simplifies to $q_{ir} = \frac{\beta_i^{(1)}}{\beta_r^{(1)}}$.

We can draw meaningful comparisons between the invader and the residents by substituting the Taylor series expansion (Eq.2.6) into the right-hand-side of the invader–resident comparison (Eq.2.7) and grouping like-terms:

$$\begin{aligned}\overline{g_i(E_i,C_i)} \approx & \underbrace{\alpha_i^{(1)}(\overline{E_i}-E_i^*)+\frac{1}{2}\alpha_i^{(2)}\mathrm{Var}(E_i)+\beta_i^{(1)}C_i^*-\sum_{r\neq i}^{S}q_{ir}\left((\overline{E_r}-E_r^*)+\frac{1}{2}\alpha_r^{(2)}\mathrm{Var}(E_r)+\beta_r^{(1)}C_r^*\right)}_{r_i',\text{Density-independent effects}} \\ & + \underbrace{\beta_i^{(1)}\overline{C_i}-\sum_{r\neq i}^{S}q_{ir}\beta_r^{(1)}\overline{C_r}}_{\Delta\rho_i,\text{Linear density-dependent effects}} \\ & + \underbrace{\frac{1}{2}\left[\beta_i^{(2)}\mathrm{Var}(C_i)-\sum_{r\neq i}^{S}q_{ir}\beta_r^{(2)}\mathrm{Var}(C_r)\right]}_{\Delta N_i,\text{Relative nonlinearity}} \\ & + \underbrace{\zeta_i\mathrm{Cov}(E_i,C_i)-\sum_{r\neq i}^{S}q_{ir}\zeta_r\mathrm{Cov}(E_r,C_r)\,.}_{\Delta I_i,\text{The storage effect}}\end{aligned} \tag{2.8}$$

The new symbols (r_i', $\Delta\rho_i$, ΔN_i, and ΔI_i) denote coexistence mechanisms.

The mathematical definition of the storage effect is

$$\Delta I_i = \zeta_i\ \mathrm{Cov}(E_i,C_i)-\sum_{r\neq i}^{S}q_{ir}\ \zeta_j\ \mathrm{Cov}(E_r,C_r)\,. \tag{2.9}$$

Our definition of the storage effect differs from previous definitions in several ways: 1) Like Barabás et al. (2018) but unlike Chesson (1994), we do not define the Taylor series coefficients $\beta_j^{(1)}$ and $\beta_j^{(2)}$ with negative signs. We do this for consistency of notation, which can prevent calculation errors. 2) In Chesson (1994), the subtraction inherent in an invader-resident comparison is built into the definition of q_{ir}. Here, the q_{ir} are positive and the subtraction is explicit. 3) Both Chesson (1994) and Barabás et al. (2018) define the storage effect with the so-called standard parameters, $\mathcal{E}_j$ and $\mathcal{C}_j$. The introduction of the standard parameters would complicate our exposition, and all aforementioned definitions for the storage effect are numerically equivalent in the limit of small noise, an assumption upon which Modern Coexistence Theory is built. See Chesson (2020) and Barabás and D'Andrea (2020) for a discussion of the merits of the standard parameters.

Coexistence mechanisms are often divided by the invader's sensitivity to competition, which we operationalize here as $\left|\beta_i^{(1)}\right|$. The rationale is that $\left|\beta_i^{(1)}\right|$ can be interpreted as the speed of population dynamics

(at least in the lottery model and annual plant model), so the scaling enables a comparison of species with slow and fast life-cycles (Chesson, 2018). Note that this scaling is distinct from the aforementioned q_{ir} scaling factors.

Scaled coexistence mechanisms are sometimes averaged over species (see Chesson, 2003, Barabás et al., 2018), either to make comparisons between communities or to quantify how a mechanism affects species *in general*. The *community-average storage effect* is defined as

$$\overline{\left(\frac{\Delta I}{\left|\beta^{(1)}\right|}\right)} = \frac{1}{S}\sum_{i=1}^{S}\frac{\Delta I_i}{\left|\beta_i^{(1)}\right|}. \tag{2.10}$$

Ingredient 2 (an EC interaction effect) and ingredient 3 (the EC covariance) are necessary for the storage effect in the sense that the right-hand-side of Eq.2.9 will be zero if $\zeta_j = 0$ and $\mathrm{Cov}(E_j, C_j) = 0$ for all j. However, the ingredients are neither necessary nor sufficient in the sense that one can construct examples where the right-hand-side of Eq.2.9 is positive despite not all species (including the focal species i) attaining the ingredients individually; or, examples where right-hand-side of Eq.2.9 is zero despite all species attaining the ingredients individually. Such constructions typically leave species with highly asymmetric ΔI_i, even though coexistence is more likely to be attained when all species have a positive ΔI_i.

As we have defined it above, ΔI_i is a species-specific quantity, whereas coexistence is a community-level property. Even though Eq.2.9 is called "the storage effect" by convention, a more sophisticated understanding of coexistence theory identifies the community-average measure as the relevant quantity (Chesson, 2003; Chesson, 2008; Yuan and Chesson, 2015). The community-average storage effect is a complicated expression (an averages of an average), and thus does not transparently reveal anything resembling a necessary or sufficient condition. However, in special cases (e.g., a single limiting factor, symmetric species), the community average measure does reveal the key role played by the three ingredients; for example, see Table 6.3 in Chesson (2008), Eq.2.41 or Eq.2.66 later on in the Appendices.

2.1.B EC covariance and causation

Mathematically, covariance is what is required of the storage effect. Why then, does ingredient 3A employ the concept of causation? Cases of correlation without causation are readily caused by latent variables — if X and Y are causally unconnected, but both are positively related to the latent variable Z, then X and Y will covary. As an ecological example, consider a hypothetical annual plant system in which soil salinity E and the probability of seed germination (which relates to competition via C = # germinant competitors = germination probability × # seeds) are causally unconnected, but positively correlated due to both factors being causally related to precipitation. Increased precipitation causes increased soil moisture, which causes

increased germination; increased precipitation causes the height of a saline water table to increase, which increases soil salinity. Note however, that while there is technically no causation between E and C as we have defined them, there is causation between the environment and competition at some level (here, between precipitation and the number of germinant competitors), and that this causal relationship is necessary for the observed correlation between E and C. Cases of EC covariance without EC causation are only made possible by causation at some level. Note also that the EC covariance is a population covariance, so a spurious covariance based on sampling error is impossible.

It is well known that correlation does not imply causation, but it is not widely recognized that the inverse is true: causation does not imply correlation. A simple example of causation without correlation is a phytoplankton species whose nitrogen uptake rate is a hump-shaped function of temperature, E. If the environment is highly autocorrelated, such that the uptake rate becomes proportional to competition C (here operationalized as the reciprocal of nitrogen concentration), then the relationship between E and C could look like a concave-up parabola in the $E-C$ plane. Since a parabola has covariance equal to zero, we could measure a zero-valued storage effect despite the presence of all ingredients, including a causal relationship between E and C. However, the storage effect has not *really* disappeared. Rather, the bit of per capita growth rate that is attributable to the storage effect has been shunted to a different coexistence mechanism: relative nonlinearity (see Eq.2.8).

The dependence of coexistence mechanism's values on different definitions of E and C is a well-known feature of Modern Coexistence Theory (Barabás et al., 2018). While this non-uniqueness is not ideal, experience suggests that there are better and worse definitions of E and C which may be judged by their naturalness, interpretability, mathematically convenience, and ability to produce ecological insights. In the current hypothetical of a phytoplankton species, the superior choice of E is the resource uptake rate, which has the virtue of separating specialization on environmental states (i.e., the storage effect) from specialization on resource variation *per se* (i.e., relative nonlinearity).

2.1.C EC covariance for a resident species

We first analyze the dynamics a single resident species, dropping species-specific subscripts for notational simplicity. The time-evolution of population density N and the environmental parameter E is given by the equations

$$\begin{aligned} N(t+\Delta t) &= N(t) + F(N(t), E(t))\Delta t \\ E(t+\Delta t) &= E(t) + G(E(t))\,\Delta t + \sigma\sqrt{\Delta t}\,\eta(t), \end{aligned} \tag{2.11}$$

where F is the deterministic growth rate function of the population, G is the deterministic change function of the environmental parameter, t is time, dt is the length of a time step, and $\eta(t)$ is a draw from the standard normal distribution, i.e., $\eta(t) \sim Normal(0, 1)$. The scaling of $\eta(t)$ by $\sqrt{\Delta t}$ is explained by the central limit theorem: the standard deviation of a sum of n i.i.d. random variables is proportional to $\sqrt{n}$, so if perturbations affecting the affecting the environmental parameter occur at a near-constant rate, then the sum of perturbations will be proportional to $\sqrt{\Delta t}$. The functions F and G are arbitrary but smooth functions. Note that the dynamics of E do not depend on population density; indeed, density-independence is the defining feature of an environmental parameter.

In the continuous-time limit (i.e., as the length of the time step shrinks), we obtain a system of stochastic differential equations (SDEs),

$$\begin{aligned} dN(t) &= F(N(t), E(t))dt \\ dE(t) &= G(E(t))dt + \sigma dW(t), \end{aligned} \tag{2.12}$$

with $dW(t)$ denoting an increment of the standard Wiener process (Karlin and Taylor, 1975, ch. 7). Suppose that in the absence of fluctuations in E (i.e., in the limit as $\sigma \to 0$), the system attains a stable equilibrium, denoted (N^*, E^*). This assumption is not very assumptive: most real-world population exhibit random fluctuations around a stable equilibrium, rather than population cycles or chaotic behavior (Turchin, 2003; Kendall et al., 1998; Louca and Doebeli, 2015). Suppose further that environmental noise is small (i.e., σ is small relative to other model parameters hidden in F and G), such that we can approximate the dynamics with a linearization about the equilibrium (see Gardiner, 1985, ch. 7 for details). The assumption of small environmental noise is not particular to our exposition — it is foundational to Modern Coexistence Theory (Chesson, 1994; Barabás et al., 2018). While the small-noise assumption ensures the accuracy of the mathematical expressions to come, a violation of the small-noise assumption does not imply that the results are quantitatively or qualitatively inaccurate; statements about accuracy would required detailed numerical analyses of particular models.

The small-noise approximation of our dynamical system is

$$\begin{aligned} dN(t) &= \left[F_N(N(t) - N^*) + F_E(E(t) - E^*)\right] dt \\ dE(t) &= \left[G_E(E(t) - E^*)\right] dt \; + \sigma dW(t), \end{aligned} \tag{2.13}$$

where F_N, F_E, and G_E are partial derivatives evaluated at equilibrium, e.g., $F_N = \frac{\partial F(N,E)}{\partial N}\Big|_{\substack{N=N^* \\ E=E^*}}$. The assumption of a stable equilibrium implies that $F_N < 0$ and $G_E < 0$.

Our ultimate goal to is to obtain the covariance between the focal residents' environmental parameter and competition parameter, $\mathrm{Cov}(E, C)$. If we suppose that competition is a function of current popula-

tion density, say $C = \widetilde{C}(N)$, then we can use a Taylor series expansion of $\widetilde{C}$ to make the approximation $\text{Cov}(E, C) \approx \widetilde{C}_N \text{Cov}(E, N)$. Thus, our proximal goal is to express $\text{Cov}(E, N)$ in terms of model parameters. It is natural to write competition as a function of population density in population models where per capita growth rates are directly affected by population densities (e.g., the competitive Lotka Volterra model). However, our main finding (that $\text{Cov}(E, C)$ increases as $T_E/T_{E\to C}$ increases) also holds true in models with explicit resource competition, and by extension, apparent competition (Section 2.1.F).

To build intuition for the derivation of $\text{Cov}(E, N)$, we first perform the simpler, univariate derivation of $\text{Var}(E)$. We translate the stochastic process to the origin (re-using the symbols N and E) such that $N^* = E^* = 0$. This does not change variances or covariances (note the property $\text{Cov}(X + a, Y + b) = \text{Cov}(X, Y)$) but it does simplify the derivation by allowing us to write $\text{Var}(E) = \mathbb{E}\left[E^2\right]$. The SDE for the environmental parameter is

$$dE(t) = [G_E E(t)]\, dt + \sigma dW(t). \tag{2.14}$$

Our general strategy is to use Itô's lemma to perform a change of variables, use the property of Itô Isometry to calculate the variance of the new variable, and then perform the inverse change of variables to obtain the variance of E.

Consider a generic univariate drift-diffusion SDE:

$$dX(t) = a(X, t)dt + b(X, t)dW(t). \tag{2.15}$$

Itô's lemma (Karlin and Taylor, 1981, p. 347–348) states that the corresponding SDE for a smooth function $f(X, t)$ is

$$df = \left[\frac{\partial f}{\partial t} + a(X, t)\frac{\partial f}{\partial x} + \frac{b(X, t)^2}{2}\frac{\partial^2 f}{\partial x^2}\right] dt + b(X, t)\frac{\partial f}{\partial x} dW(t). \tag{2.16}$$

We define the new variable $Y = f(E, t) = E(t)e^{-G_E t}$. The SDE of the new variable is

$$dY(t) = \sigma e^{-G_E t} dW(t), \tag{2.17}$$

which conveniently has no drift term. The SDE integrates to

$$Y(t) = Y(0) + \int_0^t \sigma e^{-G_E s} dW(s). \tag{2.18}$$

The property of Itô Isometry (Allen, 2010, p. 377) and the independence independence of increments of

the Weiner process implies that for any two variables X and Y,

$$\mathbb{E}\left[\left(\int_0^{t_1} X(s)dW(s)\right)\left(\int_0^{t_2} Y(s)dW(s)\right)\right] = \mathbb{E}\left[\int_0^{min(t_1,t_2)} X(s)Y(s)ds\right]. \tag{2.19}$$

Applying Itô isometry to our transformed variable Y, we find that

$$\begin{aligned}
\mathbb{E}\big[Y(t)^2\big] &= \mathbb{E}_t\left[\left(Y(0) + \int_0^t \sigma e^{-G_E s} dW(s)\right)^2\right] \\
&= \mathbb{E}\big[Y(0)^2\big] + \mathbb{E}\left[2Y(0)\int_0^t e^{-G_E s} dW(s)\right] + \mathbb{E}\left[\left(\int_0^t \sigma e^{-G_E s} dW(s)\right)^2\right] \\
&= Y(0)^2 + \mathbb{E}\left[\int_0^t \sigma^2 e^{-2G_E s} ds\right] \\
&= Y(0)^2 + \int_0^t \sigma^2 e^{-2G_E s} ds \\
&= Y(0)^2 + \frac{\sigma^2}{2G_E}\left(1 - e^{-2G_E t}\right).
\end{aligned} \tag{2.20}$$

To revert back to the environmental parameter, we apply the inverse function $f^{-1}(Y,t) = Y(t)e^{G_E t}$:

$$\mathrm{Var}(E(t)) = \mathbb{E}\big[E(t)^2\big] = E(0)^2 e^{2G_E t} - \frac{\sigma^2}{2G_E}\left(1 - e^{2G_E t}\right). \tag{2.21}$$

Recalling that $G_E < 0$, it is clear that Var $(E(t))$ converges exponentially fast to the variance of the stationary distribution,

$$\lim_{t\to\infty} \mathrm{Var}(E(t)) = -\frac{\sigma^2}{2G_E}. \tag{2.22}$$

We can apply the previous steps (Eq.2.14 – Eq.2.22) to the multivariate case. Let $\boldsymbol{X}(t)$ be the m-dimensional state of the dynamical system at time t, which may include population densities, environmental parameters, resource concentrations, etc. Additionally, $\boldsymbol{A}$ is a $m \times m$ matrix of rate per capita rate coefficients (e.g., F_N in Eq.2.13), $\boldsymbol{B}$ is a $m \times m$ matrix of diffusion coefficients, and $\boldsymbol{W}(t)$ is a length-m vector of Weiner processes. The system of SDEs can be written succinctly as

$$d\boldsymbol{X}(t) = \boldsymbol{A}\,\boldsymbol{X}(t)\,dt + \boldsymbol{B}\,d\boldsymbol{W}(t). \tag{2.23}$$

Note here that $\boldsymbol{W}$ may have correlated increments, i.e., $\mathbb{E}[dW_i(t)dW_j(t)] = \rho_{ij}\,dt$. We place these correlations in the $m \times m$ matrix $\boldsymbol{C}$, with 1's on the diagonal and correlation coefficients ρ_{ij} on the off-diagonals. We define the transformation $\boldsymbol{Y}(t) = \boldsymbol{X}(t)e^{-t\boldsymbol{A}}$, apply Itô's lemma, and arrive at the multivariate analogue

of Eq.2.20 (line 4):

$$\mathbb{E}[\boldsymbol{Y(t)Y(t)}^\intercal] = \boldsymbol{Y}(0)\boldsymbol{Y}(0)^\intercal + \int_0^t e^{-s\boldsymbol{A}}\boldsymbol{B}\boldsymbol{C}\boldsymbol{B}^\intercal e^{-s\boldsymbol{A}^\intercal}\, ds. \tag{2.24}$$

The matrix product $\boldsymbol{BCB}^\intercal$ is the covariance matrix of the noise term, $\boldsymbol{B}\, d\boldsymbol{W}(t)$. Before evaluating the above integral, we can perform the inverse transformation $\boldsymbol{X}(t) = \left(e^{-t\boldsymbol{A}}\right)^{-1}\boldsymbol{Y}(t) = e^{t\boldsymbol{A}}\boldsymbol{Y}(t)$ to obtain an intermediate expression for the matrix of covariances between states, denoted $\boldsymbol{\Sigma}(t) = \mathbb{E}[\boldsymbol{X(t)X(t)}^\intercal]$:

$$\begin{aligned}\boldsymbol{\Sigma}(t) &= e^{t\boldsymbol{A}}\left(\boldsymbol{X}(0)\boldsymbol{X}(0)^\intercal + \int_0^t e^{-s\boldsymbol{A}}\boldsymbol{B}\boldsymbol{C}\boldsymbol{B}^\intercal e^{-s\boldsymbol{A}^\intercal}\, ds\right)e^{t\boldsymbol{A}^\intercal} \\ &= e^{t\boldsymbol{A}}\boldsymbol{X}(0)\boldsymbol{X}(0)^\intercal e^{t\boldsymbol{A}^\intercal} + \int_0^t e^{(t-s)\boldsymbol{A}}\boldsymbol{B}\boldsymbol{C}\boldsymbol{B}^\intercal e^{(t-s)\boldsymbol{A}^\intercal}\, ds.\end{aligned} \tag{2.25}$$

To proceed, we need to use the Vec operator (Searle and Khuri, 2017). The Vec operator concatenates the columns of a matrix into one long column vector, with the first column on top and the mth column on the bottom. The Vec operator also has a handy property: for three arbitrary matrixes, $Vec\,(\boldsymbol{UVP}) = \left(\boldsymbol{P}^H \otimes \boldsymbol{U}\right) Vec\,\boldsymbol{V}$, where "$\otimes$" is the kronecker product, and the superscript "H" denotes the conjugate transpose. We are dealing exclusively with real matrixes, so the conjugate transpose is simply the transpose, $\boldsymbol{P}^H = \boldsymbol{P}^\intercal$. Applying the Vec operator, we obtain

$$Vec\,\boldsymbol{\Sigma}(t) = \left(e^{t\boldsymbol{A}} \otimes e^{t\boldsymbol{A}}\right)\boldsymbol{X}(0)\boldsymbol{X}(0)^\intercal + \int_0^t e^{(t-s)\boldsymbol{A}} \otimes e^{(t-s)\boldsymbol{A}}\, ds\, Vec\,(\boldsymbol{BCB}^\intercal). \tag{2.26}$$

Now we utilize the identity $e^{\boldsymbol{U}} \otimes e^{\boldsymbol{V}} = e^{\boldsymbol{U}\oplus\boldsymbol{V}}$, where "$\oplus$" is the kronecker sum. Simplifying and integrating, we arrive at explicit formulae for the covariances:

$$\begin{aligned}Vec\,\boldsymbol{\Sigma}(t) &= e^{t(\boldsymbol{A}\oplus\boldsymbol{A})}\boldsymbol{X}(0)\boldsymbol{X}(0)^\intercal + \int_0^t e^{(t-s)(\boldsymbol{A}\oplus\boldsymbol{A})}\, ds\, Vec\,(\boldsymbol{BCB}^\intercal) \\ &= e^{t(\boldsymbol{A}\oplus\boldsymbol{A})}\boldsymbol{X}(0)\boldsymbol{X}(0)^\intercal + (\boldsymbol{A}\oplus\boldsymbol{A})^{-1}\left(e^{t(\boldsymbol{A}\oplus\boldsymbol{A})} - \boldsymbol{I}\right) Vec\,(\boldsymbol{BCB}^\intercal).\end{aligned} \tag{2.27}$$

It can be shown that the eigenvalues of any two matrixes $\boldsymbol{U}\oplus\boldsymbol{V}$ are the sums of every possible pair of eigenvalues of $\boldsymbol{U}$ and $\boldsymbol{V}$ (Horn and Johnson, 2012). Since $\boldsymbol{A}$ has all negative eigenvalues (we assume a stable equilibrium), $\boldsymbol{A}\oplus\boldsymbol{A}$ has all negative eigenvalues. Therefore, in the limit as $t\to\infty$, the exponential terms in Eq.2.27 vanish and the covariances of the stationary distribution can be written as

$$\lim_{t\to\infty} Vec\,\boldsymbol{\Sigma}(t) = -\left(\boldsymbol{A}\oplus\boldsymbol{A}\right)^{-1} Vec\,(\boldsymbol{BCB}^\intercal). \tag{2.28}$$

We can use the expression above to compute the covariance between environment and competition. Returning to our original model of a single resident species (Eq.2.13), the state becomes $\boldsymbol{X}(t) = (N(t), E(t))^\intercal$,

and the matrixes become

$$\boldsymbol{A} = \begin{bmatrix} F_N & F_E \\ 0 & G_E \end{bmatrix}, \quad \boldsymbol{B} = \begin{bmatrix} 0 & 0 \\ 0 & \sigma \end{bmatrix}, \quad \text{and} \quad \boldsymbol{C} = \begin{bmatrix} 1 & 0 \\ 0 & 1 \end{bmatrix}. \tag{2.29}$$

Using Eq.2.28 and restructuring the covariances in matrix-form, we obtain

$$\lim_{t\to\infty} \boldsymbol{\Sigma}(t) = \begin{bmatrix} -\frac{\sigma^2 {F_E}^2}{2{F_N}^2 G_E + 2F_N {G_E}^2} & \frac{\sigma^2 F_E}{2G_E(F_N+G_E)} \\ \frac{\sigma^2 F_E}{2G_E(F_N+G_E)} & -\frac{\sigma^2}{2G_E} \end{bmatrix}. \tag{2.30}$$

The EC covariance experienced by the resident species is therefore

$$\text{Cov}(E,C) = \frac{\widetilde{C}_N F_E \sigma^2}{2G_E\,(F_N + G_E)}. \tag{2.31}$$

The EC covariance is always non-negative, due to assumptions about the signs of Taylor series coefficients in matrix $\boldsymbol{A}$ (Eq.2.29). Specifically, we assume that $G_E < 0$ (required for a stationary environment), $F_N < 0$ (i.e., density dependence), and $F_E > 0$ (which follows the convention in Modern Coexistence Theory that a positive environment is good for population growth). If we instead made the assumption that $F_E < 0$, then the covariance would always be non-positive; however, the EC interaction effect (i.e., ζ, see Section 2.1.A) would also flip signs, leading to the same numerical value of the storage effect .

We can re-parameterize EC covariance in terms of the time scales, which are defined as the reciprocal of rates. For example, if the rate of train arrivals is 10 trains per hour, then the time scale of a train arrival is 1/10 hours = 6 minutes.

The return rate of the environmental parameter is $-G_E$ (recall that $G_E < 0$), so the time scale of environmental change is $T_E = -1/G_E$. The rate at which the environment affects competition is $\frac{\partial \widetilde{C}}{\partial E}\Big|_{\substack{N=N^* \\ E=E^*}} = \frac{\partial \widetilde{C}}{\partial N}\Big|_{N=N^*} \frac{\partial F}{\partial E}\Big|_{\substack{N=N^* \\ E=E^*}} = \widetilde{C}_N F_E$ obtained via the chain rule; therefore, the time scale on which the environment affects competition is $T_{E\to C} = 1/(\widetilde{C}_N F_E)$. Making these substitutions, Eq.2.31 becomes

$$\text{Cov}(E,C) = \frac{(T_E \sigma)^2}{2\,T_{E\to C}\,(1 - T_E\,F_N)}. \tag{2.32}$$

By taking the partial derivatives of the right-hand-side (with respect to T_E and $T_{E\to C}$ individually), it is easy to see that $\text{Cov}(E,C)$ increases monotonically with T_E and decreases monotonically with $T_{E\to C}$. Therefore, we say that

$$\text{Cov}(E,C) \text{ is an increasing function of } \frac{T_E}{T_{E\to C}}, \tag{2.33}$$

as is claimed in the main text.

Current evidence suggests that density-dependence is often weak relative to stochastic forces (Ziebarth et al., 2010; Knape and de Valpine, 2012; Thibaut and Connolly, 2020). In that case, F_N is a small parameter and Eq.2.32 simplifies further:

$$\mathrm{Cov}(E,C) \approx \frac{(T_E\sigma)^2}{2\,T_{E\to C}}. \tag{2.34}$$

As the return rate of the environmental parameter (i.e., $-G_E$) becomes smaller, the variance of the environmental parameter increases (see Eq.2.22). Since the scale of fluctuations in E is proportional to the covariance between E and C, one may suspect that the relationship between T_E and $\mathrm{Cov}(E,C)$ is driven by the indirect effect of environmental autocorrelation, mediated through increased environmental variation; rather than environmental autocorrelation *per se*. To show that this is not the case, we can isolate the effects of environmental autocorrelation by modifying the dynamical equation for E so that

$$dE(t) = [G_E(E(t)-E^*)]\,dt + \frac{\sigma}{\sqrt{-G_E}}dW(t), \tag{2.35}$$

which ensures that the variance of E's stationary distribution is always σ^2. Under these dynamics, the EC covariance comes out to

$$\mathrm{Cov}(E,C) = \frac{T_E\sigma^2}{2\,T_{E\to C}\,(1-T_E\,F_N)}. \tag{2.36}$$

Here, just as before, $\mathrm{Cov}(E,C)$ is an increasing function of $T_E/T_{E\to C}$.

2.1.D EC covariance for the invader

Because we are now dealing with two species, we use the subscripts i and r to refer to the invader and resident. We still use F and G to refer to the deterministic growth functions of population density and the environmental parameter (respectively), but use the superscripts (i) and (r) to denote whether the state variable in question belongs to the invader or resident. For example, $G^{(i)}$ describes the time-evolution of the invader's environmental parameter, and the symbol $F^{(i)}_{N_r}$ is the partial derivative of the invader's population growth rate with respect to resident density, evaluated at equilibrium, i.e., $F^{(i)}_{N_r} = \frac{\partial F^{(i)}(N_i,N_r,E_i)}{\partial N_r}\Big|_{\substack{N_i=0,N_r=N_r^*\\E_i=E_i^*,E_r=E_r^*}}$. With this new notation, the residents' EC covariance (Eq.2.32) is

$$\mathrm{Cov}(E,C) = \frac{\widetilde{C}_{N_r}F^{(r)}_{E_r}\sigma^2}{2G^{(r)}_{E_r}\left(F^{(r)}_{N_r}+G^{(r)}_{E_r}\right)}. \tag{2.37}$$

We seek the covariance between the invader's environmental response E_i and a shared competition param-

eter C, which is determined by the resident's density. In symbols, we seek $\widetilde{C}_{N_r}\mathrm{Cov}(E_i, N_r)$, which requires us to analyze a system with three state variables: $\boldsymbol{X}(t) = (N_r(t), E_r(t), E_i(t))^\intercal$. The SDE matrixes (see Eq.2.23) are

$$\boldsymbol{A} = \begin{bmatrix} F_{N_r}^{(r)} & F_{E_r}^{(r)} & 0 \\ 0 & G_{E_r}^{(r)} & 0 \\ 0 & 0 & G_{E_i}^{(i)} \end{bmatrix}, \quad \boldsymbol{B} = \begin{bmatrix} 0 & 0 & 0 \\ 0 & \sigma_r & 0 \\ 0 & 0 & \sigma_i \end{bmatrix}, \quad \text{and} \quad \boldsymbol{C} = \begin{bmatrix} 1 & 0 & 0 \\ 0 & 1 & \rho \\ 0 & \rho & 1 \end{bmatrix}, \tag{2.38}$$

where ρ is the correlation between the two-species' environmental parameters. Applying Eq.2.28 and correctly identifying $\mathrm{Cov}(E_i, N_r) = [\lim_{t\to\infty} \boldsymbol{\Sigma}(t)]_{3,1}$, we have

$$\mathrm{Cov}(E_i, C) = \frac{\widetilde{C}_{N_r} F_{E_r}^{(r)} \rho \sigma_i \sigma_r}{(F_{N_r}^{(r)} + G_{E_i}^{(i)})(G_{E_i}^{(i)} + G_{E_r}^{(r)})}. \tag{2.39}$$

In a two-species system with a shared competition parameter C, the storage effect for invader i is defined as

$$\Delta I_i = \zeta_i \mathrm{Cov}(E_i, C) - \frac{\beta_i^{(1)}}{\beta_r^{(1)}} \zeta_r \mathrm{Cov}(E_r, C)\,, \tag{2.40}$$

recalling from Section 2.1.A that $q_{ir} = \beta_i^{(1)}/\beta_r^{(1)}$ in this context. The sensitivity to competition is $\beta_j^{(1)} = F_{N_r}^{(j)} \widetilde{C}_{N_r}$, so the scaling factor is $q_{ir} = F_{N_r}^{(i)}/F_{N_r}^{(r)}$. The EC interaction effect could be expressed as a cross partial derivative of the growth function F, i.e., $\zeta_j = F_{N_r E_j}^{(j)} \widetilde{C}_{N_r}$. Note that the Taylor series term corresponding to the coefficient $F_{N_r E_j}$ does not appear in the small-noise approximation of dynamics (Eq.2.13, Eq.2.23), since it is small compared to other terms; $F_{N_r E_j}^{(j)}(N_r - N_r^*)(E_j - E_j^*) = \mathcal{O}(\sigma^2)$ in the conventional "big-oh" notation, whereas $F_{N_r}^{(j)}(N_r - N_r^*) = \mathcal{O}(\sigma)$.

If we assume that species are symmetrical in all respects, with the exception that species respond differently to the environment (i.e., $\rho < 1$), then we no longer need to use species-specific subscripts: $\zeta_i = \zeta_r = \zeta$, $F_{N_r}^{(r)} = F_{N_r}^{(i)} = F_N$, $F_{E_r}^{(r)} = F_{E_i}^{(i)} = F_E$, and $G_{E_r}^{(r)} = G_{E_i}^{(i)} = G_E$. Using this simplified notation and plugging each species' covariances (Eq.2.37 & Eq.2.39) into the storage effect formula (Eq.2.40), we get

$$\begin{aligned} \Delta I_i &= -\zeta(1-\rho)\frac{\widetilde{C}_N F_E \sigma^2}{2G_E\,(F_N + G_E)} \\ &= -\zeta(1-\rho)\frac{(T_E\sigma)^2}{2\,T_{E\to C}\,(1 - T_E\,F_N)} \end{aligned} \tag{2.41}$$

which has the happy property of exactly matching the expanded ingredient-list definition of the storage effect. In particular, Ingredient 3A (a causal relationship between environment and competition) is captured by the fact that neither $\widetilde{C}_N$ nor F_E are zero, or equivalently, the fact that $T_{E\to C}$ is not ∞. Ingredient 3B

(that the environment does not change too quickly) is captured by the fact that T_E is not zero.

2.1.E Seasonality

Our results also hold true for periodically fluctuating environments. Consider a sinusoidal environment with small amplitude, permitting the small-noise approximation,

$$\begin{aligned} \frac{dN(t)}{dt} &= F_N(N(t) - N^*) + F_E(E(t) - E^*) \\ E(t) &= E^* + \sigma \sin\left(\frac{2\pi t}{p}\right), \end{aligned} \tag{2.42}$$

where σ and p are the amplitude and period of environmental fluctuations, respectively. Because we are only dealing with a single species, we have dropped the species-specific subscripts of the previous section in favor of the simpler notation of Section 2.1.C. For the sake of simplifying the covariance calculation, we will once again assume the system has been translated so that $N^* = 0$ and $E^* = 0$. The ordinary differential equation can be integrated via the method of exponential integrating factors, resulting in the general solution,

$$N(t) = ce^{F_N t} - \frac{F_E p\sigma\left(F_N p \sin\left(\frac{2\pi t}{p}\right) + 2\pi\cos\left(\frac{2\pi t}{p}\right)\right)}{F_N^2 p^2 + 4\pi^2}. \tag{2.43}$$

Because $F_N < 0$, the large-t limit eliminates the term $ce^{F_N t}$ without needing to know the initial condition. We can compute the covariance by integrating the large-t limit of $N(t)$ and $E(t)$ across a single period:

$$\begin{aligned} \mathrm{Cov}(E, C) &\approx \widetilde{C}_N \mathrm{Cov}(E, N) \\ &= \widetilde{C}_N \mathbb{E}[EN] \quad [\text{since } \mathbb{E}[E]\,\mathbb{E}[N] = E^* N^* = 0] \\ &= \frac{\widetilde{C}_N}{p}\int_0^p E(t)N(t)dt \\ &= \frac{\widetilde{C}_N}{p}\int_0^p \left(\sigma\sin\left(\frac{2\pi t}{p}\right)\right)\left(-\frac{F_E p\sigma\left(F_N p\sin\left(\frac{2\pi t}{p}\right) + 2\pi\cos\left(\frac{2\pi t}{p}\right)\right)}{F_N^2 p^2 + 4\pi^2}\right) dt \\ &= -\frac{\widetilde{C}_N F_N F_E p^2 \sigma^2}{2F_N^2 p^2 + 8\pi^2}. \end{aligned} \tag{2.44}$$

Re-parameterizing with $T_E = p$ and $T_{E\to C} = 1/\left(\widetilde{C}_N F_E\right)$, the covariance becomes

$$\mathrm{Cov}(E, C) = -\frac{F_N\left(\sigma T_E\right)^2}{T_{E\to C}\left(2F_N^2 T_E^2 + 8\pi^2\right)}. \tag{2.45}$$

2.1.F Explicit resource competition

In many population models, per capita growth rates are a decreasing function of species' densities. This structure is a simple representation of competition or apparent competition, but it assumes that resource (or natural enemy) dynamics are much faster than the focal population dynamics (Chesson, 1990; Kuang and Chesson, 2008). Here we show that our results are insensitive to this assumption by examining a general model of explicit resource competition. Due to the duality between resources and natural enemies (i.e., "enemy-free space" is a resource; Jeffries and Lawton, 1984), this section also covers the case of explicit apparent competition.

Here we seek the covariance between a residents' environmental response E_r and competition parameter C, the latter of which is determined by the resource concentration $R(t)$. The dynamical system is given by the equations

$$\begin{aligned} dN(t) &= F(N(t), E(t), R(t))dt \\ dE(t) &= G(E(t))dt + \sigma dW(t) \\ dR(t) &= H(N(t), E(t), R(t))dt. \end{aligned} \tag{2.46}$$

The inputs to the deterministic growth functions (F, G, and H) imply that the environmental parameter may directly affect the dynamics of both the resident and the resource (see section 2.1.H for a concrete example). The dynamics produce the multivariate small-noise approximation with the state $\boldsymbol{X}(t) = (N(t), E(t), R(t))^\intercal$ and the matrixes (see Eq.2.23),

$$\boldsymbol{A} = \begin{bmatrix} 0 & F_E & F_R \\ 0 & G_E & 0 \\ H_N & H_E & H_R \end{bmatrix}, \quad \boldsymbol{B} = \begin{bmatrix} 0 & 0 & 0 \\ 0 & \sigma & 0 \\ 0 & 0 & 0 \end{bmatrix}, \quad \text{and} \quad \boldsymbol{C} = \begin{bmatrix} 1 & 0 & 0 \\ 0 & 1 & 0 \\ 0 & 0 & 1 \end{bmatrix}. \tag{2.47}$$

Constraints on parameters are imposed by a general understanding of ecological dynamics: $F_E > 0$ (because of the sign convention where a positive environment increases population growth rates), $F_R > 0$ (resources are generally good for population growth), $G_E < 0$ (necessary for a stationary environment), $H_N < 0$ (resources are consumed), $H_E \leq 0$ (an increase in the environmental parameter either negatively affects resource dynamics by increasing resource consumption, or only directly affects population dynamics), and $H_R < 0$ (because of negative feed-backs in resource dynamics; consider chemostat or logistic dynamics around equilibrium). In order for the equilibrium (N^*, E^*, R^*) to be stable, the parameters must also satisfy the inequality: $\frac{{H_R}^2}{4F_R} \leq H_N < 0$.

We can re-write the population growth function as $F(N, E, R) = N\, f(E, R)$, where f is a *per capita*

growth rate function. Then, note that $F_N = \frac{\partial}{\partial N}\left[Nf(E,R)\right]\Big|_{\substack{N=N^*\\E=E^*\\R=R^*}} = f(E^*,R^*) + N^*\frac{\partial}{\partial N}\left[f(E,R)\right]\Big|_{\substack{E=E^*\\R=R^*}} = 0$, which explains $A_{11} = 0$. On the other hand, H_R is not zero because resource fluxes are not necessarily proportional to current resource concentrations. An example of this is a chemostat model, wherein resource input is independent of current resource concentration.

Competition can be generically defined as a decreasing function of resource concentration, $C(t) = \widetilde{C}(R(t))$. Thus, the EC covariance can be approximated as $\mathrm{Cov}(E,C) \approx \widetilde{C}_R \mathrm{Cov}(E,R)$. A particularly simple example is $C(t) = 1/R(t)$, which leads to $\mathrm{Cov}(E,C) \approx (-1/R^{*2})\mathrm{Cov}(E,R)$.

Using the standard formula (Eq.2.28), we obtain

$$\mathrm{Cov}(E,C) = -\frac{\sigma^2 \widetilde{C}_R F_E H_N}{2G_E\left(G_E\left(G_E + H_R\right) - F_R H_N\right)}. \tag{2.48}$$

Just as in the no-resource model (section 2.1.C), the time scale of environmental change is $T_E = -1/G_E$. The time scale on which the environment affects competition, $T_{E\to C}$, depends on the value of H_E. If $H_E = 0$, then the environmental parameter only directly affects population dynamics, and thus the shortest pathway from environment to competition is [environment $\to$ population density $\to$ resource concentration]. Therefore, the rate at which the environment affects competition is $\frac{\partial \widetilde{C}}{\partial R}\Big|_{R=R^*} \times \frac{\partial H}{\partial N}\Big|_{\substack{N=N^*\\R=R^*}} \times \frac{\partial F}{\partial E}\Big|_{\substack{N=N^*\\E=E^*\\R=R^*}} = \widetilde{C}_N H_N F_E$. Correspondingly, $T_{E\to C} = 1/(\widetilde{C}_N H_N F_E)$. If, on the other hand, $H_E < 0$, then the environmental parameter directly affects resource dynamics, and the time scale is instead $T_{E\to C} = 1/(\widetilde{C}_N H_E)$.

One may re-parameterize $\mathrm{Cov}(E,C)$ in terms of T_E and $T_{E\to C}$, but the resulting expression is not as simple as the analogous expression in case of implicit resource competition (i.e., Eq.2.32). In particular, the constitutive parameters of $T_{E\to C}$ are not all eliminated from the expression; the resulting dependencies between variables (say, between H_N and $T_{E\to C}$) make it difficult to understand how $T_{E\to C}$ affects the covariance. Nevertheless, we can evaluate our main result qualitatively by checking if $\mathrm{Cov}(E,C)$ responds as expected to changes in the constitutive parameters of T_E and $T_{E\to C}$.

We first consider the case where the environmental parameter does not directly affect resource dynamics (i.e., $H_E = 0$). Here, $T_{E\to C}$ is proportional to $-1/\widetilde{C}_R$, $-1/H_N$, and $1/F_E$. Equivalently, $T_{E\to C}$ increases along with $\widetilde{C}_R$ and H_N; and decreases as F_E increases. Therefore, if $\mathrm{Cov}\,(E,C)$ increases as $T_{E\to C}$ decreases (ingredient 3A), then we would expect that $\mathrm{Cov}(E,C)$ is a decreasing function of $\widetilde{C}_R$ and H_N; and an increasing function of F_E. Following similar logic, T_E is proportional to $-1/G_E$, so if $\mathrm{Cov}(E,C)$ increases as T_E increases (ingredient 3B), then we would expect that $\mathrm{Cov}(E,C)$ is an increasing function of G_E.

In the case where where the environmental parameter negatively affects resource dynamics (i.e., $H_E < 0$), the time scale parameter $T_{E\to C}$ is proportional to $-1/\widetilde{C}_R$ and $-1/H_E$. In turn, we would expect that

$\mathrm{Cov}(E, C)$ is a decreasing function of $\widetilde{C}_R$ and H_N.

Indeed, all of the relationships in the previous two paragraphs are always true. We show that this is the case by taking the partial derivatives of the right-hand-side of Eq.2.48 with respect to the aforementioned parameters (e.g., $\widetilde{C}_R$) and evaluating whether the result is positive or negative. These calculations were performed with the software *Mathematica*; see the supplementary files.

2.1.G Discrete time

Our main result — $\mathrm{Cov}(E, C)$ increases as $T_E/T_{E\to C}$ increases — is also true in discrete-time systems. Similarly to the continuous-time case, we can linearize a system of difference equations and use the approximate dynamics to compute covariances. Consider the discrete-time system with resident density N and environmental state E,

$$\begin{aligned} N(t+\Delta t) &= F'(N(t), E(t)) \\ E(t+\Delta t) &= G'(E(t)) + \sigma'\eta'(t). \end{aligned} \tag{2.49}$$

The prime superscript ("′") is used to differentiate current functions and parameters from corresponding continuous-time functions and parameters. Assuming that σ' is small and that the deterministic sub-system settles to a stable equilibrium, we can write the approximate dynamics as

$$\begin{aligned} N(t+\Delta t) - N^* &= F'_N(N(t) - N^*) + F'_E(E(t) - E^*) \\ E(t+\Delta t) - E^* &= G'_E(E(t) - E^*) + \sigma'\eta'(t). \end{aligned} \tag{2.50}$$

More generally, a system of linear stochastic difference equations can be written as

$$\boldsymbol{X}(t+\Delta t) = \boldsymbol{A'}\,\boldsymbol{X}(t) + \boldsymbol{B'}\,\boldsymbol{\eta'}(t), \tag{2.51}$$

where $\boldsymbol{X}(t)$ is m-dimensional state, $\boldsymbol{A'}$ is a $m \times m$ matrix, $\boldsymbol{B}$ is a $m \times m$ matrix, and $\boldsymbol{\eta'}$ is a draw from a multivariate normal distribution with correlation matrix $\boldsymbol{C'}$.

Assuming that the system has been translated so that $\mathbb{E}[\boldsymbol{X}] = 0$, computing the covariance matrix (denoted $\boldsymbol{\Sigma'}$) of the stationary distribution amounts to squaring both sides of Eq.2.51 and taking the expectation:

$$\lim_{t\to\infty} \boldsymbol{\Sigma'}(t) = \boldsymbol{A'}\left[\lim_{t\to\infty} \boldsymbol{\Sigma'}(t)\right]\boldsymbol{A'^{\mathsf{T}}} + \boldsymbol{B'C'B'^{\mathsf{T}}}. \tag{2.52}$$

Applying the Vec operator to both sides and solving for the stationary covariances, we obtain the explicit formula

$$\lim_{t\to\infty} Vec\,\boldsymbol{\Sigma'}(t) = \left(\boldsymbol{I} - \boldsymbol{A'} \otimes \boldsymbol{A'}\right)^{-1} Vec\left(\boldsymbol{B'C'B'^{\mathsf{T}}}\right). \tag{2.53}$$

Applying the above equation to the discrete-time system with a sole resident (i.e., Eq.2.50), we find that

$$\mathrm{Cov}(E,C) = \frac{\widetilde{C}_N F'_E G'_E \sigma'^2}{({G'_E}^2 - 1)\,(F'_N G'_E - 1)}. \tag{2.54}$$

The time scales T_E and $T_{E\to C}$ are the reciprocals of dynamical rates, but the parameters in the covariance expression above (e.g., F'_E) are not rates — they are are dimensionless. To convert the parameters to their continuous-time counterparts, we match terms in the discrete-time system (Eq.2.50) to terms in the corresponding continuous-time solution, obtained by integrating the continuous-time dynamics over a short time step. See the *Mathematica* notebook for details.

We obtain $F'_N = \exp\{F_N \Delta t\}$ and $G'_E = \exp\{G_E \Delta t\}$, the standard conversion between the finite rate of increase and per capita growth rates (Gotelli and Ulrich, 2012, p. 13). Recall that F_N and G_E are the Taylor series coefficients of the small-noise approximation of continuous-time dynamics (Eq.2.13). Following Eq.2.21, the conversion for the noise variance is $\sigma'^2 = -(\sigma^2/2G_E)(1 - \exp(2G_E\Delta t))$. The remaining coefficient conversion is more complicated: $F_E = \frac{F_E(\exp(F_N\Delta t) - \exp(G_E \Delta t))}{F_N - G_E}$.

Now, the covariance can be written as

$$\mathrm{Cov}(E,C) = -\frac{\widetilde{C}_N F_E (e^{F_N \Delta t} - e^{G_E \Delta t}) e^{G_E \Delta t} \frac{\sigma^2}{2G_E}(1 - e^{2G_E \Delta t})}{(F_N - G_E)\,(e^{2G_E \Delta t} - 1)\,(e^{(F_N + G_E)\Delta t} - 1)}. \tag{2.55}$$

For small Δt, the Taylor series approximation $e^{x\Delta t} = 1 + x\Delta t + \ldots$ can be applied. Truncating at $\mathcal{O}(1)$, the covariance can be approximated as

$$\mathrm{Cov}(E,C) \approx \frac{\widetilde{C}_N F_E \sigma^2}{2G_E\,(F_N + G_E)}, \tag{2.56}$$

which is identical to the continuous-time covariance (Eq.2.31). Substituting in T_E and $T_{E\to C}$ will result once again in Eq.2.32, thus making it clear that $\mathrm{Cov}(E,C)$ increases as $T_E/T_{E\to C}$ increases.

2.1.H A phytoplankton model with fluctuating uptake rates

Here we provide an example with the purpose of 1) demonstrating how the general methodology of section 2.1.C may be used in practice, and 2) providing intuition with regard to the biological meaning of $T_{E\to C}$.

Consider a chemostat with phytoplankton density $N(t)$ and resource concentration $R(t)$. The phytoplankton exhibits a linear functional response, but with a temporally-fluctuating uptake rate, given by $exp(E(t))$.

The environmental parameter itself follows Ornstein-Uhlenbeck dynamics. The equations are

$$\begin{aligned}\frac{dN(t)}{dt} &= N(t)\left[c\, e^{E(t)}R(t) - \delta\right] \\ \frac{dR(t)}{dt} &= \delta(S - R(t)) + e^{E(t)}N(t)R(t) \\ dE(t) &= -\theta(E(t) - \mu)dt\ + \sigma dW(t),\end{aligned} \tag{2.57}$$

where c is the resource-to-phytoplankton conversion coefficient, δ is the dilution rate (and equivalently, the death rate for phytoplankton), S is the resource supply concentration, θ is the return rate of the environmental parameter, μ is the mean of $E(t)$, and σ is the scale of perturbations to $E(t)$.

The deterministic dynamics produce a single positive equilibrium, $n^* = (ce^{\mu}S - \delta)$, $R^* = (\delta e^{-\mu})/c$, and $E^* = \mu$. Defining the full system state as $\boldsymbol{X}(t) = (N(t), R(t), E(t))^{\intercal}$, the matrixes of the linearized system are

$$\boldsymbol{A} = \begin{bmatrix} 0 & \delta e^{-\mu}\left(ce^{\mu}S - \delta\right) & c\left(ce^{\mu}S - \delta\right) \\ 0 & -\theta & 0 \\ -\frac{\delta}{c} & -\frac{\delta e^{-\mu}(ce^{\mu}S - \delta)}{c} & -ce^{\mu}S \end{bmatrix}, \quad \boldsymbol{B} = \begin{bmatrix} 0 & 0 & 0 \\ 0 & 0 & 0 \\ 0 & 0 & \sigma \end{bmatrix}, \quad \text{and} \quad \boldsymbol{C} = \begin{bmatrix} 1 & 0 & 0 \\ 0 & 1 & 0 \\ 0 & 0 & 1 \end{bmatrix}. \tag{2.58}$$

A natural choice for the competition parameter is $C(t) = \widetilde{C}(R(t)) = -\log(cR(t))$, which makes the per capita growth rate of the phytoplankton $\exp(E(t) - C(t)) - \delta$. With this choice, the interaction effect between environment and competition is $\zeta = -\delta$, which is always non-zero (as claimed in the main text).

Computing the covariances of the stationary distribution and using the approximation $\mathrm{Cov}(E, C) \approx \widetilde{C}_R \mathrm{Cov}(E, R)$, we find that the EC covariance is

$$\mathrm{Cov}(E, C) = \frac{\sigma^2\left(ce^{\mu}S - \delta\right)}{2\theta\left(ce^{\mu}S - \delta + \theta\right)}. \tag{2.59}$$

Following the mathematics of Section 2.1.D, we can obtain a simple expression for the storage effect if we assume that species have different responses to the environment but are otherwise identical. In a two-species community where the cross-species correlation in E is ρ, the storage effect is

$$\Delta I = \delta\left(1 - \rho\right)\frac{\sigma^2\left(ce^{\mu}S - \delta\right)}{2\theta\left(ce^{\mu}S - \delta + \theta\right)}. \tag{2.60}$$

The time scale on which the environment affects competition is

$$\begin{aligned} T_{E\to C} &= \frac{1}{\widetilde{C}_R H_E} \quad [H \text{ is the r.h.s. of dR(t)/dt, (Eq.2.57)}] \\ &= \frac{1}{ce^{\mu}S - \delta}. \end{aligned} \tag{2.61}$$

Intuitively, the rate at which the environment affects competition (i.e., the reciprocal of $T_{E\to C}$) increases as the rate of consumption and conversion (i.e., $c\exp(\mu)$) increases; and decreases as the process of chemostat dilution (i.e., δ) becomes stronger than resource-consumer interactions.

Combining the definition of $T_{E\to C}$ (Eq.2.61) with the definition $T_E = 1/\theta$, the EC covariance (Eq.2.59) can be rewritten as

$$\mathrm{Cov}(E,C) = \frac{(\sigma T_E)^2}{2\left(T_E + T_{E\to C}\right)}. \tag{2.62}$$

2.1.I The lottery model

In this section, we will analyze the lottery model (*sensu* Chesson, 1994), one of the canonical models in Modern Coexistence Theory. We will show that the storage effect arises readily when environmental states are uncorrelated between time steps, a result that speciously acts as counter-example to our claim that $\mathrm{Cov}(E,C)$ increases with $T_E/T_{E\to C}$. However, as we argue in the main text, E is very much autocorrelated on the more relevant within-step time scale. We will also show how the lottery model connects to our broader claim that ingredient 3B can be satisfied by a life stage, which through its numerical response to the abiotic environment, carries the effects of the environment through time.

2.1.I.1 The conventional lottery model

The lottery model describes coral reef fishes competing for space. In a single time step, adult fish produce larvae according to the time-varying per capita fecundities $\xi_j(t)$, adult fish die with probabilities δ_j, and larvae compete for the open territories. Each individual larvae has the same probability of winning a territory, hence the lottery model's name. It is assumed that the fish always produce far more larvae than are necessary to replace the dead adults, such that adult densities of all species sum to one. The per capita fecundities are assumed to be temporally uncorrelated, though there may be cross-species correlations within a time step. Unrecruited larvae die before the next time step begins, so we can track the adult densities (denoted N_j)

with one equation per species:

$$N_j(t+1) = N_j(t)\left[\overbrace{1-\delta_j}^{\text{survival prob.}} + \overbrace{\xi_j(t)}^{\text{per capita fecundity}}\left[\underbrace{\frac{\overbrace{\sum_{j=1}^{S}\delta_j N_j(t)}^{\text{open territories}}}{\sum_{j=1}^{S}\xi_j(t)N_j(t)}}_{\text{total larvae}}\right]\right]. \tag{2.63}$$

Here, S is the number of species in the community. Conventionally, the environmental parameter is per capita fecundity, and competition is the number of larvae per open territory (both on the logarithmic scale for mathematical convenience). In symbols, we have $E_j(t) = \log(\xi_j(t))$ and $C(t) = \log\left(\frac{\sum_{j\neq i}^{S}\xi_j(t)N_j(t)}{\sum_{j\neq i}^{S}\delta_j N_j(t)}\right)$. The lottery model can now be written as

$$N_j(t+1) = N_j(t)\left[1-\delta_j+\exp\{E_j(t)-C(t)\}\right]. \tag{2.64}$$

Unlike previous models in this document, the competition parameter is a function of both the environmental parameter and population density: $C(t) = \widetilde{C}(\boldsymbol{E}(t), \boldsymbol{N}(t))$, where $\boldsymbol{E}(t)$ and $\boldsymbol{N}(t)$ are S-dimensional vectors. This in itself is an indication that the lottery model contains multiple time scales. Indeed, the environment (i.e., per capita fecundity) affects the number of larvae, which affects competition (i.e., recruitment) some time later. Events on this fast time scale (from spawning to recruitment) occur within a single time step of the lottery model.

The covariance between environment and competition for species j can be approximated as

$$\begin{aligned}\mathrm{Cov}(E_j, C) &\approx \sum_{k=1}^{S}\left[\widetilde{C}_{E_k}\mathrm{Cov}(E_j, E_k) + \widetilde{C}_{N_k}\mathrm{Cov}(E_j, N_k)\right] \\ &= \sum_{k=1}^{S}\left[\widetilde{C}_{E_k}\mathrm{Cov}(E_j, E_k)\right] \quad [\text{since the } E_j(t) \text{ are temporally uncorrelated}].\end{aligned} \tag{2.65}$$

For a sole resident species, $\widetilde{C}_{E_r} = 1$, and thus the covariance is $\mathrm{Cov}(E_r, C) = \sigma_r^2$. For an invader in the presence of a sole resident, the covariance is $\mathrm{Cov}\,(E_r, C) = \rho\sigma_i\sigma_r$. The interaction effect between environment and competition is $\zeta_j = -\delta_j(1-\delta_j)$. Putting it all together, a symmetric invader and resident (which are identical with the exception of their environmental responses; i.e., $\rho \neq 1$), will produce the scaled storage effect

$$\frac{\Delta I}{\delta} \approx \sigma^2 (1-\delta)(1-\rho). \tag{2.66}$$

For the remainder of our discussion, we will consider a system with a single resident and drop all species-specific indexes. The environmental parameter of the resident is uncorrelated between time steps, which corresponds to the autoregressive-1 equation,

$$E(t+1) = E^* + G'_E(E(t) - E^*) + \sigma\eta(t) \quad [\eta(t) \sim Normal(0,1)], \tag{2.67}$$

with $G'_E = 0$. Following the logic of section 2.1.G, the return rate of the environment (i.e., the continuous-time analogue of the autoregressive parameter G'_E) is $-G_E = -\log(G'_E) = -\log(0) = \infty$; and thus the time scale of environmental change is $T_E = -1/G_E = 0$. The lottery model produces coexistence via the storage effect when $T_E = 0$ (see Eq.2.66), which seems to contradict a number of previous results (Eq.2.32, Eq.2.45, Eq.2.48, Eq.2.62) where a non-zero T_E was required for a non-zero $\mathrm{Cov}(E, C)$.

2.1.I.2 Larvae carry the environment

Even if we were to imagine that the fish spawn in an instant, it is still the case that "the environment" is autocorrelated on the within-step time scale. "The environment", broadly understood as any fluctuating, density-independent parameter, can be defined in terms of larval density. By virtue of the larva's continued existence, "the environment" is autocorrelated. Put another way, The larvae carry the effects of the abiotic environment through time, thus satisfying ingredient 3B.

To demonstrate this interpretation of the lottery model, we show how dispersal can alter the larva's ability to carry the effects of the environment. After the spawning phase, planktonic fish larvae drift offshore (ostensibly this is an adaptation for avoiding predation), returning months later to compete for open reef territories. The conventional lottery model assumes that all larvae return, but it is more likely that larvae are both lost and gained through dispersal amongst stretches of reef in a larger metapopulation. We can track larvae in a single patch with the differential equation

$$\frac{dL(s,t)}{ds} = m(\mu - L(s)), \tag{2.68}$$

where s is the number of days since the beginning of the spawning period in year t, m is the rate of dispersal, and μ is the expectation of per capita fecundity $\xi(t)$. The model assumes that there are a large number of patches and that the $\xi(t)$ of different patches are independent (so that the spatial average of $\xi(t)$ converges to the expectation μ); that dispersal between patches is equally likely throughout the time period; and that

each patch is an equally likely destination for any disperser (i.e., spatially implicit dynamics).

The initial condition in our single patch is $L(0,t) = n(t)\xi(t)$. Integrating from 0 to s_1, the number of days between the end of the spawning phase and the beginning of the recruitment phase, we obtain the larval density, $L(s_1,t) = n(t)\xi(t)e^{-ms_1} + \mu\,(1 - e^{-ms_1})$.

The density of larvae that originated in the focal patch (i.e., the larvae that carry the effects of the local environment) are $L(s,t) = n(t)\xi(t)e^{-ms}$. We re-define the environmental parameter as the per capita density of these original larvae at time s: $E(s,t) = \xi(t)e^{-ms}$. It is clear that E is autocorrelated on the time scale of days. In fact, the characteristic decay rate of E is m, which means that the time scale of environmental change is $T_E = 1/m$ days.

We note here that there are different ways to interpret the effects of dispersal. If one defines "the environment" in terms of the remaining larvae (as we have above), then T_E is inversely proportional to the dispersal rate, but $T_{E\to C}$ is relatively unaffected by dispersal. On the other hand, if one defines "the environment" in terms of the effective per capita fecundity, then T_E is unaffected by dispersal and $T_{E\to C}$ increases along with the dispersal rate. See the *Mathematica* notebook for details. While multiple interpretations are possible, the result is the same: as the dispersal rate increases, $T_E/T_{E\to C}$ decreases, and in turn, so does the EC covariance.

Acknowledgements

We would like to thank Karen Abbott for helpful suggestions, and Logan Brissette for help with Figure 2.2.

Data availability statement

Code is available on GitHub (https://github.com/ejohnson6767/storage_effect_heuristic) and on Figshare (https://doi.org/10.6084/m9.figshare.20399253.v1; https://doi.org/10.6084/m9.figshare.20399235.v1).

References

Abrams, P. (1984). Variability in resource consumption rates and the coexistence of competing species. *Theoretical Population Biology*, *25*(1), 106–124.

Adler, P. B., & Drake, J. M. (2008). Environmental variation, stochastic extinction, and competitive coexistence. *The American Naturalist*, *172*(5), E186–E195.

Adler, P. B., Ellner, S. P., & Levine, J. M. (2010). Coexistence of perennial plants: An embarrassment of niches. *Ecology Letters*, *13*(8), 1019–1029.

Adler, P. B., HilleRisLambers, J., Kyriakidis, P. C., Guan, Q., & Levine, J. M. (2006). Climate variability has a stabilizing effect on the coexistence of prairie grasses. *Proceedings of the National Academy of Sciences*, *103*(34), 12793–12798.

Allen, L. J. (2010). *An introduction to stochastic processes with applications to biology* (2nd ed.). CRC press.

Angert, A. L., Huxman, T. E., Chesson, P., & Venable, D. L. (2009). Functional tradeoffs determine species coexistence via the storage effect. *Proceedings of the National Academy of Sciences*, *106*(28), 11641–11645.

Armitage, D. W., & Jones, S. E. (2019). Negative frequency-dependent growth underlies the stable coexistence of two cosmopolitan aquatic plants. *Ecology*, *100*(5), e02657.

Armitage, D. W., & Jones, S. E. (2020). Coexistence barriers confine the poleward range of a globally distributed plant. *Ecology Letters*, *23*(12), 1838–1848.

Barabás, G., & D'Andrea, R. (2020). Chesson's coexistence theory: Reply. *Ecology*, *101*(11).

Barabás, G., D'Andrea, R., & Stump, S. M. (2018). Chesson's coexistence theory. *Ecological Monographs*, *88*(3), 277–303.

Bell, A. M., & Hellmann, J. K. (2019). An integrative framework for understanding the mechanisms and multigenerational consequences of transgenerational plasticity. *Annual Review of Ecology, Evolution, and Systematics*, *50*, 97–118.

Bogunovic, I., Mesic, M., Zgorelec, Z., Jurisic, A., & Bilandzija, D. (2014). Spatial variation of soil nutrients on sandy-loam soil. *Soil and tillage research*, *144*, 174–183.

Cáceres, C. E. (1997). Temporal variation, dormancy, and coexistence: A field test of the storage effect. *Proceedings of the National Academy of Sciences*, *94*(17), 9171–9175.

Chesson, P. (1990). Macarthur's consumer-resource model. *Theoretical Population Biology*, *37*(1), 26–38.

Chesson, P. (1991). A need for niches? *Trends in ecology & evolution*, *6*(1), 26–28.

Chesson, P. (1994). Multispecies competition in variable environments. *Theoretical Population Biology*, *45*(3), 227–276.

Chesson, P. (2000a). General theory of competitive coexistence in spatially-varying environments. *Theoretical Population Biology*, *58*(3), 211–237.

Chesson, P. (2000b). Mechanisms of maintenance of species diversity. *Annual review of Ecology and Systematics*, *31*(1), 343–366.

Chesson, P. (2003). Quantifying and testing coexistence mechanisms arising from recruitment fluctuations. *Theoretical Population Biology*, *64*(3), 345–357.

Chesson, P. (2008). Quantifying and testing species coexistence mechanisms. In *Unity in diversity: Reflections on ecology after the legacy of Ramon Margalef* (pp. 119–164). Fundacion BBVA Bilbao.

Chesson, P. (2012). Scale transition theory: Its aims, motivations and predictions. *Ecological Complexity*, *10*, 52–68.

Chesson, P. (2018). Updates on mechanisms of maintenance of species diversity. *Journal of ecology*, *106*(5), 1773–1794.

Chesson, P. (2020). Chesson's coexistence theory: Comment. *Ecology*, *101*(11), e02851.

Chesson, P., Donahue, M. J., Melbourne, B., & Sears, A. L. W. (2003). *Chapter 6: Scale Transition Theory for Understanding Mechanisms in Metacommunities* (tech. rep. Hanski 1999).

Chesson, P., Gebauer, R. L., Schwinning, S., Huntly, N., Wiegand, K., Ernest, M. S., Sher, A., Novoplansky, A., & Weltzin, J. F. (2004). Resource pulses, species interactions, and diversity maintenance in arid and semi-arid environments. *Oecologia*, *141*(2), 236–253.

Chesson, P., & Huntly, N. (1997). The roles of harsh and fluctuating conditions in the dynamics of ecological communities. *The American Naturalist*, *150*(5), 519–553.

Chesson, P., Huntly, N. J., Roxburgh, S. H., Pantastico-Caldas, M., & Facelli, J. M. (2012). The storage effect: Definition and tests in two plant communities. In *Temporal dynamics and ecological process* (pp. 11–40). Cambridge University Press.

Chesson, P., & Kuang, J. J. (2010). The storage effect due to frequency-dependent predation in multispecies plant communities. *Theoretical Population Biology*, *78*(2), 148–164.

Chesson, P. L. (1988). Interactions between environment and competition: How fluctuations mediate coexistence and competitive exclusion. In *Community ecology* (pp. 51–71). Springer.

Chesson, P. L., & Huntly, N. (1988). Community consequences of life-history traits in a variable environment. *Annales Zoologici Fennici*, 5–16.

Chu, C., & Adler, P. B. (2015). Large niche differences emerge at the recruitment stage to stabilize grassland coexistence. *Ecological Monographs*, *85*(3), 373–392.

Colicchio, J. M., & Herman, J. (2020). Empirical patterns of environmental variation favor adaptive transgenerational plasticity. *Ecology and evolution*, *10*(3), 1648–1665.

Danino, M., Kessler, D. A., & Shnerb, N. M. (2018). Stability of two-species communities: Drift, environmental stochasticity, storage effect and selection. *Theoretical Population Biology*, *119*, 57–71.

Darwin, C. M. A. (1859). *On the origins of species* (1st ed.). John Murray.

Dempster, E. R. (1955). Maintenance of genetic heterogeneity. *Cold Spring Harbor symposia on quantitative biology*, *20*.

Descamps-Julien, B., & Gonzalez, A. (2005). Stable coexistence in a fluctuating environment: An experimental demonstration. *Ecology*, *86*(10), 2815–2824.

Ellner, S. (1987). Alternate plant life history strategies and coexistence in randomly varying environments. *Vegetatio*, *69*(1), 199–208.

Ellner, S. P., Snyder, R. E., & Adler, P. B. (2016). How to quantify the temporal storage effect using simulations instead of math. *Ecology letters*, *19*(11), 1333–1342.

Ellner, S. P., Snyder, R. E., Adler, P. B., & Hooker, G. (2019). An expanded modern coexistence theory for empirical applications. *Ecology letters*, *22*(1), 3–18.

Facelli, J. M., Chesson, P., & Barnes, N. (2005). Differences in seed biology of annual plants in arid lands: A key ingredient of the storage effect. *Ecology*, *86*(11), 2998–3006.

Galloway, L. F., & Burgess, K. S. (2009). Manipulation of flowering time: Phenological integration and maternal effects. *Ecology*, *90*(8), 2139–2148.

Gardiner, C. W. (1985). *Handbook of stochastic methods* (Vol. 3). Springer.

Gause, G. F. (1934). *The struggle for existence.* Williams & Wilkins.

Geritz, S. A., Gyllenberg, M., Jacobs, F. J., & Parvinen, K. (2002). Invasion dynamics and attractor inheritance. *Journal of mathematical biology*, *44*(6), 548–560.

Gotelli, N. J., & Ulrich, W. (2012). Statistical challenges in null model analysis. *Oikos*, *121*(2), 171–180.

Grinnell, J. (1904). The Origin and Distribution of the Chest-Nut-Backed Chickadee. *21*(3), 364–382.

Gulisija, D., Kim, Y., & Plotkin, J. B. (2016). Phenotypic plasticity promotes balanced polymorphism in periodic environments by a genomic storage effect. *Genetics*, *202*(4), 1437–1448.

Haldane, J. B., & Jayakar, S. D. (1963). Polymorphism due to selection of varying direction. *Journal of Genetics*, *58*(2), 237–242.

Hallett, L. M., Shoemaker, L. G., White, C. T., & Suding, K. N. (2019). Rainfall variability maintains grass-forb species coexistence. *Ecology Letters*, *22*(10), 1658–1667.

Harper, J. L. (1977). *Population biology of plants.* Academic Press.

Hastings, A. (2010). Timescales, dynamics, and ecological understanding. *Ecology*, *91*(12), 3471–3480.

Herman, J. J., & Sultan, S. E. (2011). Adaptive transgenerational plasticity in plants: Case studies, mechanisms, and implications for natural populations. *Frontiers in plant science*, *2*, 102.

Herman, J. J., & Sultan, S. E. (2016). Dna methylation mediates genetic variation for adaptive transgenerational plasticity. *Proceedings of the Royal Society B: Biological Sciences*, *283*(1838), 20160988.

Holt, G., & Chesson, P. (2014). Variation in moisture duration as a driver of coexistence by the storage effect in desert annual plants. *Theoretical Population Biology*, *92*, 36–50.

Holt, R. D. (1977). Predation, apparent competition, and the structure of prey communities. *Theoretical Population Biology*, *12*(2), 197–229.

Horn, R. A., & Johnson, C. R. (2012). *Matrix analysis*. Cambridge university press.

Huston, M. (1979). A general hypothesis of species diversity. *The American Naturalist*, *113*(1), 81–101.

Hutchinson, G. E. (1961). The paradox of the plankton. *The American Naturalist*, *95*(882), 137–145.

Ignace, D. D., Huntly, N., & Chesson, P. (2018). The role of climate in the dynamics of annual plants in a chihuahuan desert ecosystem. *Evolutionary Ecology Research*, *19*(3), 279–297.

Jeffries, M., & Lawton, J. (1984). Enemy free space and the structure of ecological communities. *Biological Journal of the Linnean Society*, *23*(4), 269–286.

Kamenev, A., Meerson, B., & Shklovskii, B. (2008). How colored environmental noise affects population extinction. *Physical Review Letters*, *101*(26), 268103.

Karlin, S., & Taylor, H. E. (1975). *A first course in stochastic processes* (1st ed.). Academic Press.

Karlin, S., & Taylor, H. E. (1981). *A second course in stochastic processes* (1st ed.). Academic Press.

Kendall, B. E., Prendergast, J., & Bjørnstad, O. N. (1998). The macroecology of population dynamics: Taxonomic and biogeographic patterns in population cycles. *Ecology letters*, *1*(3), 160–164.

Knape, J., & de Valpine, P. (2012). Are patterns of density dependence in the global population dynamics database driven by uncertainty about population abundance? *Ecology letters*, *15*(1), 17–23.

Kuang, J. J., & Chesson, P. (2008). Predation-Competition Interactions for Seasonally Recruiting Species. *171*(3).

Kuang, J. J., & Chesson, P. (2009). Coexistence of annual plants: Generalist seed predation weakens the storage effect. *Ecology*, *90*(1), 170–182.

Kuang, J. J., & Chesson, P. (2010). Interacting coexistence mechanisms in annual plant communities: Frequency-dependent predation and the storage effect. *Theoretical Population Biology*, *77*(1), 56–70.

Lachmann, M., & Jablonka, E. (1996). The inheritance of phenotypes: An adaptation to fluctuating environments. *Journal of theoretical biology*, *181*(1), 1–9.

Letten, A. D., Dhami, M. K., Ke, P.-J., & Fukami, T. (2018). Species coexistence through simultaneous fluctuation-dependent mechanisms. *Proceedings of the National Academy of Sciences*, *115*(26), 6745–6750.

Levin, S. A. (1970). Community equilibria and stability, and an extension of the competitive exclusion principle. *The American Naturalist*, *104*(939), 413–423.

Levins, R. (1979). Coexistence in a variable environment. *The American Naturalist*, *114*(6), 765–783.

Lewens, T. (2010). Natural selection then and now. *Biological Reviews*, *85*(4), 829–835.

Lewontin, R. C., & Cohen, D. (1969). On population growth in a randomly varying environment. *Proceedings of the National Academy of Sciences of the United States of America*, *62*(4), 1056–1060.

Li, L., & Chesson, P. (2016). The effects of dynamical rates on species coexistence in a variable environment: The paradox of the plankton revisited. *The American Naturalist*, *188*(2), E46–E58.

Loreau, M. (1989). Coexistence of temporally segregated competitors in a cyclic environment. *Theoretical Population Biology*, *36*(2), 181–201.

Loreau, M. (1992). Time scale of resource dynamics and coexistence through time partitioning. *Theoretical Population Biology*, *41*(3), 401–412.

Lotka, A. J. (1932). The growth of mixed populations: Two species competing for a common food supply. *Journal of the Washington Academy of Sciences*, *22*(16-17), 461–469.

Louca, S., & Doebeli, M. (2015). Detecting cyclicity in ecological time series. *Ecology*, *96*(6), 1724–1732.

May, R. M. (1974). On the theory of niche overlap. *Theoretical Population Biology*, *5*(3), 297–332.

Meyer, I., & Shnerb, N. M. (2018). Noise-induced stabilization and fixation in fluctuating environment. *Scientific Reports*, *8*(1), 1–12.

Muko, S., & Iwasa, Y. (2000). Species coexistence by permanent spatial heterogeneity in a lottery model. *Theoretical Population Biology*, *57*(3), 273–284.

Mylius, S. D., & Diekmann, O. (2001). The resident strikes back: Invader-induced switching of resident attractor. *Journal of Theoretical Biology*, *211*(4), 297–311.

Pake, C. E., & Venable, D. L. (1995). Is coexistence of sonoran desert annuals mediated by temporal variability reproductive success. *Ecology*, *76*(1), 246–261.

Pake, C. E., & Venable, D. L. (1996). Seed banks in desert annuals: Implications for persistence and coexistence in variable environments. *Ecology*, *77*(5), 1427–1435.

Pande, J., Fung, T., Chisholm, R., & Shnerb, N. M. (2020). Mean growth rate when rare is not a reliable metric for persistence of species. *Ecology letters*, *23*(2), 274–282.

Price, T. (1998). Maternal and paternal effects in birds. In *Maternal effects as adaptations* (pp. 202–226). Oxford University Press.

Reinhold, K. (2000). Maintenance of a genetic polymorphism by fluctuating selection on sex-limited traits. *Journal of Evolutionary Biology*, *13*(6), 1009–1014.

Schreiber, S. J. (2021). Positively and negatively autocorrelated environmental fluctuations have opposing effects on species coexistence. *The American Naturalist*, *197*(4), 000–000.

Schreiber, S. J., Benaïm, M., & Atchadé, K. A. (2011). Persistence in fluctuating environments. *Journal of Mathematical Biology*, *62*(5), 655–683.

Searle, S. R., & Khuri, A. I. (2017). *Matrix algebra useful for statistics*. John Wiley & Sons.

Sears, A. L., & Chesson, P. (2007). New methods for quantifying the spatial storage effect: An illustration with desert annuals. *Ecology*, *88*(9), 2240–2247.

Snyder, R. (2012). Storage effect. In *Encyclopedia of theoretical ecology* (1st ed., pp. 722–726). University of California Press.

Snyder, R. E., & Chesson, P. (2003). Local dispersal can facilitate coexistence in the presence of permanent spatial heterogeneity. *Ecology letters*, *6*(4), 301–309.

Snyder, R. E., & Chesson, P. (2004). How the spatial scales of dispersal, competition, and environmental heterogeneity interact to affect coexistence. *The American Naturalist*, *164*(5), 633–650.

Stomp, M., van Dijk, M. A., van Overzee, H. M., Wortel, M. T., Sigon, C. A., Egas, M., Hoogveld, H., Gons, H. J., & Huisman, J. (2008). The timescale of phenotypic plasticity and its impact on competition in fluctuating environments. *The American Naturalist*, *172*(5), E169–E185.

Stump, S. M., & Chesson, P. (2017). How optimally foraging predators promote prey coexistence in a variable environment. *Theoretical Population Biology*, *114*, 40–58.

Thibaut, L. M., & Connolly, S. R. (2020). Hierarchical modeling strengthens evidence for density dependence in observational time series of population dynamics. *Ecology*, *101*(1).

Thibaut, L. M., Connolly, S. R., & Sweatman, H. P. (2012). Diversity and stability of herbivorous fishes on coral reefs. *Ecology*, *93*(4), 891–901.

Tilman, D. (1982). *Resource competition and community structure*. Princeton University Press.

Towers, I. R., Bowler, C. H., Mayfield, M. M., & Dwyer, J. M. (2020). Requirements for the spatial storage effect are weakly evident for common species in natural annual plant assemblages. *Ecology*, *101*(12), e03185.

Turchin, P. (2003). *Complex population dynamics: A theoretical/ empirical synthesis* (1st ed.). Princeton University Press.

Usinowicz, J., Chang-Yang, C.-H., Chen, Y.-Y., Clark, J. S., Fletcher, C., Garwood, N. C., Hao, Z., Johnstone, J., Lin, Y., Metz, M. R., Masaki, T., Nakashizuka, T., Sun, I.-F., Valencia, R., Wang, Y., Zimmerman, J. K., Ives, A. R., & Wright, S. J. (2017). Temporal coexistence mechanisms contribute to the latitudinal gradient in forest diversity. *Nature*, *550*(7674), 105–108.

Usinowicz, J., Wright, S. J., & Ives, A. R. (2012). Coexistence in tropical forests through asynchronous variation in annual seed production. *Ecology*, *93*(9), 2073–2084.

Venable, D. L., Pake, C. E., & Caprio, A. C. (1993). Diversity and coexistence of sonoran desert winter annuals. *Plant Species Biology*, *8*(2-3), 207–216.

Vittoz, P., & Engler, R. (2007). Seed dispersal distances: A typology based on dispersal modes and plant traits. *Botanica Helvetica*, *117*(2), 109–124.

Volterra, V. (1926). Variations and fluctuations of the number of individuals in animal species living together. *Animal Ecology*, 409–448.

Yamamichi, M., & Hoso, M. (2017). Roles of maternal effects in maintaining genetic variation: Maternal storage effect. *Evolution*, *71*(2), 449–457.

Yuan, C., & Chesson, P. (2015). The relative importance of relative nonlinearity and the storage effect in the lottery model. *Theoretical population biology*, *105*, 39–52.

Zepeda, V., & Martorell, C. (2019). Fluctuation-independent niche differentiation and relative non-linearity drive coexistence in a species-rich grassland. *Ecology*, *100*(8), e02726.

Ziebarth, N. L., Abbott, K. C., & Ives, A. R. (2010). Weak population regulation in ecological time series. *Ecology Letters*, *13*(1), 21–31.

2.2 Interpreting other coexistence mechanisms

Why coexistence mechanisms? Why not use some other scheme for partitioning invasion growth rates? For one, the coexistence mechanisms are demarcated with respect to the absence vs. presence of density-dependence (i.e., E_j vs. C_j) and variation (i.e., $\mathbb{E}_{x,t}[C_j]$ vs. $\text{Var}_{x,t}(C_j)$), two integral concepts in population biology. Second, the coexistence mechanisms are distinct from a historical perspective: nobody discovered two coexistence mechanisms in the same paper (though fitness-density covariance is an amalgam of several previously proposed explanations). Finally, the coexistence mechanisms reveal commonalities between seemingly disparate explanations for coexistence. Herbivores are physically very different from soil nutrients, but both can behave similarly from a population-dynamical perspective (Chesson and Kuang, 2008).

That is not to say that the coexistence mechanisms are the only reasonable way partition the invasion growth rate. Ellner et al. (2019) give a generic method for calculating unorthodox partitions and provide an example involving species' traits. One may decompose the conventional coexistence mechanisms further into contributions from individual (or subsets of) regulating factors or into contributions from spatial variation and temporal variation. One may also aggregate coexistence mechanisms to compare the main effect of density-independent factors (i.e., ΔE_i) to the main effect of density-dependent factors (i.e., $\Delta\rho_i + \Delta N_i$); or to compare all spatial mechanisms to all temporal mechanisms (Johnson and Hastings, 2022a, Section 4.1).

Causal diagrams (Fig. 2.4, 2.5, 2.6, 2.8) can be used to demonstrate how each coexistence mechanism operates. With the exception of density-independent effects (ΔE_i), each coexistence mechanism has two features: 1) a negative feedback loop involving population density n_j and per capita growth rates r_j, and 2) some degree of specialization / exclusivity / ecological differentiation. For example, in the causal diagram for the linear density-dependent effects, $\Delta\rho_i$ (Fig. 2.5), species j has a species-specific competition parameter C_j, implying that species j specializes on particular resources or natural enemies. Note that the causal diagrams are highly stylized; they focus on a feedback loop corresponding to a single species, and therefore only show a small subset of a much larger community-level causal diagram.

There are at least two reasons for relating simple explanations for coexistence to the coexistence mechanisms. First, the resulting taxonomy of models can serve as a heuristic guide for determining the precise causes of coexistence in a new model. Second, we need disparate models to give a fully generally interpretation of coexistence mechanisms. As we will see, it is likely that some misconceptions about relative nonlinearity and the storage effect are the consequence of over-generalizing from two highly-similar models (the lottery model and the annual plant model; Chesson, 1994).

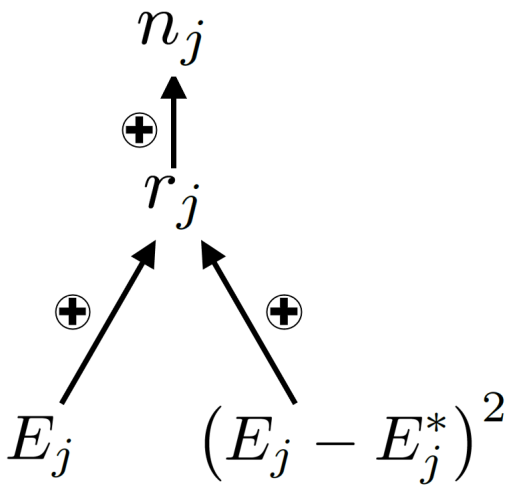

Figure 2.4: Density-independent effects. The density-independent factors (captured by E_j and $\text{Var}(E_j)$) affect growth rates and population density. Note the absence of any feedback loops. The quantity $\left(E_j - E_j^*\right)^2$ becomes $\text{Var}_{x,t}(E_j)$ when averaged across space and time.

.

2.2.1 ΔE_i Density-independent effects

The first coexistence mechanism, ΔE_i, is termed *density-independent effects* and can be interpreted as the degree to which density-independent factors favor the invader. The value of ΔE_i does not depend on any species' density. This represented by the lack of a feedback loop in clearly in Figure 2.4. Consequentially, one species will have the largest ΔE_i, regardless of which species is the invader; if all other terms in the invasion growth rate partition are zero, then all other species in the community will be excluded (Chesson and Huntly, 1997). This thought experiment demonstrates 1) that density-dependent factors are necessary for coexistence and therefore ΔE_i might rightfully not deserve the title of "coexistence mechanism"; and 2) why all the Taylor series terms containing only E_j's are shunted into ΔE_i, while the growth rate components containing only C_j's are split between $\Delta\rho_i$ and ΔN_i: the density-independent effects are between-species differences that cannot be responsible for coexistence, so it is often uninteresting to partition them further (but see Ellner et al., 2019).

2.2.2 $\Delta\rho_i$ Linear density-dependent effects

The second quantity, $\Delta\rho_i$, is called the *linear density-dependent effects*. The linear density-dependent effects is best understood as the class of classic explanations for coexistence: resource and natural-enemy partitioning. More precisely, $\Delta\rho_i$ is the rare-species advantage resulting from specialization on the mean level of density-dependent factors, which could take the form of mineral nutrients, water, carbon, prey species, light, space, refugia, pathogens, parasites, parasitoids, predators, herbivores, etc. The "specialization" need not

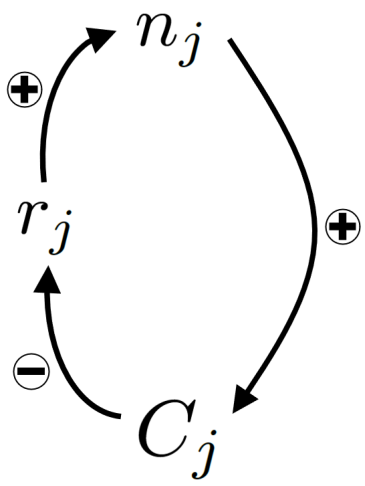

Figure 2.5: Linear density-dependent effects. The negative feedback loop involves the species-specific competition parameter C_j, which includes the effects of resources and natural enemies.

be complete in the sense that each species only affects and is affected by a single density-dependent factor. Rather, there is some contingent (i.e., model specific) threshold of specialization needed in order to attain coexistence (Barabás et al., 2016). In the two-species Lotka-Volterra model, there is a simple mathematical condition for the "specialization threshold" (i.e., intraspecific competition > interspecific competition). In more speciose communities, such simple equations do not generally exist (Saavedra et al., 2017; Logofet, 1993).

Naturally, coexistence in explicit resource-consumer models can be attributed to $\Delta\rho_i$ (e.g., Ellner et al., 2019). The same can be said of coexistence in Lotka-Volterra-like models (Volterra, 1937; Hassell and Comins, 1976; Walters and Korman, 1999; Dallas et al., 2021), where species densities themselves can be treated as density-dependent factors. Lotka-Volterra dynamics are usually viewed as a useful but imperfect simile for the dynamics associated with competition or apparent-competition (Abrams et al., 2008; Mayfield and Stouffer, 2017; O'Dwyer, 2018). However, when resource dynamics are fast, a specific form of resource-consumer dynamics are well-approximated by Lotka-Volterra dynamics (MacArthur, 1970; Chesson, 1990).

The linear density-dependent effects encompasses several notable explanations for coexistence. First, $\Delta\rho_i$ captures coexistence mechanisms that operate on finer-grained spatial or temporal scales than that of observation/data-collection. For example, the competition–colonization trade-off can be attributed to fitness-density covariance from a "worm's-eye view" (Bolker and Pacala, 1999; Shoemaker and Melbourne, 2016), but can be attributed to the linear density-dependent effects from a "bird's-eye view". the competition–colonization trade-off (Skellam, 1951; Levins and Culver, 1971) can be attributed to $\Delta\rho_i$. The same is true for related explanations, such as the fecundity-dispersal trade-off (Yu and Wilson, 2001) and a seed

size-number trade-off (Turnbull et al., 1999; Muller-Landau, 2010). The latter factoid can be verified by looking at the equations in Levins and Culver's (1971) classic paper on the competition–colonization trade-off and using the process of elimination to exclude fluctuation-dependent coexistence mechanisms. There are no patch-level equations, which excludes spatial fluctuation-dependent coexistence mechanisms; and the per capita growth rate equation is linear and deterministic, which excludes temporal fluctuation-dependent coexistence mechanisms.

Second, the Janzen-Connell hypothesis of tropical tree coexistence (Janzen, 1970; Connell, 1971) also falls under the umbrella of $\Delta\rho_i$. Unlike ordinary natural-enemy partitioning, the Janzen-Connell hypothesis posits that coexistence is boosted further by *distance-responsive predation*: parasites and diseases tend to kill seeds and seedlings which are near to their parent trees. However, Stump and Chesson (2015) used MCT to show that distance-responsive predation generally undermines coexistence, thus disproving the Janzen-Connell hypothesis in its most platonic form.

Finally, coexistence via intransitive competition (Soliveres and Allan, 2018) is *partially* captured by $\Delta\rho_j$. Intransitive competition means that there is no best competitor in all settings, such that coexistence occurs via indirect effects that span across a network of interspecific interactions. This process is well-caricatured by Rock-Paper-Scissors dynamics, where species A beats B, B beats C, C beats A, and so on (May and Leonard, 1975, Gilpin, 1975). Intransitive competition is normally studied with Lotka-Volterra models, it can also arise in more complex, multi-trophic models (Schreiber and Rittenhouse, 2004; Schreiber et al., 2018). While it has not been documented empirically or theoretically (to our knowledge), intransitivity can be mediated through other coexistence mechanisms. For instance, intransitivity via relative nonlinearity may occur if species A generates a lot of resource variation, which disproportionately hurts species B via relative nonlinearity, and so on.

Invasion analysis is generally seen as incompatible with coexistence via intransitive competition. The problem is that in perturbing a species to invader state, intransitive loops (*sensu* Gallien et al., 2017, Fig. B3) involving the invader are destroyed, which may cause knock-on extinctions. However, intransitive loops among the resident species affect the densities of the those species, and thus the level of competition felt by the invader. It is in this sense that $\Delta\rho_i$ partially captures the effects of intransitive competition.

Gallien et al. (2017) suggest a measure of the effects of intransitive competition on coexistence: the difference between invasion growth rate in the real world, and a hypothetical world where an some intransitive loops have been broken by removing a single resident species (this is repeated for each resident, and then averaged). This measure captures the effects of some intransitive loops (i.e., all the loops that pass through a single resident), but not all of them (i.e., the loops among the $S-2$ remaining residents). We suggest the following method for measuring the effects of all intransitive loops (excluding those involving the invader)

simultaneously: take the difference between the true invasion growth rate, and the invasion growth rate where there is a single resident species; naturally, this is repeated across all resident, and then averaged. To be clear, our suggestion is tentative and untested; more work is needed to integrate Modern Coexistence Theory with the reality of intransitive competition.

2.2.3 $\Delta \mathrm{N}_i$ Relative nonlinearity

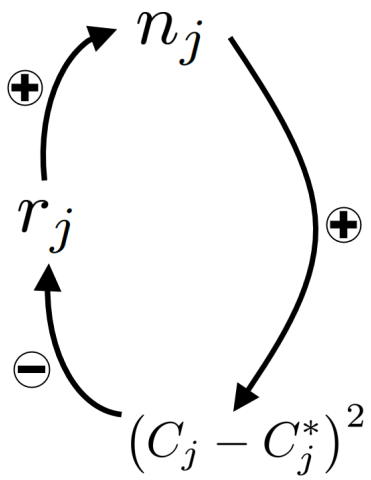

Figure 2.6: Relative nonlinearity. The negative feedback loop is mediated through the variance of regulating factors. The quantity $\left(C_j - C_j^*\right)^2$ becomes $\mathrm{Var}_{x,t}(C_j)$ when averaged across space and time. Increased population density n_j increases the magnitude of fluctuations in competition, $\left(C_j - C_j^*\right)^2$. These fluctuations may affect the metapopulation growth rate r_j either positively or negatively through the coefficient $\beta_j^{(2)}$; here we show a negative effect, as this is the case in resource-consumer models where the consumer has a type II functional response and the competition parameter is $C_j = 1/$"resource concentration".

The first fluctuation-dependent mechanism, $\Delta \mathrm{N}_i$, is called *relative nonlinearity*. It can be interpreted as the rare-species advantage that results from specialization on the variation in a density-dependent factors (Levins, 1979; Tilman, 1982). The variation can be generated endogenously via population dynamics (Armstrong and McGehee, 1976, 1980); or exogenously, either directly via a fluctuating resource supply (Stewart and Levin, 1973; Hsu, 1980; Smith, 1981; Butler et al., 1985; Abrams, 2004), or indirectly via environmental fluctuations (Chesson, 1994; Yuan and Chesson, 2015).

Compared to other coexistence-promoting mechanisms — specifically $\Delta\rho_i$ and ΔI_i — relative nonlinearity is understudied. The relegation of relative nonlinearity probably has several causes. For one, Chesson (1994) showed that in systems with a single competitive factor, only one species can coexist via relative nonlinearity, but an unlimited number of species could coexist via the storage effect. Further, Chesson (2000) found that there is no relative nonlinearity in the annual plant model and the lottery model with only spatial variation. In

models where relative nonlinearity can arise, Chesson (2000) writes that "... the limited ability for relative nonlinearity to promote coexistence when acting alone means that it is best viewed as modifying other mechanisms ... by decreasing the degree of dominance of a superior competitor with a relatively concave growth rate ... ". As we will show below, this is only generally true for models where resource variation is driven by environmental stochasticity: fluctuations in the per capita demographic rates of of resources or consumers.

Theoretically, many species *can* coexist via relative nonlinearity when there are many competitive factors. In a system with L regulating factors, there are $L(L+1)$ unique spatial and temporal covariances; treating the covariance between regulating factors as an effective regulating factor and following the mathematics of the competitive exclusion principle, we conclude that the maximum number of species that can coexist via relative nonlinearity is $L(L+1)$. However, it is unclear how to devise a concrete model in order to attain this outcome, to say nothing of how representative such a model would be of real-world population dynamics.

To better understand the relationship between resource variation and coexistence, we consider a community with a single resource and two consumers that exhibit an opportunist-gleaner tradeoff (Fig. 2.7). We also use a heuristic that originates from Tilman's (1980, 1982) graphical analysis of resource-consumer models: For coexistence to occur, species must consume proportionately more of that which most limits their own growth. In the example portrayed in Figure 2.7, the gleaner is hurt by resource variation, so it is most limited by mean resource levels. Thus, coexistence requires that the gleaner disproportionately decreases mean resource levels, or equivalently, increases resource variation when it is abundant.

The gleaner can increase variation (and thus promote coexistence) by inducing cyclical resource-consumer dynamics (Armstrong and McGehee, 1976, 1980). This outcome is contingent upon model parameters, but it is not a quirk: the gleaner has a faster consumption rate (at low resource concentrations), and is therefore inherently more destabilizing than the opportunist.

If resource dynamics are subject to environmental stochasticity, then resource variation should scale monotonically with mean resource levels (according to the small-noise approximation of population dynamics; Gardiner, 1985; Lande et al., 2003). Here, since the gleaner has a lower R^* than the opportunist, the gleaner tends to decrease resource variation, thus undermining coexistence. There is some reason to believe that this outcome is common in the real-world: Taylor's law (Taylor, 1961; Taylor, 2019) shows that the aforementioned relationship between the mean and variance is common, at least for biotic resources. Though relative nonlinearity cannot promote coexistence in the case of environmental stochasticity, it is nevertheless important because it can change competitive outcomes (e.g., if resource variation is severe enough, then the opportunist will exclude the gleaner).

When the resource supply rate fluctuate through time, the gleaner tends to increase resource variation,

thus promoting coexistence (Hsu, 1980; Smith, 1981). The reason for the increase in variation is related to the different slopes the two consumer's birth-rate curves around their respective equilibrium resource levels (at R_1^* and R_2^*; see Fig. 2.7). If the slope is steep, a resource surplus causes a dramatic increase in consumer birth rates; the subsequently large consumer population then reduces resource levels. In other words, resource levels are regulated via a negative feedback loop with consumers, and the strength of this negative feedback is proportional to the slope of the birth rate function. Because the gleaner species necessarily has a shallow slope (than the opportunist), it necessarily increases resource variation. Note here that coexistence is possible but not guaranteed. Experimental work with phytoplankton microcosms supports the idea that fluctuating resource supply changes population dynamics and sometimes causes coexistence (Grover, 1990; Grover, 1991; Grover, 1997, ch. 5).

So far in this section, we have discussed temporal relative nonlinearity in the context of resource competition. However, relative nonlinearity should work similarly in the apparent competition module (i.e., two prey, one predator), due to duality between resource concentration and the inverse of predator density ("enemy-free space" Jeffries and Lawton, 1984). Indeed, previous research has already demonstrated that in models with apparent competition, relative nonlinearity via endogenous cycles can promote coexistence (Schreiber, 2004) and that relative nonlinearity via environmental stochasticity does not permit multiple species to coexist (Stump and Chesson, 2017, Appendix D.2).

Spatial relative nonlinearity has only been explicitly studied in a few papers (Chesson, 2000; Snyder and Chesson, 2004; Stump et al., 2018). It has been suggested that spatial relative nonlinearity should arise less readily than temporal relative nonlinearity (Chesson, 2000; Snyder and Chesson, 2004; Barabás et al., 2018) but this suggestion is clearly an extrapolation from the lottery model and annual plant model with fluctuating fecundity. Within the context of resource-consumer models with opportunist-gleaner trade-offs, we expect that spatial relative nonlinearity behaves similarly to temporal relative nonlinearity (Table 2.1). There is one exception: population cycles are necessarily a temporal phenomenon, so there is no purely spatial analogue of the endogenously generated resource-consumer cycles.

If there is spatial variation in the per capita (or per concentration) parameters of resource dynamics, then we can apply the same argument that we used in the case of temporal environmental stochasticity: resource variation is proportional to mean resource levels, so the dominant competitor in the absence of fluctuations — the gleaner — tends to decrease resource variation, thus undermining coexistence. This coexistence-undermining effect is strongest when there is complete local retention (i.e., individuals never disperse away from their home patches). Local retention in spatial models plays a similar role to temporal autocorrelation in temporal models, in the sense that both allow population buildup when/where conditions are favorable (see Johnson and Hastings, 2022b). As we will see, local retention tends to boost the spatial storage effect

and fitness-density covariance.

If there is spatial variation in resource supply rates, then we can apply the same argument that we used in the case of temporally-fluctuating resource supply: The gleaner is less capable of dampening fluctuations in resource concentrations, which increases resource variation (relative to the opportunist), and in-turn promotes coexistence. There is an interesting twist: the coexistence-promoting effect of this mechanism is strongest when there is no local retention of consumers. Local retention strengthens the feedback loop between population density and resource concentration, such that consumers tamp-down resources in good patches (i.e., patches with high resource supply rates). When consumers disperse, good patches lose consumers (on net), which increases the spatial variation in resource concentrations. In Appendix 2.2.B, we analyze a model and show — with simulations and math — that spatial variation in resource supply can indeed promote coexistence.

In conclusion, whether or not relative nonlinearity promotes coexistence in opportunist-gleaner models depends on the ultimate source of resource variation (Table 2.1). While "it depends" is perhaps an unsatisfactory answer, it is valuable in that it refutes the conventional wisdom that relative nonlinearity simply tweaks growth rates or switches competitive outcomes.

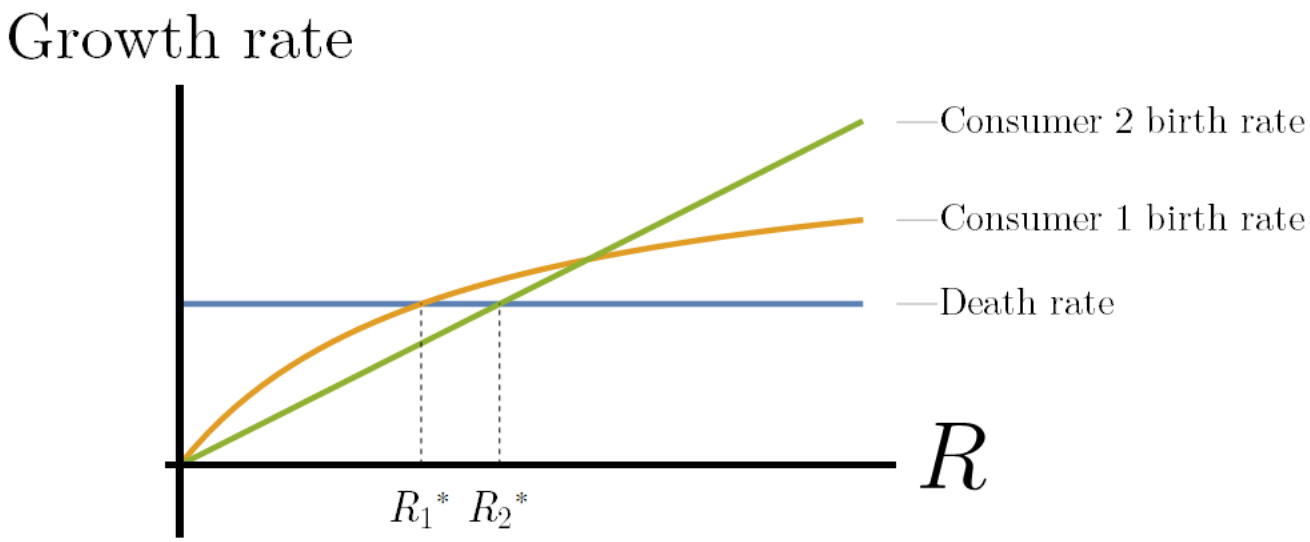

Figure 2.7: An opportunist-gleaner trade-off. Consumer 1 (the "gleaner") excludes consumer 2 (the "opportunist"), but consumer 2 benefits from relative nonlinearity in the presence of resource fluctuations. Figure modified from Figure 1.1, Chapter 1.

Table 2.1: Does relative nonlinearity promote coexistence in a model with an opportunist gleaner trade-off? Here, *Promotes coexistence = Yes* means that it is possible for both species to coexist. *No* means only one species can persist.

Source of resource/natural-enemy variation	Promotes coexistence?
Temporal variation	
Endogenous population cycles	Yes
Environmental stochasticity	No
Fluctuating resource supply rate	Yes
Spatial variation	
Endogenous population cycles	N/A
Environmental stochasticity	No
Fluctuating resource supply rate	Yes

2.2.4 $\Delta\kappa_i$ Fitness-density covariance

The final fluctuation-dependent mechanism, $\Delta\kappa_i$, is known as *fitness-density covariance* (also sometimes called *growth-density covariance*). This term can be interpreted as the differential ability of an invader's individuals to end up in locations where they have high fitness (Chesson, 2000; Chesson et al., 2005; Chesson, 2012). Fitness-density covariance accounts for the tremendous potential for biodiversity that can result from the spatial partitioning of density-dependent factors. Examples include phytoplankton partitioning a light gradient in the water column (Huisman et al., 1999; Gervais et al., 2003), nesting birds partitioning tree branches (MacArthur, 1958), and plants partitioning microhabitats with different ratios of resource-supply rates (Tilman, 1982; Crozier and Boerner, 1984). Fitness-density covariance also accounts for the spatial partitioning of density-independent factors (i.e., environmental niche partitioning), the competition–colonization trade-off, and heteromyopia.

We can immediately see that $\Delta\kappa_i$ contains enormous complexity in a simple formula: relative density is the outcome of a multi-generational interplay between dispersal and local growth, and "fitness" itself can be decomposed into many parts. To get a better grasp on this complexity, we will look at several scenarios that do not lead to fitness-density covariance, followed by several scenarios that do.

First, consider a landscape with a homogeneous environment. If per capita growth rates decrease with population density, then chance fluctuations in relative density will generate a negative $\mathrm{Cov}_x(\nu_j, \lambda_j)$ (Lloyd and Dybas, 1966; Lloyd, 1967; Matsuda et al., 1992). However, if there are no systematic differences between species, an invader will quickly attain the same spatial correlations as the resident, resulting in $\Delta\kappa_i = 0$ (Chesson, 1991). On the other hand, $\Delta\kappa_i$ will be positive if individuals aggregate semi-independently across space, as will occur naturally for invaders with herding, swarming, and/or mate-finding behavior. This scenario demonstrates that environmental niche differences are not necessary for coexistence, but that niche

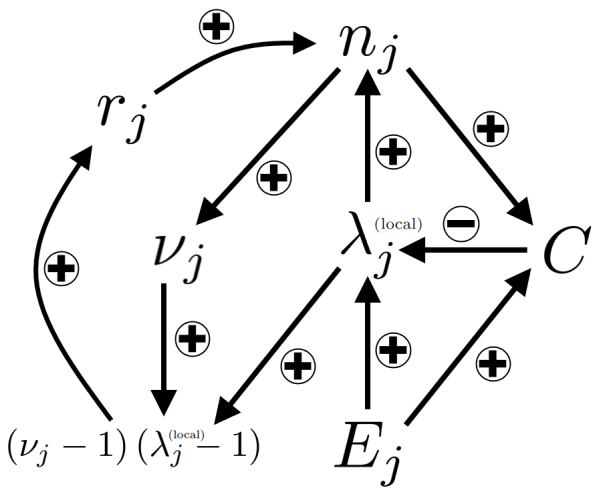

Figure 2.8: Fitness-density covariance. The full negative feedback loop is $n_j \to C \to \lambda_j^{(\text{local})} \to n_j \to \nu_j \to (\nu_j - 1)(\lambda_j^{(\text{local})} - 1) \to r_j \to n_j$. The local finite rate of increase is given to superscript "(local)" to help differentiate it from the metapopulation growth rate, r_j. The product of fluctuations in relative density and fitness, $(\nu_j - 1)(\lambda_j^{(\text{local})} - 1)$ becomes $\mathbb{E}_t\left[\text{Cov}_x\left(\nu_j, \lambda_j^{(\text{local})}\right)\right]$ when properly averaged across time and space. Local population growth along with the *local retention* of individuals leads to a buildup of population density in certain patches. This *local* process is represented by the subset of the feedback loop $n_j \to C \to \lambda_j^{(\text{local})} \to n_j$. Local population density affects relative density, ν_j, and local fitness, $\lambda_j^{(\text{local})}$. Then, local densities and finite rates of increase feed into the term $(\nu_j - 1)(\lambda_j^{(\text{local})} - 1)$, which affects the metapopulation growth rate r_j. This process is represented by the subset of the feedback loop $n_j \to \nu_j \to (\nu_j - 1)(\lambda_j^{(\text{local})} - 1) \to r_j \to n_j$. As in the causal diagram of the storage effect, the species-specific environmental parameter functions to imbue the negative feedback loop with some degree of specialization.

differences of some kind — whether they be environmental or behavioral — are still required.

Second, consider a landscape with a heterogeneous environment which is inhabited by organisms that have complete information, can disperse at no cost, and do not exhibit interference competition. Here, residents will attain the *ideal free distribution* (Fretwell, 1969): the spatial distribution of a resident s where fitness is constant at $\lambda_s = 1$ across the landscape. If the invader has environmental niche differences, it will concentrate in its best patches without increasing competition, thus producing a positive $\Delta\kappa_i$. If the invader has the same environmental niche as the resident, then $\Delta\kappa_i$ equals zero. This scenario demonstrates that fitness-density covariance is not merely a measure of how good species are at actively dispersing to "good" patches. Since the local fitness of a patch depends on the number of competitors in that patch, the ability to *end up* in location with high fintess is inextricably tied to abundance.

For our final no-coexistence scenario, consider a heterogeneous environment with organisms that exhibit *widespread dispersal*: in each time-step, all individuals disperse and rain uniformly across the landscape. Here, relative density is the same in every patch, and thus fitness-density covariance is zero.

What does generate a positive $\Delta\kappa_i$? Environmental niche differences, environmental heterogeneity, and

local retention naturally engender a positive fitness-density covariance:. A good environment for a resident leads to a buildup of resident individuals, but a good environment for an invader does not lead to a buildup of invader individuals. This asymmetry leads to reduced fitness for residents in high density patches, which translates to a positive $\Delta\kappa_i$. This whole process can also generate a storage effect if the interaction effect between environment and competition is non-zero. As Chesson (2000) points out, variation in relative density can generate a positive covariance between environment and competition, even if a negative covariance would be attained in the absence of density variation.

Fitness-density covariance accounts for the coexistence of competitors in patches with varying resource supply rates (Chase and Leibold, 2003, ch. 6). Resources in different patches can be treated (mathematically) as separate regulating factors (Levins, 1974; Szilágyi and Meszéna, 2009). Alternatively, this process can be thought of as a special case of the environmental niche partitioning described in the previous paragraph, where the spatially fluctuating resource supply point *is* the environmental parameter E_j. Even though E_j is typically a demographic parameter that directly affects some focal species (e.g., the probability of germination), E_j can just as easily directly affect the regulating factors (for an example, see Appendix 2.2.B.

Fitness-density covariance also accounts for two previously proposed explanations for coexistence: the *competition–colonization trade-off* (Skellam, 1951; Levins and Culver, 1971) and *heteromyopia* (Murrell and Law, 2003). In the competition–colonization trade-off, the superior colonizer has a positive $\Delta\kappa_i$ (Shoemaker and Melbourne, 2016) because it ends up in recently disturbed patches which are devoid of competitors. In the case of heteromyopia — the phenomenon where intraspecific competition occurs over longer distances than interspecific competition — intraspecific competition lowers the residents' density, creating small holes in the landscape. The invader settles into theses holes and only competes strongly with a few conspecific in the near vicinity, resulting in a positive $\Delta\kappa_i$ (Snyder, 2008).

Another way to understand fitness-density covariance is to understand how it differs from other coexistence mechanisms. The spatial storage effect and fitness-density covariance seem inextricably related, since they both arise readily in models with environmental niche differences, environmental heterogeneity, and local retention. However, we can tease out differences just by looking at the mathematical definitions of the two coexistence mechanisms. For one, the spatial storage effect requires spatial variation in the environment, whereas fitness-density covariance does not. Species may have biased dispersal based on sensory preferences of environmental conditions that otherwise do not affect growth rates (Barabás et al., 2018, Appendix S5); though this is environmental variation in the colloquial sense (species are responding to environmental cues), there is "no environmental variation" in the technical sense that there is no varying demographic parameter than affects the local finite rate of increase.

A fitness-density covariance can potentially emerge in a truly homogeneous environment if species engage

in aggregating behavior (e.g., swarming, schooling, herding, "natal homing"). It is quite possible that such behavior will generate a positive fitness-density covariance: the clustered resident individuals experience lower fitness λ (via increased competition), but continue to aggregate because there is an individual-level fitness benefit for doing so. However, aggregating behavior could also lead to a negative fitness-density covariance. If aggregation is strong enough, invader populations can be regionally rare but locally abundant, thus eliminating a rare-species advantage. Alternatively, aggregation can have positive fitness consequences (e.g., increased mating-finding ability, group-level vigilance) such that the residents benefit on-net.

Even in the face of environmental heterogeneity, there are still notable differences between the spatial storage effect and fitness-density covariance. In Appendix 2.2.A we derive expressions for both coexistence mechanism in an arbitrary model with two species, permanent spatial heterogeneity, and dispersal. When species are identical except for their responses to the environment, we find that

$$\Delta I = \frac{qN_0^*\alpha^{(1)}}{1-q(\theta N_0^*\beta^{(1)}+1)}\left[\zeta\sigma^2(\phi-1)\right], \text{and} \tag{2.69}$$

$$\Delta\kappa = \frac{qN_0^*\alpha^{(1)}}{1-q(\theta N_0^*\beta^{(1)}+1)}\left[\frac{q}{1-q}2\alpha^{(1)}\theta\beta^{(1)}\sigma^2(\phi-1)\right]. \tag{2.70}$$

All of the symbols are described in and Appendix 2.2.A; but notably, σ^2 is the variance in the environmental parameter E_j; ϕ is the spatial correlation between the two species' environmental parameters; ζ is the interaction effect between environmental and competition; and q is the local retention fraction (a $(1-q)$ fraction of individuals disperse after each time-step).

Both the spatial storage effect and fitness-density covariance are proportional to $q \times \sigma^2 \times (1-\phi)$, respectively representing local retention, environmental heterogeneity, and spatial niche differences. Under these conditions, fitness-density covariance is all but inevitable, whereas the spatial storage effect depends on there being a substantial interaction effect ζ. This may explain why some simple spatial models produce fitness-density covariance but not the spatial storage effect (e.g., Amarasekare and Nisbet, 2001; Muko and Iwasa, 2000).

Another notable difference is that the spatial storage effect is proportional to $q/(1-q)$, whereas fitness-density covariance is nearly proportional to $(q/(1-q))^2$, which is very large when the local retention q is large. The discrepancy occurs because the density of a species is proportional to $q/(1-q)$; in turn, the density of species is only proportional to competition (which shows up in the spatial storage effect), but is proportional to both relative density ν and fitness λ (the product of which shows up in fitness-density covariance). This may explain Shoemaker and Melbourne's (2016) finding that fitness-density covariance is more important than the spatial storage effect: the authors used large retention fractions ($q \approx 0.9$).

It has been argued that the spatial storage effect "seems to be inevitable under realistic scenarios" (Chesson, 2000), and that "...space itself is often the bet-hedging strategy that generates storage ..." (Barabás et al., 2018). However, we believe that these statements are over-generalizations from particular versions of the lottery model and annual plant model, where spatially-fluctuating fecundity automatically generates an interaction effect ζ_j. However, with a slight tweak to these models, we see exactly the opposite: when survival fluctuates instead of fecundity, the interaction effect is automatically zero. The spatial storage effect may indeed be prevalent in nature, but it is by no means inevitable (e.g., Towers et al., 2020).

We have shown that the relative importance of the spatial storage effect and fitness density covariance are context dependent: fitness density covariance tends to be be comparatively large when local retention is large and when fecundity doesn't vary across space. Much like the contingent effects of relative nonlinearity (Table 2.1), this contingency implies that very little can be said about the relative importance of coexistence mechanisms, *a priori*. To determine how species are coexisting (or failing to coexist), one must fit a model and quantify coexistence mechanisms.

Appendices

2.2.A The spatial storage effect vs. fitness-density covariance

Consider a community with scalar populations inhabiting discrete patches (indexed by x), with discrete-time dynamics (indexed by t). In each time-step, there are two events. First is a bout of local population growth, determined by the local finite rate of increase, $\lambda_j(x,t)$. Second is a dispersal event, where in each patch a proportion of individuals, p_j, disperse and are distributed uniformly over all patches (including the patch of origin). It follows that a proportion of individuals, $q_j = (1-p_j)$, are retained locally; We call q the *retention proportion*. To simplify the expressions for coexistence mechanisms, we assume that there is no temporal variation, and that population densities N_j and relative densities ν_j settle to an equilibrium in each patch. The time-evolution of population density N_j at patch x is given by

$$N_j(x,t+1) = q_j N_j(x,t)\lambda_j(x,t) + \frac{1-q_j}{K}\sum_{s=1}^{K} N_j(s,t)\lambda_j(s,t). \tag{2.71}$$

Often in MCT, the competition parameter is a function of both species densities and the environmental parameter; However, in such models, there is an implicit time-lag between the effects of environment and competition on population dynamics, such that the environment has enough time to affect competition within a time-step. For instance, in the lottery model, per capita fecundity (the environmental parameter) affects the per larva recruitment probability (the competition parameter), but recruitment occurs weeks or months after reproduction, a fact which is hidden by the simple structure of the lottery model equations. In this appendix, we only consider models in which the competition parameter is a function of a single residents s's population density: $C_j = h_j(N_s)$. This simplifies things because it prevents the environment from affecting competition on two separate time-scales: within a time-step (as in the lottery model) and between time-steps (via inter-generational population growth).

To obtain the spatial storage effect, we must obtain the quantity $\mathrm{Cov}_x(E_j, C_j)$, which in the two-species/single-resident case can be approximated as $\mathrm{Cov}_x(E_j, \theta_{jr}N_s)$, where θ_{jr} is is a constant that converts species s's density to species j's competition: $\theta_{jr} = \frac{dh_j(N_s^*)}{dN_s}$. Using perturbation theory and the properties of geometric series, fitness-density covariance can be approximated (Appendix 1.2.D) as

$$\mathbb{E}_t[\mathrm{Cov}_x(v_j,\lambda_j)] \approx \frac{q_j}{1-q_j}\mathrm{Var}_x\Big(\alpha_j^{(1)}(E_j - E_j^*) + \beta_j^{(1)}(C_s - C_s^*)\Big), \tag{2.72}$$

which — again assuming that the competition parameter is a function of only the resident's density — can

be approximated as

$$\mathbb{E}_t[\mathrm{Cov}_x(v_j,\lambda_j)] \approx \frac{q_j}{1-q_j}\left[\left(\alpha_j^{(1)}\right)^2 \mathrm{Var}_x(E_j) + 2\alpha_j^{(1)}\beta_j^{(1)}\mathrm{Cov}_x(E_j,\theta_{jr}N_s) + \left(\beta_j^{(1)}\right)^2 \mathrm{Var}_x(\theta_{jr}N_s)\right]. \quad (2.73)$$

Now, it is clear that simplifying the expressions for the coexistence mechanisms will require us to find the residents' density, N_s. Specifically, re-expressing N_s in terms of the environmental parameter, E_s, will allow us to express the coexistence mechanisms in terms of spatial variation and between-species correlation in the environment.

To find N_s, we take a perturbative approach, where both N_j and λ_j are expanded in powers of the small parameter σ: $N_j(x,t) = N_{j,0}(x,t) + \sigma N_{j,1}(x,t) + ...$; and $\lambda_j(x,t) = \lambda_{j,0}(x,t) + \sigma\lambda_{j,1}(x,t) + ...$ With this, we re-write the population dynamics (Eq.2.71) as

$$\begin{aligned} N_{j,0}(x,t+1) + \sigma N_{j,1}(x,t+1) + \ldots =& q_j(N_{j,0}(x,t) + \sigma N_{j,1}(x,t) + \ldots)(\lambda_{j,0}(x,t) + \sigma\lambda_{j,1}(x,t) + \ldots) \\ &+ \frac{1-q_j}{K}\sum_{s=1}^{K}(N_{j,0}(s,t) + \sigma N_{j,1}(s,t) + \ldots)(\lambda_{j,0}(s,t) + \sigma\lambda_{j,1}(s,t) + \ldots). \end{aligned} \quad (2.74)$$

The zeroth-order dynamics are the same in every patch (because environmental fluctuations are $\mathcal{O}(\sigma)$). Assuming that there are no complex dynamics, the resident density reaches a stable equilibrium, denoted $N_{s,0}^*$, that is the same in each patch and which can be obtained by solving

$$N_s = N_s\, g_s(E_s^*, h_s(N_s)) \quad (2.75)$$

for N_s. For example, if the population model is $\lambda_s(x,t) = s + E(x)/(1 + cN_s(x,t))$, then $N_{s,0}^* = \frac{E_s^*}{c(1-s)} - \frac{1}{c}$.

Noting that $\lambda_{j,0}^* = g_j(E_j^*, h_j(N_{s,0}^*)) = 1$, the first-order dynamics can be written as

$$\sigma N_{j,1}(x,t+1) = \sigma\left[q_j\left(N_{j,0}^*\lambda_{j,1}(x,t) + N_{j,1}(x,t)\right) + (1-q_j)\left(N_{j,0}^*\mathbb{E}_x[\lambda_{j,1}(t)] + \mathbb{E}_x[N_{j,1}(t)]\right)\right]. \quad (2.76)$$

MCT is based on small-noise assumptions (details in Chesson, 1994; Chesson, 2000) that ensure that all terms in the mathematical expression of the invasion growth rate are of commensurable magnitude. Specifically, MCT assumes that environmental fluctuations are small and that the average of fluctuations is even smaller; Or put into symbols, $E_j - E_j^* = \mathcal{O}(\sigma)$ and $\mathbb{E}_{x,t}\left[E_j - E_j^*\right] = \mathcal{O}(\sigma^2)$. Analogous bounds can be put on population density, relative density, and the competition parameter, as all of these a ultimately functions of the environment. These small-noise assumptions can be used to match terms from the perturbative

expansion above and the Taylor series expansion of λ_j (see Section 3, Eq.3 in the main text), resulting in $\sigma\lambda_{j,1}(x,t) = \alpha_j^{(1)}(E_j(x,t)-E_j^*)+\beta_j^{(1)}(C_j(x,t)-C_j^*)$. The small-noise assumptions also mean that $\mathbb{E}_x[\lambda_{j,1}(t)]$ and $\sigma\mathbb{E}_x[N_{j,1}]$ are $\mathcal{O}(\sigma^2)$, which simplifies Eq.2.74 to

$$\sigma N_{j,1}(x,t+1) = \sigma\left[q_j\left(N_{j,0}^*\lambda_{j,1}(x,t) + N_{j,1}(x,t)\right)\right]. \tag{2.77}$$

Using the relationship $\sigma\lambda_{j,1}(x,t) = \alpha_j^{(1)}(E_j(x,t) - E_j^*) + \beta_j^{(1)}(C_j(x,t) - C_j^*) \approx \alpha_j^{(1)}(E_j(x,t) - E_j^*) + \beta_j^{(1)}\theta_{jr}N_{s,1})$ to substitute for $\lambda_{j,1}(x,t)$, we can solve for the equilibrium density of the resident

$$N_s^* \approx N_{s,0}^* + \sigma N_{s,1}^*, \text{ where} \tag{2.78}$$

$$\sigma N_{s,1}^* = \frac{q_s N_{s,0}^* \alpha_s^{(1)}(E_s - E_s^*)}{1 - q_s(\theta_{ss}N_{s,0}^*\beta_s^{(1)} + 1)}. \tag{2.79}$$

Plugging the above expression into the formulas for coexistence mechanisms (see Section 3 in the main text), and writing the covariance between the two species' environmental responses as $\phi\sigma_1\sigma_2$ (where ϕ is the correlation coefficient), we find that the spatial storage effect is

$$\Delta I_i = \frac{q_s N_{s,0}^* \alpha_s^{(1)}}{1 - q_s(\theta_{ss}N_{s,0}^*\beta_s^{(1)} + 1)}\left[\zeta_i\phi\sigma_i\sigma_s - \zeta_s\sigma_s^2\right], \tag{2.80}$$

and fitness-density covariance is

$$\begin{aligned}\Delta\kappa_i =& \frac{q_i}{1-q_i}\left[\left(\alpha_i^{(1)}\right)^2\sigma_i^2 + \frac{2\alpha_i^{(1)}\alpha_s^{(1)}\theta_{ir}\beta_i^{(1)}\phi\sigma_i\sigma_s q_s N_{s,0}^*}{1 - q_s(\theta_{ss}N_{s,0}^*\beta_s^{(1)} + 1)} + \left(\frac{\alpha_s^{(1)}\theta_{ir}\beta_i^{(1)}\sigma_s q_s N_{s,0}^*}{1 - q_s(\theta_{ss}N_{s,0}^*\beta_s^{(1)} + 1)}\right)^2\right] \\ & - \frac{q_s}{1-q_s}\left[\left(\alpha_s^{(1)}\right)^2\sigma_s^2 + \frac{2\left(\alpha_s^{(1)}\right)^2\theta_{ss}\beta_s^{(1)}\sigma_s^2 q_s N_{s,0}^*}{1 - q_s(\theta_{ss}N_{s,0}^*\beta_s^{(1)} + 1)} + \left(\frac{\alpha_s^{(1)}\theta_{ss}\beta_s^{(1)}\sigma_s q_s N_{s,0}^*}{1 - q_s(\theta_{ss}N_{s,0}^*\beta_s^{(1)} + 1)}\right)^2\right].\end{aligned} \tag{2.81}$$

Here, we can see that the invader's dispersal dynamics (i.e., the value of q_i) does not play a role in the spatial storage effect, but does play a role in fitness-density covariance. The resident's dispersal dynamics, on the other hand, play a role in both mechanisms.

If the invader and resident have identical demographic parameters but partially uncorrelated environmental responses, then we can drop the species-specific subscripts, and the coexistence mechanisms simplify to

$$\Delta I = \frac{qN_0^*\alpha^{(1)}}{1-q(\theta N_0^*\beta^{(1)}+1)}\left[\zeta\sigma^2(\phi-1)\right], \text{and} \tag{2.82}$$

$$\Delta\kappa = \frac{qN_0^*\alpha^{(1)}}{1-q(\theta N_0^*\beta^{(1)}+1)}\left[\frac{q}{1-q}2\alpha^{(1)}\theta\beta^{(1)}\sigma^2(\phi-1)\right]. \tag{2.83}$$

2.2.B Spatial variation in resource supply promotes coexistence

Here, we analyze a 2-consumer, 1-resource model in which the two consumers exhibit an opportunist-gleaner trade-off. The model can also be described as a discrete-time approximation of a continuous-time chemostat model. The local finite rate of increase for the consumer is

$$\lambda_j(x,t) = 1 + \left(\frac{w\mu_j R(x,t)}{K_j + R(x,t)} - d\right)\Delta t, \quad j = (1,2), \tag{2.84}$$

where w is an efficiency constant (converts resource uptake to consumer biomass), μ_j is the resource maximum uptake rate, K_j is the half-saturation constant, d is the dilution/death rate, Δt is the length of a time-step, and $R(x,t)$ is the concentration of the resource at location x and time t.

Each time-step is split into two phases: growth and dispersal. Growth follows the equations above. The dispersal phase can be described as *local retention with global dispersal*, and follows Eq.2.71 in 2.2.A.

The resource dynamics are given by the equation,

$$R(x,t+1) = R(x,t) + \left(d(S(x) - R(x,t)) - \sum_{j=1}^{2}\frac{\mu_j N_j(x,t)R(x,t)}{K_j + R(x,t)}\right)\Delta t, \tag{2.85}$$

where $S(x)$ is the patch-specific *resource supply point*. Here, $S(x)$ is effectively the environmental parameter, so $S(x) - S^* = \mathcal{O}(\sigma)$. Resources do not disperse.

First we verify a claim in the main text: coexistence via spatial relative nonlinearity is not possible if there is complete local retention. With no dispersal, we can straightforwardly solve for the equilibrium resource concentration. When there is only a single resident s,

$$R^* = \frac{dK_s}{\mu_s w - d} \tag{2.86}$$

in each and every patch. There is no spatial variation in resource concentration, so there can be no spatial relative nonlinearity (assuming that local populations reach equilibrium and do no experience endogenously-driven population cycles).

As discussed in Section 4.3 in the main text, coexistence is possible if the gleaner species tends to increase resource variation, compared to the opportunist. The opportunist-gleaner continuum is controlled by μ_j and K_j, with higher parameter values corresponding to more opportunism. We can fix the equilibrium resource concentration at some arbitrary value R_0^*, so that both species are competitively equivalent in the absence of spatial resource variation, via Tilman's (1982) R^* rule. We can then solve for μ_j,

$$\mu_j = \frac{d(K_j + R_0^*)}{R_0^* w}, \tag{2.87}$$

and substitute the right-hand-side into the dynamical equations. With this substitution, K_j becomes the only parameter that controls the degree of opportunism, but modulating K_j does not change the (equilibrium) competitive equivalence of species.

We will now calculate the resource variation in the case of a single-resident, using the same perturbative approach as in 2.2.A. Writing the dynamics of resource concentration (i.e., the right-hand-side of Eq.2.85) as the function $\Phi(R(x,t), N_s(x,t), S(x))$, the first-order dynamics are

$$\sigma N_{s,1}(x, t+1) = \sigma q_s \left(N_{s,0}^* \frac{d\lambda_s(R^*)}{dR} R_1 + N_{s,1}(x,t) \right), \text{ and} \tag{2.88}$$

$$\sigma R_1(x, t+1) = \frac{d\Phi(R_0^*, N_{s,0}^*, S^*)}{dR} \sigma R_1(x,t) + \frac{d\Phi(R_0^*, N_{s,0}^*, S^*)}{dR} \sigma N_{s,1}(x,t) + \frac{d\Phi(R_0^*, N_{s,0}^*, S^*)}{dS} (S(x) - S^*). \tag{2.89}$$

After substituting in the Taylor series coefficients, we can solve for the equilibrium resource concentration:

$$R_s^* \approx R_0^* + \sigma R_{s,1}^*, \text{ where} \tag{2.90}$$

$$R_{s,1}^* = (S(x) - S^*) \frac{(1 - q_s) R_0^* (K_s + R_0^*)}{dK_s q_s (R_0^* - S^*) + (q_s - 1)\left(K_s S^* + R_0^{*2}\right)}. \tag{2.91}$$

Recall that R_0^* is fixed. Using the fact that $\text{Var}_x(R_s) \approx \mathbb{E}_x\left[R_{s,1}^2\right]$ and $\text{Var}_x(S) = \sigma^2$, we find that resource variation is

$$\text{Var}_x(R_s) \approx \sigma^2 \left[\frac{(1 - q_s) R_0^* (K_s + R_0^*)}{dK_s q_s (R_0^* - S^*) + (q_s - 1)\left(K_s S^* + R_0^{*2}\right)} \right]^2. \tag{2.92}$$

In the *Mathematica notebook*, `spatial_DeltaN.nb` (https://github.com/ejohnson6767/MCT_review), we prove that the resource variation decreases monotonically with the parameter K_s. This result confirms

our earlier claim that gleaner species increase resource variation, compared to opportunist species. In the *R script* `spatial_opportunist_gleaner_sims.R` (https://github.com/ejohnson6767/MCT_review), we provide a simulation example to show species can indeed coexist.

Data availability statement

Code is available on GitHub, https://github.com/ejohnson6767/MCT_review.

References

Abrams, P. A. (2004). When does periodic variation in resource growth allow robust coexistence of competing consumer species? *Ecology*, *85*(2), 372–382.

Abrams, P. A., Rueffler, C., & Dinnage, R. (2008). Competition-similarity relationships and the nonlinearity of competitive effects in consumer-resource systems. *The American Naturalist*, *172*(4), 463–474.

Amarasekare, P., & Nisbet, R. M. (2001). Spatial heterogeneity, source-sink dynamics, and the local coexistence of competing species. *The American Naturalist*, *158*(6), 572–584.

Armstrong, R. A., & McGehee, R. (1976). Coexistence of species competing for shared resources. *Theoretical Population Biology*, *9*(3), 317–328.

Armstrong, R. A., & McGehee, R. (1980). Competitive exclusion. *The American Naturalist*, *115*(2), 151–170.

Barabás, G., D'Andrea, R., & Stump, S. M. (2018). Chesson's coexistence theory. *Ecological Monographs*, *88*(3), 277–303.

Barabás, G., J. Michalska-Smith, M., & Allesina, S. (2016). The effect of intra-and interspecific competition on coexistence in multispecies communities. *The American Naturalist*, *188*(1), E1–E12.

Bolker, B. M., & Pacala, S. W. (1999). Spatial moment equations for plant competition: Understanding spatial strategies and the advantages of short dispersal. *The American Naturalist*, *153*(6), 575–602.

Butler, G., Hsu, S.-B., & Waltman, P. (1985). A mathematical model of the chemostat with periodic washout rate. *SIAM Journal on Applied Mathematics*, *45*(3), 435–449.

Chase, J. M., & Leibold, M. A. (2003). *Ecological niches: Linking classical and contemporary approaches*. University of Chicago Press.

Chesson, P. (1990). Macarthur's consumer-resource model. *Theoretical Population Biology*, *37*(1), 26–38.

Chesson, P. (1991). A need for niches? *Trends in ecology & evolution*, *6*(1), 26–28.

Chesson, P. (1994). Multispecies competition in variable environments. *Theoretical Population Biology*, *45*(3), 227–276.

Chesson, P. (2000). General theory of competitive coexistence in spatially-varying environments. *Theoretical Population Biology*, *58*(3), 211–237.

Chesson, P. (2012). Scale transition theory: Its aims, motivations and predictions. *Ecological Complexity*, *10*, 52–68.

Chesson, P., Donahue, M. J., Melbourne, B. A., & Sears, A. L. (2005). Scale transition theory for understanding mechanisms in metacommunities. *Metacommunities: Spatial dynamics and ecological communities*, 279–306.

Chesson, P., & Huntly, N. (1997). The roles of harsh and fluctuating conditions in the dynamics of ecological communities. *The American Naturalist*, *150*(5), 519–553.

Chesson, P., & Kuang, J. J. (2008). The interaction between predation and competition. *Nature*, *456*(7219), 235–238.

Connell, J. H. (1971). On the role of natural enemies in preventing competitive exclusion in some marine animals and in rain forest trees. In *Dynamics of populations* (pp. 298–312). Wageningen, The Netherlands.

Crozier, C. R., & Boerner, R. E. (1984). Correlations of understory herb distribution patterns with microhabitats under different tree species in a mixed mesophytic forest. *Oecologia*, *62*(3), 337–343.

Dallas, T., Melbourne, B. A., Legault, G., & Hastings, A. (2021). Initial abundance and stochasticity influence competitive outcome in communities. *Journal of Animal Ecology*.

Ellner, S. P., Snyder, R. E., Adler, P. B., & Hooker, G. (2019). An expanded modern coexistence theory for empirical applications. *Ecology letters*, *22*(1), 3–18.

Fretwell, S. D. (1969). On territorial behavior and other factors influencing habitat distribution in birds. *Acta Biotheoretica*, *19*(1), 45–52.

Gallien, L., Zimmermann, N. E., Levine, J. M., & Adler, P. B. (2017). The effects of intransitive competition on coexistence. *Ecology Letters*, *20*(7), 791–800.

Gardiner, C. W. (1985). *Handbook of stochastic methods* (Vol. 3). Springer.

Gervais, F., Siedel, U., Heilmann, B., Weithoff, G., Heisig-Gunkel, G., & Nicklisch, A. (2003). Small-scale vertical distribution of phytoplankton, nutrients and sulphide below the oxycline of a mesotrophic lake. *Journal of Plankton Research*, *25*(3), 273–278.

Gilpin, M. E. (1975). Limit cycles in competition communities. *The American Naturalist*, *109*(965), 51–60.

Grover, J. P. (1990). Resource competition in a variable environment: Phytoplankton growing according to monod's model. *The American Naturalist*, *136*(6), 771–789.

Grover, J. P. (1991). Resource competition in a variable environment: Phytoplankton growing according to the variable-internal-stores model. *The American Naturalist*, *138*(4), 811–835.

Grover, J. P. (1997). *Resource competition*. Springer.

Hassell, M., & Comins, H. (1976). Discrete time models for two-species competition. *Theoretical Population Biology*, *9*(2), 202–221.

Hsu, S.-B. (1980). A competition model for a seasonally fluctuating nutrient. *Journal of Mathematical Biology*, *9*(2), 115–132.

Huisman, J., Jonker, R. R., Zonneveld, C., & Weissing, F. J. (1999). Competition for light between phytoplankton species: Experimental tests of mechanistic theory. *Ecology*, *80*(1), 211–222.

Janzen, D. H. (1970). Herbivores and the number of tree species in tropical forests. *The American Naturalist*, *104*(940), 501–528.

Jeffries, M., & Lawton, J. (1984). Enemy free space and the structure of ecological communities. *Biological Journal of the Linnean Society*, *23*(4), 269–286.

Johnson, E. C., & Hastings, A. (2022a). Methods for calculating coexistence mechanisms: Beyond scaling factors. *arXiv preprint arXiv:2201.06666*.

Johnson, E. C., & Hastings, A. (2022b). Towards a heuristic understanding of the storage effect. *arXiv preprint arXiv:2201.06691*.

Lande, R., Engen, S., & Saether, B.-E. (2003). *Stochastic population dynamics in ecology and conservation*. Oxford University Press.

Levins, R. (1974). Discussion paper: The qualitative analysis of partially specified systems. *Annals of the New York Academy of Sciences*, *231*(1), 123–138.

Levins, R. (1979). Coexistence in a variable environment. *The American Naturalist*, *114*(6), 765–783.

Levins, R., & Culver, D. (1971). Regional coexistence of species and competition between rare species. *Proceedings of the National Academy of Sciences*, *68*(6), 1246–1248.

Lloyd, M. (1967). Mean crowding. *The Journal of Animal Ecology*, 1–30.

Lloyd, M., & Dybas, H. S. (1966). the Periodical Cicada Problem. I. Population Ecology. *Evolution*, *20*(2), 133–149.

Logofet, D. O. (1993). *Matrices and graphs: Stability problems in mathematical ecology*. CRC Press.

MacArthur, R. (1970). Species packing and competitive equilibrium for many species. *Theoretical Population Biology*, *1*(1), 1–11.

MacArthur, R. H. (1958). Population ecology of some warblers of northeastern coniferous forests. *Ecology*, *39*(4), 599–619.

Matsuda, H., Ogita, N., Sasaki, A., & Satō, K. (1992). Statistical mechanics of population: The lattice lotka-volterra model. *Progress of theoretical Physics*, *88*(6), 1035–1049.

May, R. M., & Leonard, W. J. (1975). Nonlinear Aspects of Competition Between Three Species. *SIAM Journal on Applied Mathematics*, *29*(2), 243–253.

Mayfield, M. M., & Stouffer, D. B. (2017). Higher-order interactions capture unexplained complexity in diverse communities. *Nature ecology & evolution*, *1*(3), 1–7.

Muko, S., & Iwasa, Y. (2000). Species coexistence by permanent spatial heterogeneity in a lottery model. *Theoretical Population Biology*, *57*(3), 273–284.

Muller-Landau, H. C. (2010). The tolerance–fecundity trade-off and the maintenance of diversity in seed size. *Proceedings of the National Academy of Sciences*, *107*(9), 4242–4247.

Murrell, D. J., & Law, R. (2003). Heteromyopia and the spatial coexistence of similar competitors. *Ecology letters*, *6*(1), 48–59.

O'Dwyer, J. P. (2018). Whence lotka-volterra? *Theoretical Ecology*, *11*(4), 441–452.

Saavedra, S., Rohr, R. P., Bascompte, J., Godoy, O., Kraft, N. J., & Levine, J. M. (2017). A structural approach for understanding multispecies coexistence. *Ecological Monographs*, *87*(3), 470–486.

Schreiber, S. J. (2004). Coexistence for species sharing a predator. *Journal of Differential Equations*, *196*(1), 209–225.

Schreiber, S. J., Patel, S., & terHorst, C. (2018). Evolution as a coexistence mechanism: Does genetic architecture matter? *The American Naturalist*, *191*(3), 407–420.

Schreiber, S. J., & Rittenhouse, S. (2004). From simple rules to cycling in community assembly. *Oikos*, *105*(2), 349–358.

Shoemaker, L. G., & Melbourne, B. A. (2016). Linking metacommunity paradigms to spatial coexistence mechanisms. *Ecology*, *97*(9), 2436–2446.

Skellam, J. G. (1951). Random dispersal in theoretical populations. *Biometrika*, *38*(1/2), 196–218.

Smith, H. L. (1981). Competitive coexistence in an oscillating chemostat. *SIAM Journal on Applied Mathematics*, *40*(3), 498–522.

Snyder, R. E. (2008). When does environmental variation most influence species coexistence? *Theoretical Ecology*, *1*(3), 129–139.

Snyder, R. E., & Chesson, P. (2004). How the spatial scales of dispersal, competition, and environmental heterogeneity interact to affect coexistence. *The American Naturalist*, *164*(5), 633–650.

Soliveres, S., & Allan, E. (2018). Everything you always wanted to know about intransitive competition but were afraid to ask. *Journal of Ecology*, *106*(3), 807–814.

Stewart, F. M., & Levin, B. R. (1973). Partitioning of resources and the outcome of interspecific competition: A model and some general considerations. *The American Naturalist*, *107*(954), 171–198.

Stump, S. M., & Chesson, P. (2015). Distance-responsive predation is not necessary for the janzen–connell hypothesis. *Theoretical Population Biology*, *106*, 60–70.

Stump, S. M., & Chesson, P. (2017). How optimally foraging predators promote prey coexistence in a variable environment. *Theoretical Population Biology*, *114*, 40–58.

Stump, S. M., Johnson, E. C., Sun, Z., & Klausmeier, C. A. (2018). How spatial structure and neighbor uncertainty promote mutualists and weaken black queen effects. *Journal of theoretical biology*, *446*, 33–60.

Szilágyi, A., & Meszéna, G. (2009). Limiting similarity and niche theory for structured populations. *Journal of theoretical Biology*, *258*(1), 27–37.

Taylor, L. R. (1961). Aggregation, variance and the mean. *Nature*, *189*(4766), 732–735.

Taylor, R. A. (2019). *Taylor's power law: Order and pattern in nature*. Academic Press.

Tilman, D. (1980). Resources: A graphical-mechanistic approach to competition and predation. *The American Naturalist*, *116*(3), 362–393.

Tilman, D. (1982). *Resource competition and community structure*. Princeton University Press.

Towers, I. R., Bowler, C. H., Mayfield, M. M., & Dwyer, J. M. (2020). Requirements for the spatial storage effect are weakly evident for common species in natural annual plant assemblages. *Ecology*, *101*(12), e03185.

Turnbull, L. A., Rees, M., & Crawley, M. J. (1999). Seed mass and the competition/colonization trade-off: A sowing experiment. *Journal of Ecology*, 899–912.

Volterra, V. (1937). Principes de biologie mathématique. *Acta Biotheoretica*, *3*(1), 1–36.

Walters, C., & Korman, J. (1999). Linking recruitment to trophic factors: Revisiting the beverton–holt recruitment model from a life history and multispecies perspective. *Reviews in Fish Biology and Fisheries*, *9*(2), 187–202.

Yu, D. W., & Wilson, H. B. (2001). The competition-colonization trade-off is dead; long live the competition-colonization trade-off. *The American naturalist*, *158*(1), 49–63.

Yuan, C., & Chesson, P. (2015). The relative importance of relative nonlinearity and the storage effect in the lottery model. *Theoretical population biology*, *105*, 39–52.

Chapter 3

Complex population dynamics

Chapter Contents

3.1 An explanation for unexpected population crashes in a constant environment

3.1.1 Abstract

Unexpected population crashes are an important feature of natural systems, yet many observed crashes have not been explained. Two difficulties in explaining population crashes are their relative rarity and the multi-causal nature of ecological systems. We approach this issue with experimental microcosms, with large numbers of replicates of red flour beetle populations (*Tribolium castaneum*). We determined that population crashes are caused by an interaction between stochasticity and successive episodes of density dependence: demographic stochasticity in oviposition rates occasionally produces a high density of eggs; so high that there are insufficient flour resources for subsequent larvae. This mechanism can explain unexpected population crashes in more general settings: stochasticity "pushes" population into a regime where density-dependence is severely overcompensatory. The interaction between nonlinearity and stochasticity also produces chaotic population dynamics and a double-humped one-generation population map, suggesting further possibilities for unexpected behavior in a range of systems. We discuss the generality of our proposed mechanism, which could potentially account for previously inexplicable population crashes.

3.1.2 Introduction

Most of the time, populations can be described as fluctuating randomly around a weakly-stable equilibrium (Ziebarth et al., 2010; Thibaut and Connolly, 2020). However, some populations experience unexpected population crashes, also known as catastrophes, extreme events, or ecological black swan events. These crashes, however rare, have outsized consequences for conservation and management (Drake, 2005; Granéli and Turner, 2006; Mangel and Tier, 1994; Raffa et al., 2008).

Colloquially, black swans are rare events that have large impacts. Technically, black swans are sampled from the tail of a heavy-tailed or fat-tailed probability distribution. Such distributions may be contrasted with the gaussian distribution, whose thin, exponentially decaying tails preclude extreme events. In the context of ecology, population crashes are simply black swan events from the left tail of the distribution of per capita growth rates.

Ecological black swans are rare by definition. Nevertheless, they have been documented in a range of populations: temperate lake phytoplankton (Batt et al., 2017), Baltic sea phytoplankton (Segura et al., 2013), North American nesting birds (Keitt and Stanley, 1998), marine copepods (Schmitt et al., 2008), a number of seal and sea lion species (Gerber and Hilborn, 2001), water flea (Daphnia) microcosms (Drake, 2014), and 25 (out of 609) populations in the Global Population Dynamics Database (Anderson et al., 2017). Additionally, there are a great number of putative black swans that are labeled in the ecological literature as "catastrophes" (reviewed by Mangel and Tier, 1994).

Although it is premature to make any claims about the prevalence of ecological black swans, there are several pieces of evidence to suggest that black swans are more common than a naïve survey of the literature would indicate. First, Anderson et al. (2017) found that the probability of detecting black swans increases with time-series length. Second, some of the longest ecological time series in existence contain black swans (Batt et al., 2017; Segura et al., 2013). Finally, it is nearly impossible to determine statistically that a distribution does not have heavy tails (Weron, 2001).

Even when it is known that a distribution has heavy tails, forecasting is precarious. Standard measures of spread or risk — like the standard deviation — can converge so slowly to their true values that they fail out-of-sample (Taleb, 2019). Even worse, black swan events dominate the standard deviation, such that a single observation can completely change one's model (e.g., Fig. 3.21 in Taleb, 2020). This phenomenon is familiar in finance (Mandelbrot and Hudson, 2007) hence the investor's dictum "past performance is not indicative of future results", even though financial time series have thousands of data points. The prospect of forecasting crashes is somewhat more dismal in ecology, where typical time series have tens of data points.

Because statistics and time series analysis are unlikely to be informative, we would like a mechanistic

explanation to help identify, ahead of time, systems in which population crashes may occur. Here, we use mechanistic models and flour beetle microcosms experiments to derive a novel mechanism of population crashes. Our mechanism combines the universal feature of stochasticity with the common feature of successive rounds of density dependence. To put it simply, population crashes can occur when stochasticity occasionally "pushes" population density into a regime where overcrowding is severe.

3.1.3 Methods

3.1.3.1 Experimental microcosms

Flour beetles (*Tribolium castaneum*) between 1 and 2 weeks of age (i.e., time since eclosion) were obtained from laboratory stock populations. Beetles were counted or weighed into 4 x 4 x 6 cm plastic enclosures which were partially filled with 20 g of standard media (95% enriched wheat flour and 5% brewer's yeast by mass). After a variable number of days which we call the oviposition period, adult beetles were sifted out of the media, leaving only the media and eggs. The complete *T. castaneum* life cycle takes 4–5 weeks (Sokoloff, 1974, p. 66), so we census the resulting adult beetles 6 weeks after the inoculation of stock beetles.

Censusing is carried out via one of two methods: 1) taking a picture of frozen beetles, using an *ImageJ Fiji* (Schindelin et al., 2012) macro to automatically count the beetles, and reviewing all pictures to manually correct any mistakes; or 2) estimating the total number of beetles using the total weight of all beetles, based on extrapolating the weight of 50 beetles. In previous experiments the weight-based method resulted in less than 1% error, which we deem negligible.

Our experimental setup enforces non-overlapping generations and synchronized life cycles, whereas previous *Tribolium* experiments have allowed a continual mixing of life-stages (e.g. Costantino et al., 1997). Our approach has several benefits. 1) The number of larvae and pupae at census-time are negligible, allowing for high-throughput computer-assisted beetle counting. 2) The only relevant inter-stage interaction is adult-on-egg cannibalism (Appendix 3.1.A). Allowing more inter-stage interactions would add to the complexity of the system, thus complicating the processes of model fitting and model adequacy analysis. 3) Our setup simulates the lifecycles of many univoltine and bivoltine insects.

3.1.3.2 Datasets

When not being handled, both stock and experimental populations were maintained in dark incubators at 60±10% relative humidity. Data was collected for 2197 one-generation experimental replicates. A single replicate is constituted by a population of *T. castaneum* in a single plastic enclosure. The data may be divided into three distinct datasets (collections of replicates) that correspond to distinct combinations of

temperature and genetic strain of beetle.

Dataset 1 (# replicates = 243; collected in 2020 and 2021): Stock populations were maintained at 31 degrees C. Adult beetles (and their subsequent eggs) were exposed to 22.5 degrees C for the entirety of a 7-day oviposition period but were returned to 31 degree C conditions afterwards.

Dataset 2 (# replicates = 1678; collected in 2019 and 2020): Stock populations and experimental units were always kept at 31 degrees C. Oviposition periods include 1,2, 3, 5, and 7 days. The various oviposition periods proved useful in model comparisons and graphical model validation (Appendix 3.1.D). In our main results (Fig. 3.2–3.4), we present only the subset of Dataset 2 where the oviposition period is 7 days (# replicates = 816). This isolates initial population size as the independent variable, and enables a fair comparison with Datasets 1 and 3.

Dataset 3 (# replicates = 276; collected in 1997): Stock populations and experimental units were maintained at 34 degrees C. The oviposition period was 7 days. Dataset 3 contains a higher maximum number of beetles at time t+1 than Dataset 1 or 2. Our recent experiments at 34 degrees C (data not published) show that this difference cannot be explained solely by differences in experimental temperatures. Instead, we suspect that the stark difference can be attributed to genetic differences in *T. castaneum* strains. After Dataset 3 was collected (but before Dataset 1 or 2) our beetle populations became infested with parasitic mites, which forced us to purge all populations and start anew with a different strain.

3.1.3.3 Model description

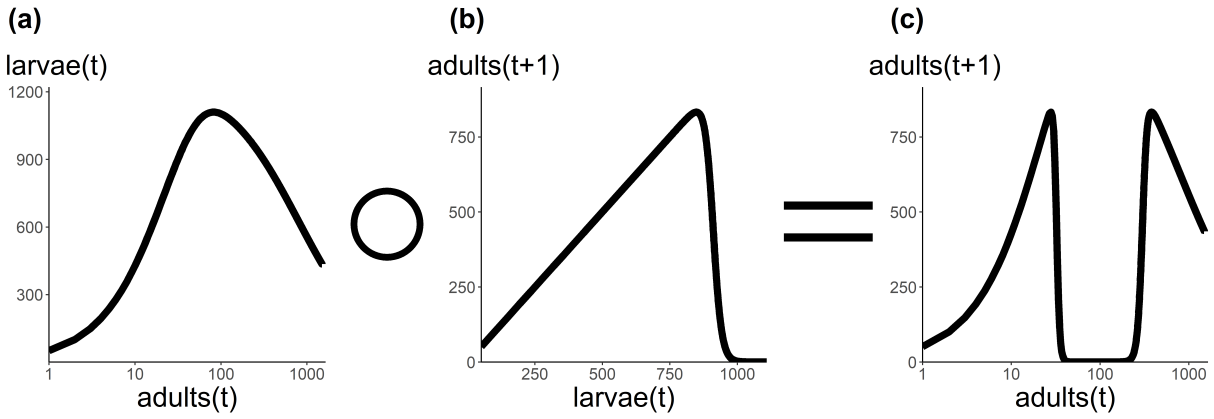

Figure 3.1: Visual summary of flour beetle population dynamics. The composition (denoted with the "o" symbol) of (a) the adult(t) → larvae(t) map with (b) the larvae(t) → adult (t+1) map can produce (c) a double-humped time-1 (i.e., adult(t) → adult(t+1)) population map. These plots depict the deterministic model with hypothetical parameters.

Our experimental populations experience two rounds of density dependence at successive life stages (Fig. 3.1): density-dependent egg production due to adult-on-egg cannibalism (Fig. 3.1a), and density-dependent larval survival due to scramble competition (Fig. 3.1b). When adults are placed into fresh media, they begin to oviposit eggs and eat eggs. The egg dynamics can be captured by the simple linear differential equation,

$$\frac{dz}{dh} = \frac{n\left(t\right)}{2}\left(\alpha - \beta z\left(h\right)\right), \quad \text{initial conditions : z(0)} = 0, \tag{3.1}$$

where z is the number of eggs; n is the number of adult beetles (hence $n/2$ is the number of females); h is the number of days since the start of the oviposition period; t is the generation number of the adult beetles, α is the per-adult, per-day oviposition rate; and β is the per-adult, per-egg, per-day cannibalism rate.

Obviously, only females can oviposit. Less obviously, females are far more voracious egg cannibals than males — using industrial die to perform an egg mark-recapture experiment, Sonleitner (1961) found that *Tribolium castaneum* females ate 19 times as many eggs as males. Although there are large differences between species and strains of *Tribolium* with respect to multiple elements of life history (Park et al., 1965; Sokoloff, 1974), the relatively greater voracity of females appears to hold true across *Tribolium* species and strains (Boyce, 1946; Rich, 1956; Stanley, 1942). For this reason and for mathematical convenience, our models assume that only females eat eggs.

When the initial number of adult beetles is large, both oviposition and cannibalism rates decrease (Rich, 1956; Sonleitner, 1961), due primarily to the density-dependent secretion of allelopathic ethylquinones (Bullock et al., 2020; Park, 1934; Park, 1935; Sonleitner and Gutherie, 1991). The decrease in the oviposition rate is comparatively large, such that the mean number of eggs decreases for high numbers of initial adults. We modelled this phenomenon by allowing the cannibalism rate β (which may more aptly be called the effective cannibalism rate) to increase linearly with initial adults: $\beta(t) = \beta_0 + \beta_0 n\left(t\right)$. This modelling decision (which may be contrasted with allowing α to decrease with adult density) allows the mean number of eggs to smoothly approach zero at high adult density. Previous research has verified that the oviposition rate α and cannibalism rate β are approximately constant over the duration of the oviposition period (Howe, 1962; Rich, 1956; Sonleitner, 1961).

After an oviposition period of s days, the number of eggs is

$$z\left(n\left(t\right)\right) = \frac{\alpha - e^{-s\ (n(t)/2)\ (\beta_0\ +\ \beta_1 n(t))}}{\beta_0\ +\ \beta_1 n(t)}. \tag{3.2}$$

Thus, eggs are a unimodal, hump-shaped function of initial adults (Fig. 3.1a). Because β_1 is very small in our system, the number of eggs produced by an intermediate number of initial adults is approximately α/β_0, the oviposition rate divided by the maximum cannibalism rate.

Once the adult beetles are sifted-out of the microcosms, the eggs hatch and become larvae. Most larvae survive to the pupal stage, and most pupae survive to the adult stage. However, at extremely high larval densities, there is not enough flour for early instar larvae to survive; scramble competition between larvae is the proximal cause of population crashes. This is evidenced by the fact that replicates with large $n(t)$ and small $n(t+1)$ (i.e., populations that have crashed) have a large number of eggs at the end of the oviposition period (Fig. 3.2c) and a large number of dead larvae at census time (Fig. 3.2a & 3.2b).

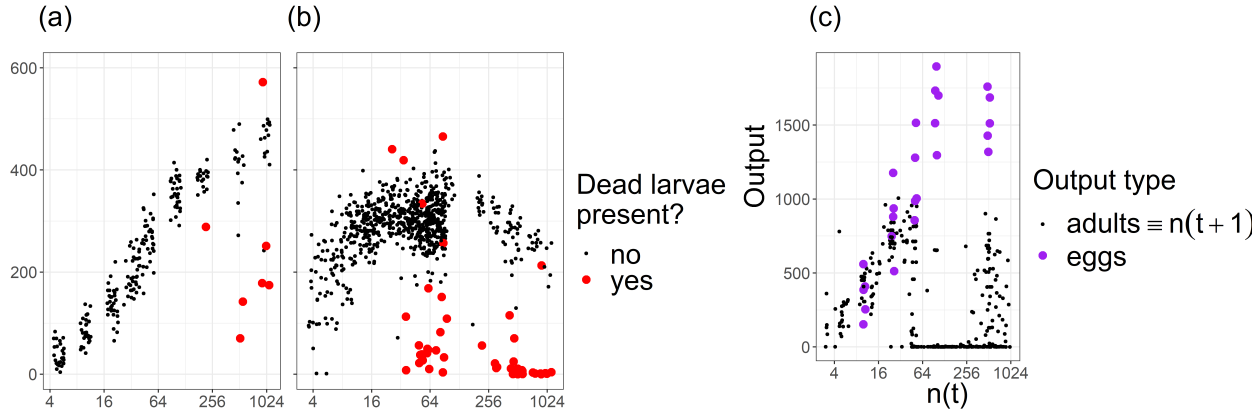

Figure 3.2: **Panel (a)**: In Datasets 1 and 2 (**Panels (a) and (b)** respectively), dead larval carcasses are observed in replicates that experienced population crashes. **Panel (c)**: A small egg-counting experiment in Dataset 3 reveals that population crashes are not caused by insufficient egg-production.

We model egg-to-adult survival using a reversed logistic function. The number of adults of generation $t+1$, as a function of the number of eggs, is

$$n\left(t+1\right)=z\left(n\left(t\right)\right)\left(\theta_L-\frac{\theta_L}{1+e^{-k(z(n(t))-z^*)}}\right), \tag{3.3}$$

where θ_L is the maximum egg-to-adult survival probability, i.e., the egg-survival probability when there are Low numbers of eggs. Here, z^* is the die-off threshold, which is more precisely defined as the number of eggs necessary to bring per-capita egg-to-adult survival probability to $\theta_L/2$. The parameter k controls the speed at which this transition occurs. The larvae-to-adult map has the appearance of being nearly discontinuous (Fig. 3.1b), partly because it is highly nonlinear (the egg-to-adult survival probability is multiplied by the number of eggs), and partly because k is relatively large.

The maximum egg-to-adult survival probability is fixed at $\theta_L = 0.91$, which was derived from an experiment where we found that 182/200 (91%) of individual eggs in abundant flour survive to adulthood. There is strong evidence (Appendix 3.1.B) that the die-off threshold decreases with initial population density, likely

due to adults conditioning the flour with feces, pheromones, and ethylquinones; we model this relationship with a simple linear function: $z^* = \gamma_0 - \gamma_1 n\,(t)$.

Combining the function for net egg production with the function for egg survival produces the time-1 population map,

$$n\,(t+1) = \frac{\alpha - e^{-s\ (n(t)/2)\ (\beta_0\ +\ \beta_1 n(t))}}{\beta_0\ +\ \beta_1 n(t)} \left(\theta_L - \frac{\theta_L}{1 + e^{-k\left(\frac{\alpha - e^{-s\ (n(t)/2)\ (\beta_0\ +\ \beta_1 n(t))}}{\beta_0\ +\ \beta_1 n(t)} \ -\ z^* \right)}} \right). \tag{3.4}$$

While the deterministic model above may appear complicated, it is merely the composition of banal density-dependent functions representing egg production and egg survival (Fig 3.1). Further justification of our model's structure can be found in the Supporting Information. Specifically, Appendix 3.1.B justifies several ostensible limitations of the model, including fixing θ_L and using eggs as a proxy for larvae.

3.1.3.4 Stochastic model fitting

3.1.4 Results

Using model comparisons, *a priori* arguments, and graphical evidence (Appendix 3.1.D & Tables 3.2–3.4), we determined that the relevant sources of stochasticity in flour beetle dynamics were sex-ratio stochasticity and demographic stochasticity in oviposition rates. The full stochastic model (described fully in Appendix 3.1.E) faithfully recreates patterns in empirical one-generation population maps (Fig. 3.3).

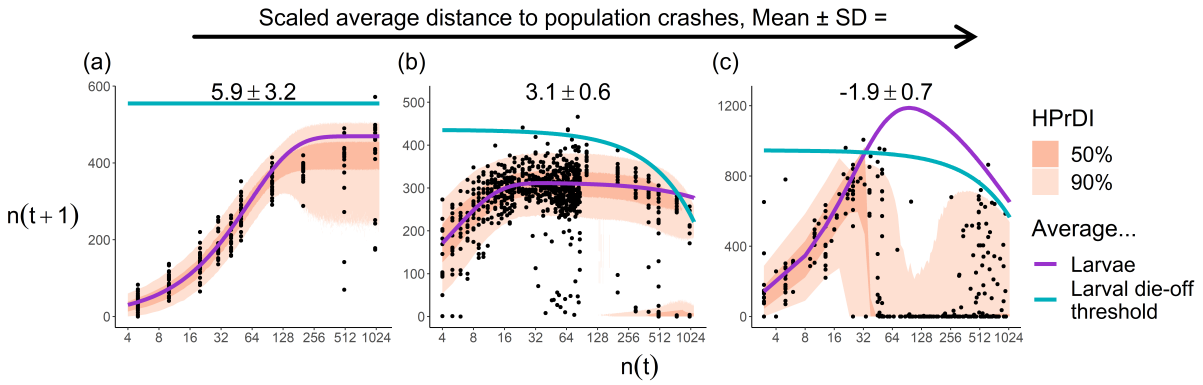

Figure 3.3: Time-1 population maps for *Tribolium castaneum*. Panels are arranged in order of an increasing scaled average distance to population crashes, a system-specific metric of complexity that is defined in the Results; Mean ± SD refers to the posterior predictive density of the metric. The solid black dots are experimental data; panels (a), (b), and (c) correspond to Datasets 1, 2, and 3 respectively. Dataset 2 is subsetted so that the oviposition period is 7 days. The salmon-colored ribbons are High Predictive Density Intervals (HPrDI) for $n(t+1)$, which were obtained by simulating from the full stochastic model. Experimental temperature is the ultimate cause of the difference between panels (a) and (b). Beetle genetic strain likely explains the difference between panels (b) and (c).

By modulating experimental conditions, we can modulate the values of demographic parameters, and in turn, the probability of population crashes. At the low temperature of Dataset 1 (see Methods, subsection datasets), the empirical population map is perfectly compensatory (Fig. 3.3a), i.e., for sufficiently high population density, increasing population density further will not decrease population density at time $t+1$. The compensatory nature of population dynamics reflects a stochastic equilibrium between oviposition and egg-cannibalism. Population crashes do not occur frequently because the die-off threshold is high, likely due to the flour being less polluted (with feces, pheromones, and ethylquinones) at lower temperatures (Fig. 3.1). Egg production does not decrease appreciably with increasing initial adults (i.e., $\beta_1 \approx 0$), likely for the same reason.

At the intermediate temperature of Dataset 2, larval production does not usually exceed the larval-density threshold for population crashes. However, on rare occasion, demographic stochasticity "pushes" the number of larvae over the threshold. The emergent pattern is a bimodal distribution of adult beetles at time $t+1$, with the low-density mode representing population crashes (Fig. 3.2b). Although sex-ratio stochasticity is present in our beetle system (see Appendix 3.1.D and Fig. 3.2), it has negligible effects in large populations, and therefore plays a relatively minor role in inducing population crashes.

These crashes are truly black swan events, both in the sense that they are unexpected, and in the sense that they are related to heavy-tailed distributions. For Dataset 2, population crashes (here operationalized as $n(t+1) < 150$)) occur in approximately 3.6% of the replicates in the range $n(t) \in= [12, 400]$. Because the distribution of $n(t+1)$ is approximately stationary in this range, population crashes are identically and independently distributed random variables. Thus, the time until the first crash is given by a geometric distribution with success parameter $p = 0.036$ and mean wait time $1/p \approx 27$ generations. For the fast-growing *Tribolium* genus, 27 generations take over 3 years. Regardless of generation time, a time series of length 27 is long by ecological standards: in the Global Population Dynamics Database (Prendergast et al., 2010), 66% of the time series had fewer than 27 observations. Further, in Appendix 3.1.H, we use minimal mathematics and empirical CDF plots to show that the population crashes come from a heavy-tailed distribution of per capita growth rates.

A highly productive strain of *T. castaneum* at high temperatures (i.e., Dataset 3) can regularly produce enough larvae to induce population crashes. The composition of two rounds of overcompensatory density-dependence produces a double-humped population map (Fig. 3.3c): Larval die-offs do not occur for low numbers of initial adults (because few adults produce few larvae) and are less common for high numbers of initial adults (because adult overcrowding reduces oviposition rates). It is only at intermediate numbers of initial adults that larval population crashes occur predictably.

Our three distinct datasets correspond to distinct experimental conditions (beetle genetics and incubator temperature), which in turn influence population dynamics. Though the datasets differ with respect to many demographic parameters, they can be arranged along a continuum of a synthetic parameter, the scaled average distance to population crashes (Fig. 3.3). First, we denote the number of eggs required for a population crash as ϕ. Then, the scaled average distance to population crashes can be written as $\mathbb{E}\Big[[\phi - z]/\sqrt{Var(\phi - z)}\Big]$, the average distance between egg production and that which is required for population crashes, scaled by the magnitude of typical fluctuations (see Appendix 3.1.F for more details). A substantially positive value indicates that population crashes are rare, whereas a negative value indicates that population crashes are more likely than not.

Note that we can manipulate the scaled average distance to population crashes by modulating the oviposition rate, α, and fixing all other variables. Therefore, to explore the full extent of the beetle system's dynamical behavior — for both the full stochastic model and the underlying "deterministic skeleton" — we simulated beetle dynamics forward in time for a variety of hypothetical oviposition rates (Fig. 3.4). To better simulate a real-world analogue of our beetle system, we also examine the distribution of population sizes in the face of weak immigration (1 female per generation).

Dataset 3 provides evidence of chaotic population dynamics. The estimated oviposition rate for Dataset

3 is approximately 15.8 eggs per day, placing the actual population in the chaotic regime of Figure 3.4a. Analogous figures corresponding to Dataset 1 & 2 (not shown) did not provide evidence of chaos. The deterministic dynamics generate a menagerie of interesting dynamical behavior: chaos, crisis, and period-doubling bifurcations (Strogatz, 1994) (Fig. 3.4a); and immigration-induced population cycles (Stone and Hart, 1999) (Fig. 3.4e). Adding stochasticity to the model erases the interesting structure of the deterministic bifurcation diagrams (see Fig. 3.4b, 3.4d, and 3.4f). In the short-term, the beetle system can persist (Fig. 3.4c). In the long-term, rare population crashes predictably lead to extinction (Fig. 3.4b & 3.4d), an outcome that is mitigated by weak immigration (Fig. 3.4f).

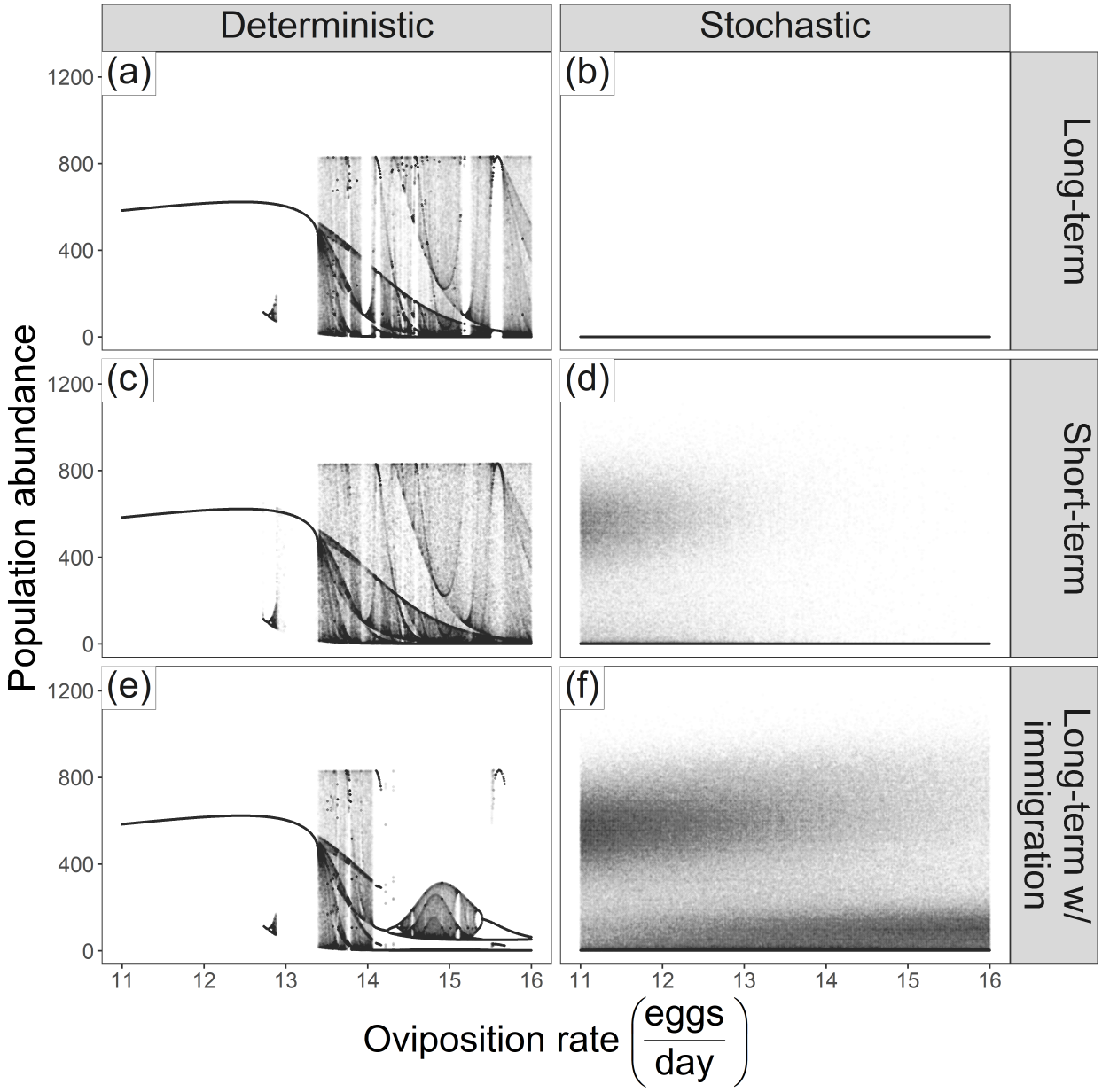

Figure 3.4: Bifurcation diagrams for factorial 'treatments' (shown on the top and right margins of the figure). All demographic parameters besides the oviposition rate, α, were selected as the posterior means of the stochastic model corresponding to Dataset 3. The oviposition period is 7 days. Deterministic refers to the 'deterministic skeleton' of the full stochastic model. Stochastic refers to the output of the full model. Long-term simulations are 500 generations. Short-term simulations are 20 generations. Immigration amounts to one adult per generation. The deterministic dynamics generate period-doubling bifurcations, crisis bifurcations, chaos (**panel a**), and transient chaos (**panel c**). Weak immigration induces population cycles (**panel e**, $\alpha > 15.7$). The inclusion of stochasticity causes extinction (**panel b**). Extinction becomes likely at higher oviposition rates (**panel d**) but can be avoided with weak immigration (**panel f**). Dataset 3 exhibits chaotic population dynamics (α is estimated at approximately 15.8 eggs/day).

3.1.5 Discussion

In our flour beetle microcosms, rare population crashes arise from a combination of noise and nonlinear density-dependence. Without noise, the number of larvae would not exceed the threshold for larval die-offs. Without a nonlinear response to competition between larvae, an excess of larvae would lead to only a slight reduction in larval survival.

Although our beetle model has some system-specific features (e.g., the effective cannibalism rate increases with initial population size), the observed mechanism of population crashes can be boiled down to a few essential ingredients: two rounds of density-dependence and some form of stochasticity. The first round of density-dependence must be compensatory or weakly overcompensatory in order to set the average number of individuals slightly below the density at which the second round has severe effects. The stochasticity (whether demographic or environmental; endogenous or exogenous) occasionally pushes population density into a regime where the second round of density-dependence is severely overcompensatory.

Because two rounds of density dependence are required, our mechanism of population crashes naturally emerges as an intergenerational phenomenon (Fig. 3.5). As we have seen, crashes occur as a within-generation phenomena if different forms of density dependence are experienced by different life stages (e.g., adult-on-egg-cannibalism vs. larval overcrowding, as in our beetle system), or in different seasons (e.g., nesting birds limited by territories in the spring vs. food availability in the winter). Many insect populations display density dependence at multiple life-stages. The discreteness of developmental stages or environmental states is not integral to our explanation; in many ways, a two-stage juvenile-adult model is a faithful approximation of a population with continuous age/size-structure (de Roos and Persson, 2013). Similarly, discrete-time dynamics are not required; overcompensatory population maps emerge from the discretization of continuous-time dynamics (see Fig. 5 in Hastings and Powell, 1991).

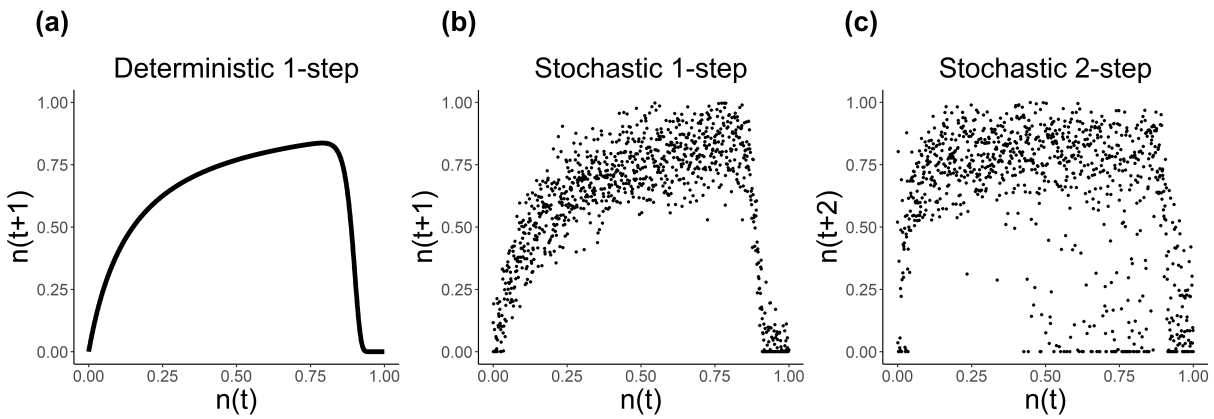

Figure 3.5: Population crashes in a scalar population. Population crashes are caused by stochasticity and the successive application of a single density-dependent process. **Panel (a)**: the time-1 population map displays severe density dependence. **Panel (b)**: the noisy time-1 population map. **Panel (c)**: the noisy time-2 population map

In flour beetle microcosms, stochasticity causes crashes by pushing larval density over the larval die-off threshold. More generally, an abnormally favorable environment (or pure luck) may produce a large number of individuals; too many to be sustained by a subsequent normal environment. For instance, a population of water voles (*Arvicola amphibius*; Le Pont, Switzerland; circa 1970) crashed (Saucy, 1994), plausibly because a sequence of abnormally warm winters (personal observations based on meteorological data) amplified the growth-phase of a predator-prey cycle, subsequently exacerbating the downward phase.

Alternatively, we may think of stochasticity as acting on the shape of the growth rate function itself, effectively lowering the threshold for severe density-dependence. From this perspective, the severe threshold-like density dependence of Fig. 3.1b & Fig. 3.5a appears less assumptive — severe density-dependence can be induced by poor environmental conditions, rather than being an invariant feature of the growth rate function. For instance, an Icelandic population of Rock ptarmigan (*Lagopus mutus*; Iceland; circa 1880) experienced a severely cold winter, which likely caused the birds to feed at an increased rate, leading to rapid depletion of the most nutritious food items and subsequent starvation (Andreev, 1991; Williams, 1954). Of course, some population crashes appear to be induced entirely by extreme environmental conditions. For example, a population of Eurasian wrens (*Troglodytes troglodytes*; circa 1960, England) was eradicated after its seed supply was buried under snow for 45 days (a period of snow cover more than four times longer than the historical average; Newton et al., 1998). It is hard to imagine that any wrens could survive this event, even if population density had been lower.

It is well known that extreme density-dependence can cause wild fluctuations in population size, the

canonical example being the chaotic dynamics of May's (1976) logistic model. In such models and in Dataset 3 (see Fig. 3.3c), populations densities naturally increase until they are in the regime of extreme overcompensation. In our mechanism of population crashes and Dataset 2 (Fig. 3.2b), the regime of extreme overcompensation can only be reached through rare fluctuations. Thus, our mechanism is distinct from chaos in the sense that 1) crashes are rare, 2) stochasticity is required, and 3) extreme overcompensation is the exception, not the rule.

We note that our explanation (i.e., noise plus overcompensatory density-dependence) bears similarity to John Wiens's (1977) theory of "ecological crunches", which posits that density dependence is only detectable under poor environmental conditions. However, we show that overcrowding can also be catalyzed by pure luck — demographic stochasticity, demographic heterogeneity, and sex-ratio stochasticity. If overcrowding is indeed catalyzed by luck, and data on the abundance of intermediate stages (here, beetle larvae) is not collected, then population crashes can occur for no discernible reason.

Our mechanism for population crashes is consistent with Anderson et al.'s (2017) finding the that the vast majority of black swan events (87%) were downwards. Anderson explains that this result stems from the asymmetry between reproduction and mortality: In most animals, the reproductive speed limit is set by age-of-maturity, gestation, and fecundity, but "there is no limit on how dramatically a population can be cut in size" (Anderson quoted in Ogden, 2018). Our mechanism offers an additional (non-mutually exclusive) explanation for the prevalence of downward black swans: the per-capita growth rate function is a concave-down function of population density, such that an increase in population density can have a disproportionately negative effect on population growth.

Anderson (2015) summarized the published descriptions (or lack thereof) of black-swan events in the Global Population Dynamics Database and found that approximately 50% of black swan events have an unknown cause. It is possible that some of these events are inexplicable, precisely because (as in our flour beetle microcosms) demographic stochasticity induces overcrowding. The effects of demographic stochasticity are often overlooked, since fluctuations due to environmental stochasticity scale with population size n, whereas fluctuations due to demographic stochasticity only scale with $\sqrt{n}$. However, an analysis of the relationship between the mean and standard deviation of population sizes was consistent with demographic stochasticity having substantial effects on real-world population fluctuations (Reed and Hobbs, 2004). A number of studies (reviewed by Lande et al., 2010, Table 1.2) have found that the typical between-individual differences are much larger than the typical between-year (environmental) differences. More recently, Snyder and Ellner (2022) used complex stage-structured models to partition the variation in lifetime reproductive success into contributions from environmental stochasticity, demographic stochasticity, and demographic heterogeneity (i.e., trait variation). Across several case studies, demographic stochasticity contributed far more

than environmental or trait variation (the exception being a case study of *Lomatium bradshawii* where "the environment" was the absence/presence of experimentally-prescribed burns), suggesting that demographic stochasticity can be a potent force in intermediate-to-large sized populations.

It would be premature to make any definitive statements about the frequency of ecological "black swan" events in the real-world (see the Introduction), let alone the generality of our proposed mechanism. Even speculation is difficult, given that the most conspicuous feature of our explanation is severe, threshold-like density-dependence and that there is great uncertainty about the strength of density-dependence in real-world populations. On one hand, substantial density-dependence is usually "detected" in field or lab-based density-manipulation experiments (see Thibaut and Connolly, 2020, Appendix S1 and sources therein), observational studies of individual insect life stages (Hassell et al., 1989), and microcosm experiments (Benincà et al., 2008; Costantino et al., 1997; Gurney et al., 1980). On the other hand, most analyses of ecological time series find that density-dependence is weak (Knape and de Valpine, 2012; Ziebarth et al., 2010).

At least two theories can explain why time series analyses conclude that density-dependence is weak. Theory 1: Density-dependence only appears to be weak because time-series data is collected on a larger spatial scale than that of density-dependent processes (Ray and Hastings, 1996; Thorson et al., 2015). Under this theory, abundance/density data reflects a spatial average over a number of semi-independently fluctuating sub-populations, such that the statistical signal of density-dependence is lost. Theory 2: There is substantial density-dependence at one life-history stage, but the resulting numerical response is diffused across space. For example, if an annual plant community on a small spatial scale ($\approx 100cm^2$) is well-under carrying capacity, competition between germinants will be weak and per capita seed yields will be large. However, because germinants compete for soil resources on the scale of centimeters, and seeds disperse on the scale of meters, most of the seeds will not be retained locally. On the small spatial scale, there will be a weak statistical relationship between seed densities in successive years (assuming that these small-scale populations are not spatially synchronized).

Both theories explain the aforementioned discrepancy between time-series analyses and microcosm experiments. Under the first theory, microcosms uncover true density-dependence because they because they are deliberately constructed at the scale of density-dependent processes. Under the second theory, microcosms artificially induce severe density dependence because they prevent dispersal. Although outside the scope of this paper, the veracities of these theories have wide-reaching implications, with the second theory questioning the external validity of microcosm experiments in general.

With slight modification, the mechanism responsible for population crashes can also generate an odd-looking generation-to-generation population map (Fig. 3.2c). We demonstrate here that such maps could actually be quite general at the appropriate spatial scale of description. It has previously been recognized that

the composition of two overcompensatory population maps can result in a double-humped "time-2" population map (May and Oster, 1976; Schaffer, 1985). Our work builds on this important idea by showing that double-humped maps can be produced by intra-generational interactions within successive developmental stages, rather than inter-generational population growth. Double-humped maps may also emerge from more complex and realistic settings. For instance, a double-humped Poincare map — which itself can be conceptualized as the composition of two overcompensatory Poincare maps — was discovered in a continuous-time, tri-trophic model (Hastings and Powell, 1991).

Here, we used flour beetle microcosms to demonstrate a novel mechanism for population crashes: environmental or demographic noise 'pushes' population density into a regime where overcompensatory density dependence causes population crashes. We recognize that there is also evidence for other mechanisms, like extreme density-independent mortality (Newton et al., 1998; Potts et al., 1980), volatility clustering (Segura et al., 2013; Segura and Perera, 2019; where seasonal resource supply modulates the variance in growth rates), or more generally, 'mixtures of distributions' (Allen et al., 2001; Keitt and Stanley, 1998; Marquet et al., 2005; McGill, 2003; Newman, 2005; Solow, 2005). A full understanding of population dynamics will require much more attention to interactions between stochasticity, stage-structure, and density-dependence.

Appendices

3.1.A Justification of limited inter-stage interactions

In our experimental setup, individuals have mostly synchronized life cycles. This significantly simplifies the population dynamics under study, since it has long been known that larvae eat eggs (Chapman, 1933) and pupae (Chapman, 1928); and that adults eat eggs (Chapman, 1928; Park, 1934) and pupae (Chapman, 1928; Strawbridge, 1953). Even though some individuals may hatch/pupate/metamorphose earlier than others, rendering a population with temporarily intermingling stages, there are good reasons to believe that this does not appreciably influence population dynamics.

Early instar larvae have low egg cannibalism rates (Hastings and Costantino, 1991; Park et al., 1974). This is likely due to limited mobility and the difficulty of consuming large eggs, the latter of which is evidenced by *Tribolium* larvae's general preference for small eggs (Craig, 1986; Ho and Dawson, 1966; Park et al., 1965) and their small mouthparts relative to adults.

Both adult-on-pupa and larva-on-pupa cannibalism can be substantial if the stages intermingle for a long time (Park et al., 1965), but the cannibalism rates are typically low. For example, if we take Park et al.'s (1965) data corresponding to the *T. castaneum* strain with the highest total intraspecific larva-on-pupa cannibalism (Table 12, treatment J), and assume that the per-larva, per-pupa cannibalism rate is constant through time, we calculate that the per day rate is approximately 0.0028. This rate is an order of magnitude smaller than typical adult-on-egg cannibalism rates (as estimated via our models). Using Park et al.'s data for adult-on-pupa cannibalism, a similar calculation yields a similar conclusion. In our beetle system, where pupae only mix with young adults, adult-on-pupa cannibalism should be even rarer: young adults hardly move at all until several days after eclosion (Hagstrum and Smittle, 1980). It has also been noted that a cannibalized pupa is "frequently left to be counted and plainly bears its mortal scars." (Park et al., 1965). We have never observed wounded or partial pupae, which is further evidence that both adult-on-pupa and larva-on-pupa cannibalism is negligible.

There are a few old reports of adults consuming larvae (Chapman, 1928), but it has often been assumed (Sokoloff, 1974, p. 138) that this interaction is negligible, given the high mobility of both life-stages. Adults can take up to 15 minutes to eat a single egg (Park, 1934), so it is hard to imagine that an adult could capture a larva for long enough to inflict a mortal wound. To our knowledge, no direct experimental evidence is available, but Strawbridge (1953) used a regression approach and concluded that adults cannibalized the immobile but sclerotized last-instar larvae more than early-instar larvae. Given the similarity between the last-instar larvae and the pupae, and the low rate of adult-on-pupa cannibalism, it is reasonable to assume that adult-on-larva cannibalism is small. It has also been suggested that Strawbridge's estimates of adult-

on-early-instar cannibalism could be entirely accounted for by density-independent larval mortality (Park et al., 1965).

Given the highly cannibalistic nature of *Tribolium* and the size disparity between early and late instar larvae, one might rightfully wonder whether larva-on-larva cannibalism is significant. However, larva-on-larva cannibalism is negligible, if not non-existent (Park et al., 1965). This finding, taken with 1) the finding that adult-on-larva cannibalism is rare, and 2) that egg consumption can take 15 minutes, suggests that the adult beetles need immobile prey.

3.1.B Further justification of model structure

Here we justify — mostly on pragmatic & computational grounds — a few peculiar aspects of our model. First, it may seem strange that we fix the maximum egg-to-adult survival probability at $\theta_L = 0.91$; after all, the three datasets clearly correspond to systems with different demographic parameters. When fitting the stochastic models, we found that θ_L and α were effectively non-identifiable when we allowed both parameters to be estimated from the data (constrained only by weakly informative priors) i.e., θ_L and α are highly correlated in regions of high posterior density. Non-identifiability leads to large uncertainties in the values of either parameter. More importantly, it causes computational issues (specifically, divergences in the trajectories of Hamiltonian Monte Carlo) that can lead to biased estimation for all parameters.

Because θ_L and α are nearly non-identifiable, any difference between 0.91 and the true value of θ_L will be "absorbed" by the estimate of α. For example, if the true effective fecundity is $\alpha\theta_L = 10$, and the true maximum egg-to-adult survival is $\theta_L = 0.80$, then an unbiased model fitting procedure will produce $\widehat{\alpha}0.91 = 10$, where the estimate of the oviposition rate is $\hat{\alpha} = \theta_L/0.91$. Therefore, fixing θ_L does not dramatically change model predictions, though it does pollute the interpretation of $\hat{\alpha}$. We also have good reason to believe that $\theta_L = 0.91$ is approximately correct, since survival probabilities are relatively invariant in the temperature range 22.5- 37.5 degrees C (Sokoloff, 1974, p. 57-66).

Second, in the full stochastic model (Appendix 3.1.E), the number of eggs surviving to adulthood in non-crash replicates is modelled as binomial distributed with $z\,(t)$ trials (i.e., the number of eggs) and success probability θ_L. A more complete model would incorporate several rounds of binomial survival — one for each life stage transition. However, we do not have the data to estimate these transition probabilities. Such experiments would be difficult, since counting eggs is arduous, early instar larvae fall through our finest sieves, and handling causes significant pupal mortality (Ryan and Nathanson, 1969). Estimating these transition probabilities indirectly (i.e., integrating / summing conditional likelihoods over possible combinations of eggs, larval instars, and pupae) is computationally infeasible. We would expect that this limitation of our model

would result in artificially thin tails in the distribution of beetles surviving to adulthood (it is well-known that mixtures of distributions produce heavy-tailed distributions; e.g., Allen et al., 2001). However, this appears not to be the case (Fig.3.9, right panel).

Third, we model egg-to-adult survival as a function of egg density, even though population crashes are caused by high larval density. This modelling decision can be justified on the grounds that egg density is a good proxy for larval density. The egg-hatch probability is necessarily independent of egg-density (because eggs are sedentary and non-interactive), so the average number of larvae is always proportional to the number of eggs.

Finally, our model states that the die-off threshold decreases with initial population size: $z^* = \gamma_0 - \gamma_1 n(t)$. If the die-off threshold did not decrease with $n(t)$, one would expect that population crashes would become less frequent at sufficiently high $n(t)$, since the average number of eggs decreases with $n(t)$ (as the effective cannibalism rate increases). This is not the case. In Dataset 2, for very large $n(t)$, we see an increase the frequency of crashes, along with a decrease in the average $n(t+1)$ for non-crashing replicates (Fig. 3.2 in the main text) consistent with an increase in the effective cannibalism rate. Figure 3.6 clearly shows that the crash frequency increases with $n(t)$ and the length of the oviposition period. Both of these factors contribute to the "conditioning of the medium" (Sokoloff, 1974, p. 150) — the nutritive depletion of the flour, along with the accumulation of feces and ethylquinones — which likely engenders larval die-offs. The length of the oviposition period does not need to be factored into the die-off threshold equation (i.e., $z^* = \gamma_0 - \gamma_1 n(t)$), since the full stochastic model is fit with the subset of data where oviposition period $\approx$ 7days.

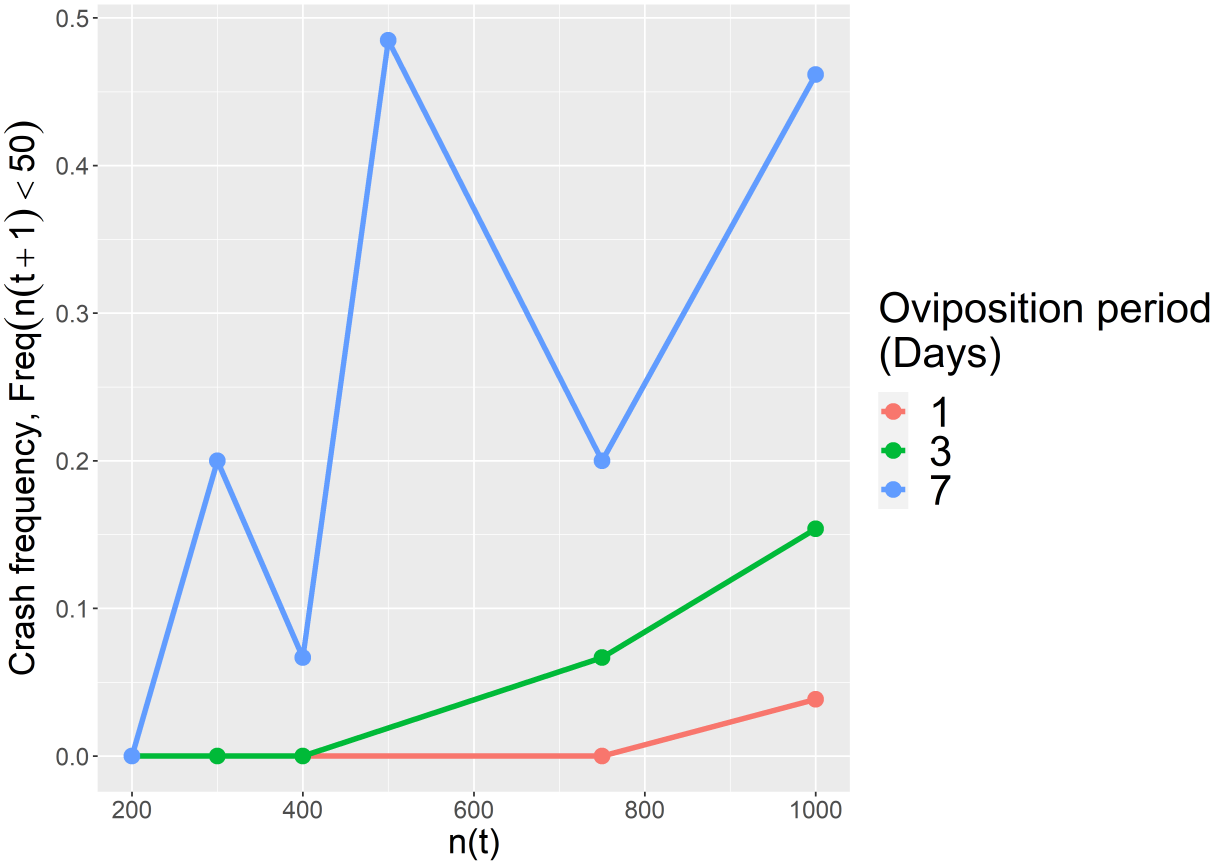

Figure 3.6: The frequency of population crashes increases with $n(t)$ and the length of the oviposition period; data from Dataset 2. Sample sizes for each point ranges from 13 to 33 replicates.

3.1.C Stochastic modelling general information

All modelling code is available at https://github.com/ejohnson6767/castaneum_crash. See the file `README.txt` for file descriptions. Our modelling approach has two steps.

1. We determined the important sources of stochasticity in beetle dynamics by comparing eleven sub-models with different combinations and variants of the four main sources of stochasticity: demographic stochasticity, demographic heterogeneity, sex-ratio stochasticity, and environmental stochasticity. For technical / computational reasons that will be explained, these sub-models do not include demographic stochasticity in egg-to-adult survival, nor do they include our mechanism of population crashes; naturally, they are fit using only the subset of data for which population crashes did not occur (see Appendix 3.1.D for details). Using graphical evidence and cross-validation, we select a single best-fit model (described fully in Appendix 3.1.E), which happens to include the processes of sex-ratio stochasticity and demographic stochasticity in oviposition.

2. We fit the full stochastic model, which includes the processes of sex-ratio stochasticity, demographic stochasticity in oviposition, demographic stochasticity in egg-to-adult survival, and the mechanism of population crashes (i.e., egg-to-adult survival is a decreasing function of egg-density).

All model-fitting was performed in the R software environment using the Stan program's implementation of Hamiltonian Monte Carlo. All models were formulated in a Bayesian framework, which in the current context has several benefits (in comparison with a Maximum Likelihood approach). 1) Models with latent variables can be efficiently fit using the program Stan, which only requires a conditional likelihood function. Computing the marginal likelihood function for our full model would involve a (computationally infeasible) triply-nested integration over latent females, eggs, and die-off thresholds. 2) Pair plots (i.e., bivariate plots of posterior samples) can be used to troubleshoot — to identify non-identifiable parameters and posterior multi-modality. 3) The joint posterior distribution of model parameters can be used to characterize parameter uncertainty, which is useful in comparing the overall fit of different models. 4) Overfitting is avoided because of the regularizing property of the prior distribution, and the fact that Bayesian inference is a form of model-averaging (Hastie et al., 2009, Section 8.8) and thus avoids giving full credulity to parameter combinations associated with spuriously large likelihoods.

All models were fit using weakly informative priors. The influence of the prior distributions were assessed with the posterior contraction (Gelman et al., 2014), a measure of how much parameter uncertainty shrinks a posteriori. The posterior contraction is defined as

$$c\left(\theta|D\right) = 1 - \frac{Var_{post}\left(\theta|D\right)}{Var_{prior}\left(\theta\right)}, \tag{3.5}$$

where θ is an arbitrary parameter, D is the data, $\text{Var}_{post}\left(\theta|D\right)$ is the variance of the marginal posterior distribution of θ, and $Var_{prior}\left(\theta\right)$ is the variance of the marginal prior distribution of θ. To further ensure model adequacy, we assessed a number of model diagnostics; see `scripts/model_diagnostics.R` at https://github.com/ejohnson6767/castaneum_crash.

3.1.D Determining the important sources of stochasticity

In order to determine the important sources of stochasticity in beetle dynamics, we fit 11 sub-models that contained various combinations of stochastic forces (full descriptions and likelihood functions are provided in Appendix 3.1.G). The sub-models do not include demographic stochasticity in egg-to-adult survival, nor do they include the mechanism of population crashes (i.e., egg-to-adult survival decreases with increasing egg density). This focused approach is purely pragmatic: marginal likelihoods are required for model comparisons (Merkle et al., 2019), and the marginal likelihood function of the full stochastic model is computationally

intractable (due to nested integrations over the latent number of females, eggs, and die-off thresholds). The sub-models are considerably simpler.

In addition, we do not expect that demographic stochasticity in egg-to-adult survival will contribute significantly to the total variation in $n(t+1)$. In Dataset 2, sufficiently large $n(t)$ produces an average non-crash $n(t+1)$ of approximately 300 individuals. Conditioned on the average number of eggs, the standard deviation of $n(t+1)$ (attributed only to stochasticity in egg-to-adult survival) is approximately $\sqrt{(300/0.91)\,0.91\,(1-0.91)} \approx 5$, whereas the unconditional standard deviation of $n(t+1)$ is approximately 60. At $n(t) = 5$ and oviposition period = 1day, the average $n(t+1)$ is 17 individuals; thus, the standard deviation of $n(t+1)$ (attributed only to stochasticity in egg-to-adult survival) is approximately $\sqrt{(17/0.91)\,0.91\,(1-0.91)} \approx 1$, whereas the unconditional standard deviation of n(t+1) is approximately 23. Regardless of the number of eggs, the scale of variation in survival is only $\sqrt{0.91\,(1-0.91)} \approx 0.28$, a small number. Even if θ_L is not exactly equal to 0.91, any high survival probability will lead to low variance in Bernoulli sampling; as it turns out, survival probabilities are high for all life stages in the range of temperature and humidity conditions that our beetles experienced (Sokoloff, 1974, p. 57-66).

The sub-models were fit for each dataset separately. We fit the sub-models to a subset of data — replicates for which population crashes had not occurred — determined visually via one-generation populations maps. Almost all parameters had marginal posterior contractions greater than 0.96, indicating that the prior distribution had negligible influence. The sole exception was the return-rate parameter (for all three datasets) of sub-model 3, the model with temporally autocorrelated fluctuations in oviposition rates. The autoregressive parameter ρ was nearly non-identifiable with the demographic stochasticity parameter η_α, leading to large posterior uncertainties. Diagnostics indicated that all sub-models — with the exception of sub-models 10 and 11 — converged to the posterior distribution and had low Monte Carlo error.

Sub-models were compared using Pareto-Smoothed Importance Sampling Leave-One-Out Cross Validation (PSIS LOOCV; Vehtari et al., 2017) with expected log predictive density as the loss function. This method of model comparison is preferable to information criteria-based methods, which do not account for parameter uncertainty, are not well-defined for hierarchical models, and which only approximate cross-validation error asymptotically for linear models.

Cross Validation results are presented in Tables 3.2–3.4. Across all datasets, many of the best-fit sub-models included demographic stochasticity and/or some form of demographic heterogeneity (recall that sex-ratio stochasticity is a special case of demographic heterogeneity). There seems to be no predictive benefit to including demographic stochasticity in cannibalism, indicating that either cannibalism rates do not vary appreciably over time (which is doubtful), or that demographic stochasticity in cannibalism is effectively modelled by increasing the demographic stochasticity in oviposition. There also seems to be

no predictive benefit of including both demographic heterogeneity and sex-ratio stochasticity. Sub-models with environmental stochasticity performed poorly, either running into computational issues or generating low likelihoods. This is not too surprising, seeing as how the beetles lived in temperature and humidity-controlled incubators.

We give special attention to the Cross Validation results of Dataset 2 (Table 3.3). Dataset 2 has multiple oviposition period lengths and the most replicates by far. Without multiple oviposition period lengths, the parameters α and β_0 are highly correlated among posterior samples, leading to high uncertainty in the marginal posteriors of both parameters.

According to Cross Validation, the best-fit sub-model for Dataset 2 was sub-model 5, which featured demographic stochasticity and demographic heterogeneity in oviposition rates. However, there is not strong evidence for the superiority of sub-model 5 compared to sub-models 1, 5, and 6. Because Model 1 is more parsimonious, represents the same process (sex-ratio stochasticity is a type of demographic heterogeneity), and is more plausible *a priori* (we know that there is randomness in the sex-ratio), we regard sub-model 1 as the best sub-model for Dataset 2. Sub-models 2, 3, 7, 8, 9, and 11 were clearly worse.

There was no clear relationship between complexity and fit, with complexity being defined in relation to sub-model 1: Sub-models 2, 3, 4, and 9 are more complex; sub-models 5 and 8 are similarly complex; and sub-models 6, 7, and 11 are less complex. Interestingly, the sub-model with only demographic stochasticity did not perform terribly worse than the best-fit sub-model. This is some indication that demographic stochasticity is the dominant stochastic force in our beetle microcosms.

However, we believe that demographic heterogeneity of some sort (recall sex-ratio stochasticity is a special case of demographic heterogeneity) plays an important role in our system. There are two pieces of evidence for this. First, sex ratio stochasticity undeniably exists in our system, *a priori* (Howe, 1956). Second, demographic heterogeneity accounts for the high variance in $n(t+1)$ at small $n(t)$ for experiments with a long oviposition period: a fluctuation in the sex ratio has compounding effects on egg production over the oviposition period (because the sex ratio stays the same), whereas demographic stochasticity does not (a large number of eggs one day is likely to be cancelled out by a small number of eggs the next day).

The verbal argument above is supported by the conjunction of mathematical and graphical evidence. In the sub-model with only demographic stochasticity (sub-model 6, Appendix 3.1.G) the variance of $n(t+1)$ is necessarily an increasing function of $n(t)$. This is what we see in experimental data with a 1-day oviposition period (Fig. 3.7, left panels). In the sub-model with both demographic stochasticity and demographic heterogeneity (sub-model 2, Appendix 3.1.G) the variance of $n(t+1)$ is necessarily an increasing function of $n(t)$ when the oviposition period is short. However, when the oviposition period is long, it is possible for the variance of $n(t+1)$ to be a decreasing function of $n(t)$. This is precisely what we see in experimental

data with a 7-day oviposition period (Fig. 3.7, right panels).

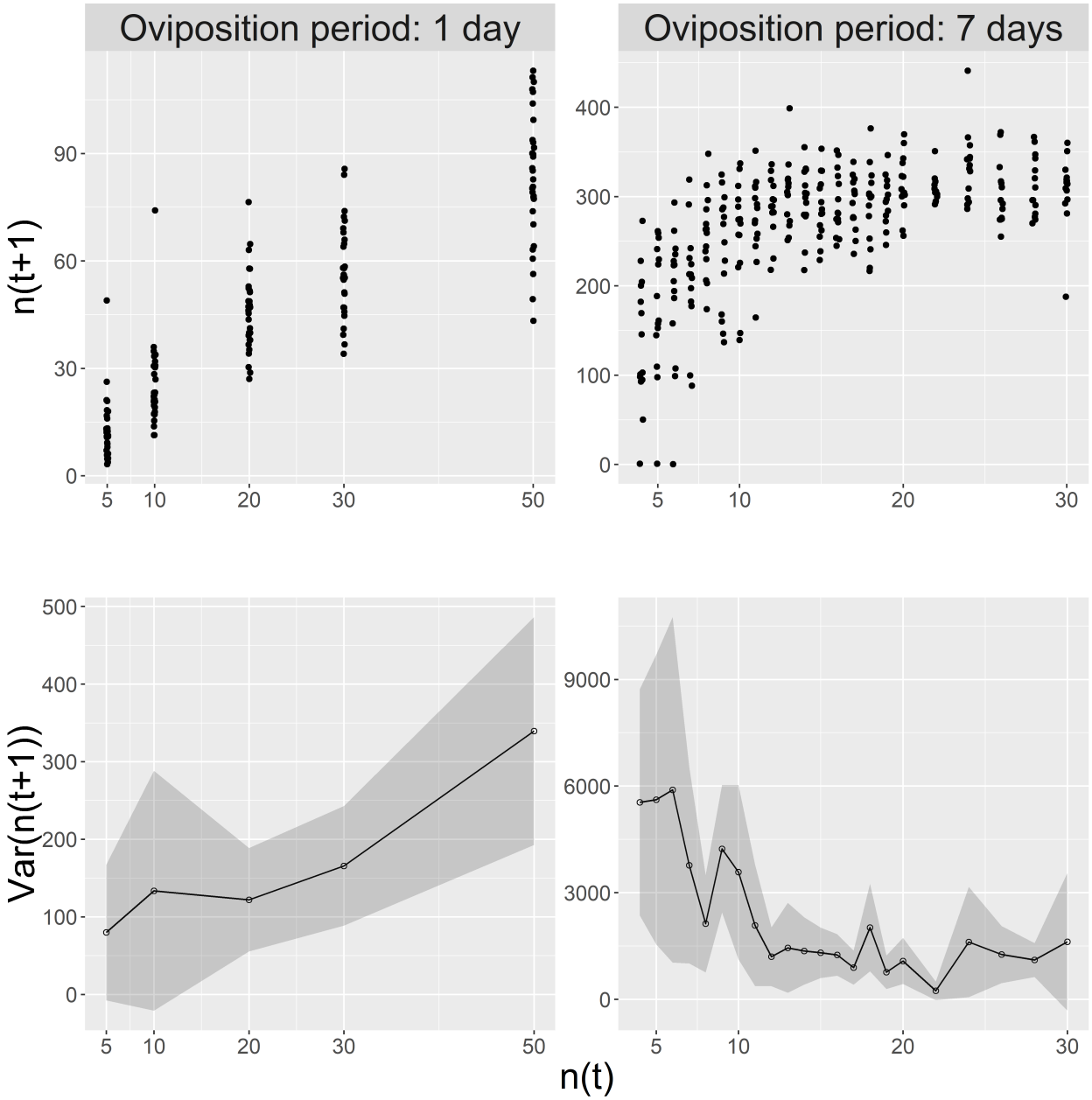

Figure 3.7: The variance of $n(t+1)$ increases with $n(t)$ when the oviposition period is short, but decreases with $n(t)$ when the oviposition period is long; data from Dataset 2. The shaded regions on the bottom panels represent the sample variance $\pm$ 2 standard errors. The formula for the standard error of the variance is given by Rao (1973, p. 438). An outlier with $n(t) = 5$ and $n(t+1) > 125$ has been excluded from the left panels (the 1-day oviposition period data), since this datum almost certainly represents experimental error.

Undeniably, demographic stochasticity plays a large role in our beetle microcosms. In a sub-model with

only demographic heterogeneity (sub-model 7, Appendix 3.1.G), the variance of $n\,(t+1)$ goes to zero for sufficiently large $n\,(t)$. This prediction is obviously contradicted by the empirical time-one population maps (Fig. 3.3 in the main text). In a model with only environmental stochasticity (sub-model 11, Appendix 3.1.G), the variance of $n\,(t+1)$ should increase quadratically with $n\,(t)$ for sufficiently small $s \times n\,(t)$. Again, this pattern does not appear in the data (Fig. 3.7, bottom-left panel).

We selected sub-model 1 as the all-purpose, best-fit sub-model for all datasets. This decision was based on 1) the strong *a priori* evidence for sex ratio stochasticity, 2) the strong graphical evidence for both demographic stochasticity and demographic heterogeneity (of some variety), 3) the evidence (*a priori*, graphical, and Cross Validation) against the appreciable influence of environmental stochasticity, and 4) the Cross Validation results for dataset 2 (which are given more inferential weight for reasons previously discussed).

3.1.E Full stochastic model description

Here we describe the full stochastic model, i.e., sub-model 1 (with sex-ratio stochasticity and demographic stochasticity) with the mechanism of population crashes and demographic stochasticity in egg-to-adult survival. Because Hamiltonian Monte Carlo is a gradient-based method, all of the model's parameters (including the number of females and eggs) are treated as continuous variables. Therefore, we often utilize the normal approximation to the binomial distribution: a binomial distribution with n trials and success probability p is approximated by a zero-truncated normal (hereby denoted $Normal_{trunc}$) with mean np and variance $np(1-p)$. model parameters are described in Appendix, Table S3.1.

The full stochastic model has several notable features:

1. Sex-ratio stochasticity. Even though flour beetles have a $50:50$ sex ratio in large populations (Howe, 1956), the sex ratio may fluctuate substantially in small populations. The number of females is binomial distributed with success probability $= 1/2$. We used the normal approximation, such that the number of females given x adults is drawn from a zero-truncated normal distribution with mean $x/2$ and variance $x/4$.

2. Demographic stochasticity in oviposition. In each moment, each female has an oviposition rate that is drawn from a normal distribution with mean α and variance ${\eta_\alpha}^2$. Because each female's oviposition rate is drawn independently, the sum of oviposition rates fluctuates with variance $f\ {\eta_\alpha}^2$ in a population with f females. For notational simplicity, the explicit generation-time dependence (e.g., $f(t)$) has been suppressed. The differential equation for egg-production in the main text (see Methods) becomes the stochastic differential equation (SDE),

$$dz(h) = f\left(\alpha - \beta\ z\left(h\right)\right) dh + \sqrt{f}\ \eta_\alpha dW_h, \tag{3.6}$$

where h is the number of days since the beginning of the oviposition period, β is the effective cannibalism rate, and dW_h is an increment of the Weiner Process. Recall that $\beta = \beta(t)\ = \beta_0 - \beta_1 n(t)$. The above SDE is associated with a Fokker-Planck equation for the probability of egg density $p(z)$. The Fokker-Planck equation is

$$\frac{dp\left(z,h\right)}{dh} = -\frac{\partial}{\partial z}\left[f\ \ (\alpha - \beta\ z)\ \ p\left(z,h\right)\right]\ \frac{1}{2}\frac{\partial^2}{\partial z^2}\left[f\ \eta_\alpha^2\ p\left(z,h\right)\right], \quad \textit{boundary conditions}:\ p(z,0) = \delta\left(z\right), \tag{3.7}$$

where $\delta\left(z\right)$ is the Dirac-delta function. This partial differential equation can be solved using the Fourier method. After an oviposition period of s days, the egg 'density' z is distributed normally with mean $\frac{\alpha\left(1-e^{-f\beta s}\right)}{\beta}$ and standard deviation $\sqrt{\frac{\eta_\alpha^2\left(1-e^{-2f\beta s}\right)}{2\beta}}$.

3. Varying thresholds for die-offs. If the die-off threshold (denoted z^*) was the same for every replicate population, the minimum z^* would be determined by the largest $n(t+1)$ across replicates. Put another way, a fixed z^* would not allow for an anomalously large number of eggs to survive to adulthood. Instead, we let each replicate have its own threshold, drawn from a zero-truncated normal distribution with mean μ_{z^*} and standard deviation σ_{z^*}.

   Demographic stochasticity in egg-to-adult survival. We found that for replicates with population crashes, $Var\left(n\left(t+1\right)\right)$ was larger than expected under binomial survival. This may be a consequence of multiple rounds of survival (for different life-stages) or microenvironments within a single replicate. Regardless, we accounted for this excess noise with the parameter, ϵ_H, the scale of fluctuations in the egg-to-adult survival probability when there are High numbers of eggs. Because egg survival depends on both the replicate-specific adults $n(t)$ and the replicate-specific die-off threshold z^*, egg-to-adult survival (simply denoted θ) is also a replicate-specific parameter.

3.1.F Full stochastic model, fitting details

We use the variables x_i and y_i to denote the $n(t)$ and $n(t+1)$ of the i-th replicate, respectively. The subscript i also indexes replicate-specific parameters and oviposition period. Again, we suppress the notation for dependence on the generation number t. A table of model variables is provided in the Appendix, Table S2.

The model is technically a doubly-nested hierarchical model, with parameters θ_i and ϵ_i (for each replicate

i); hyperparameters z_i and z_i^*; and hyper-hyperparameters $\alpha, \eta_\alpha, \beta_0, \beta_1, k, \sigma_{z^*}, \gamma_0, \gamma_1, \theta_L,\ \epsilon_H,\ f_i$. There are many parameters for the numbers of females, f_i (one for each replicate), but these are highly constrained by Mendel's law of segregation: females are binomial distributed with x_i trials and success probability 1/2. The variables $\mu_{Z_i}, \sigma_{Z_i}, \mu_{z_i{}^*}, \beta_i$, and ϵ_L are intermediate quantities (i.e., they can be derived from parameters).

(Approximate) Binomial sampling of females

$$f_i \sim Normal_{trunc}(mean = x_i/2, sd = \sqrt{x_i}/2) \tag{3.8}$$

Process model for egg production

$$\mu_{Z_i} = \frac{\alpha\left(1 - e^{-f_i\beta_i s_i}\right)}{\beta_i} \tag{3.9}$$

$$\sigma_{Z_i} = \sqrt{\frac{\eta_\alpha^2\left(1 - e^{-2f_i\beta_i s_i}\right)}{2\beta_i}} \tag{3.10}$$

$$\beta_i = \beta_0 + \beta_1 x_i \tag{3.11}$$

(latent) data model for egg production

$$z_i \sim Normal_{trunc}\left(mean = \mu_{Z_i}, sd = \sigma_{Z_i}\right) \tag{3.12}$$

Varying thresholds for larval die-offs

$$z_i^* \sim Normal_{trunc}\left(mean = \mu_{z_i{}^*}, sd = \sigma_{z^*}\right) \tag{3.13}$$

$$\mu_{z_i{}^*} = \gamma_0 + \gamma_1 x_i \tag{3.14}$$

Per-capita larval survival

$$\theta_i = \theta_L - \frac{\theta_L}{1 + e^{-k\left(z_i - z_i^*\right)}} \tag{3.15}$$

$$\epsilon_L = \sqrt{\theta_L\left(1 - \theta_L\right)} \tag{3.16}$$

$$\epsilon_i = \epsilon_L - \frac{\epsilon_L - \epsilon_H}{1 + e^{-k\left(z_i - z_i^*\right)}} \tag{3.17}$$

Data model for beetle abundance at time t+1

$$y_i \sim Normal_{trunc}(mean = \theta_i z_i, sd = \epsilon_i\sqrt{z_i}\ ) \tag{3.18}$$

3.1.G Sub-model likelihood functions

For each sub-model, we describe the probability of attaining z eggs given f female beetles. Here we suppress the notation for dependence on the generation number and the replicate number. Since the egg-to-adult survival probability is treated as a constant 0.91 in the sub-models, the probability of attaining y adults given f females is $\text{prob}\,(y|f) = \text{prob}\,(z\ /0.91|f)$. The probability of y adults given x initial adults can be computed by marginalizing over the latent number of females: $\text{prob}\,(y|f) = \sum_{f=0}^{x} \text{prob}\,(z/0.91|f)\,\text{prob}\,(f|x)$.

For some of the models, the true probability distribution of z given f is not a gaussian, but we will nevertheless model the data as if it came from the gaussian. This is done for the pragmatic reason that the PDF is often difficult or impossible to compute analytically, but the mean and variance of the PDF are easy to compute using the property of Ito Isometry. Many distributions can approximate the normal distribution (e.g., the gamma distribution as the shape parameter becomes large), and our data (for non-crash replicates) appears to be approximately normally distributed for nearly every $n(t)$. In models without sex-ratio stochasticity, the number of females is defined as $f = x/2$.

1. **Model with only demographic stochasticity (in oviposition rates) and sex-ratio stochasticity.** This model is described in Appendix 3.1.E, point 2. Each female has an independently fluctuating oviposition rate with temporal mean α. The likelihood function is the density of a normal distribution with mean $\alpha\left(1-e^{-f\beta s}\right)/\beta$ and variance ${\eta_\alpha}^2\left(1-e^{-2f\beta s}\right)/(2\beta)$. The likelihood is

$$\text{prob}\,(z|f,\alpha,\beta,\eta_\alpha) = \frac{\exp\left(-\frac{\beta e^{2\beta f s}\left(z-\frac{\alpha-\alpha e^{\beta(-f)s}}{\beta}\right)^2}{\eta_\alpha^2(e^{2\beta f s}-1)}\right)}{\sqrt{\pi}\sqrt{\frac{\eta_\alpha^2 e^{-2\beta f s}(e^{2\beta f s}-1)}{\beta}}} \tag{3.19}$$

2. **Model with demographic stochasticity (in oviposition rates), sex-ratio stochasticity, and demographic heterogeneity (in oviposition rates)**. Each female's time-averaged oviposition rate is an independently and identically distributed random variable with mean μ_α and variance σ_α^2 such that the population-average oviposition rate α is drawn from a normal distribution with mean μ_α and variance σ_α^2/f. To obtain the PDF for the number of eggs, we marginalize over the population average oviposition rate,

$$\int_{-\infty}^{\infty} \text{prob}\,(z|f,\alpha,\beta,\eta_\alpha)\,\text{prob}\,(\alpha|\mu_\alpha,\sigma_\alpha)\,d\alpha = \frac{\beta\exp\left(\beta f s - \frac{f\left(\mu_\alpha+e^{\beta f s}(\beta z-\mu_\alpha)\right)2}{(e^{\beta f s}-1)(\beta f\eta_\alpha^2(e^{\beta f s}+1)+2\sigma_\alpha^2(e^{\beta f s}-1))}\right)}{\sqrt{\frac{\pi(e^{\beta f s}-1)(\beta f\eta_\alpha^2(e^{\beta f s}+1)+2\sigma_\alpha^2(e^{\beta f s}-1))}{f}}} \tag{3.20}$$

The integral of from $-\infty$ to ∞ clearly produces an approximation, since oviposition rates cannot be negative. The resulting PDF is a gaussian with mean $\mu_\alpha \left(1 - e^{-f\beta s}\right)/\beta$ and variance

$$\frac{e^{-2\beta fs}\left(e^{\beta fs}-1\right)\left(\beta f\eta_\alpha^2\left(e^{\beta fs}+1\right)+2\sigma_\alpha^2\left(e^{\beta fs}-1\right)\right)}{2\beta^2 f} \tag{3.21}$$

3. **Model with demographic stochasticity (in oviposition rates) with temporal autocorrelation, and sex-ratio stochasticity.** Here, females' oviposition rates are temporally autocorrelated. This model can be thought of as providing a sliding scale between demographic stochasticity and demographic heterogeneity. When the autocorrelation time is short, females' oviposition rates fluctuate quickly as in the case of demographic stochasticity. When the autocorrelation time is very long, the females' oviposition rates are effectively constant over the course of the oviposition period (i.e., demographic heterogeneity).

   Female number i has an oviposition rate $\mu_\alpha + \zeta_i$, where the deviation from the mean oviposition rates μ_α evolves in accordance with an Ornstein Uhlenbeck process:

$$d\zeta_i = \frac{1}{\rho}\zeta_i dt + \eta_\alpha dW_i, \tag{3.22}$$

   where ρ is the characteristic timescale of autocorrelation, and dW_i is an increment of the Weiner Process.

   The egg dynamics are given by the differential equation

$$\frac{dZ}{dt} = f\left(\mu_\alpha - \beta Z\right) + f\overline{\zeta}, \tag{3.23}$$

   where $\overline{\zeta} = \frac{1}{f}\sum_{i=1}^{f}\zeta_i$ is the population average deviation. With the assumption that perturbations to females' oviposition rates are independent, $\overline{\zeta}$ evolves according to the stochastic differential equation,

$$d\overline{\zeta} = \frac{1}{\rho}\overline{\zeta}dt + \frac{\eta_\alpha}{\sqrt{f}}dW. \tag{3.24}$$

   We may now compute the mean and variance of Z using Ito Isometry. The mean is

$$\alpha\left(1 - e^{-f\beta s}\right)/\beta, \tag{3.25}$$

   and the variance is

$$-\frac{\rho^2\eta_\alpha^2 e^{-2s\left(\beta f+\frac{1}{\rho}\right)}\left(\left(\beta f\rho-1\right)^2\left(-e^{2s\left(\beta f+\frac{1}{\rho}\right)}\right)-4\beta f\rho e^{s\left(\beta f+\frac{1}{\rho}\right)}+e^{\frac{2s}{\rho}}\left(\beta f\rho+1\right)+\beta f\rho\left(\beta f\rho+1\right)e^{2\beta fs}\right)}{2\beta\left(\beta f\rho-1\right)^2\left(\beta f\rho+1\right)} \tag{3.26}$$

4. **Model with demographic stochasticity (in both oviposition and cannibalism rates), and sex-ratio stochasticity.** In this model, cannibalism rates fluctuate over time. Individuals' cannibalism rates are drawn from a normal distribution with mean $\mu_\beta = \beta_0 + \beta_1 n_t$ and variance ${\eta_\beta}^2$. Fluctuations in cannibalism rates are independent of fluctuations in oviposition rates, leading to the stochastic differential equation

$$dZ = f\left(\mu_\alpha - \beta Z\right)dt + \sqrt{f}\eta_\alpha dW_1 + \sqrt{f}Z\eta_\beta dW_2. \tag{3.27}$$

The mean is $\alpha\left(1-e^{-f\beta s}\right)/\beta$ and the variance is

$$\frac{e^{-2\beta fs}\left(\alpha^2\left(2\beta^2\left(e^{fs\eta_\beta^2}-1\right)+\eta_\beta^4\left(-\left(e^{\beta fs}-1\right)^2\right)+\beta\eta_\beta^2\left(-4e^{\beta fs}+e^{2\beta fs}+3\right)\right)+\beta^2\eta_\alpha^2\left(\beta-\eta_\beta^2\right)\left(e^{2\beta fs}-e^{fs\eta_\beta^2}\right)\right)}{\beta^2\left(2\beta^2+\eta_\beta^4-3\beta\eta_\beta^2\right)} \tag{3.28}$$

5. **Model with demographic stochasticity in oviposition rates and demographic heterogeneity and oviposition rates.** This model is the same as model 2 above, except that there is no sex-ratio stochasticity. The number of females is simply $f = n_t/2$.

6. **Model with only demographic stochasticity.** Same as model 1, but without sex-ratio stochasticity.

7. **Model with only demographic heterogeneity.** The population-average oviposition rate α is drawn from a normal distribution with mean μ_α and variance σ_α^2/F. Because there is no demographic stochasticity, conditioned on α, the number of eggs is always $\alpha\left(1-e^{-f\beta s}\right)/\beta$. Using the standard transformation of variables formula to transform the PDF of α to the PDF of Z, we get

$$\text{prob}\left(z|f,\mu_\alpha,\beta,\sigma_\alpha\right) = \frac{\beta\sqrt{f}\exp\left(\beta fs - \frac{f\left(\mu_\alpha - \frac{\beta z e^{\beta fs}}{e^{\beta fs}-1}\right)^2}{2\sigma_\alpha^2}\right)}{\sqrt{2\pi}\sigma_\alpha\left(e^{\beta fs}-1\right)} \tag{3.29}$$

which is a normal distribution with mean $\alpha\left(1-e^{-f\beta s}\right)/\beta$ and variance $\frac{\sigma_\alpha^2 e^{-2\beta fs}\left(e^{\beta fs}-1\right)^2}{\beta^2 f}$.

8. **Model with demographic heterogeneity and sex-ratio stochasticity.** Same as model 7, but with sex-ratio stochasticity.

9. **Model with demographic stochasticity, sex-ratio stochasticity, and environmental stochasticity.** Each female in a replicate population has the same time-averaged oviposition rate, α. However, α is different from replicate-to-replicate, because α is drawn from a normal distribution with mean μ_α and variance γ_α^2. To obtain the PDF for the number of eggs, we marginalize over α:

$$\int_{-\infty}^{\infty} \text{prob}\left(z|f,\alpha,\beta,\eta_\alpha\right)\ \text{prob}\left(\alpha|\mu_\alpha,\gamma_\alpha\right) d\alpha = -\frac{\beta \exp\left(\beta f s - \frac{\left(\mu_\alpha + e^{\beta f s}(\beta z - \mu_\alpha)\right)2}{(e^{\beta f s}-1)(2\gamma_\alpha^2(e^{\beta f s}-1)+\beta\eta_\alpha^2(e^{\beta f s}+1))}\right)}{\sqrt{\pi\left(e^{\beta f s}-1\right)\left(2\gamma_\alpha^2\left(e^{\beta f s}-1\right)+\beta\eta_\alpha^2\left(e^{\beta f s}+1\right)\right)}}. \tag{3.30}$$

The resulting PDF is a gaussian with mean $\mu_\alpha\left(1-e^{-f\beta s}\right)/\beta$ and variance

$$\frac{e^{-2\beta f s}\left(e^{\beta f s}-1\right)\left(2\gamma_\alpha^2\left(e^{\beta f s}-1\right)+\beta\eta_\alpha^2\left(e^{\beta f s}+1\right)\right)}{2\beta^2} \tag{3.31}$$

10. **Model with sex-ratio stochasticity and environmental stochasticity.** The population-specific oviposition rate α (shared across all females in a replicate population) is drawn from a normal distribution with mean μ_α and variance γ_α^2. Conditioned on α, the number of eggs is always $\alpha\left(1-e^{-f\beta s}\right)/\beta$. Using the standard transformation of variables formula to transform the PDF of α to the PDF of Z, we get

$$\text{prob}\left(z|f,\mu_\alpha,\beta,\gamma_\alpha\right) = \frac{\beta \exp\left(\beta f s - \frac{\left(\mu_\alpha - \frac{\beta z e^{\beta f s}}{e^{\beta f s}-1}\right)2}{2\gamma_\alpha^2}\right)}{\sqrt{2\pi}\gamma_\alpha\left(e^{\beta f s}-1\right)} \tag{3.32}$$

which is a normal distribution with mean $\alpha\left(1-e^{-f\beta s}\right)/\beta$ and variance

$$\frac{e^{-2\beta f s}\left(e^{\beta f s}-1\right)\left(2\gamma_\alpha^2\left(e^{\beta f s}-1\right)\right)}{2\beta^2} \tag{3.33}$$

11. **Model with environmental stochasticity.** Same as model 10, but with no sex-ratio stochasticity.

3.1.H Heavy tails

Here we examine the per capita growth rates (i.e., $r = \log\left(n\left(t+1\right)/n\left(t\right)\right)$) of Dataset 2 in the range $n(t) \in [12,\ 400]$. Visually, the distribution of per capita growth rates appears has a heavy left tail (Fig. 3.8).

There is no universal definition of a heavy-tailed distribution, but we will examine our data in light of two common definitions of heavy-tailed distributions: sub-exponential tail decay and infinite variance.

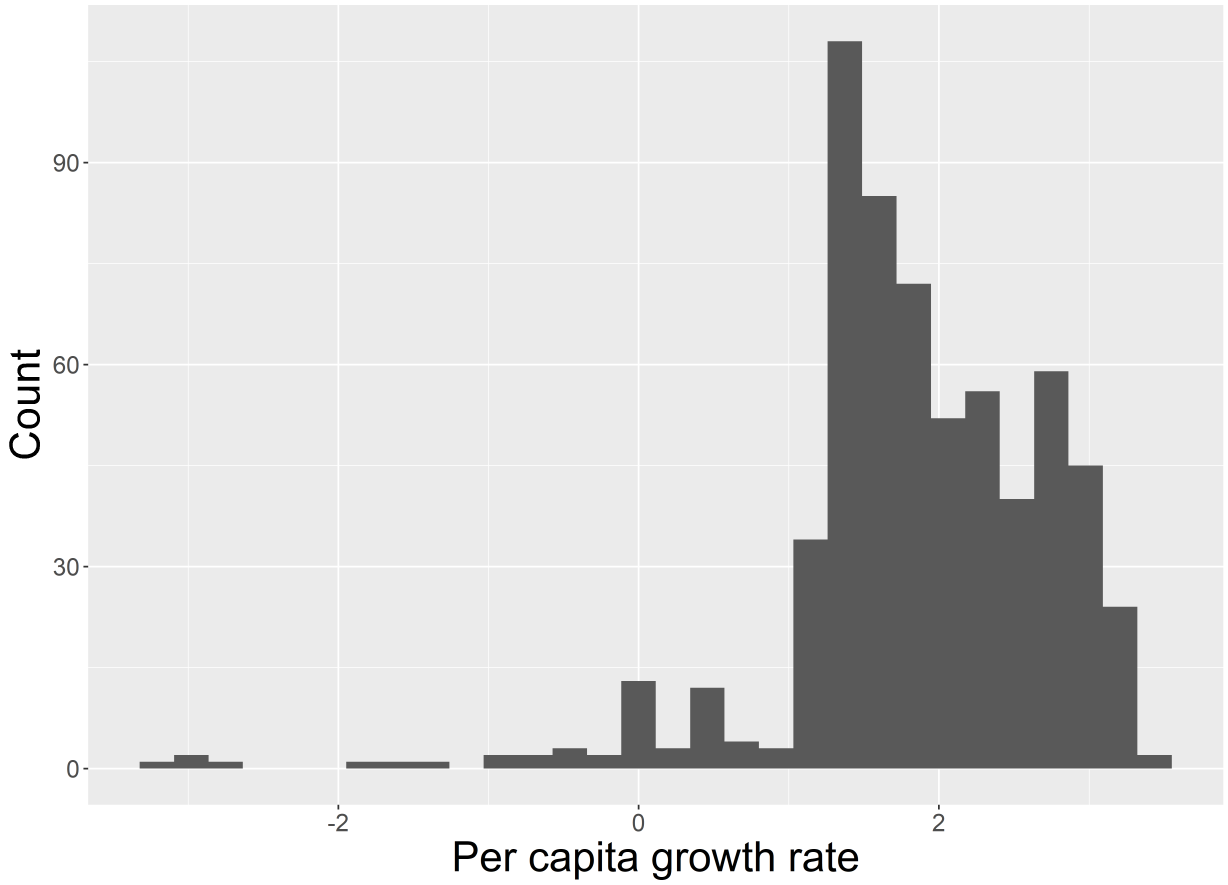

Figure 3.8: The histogram of per capita growth rates displays substantial right skew, with a putatively heavy left tail. The data is from Dataset 2, subsetted so that oviposition period = 7 days, and $n\,(t) \in [12, 400]$. Visually, the distribution of $n(t+1)$ is very similar over this range of $n(t)$, thus justifying the aggregation of data.

The one-sided exponential distribution with rate parameter λ has the probability density

$$f\,(x;\lambda) = \lambda e^{-\lambda x} \tag{3.34}$$

for $x \geq 0$. The tail probability is equivalent to the inverse cumulative distribution function,

$$\int_x^\infty f\,(s;\lambda)\,ds = e^{-\lambda x}, \tag{3.35}$$

the logarithm of which is simply $-\lambda x$.

We can distinguish heavy-tailed and thin-tailed distributions from each other by plotting the logarithm of the inverse empirical CDF (inverse eCDF), on the y-axis and the absolute deviation from the mean on the x-axis. Thin-tailed distributions should display a linear or concave-down relationship. Heavy-tailed distributions should display a concave-up relationship. Figure 3.9 shows that the right tail of the distribution of r is concave-down, whereas the left tail (which includes population crashes) is concave-up.

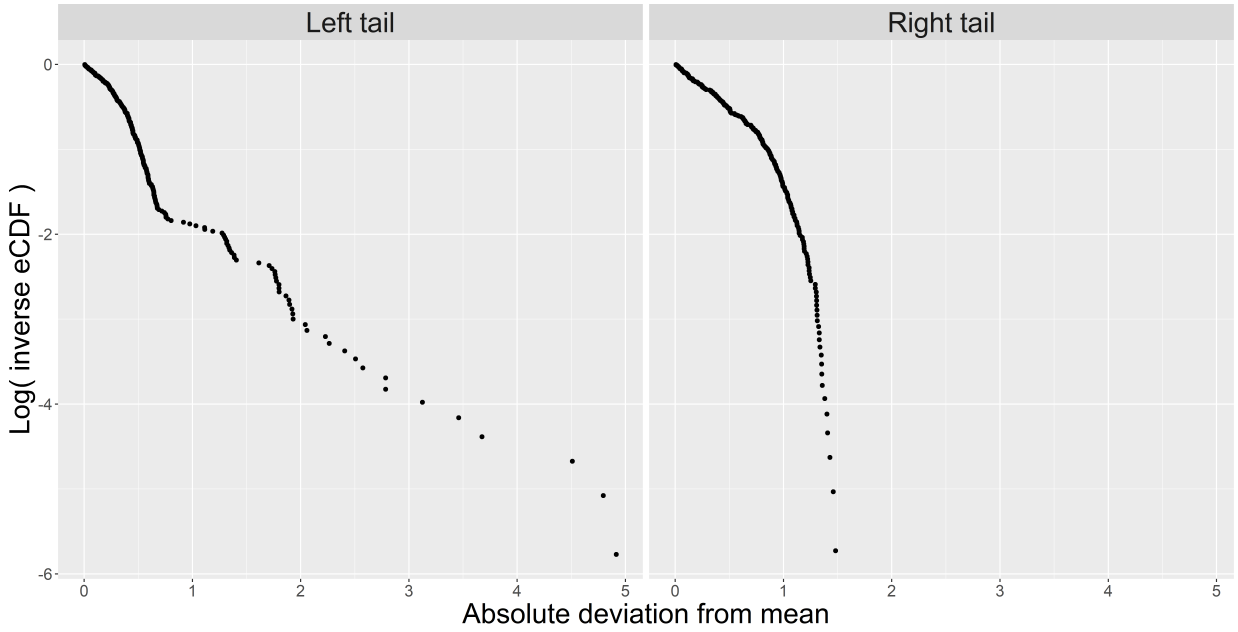

Figure 3.9: The logarithm of the inverse empirical cumulative distribution function, as a function of the Absolute value of $n(t+1) - \overline{n(t+1)}$. A concave-up relationship indicates sub-exponential tail decay, i.e., a heavy tail. The data is from Dataset 2, subsetted so that oviposition period = 7 days, and $n(t) \in [12, 400]$.

Another definition of a heavy-tailed distribution is any distribution with infinite variance. A power law distribution has the probability density

$$f(x;\omega) = cx^{-\omega}, \tag{3.36}$$

for sufficiently large x (the symbol c is a normalizing constant). The contribution of a tail to the variance is

$$\int_x^{\infty} (s-\mu)^2 f(s;\omega)\, ds \to \frac{cx^{3-\omega}}{\omega - 3}, \quad as\ x\ \to \infty. \tag{3.37}$$

The contribution of the tail to the variance grows when $\omega \leq 3$, so the variance is finite only when $\omega > 3$. The inverse CDF goes to $\frac{c\ x^{1-\omega}}{-1+\omega}$ as $x\ \to \infty$. In turn, the logarithm of the inverse CDF goes to

$$log\left(\frac{c}{\omega - 1}\right) - (1 - \omega)\, log(x), \quad as\ x\ \to \infty. \tag{3.38}$$

From this equation, we can see that the logarithm of the inverse CDF is a linearly decreasing function of $\log(x)$. When the distribution has infinite variance, the linear relationship has slope ≥ -2. When the distribution has finite variance, the linear relationship has slope < -2.

Figure 3.10 shows the tail data with overlaid lines of slope $= -2$. The right tail shows faster than cubic decay, the hallmark of finite variance. The left tail is irregular, showing approximately cubic decay *en masse*, but possibly settling on faster than cubic decay in the far reaches of the tail. The distribution of r is borderline infinite-variance. Technically, the variance is automatically infinite since extinction events correspond to $r = log(0) = -\infty$, but we have omitted extinction events from our analysis here.

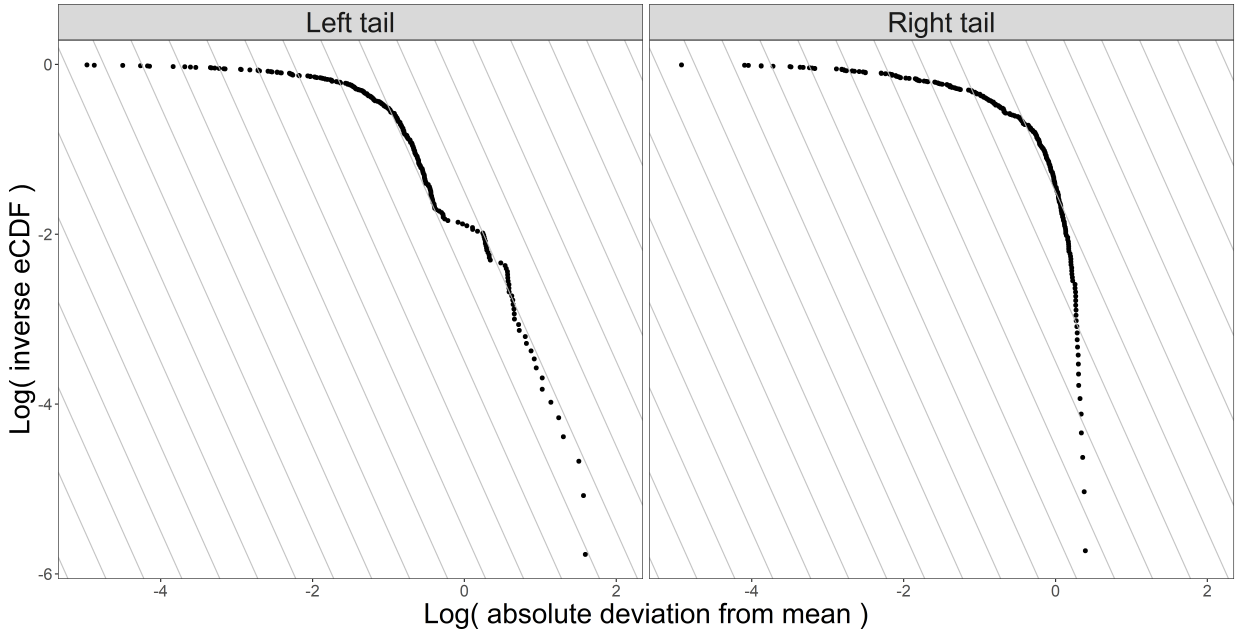

Figure 3.10: The logarithm of the inverse empirical cumulative distribution function, as a function of $log\left(\left|n\,(t+1) - \overline{n\,(t+1)}\right|\right)$. A tail with slope ≥ -2 indicates that the distribution has infinite variance. The data is from Dataset 2, subsetted so that oviposition period $= 7$ days, and $n\,(t) \in [12, 400]$.

Data availability statement

Code is available on GitHub, https://github.com/ejohnson6767/castaneum_crash.

Table 3.1: Symbols for data and model parameters.

	Description	Units
Inputs/ Outputs		
x_i	final abundance, $n(t)$, of the ith replicate	beetles
y_i	final abundance, $n(t+1)$, of the ith replicate	beetles
s_i	oviposition period; how long adults are allowed to oviposit in fresh media	days
Parameters		
f_i	abundance of females	beetles
z	number of eggs	eggs
α	mean average oviposition rate, i.e., the oviposition rate, averaged across time and all females	eggs per female per day
β_i	mean cannibalism rate, i.e., the cannibalism rate averaged across time and all females in replicate i	eggs per female per egg per day
β_0	the cannibalism rate when there are zero adult beetles	eggs per female per egg per day
β_1	the number of units by which cannibalism rate changes for each additional adult.	eggs per female per egg per day per n_t
η_α	scale of demographic stochasticity in oviposition rates; the standard deviation of the distribution from which oviposition rates are drawn at each point in time	eggs per female per day
z_i^*	replicate-specific die-off threshold. When approximately z_i^* eggs are present, the egg-to-adult survival is halfway between $\theta_L = 0.91$ and θ_H	eggs
$\mu_{z_i{}^*}$	mean of the truncated normal distribution from which replicate-specific die-off thresholds are drawn	eggs
σ_{z^*}	standard deviation of the truncated normal distribution from which replicate-specific die-off thresholds are drawn	eggs
θ_L	egg-to-adult survival probability when there are few eggs; value is fixed at 0.91 based on a previous experiment	dimensionless
θ_i	The mean egg-to-adult survival probability of the ith replicate; given z eggs, the mean number of adults is $\theta_i z$	dimensionless
ϵ_L	The scale of fluctuations in the egg-to-adult survival probability when there are a Low number of eggs; defined as $\sqrt{\theta_L\,(1-\theta_L)}$.	dimensionless
ϵ_H	The scale of fluctuations in the egg-to-adult survival probability when there are a High number of eggs; analogous to the standard deviation of a Bernoulli random variable.	dimensionless
ϵ_i	The standard deviation in the egg-to-adult survival probability of the ith replicate; given z eggs, the standard deviation of the number of adults is $\epsilon_i\sqrt{z}$	dimensionless
γ_0	the mean die-off threshold when there are zero adult beetles	dimensionless
γ_1	the number of units by which the mean die-off threshold decreases for each additional adult.	per adult

Table 3.2: Sub-model comparisons for the non-crash subset of Dataset 1 (# replicates = 237). The acronym "*elpd*" stands for expected log predictive density. $\widehat{elpd}$ is an estimate of elpd, computed using Pareto Smoothed Importance Sampling, Leave-One-Out Cross Validation (PSIS LOO) as implemented by the *loo* package (Vehtari et al., 2017). $\Delta\widehat{elpd}$ is the difference with respect to the best-fit model. $SE\left(\Delta\widehat{elpd}\right)$ is the estimate of the standard error of $\Delta\widehat{elpd}$. The effective number of parameters is calculated as the difference between $\widehat{elpd}$ and the non-cross-validated log predictive density; this quantity is analogous to the bias correction term in AIC. Sub-models 4 & 10 could not be effectively fit, hence the NAs; diagnostics indicated high Monte Carlo error and that the sampler did not converge.

Description	$\Delta\widehat{elpd}$	$SE\left(\Delta elpd\right)$	# Effective parameters
demographic stochasticity (oviposition)	0.00	0.00	6.97
demographic stochasticity (oviposition), and demographic heterogeneity (oviposition)	-0.15	0.38	6.93
demographic stochasticity (oviposition), sex-ratio stochasticity	-9.55	1.32	7.30
demographic stochasticity (oviposition), sex-ratio stochasticity, and demographic heterogeneity (oviposition)	-10.69	1.52	7.56
demographic stochasticity (oviposition), sex-ratio stochasticity, and environmental stochasticity (oviposition)	-12.47	16.37	25.13
environmental stochasticity (oviposition), sex-ratio stochasticity	-13.02	18.39	1.71
demographic stochasticity (oviposition) with temporal autocorrelation, sex-ratio stochasticity	-18.17	2.61	7.62
environmental stochasticity (oviposition)	-30.21	19.43	4.11
demographic heterogeneity (oviposition)	-99.94	10.33	10.98
demographic heterogeneity (oviposition), sex-ratio stochasticity	-104.57	10.25	10.88
demographic stochasticity (oviposition and cannibalism), sex-ratio stochasticity	-320.27	171.91	337.24

Table 3.3: Sub-model comparisons for the non-crash subset of Dataset 2 (# replicates = 1548). The acronym "*elpd*" stands for expected log predictive density. $\widehat{elpd}$ is an estimate of elpd, computed using Pareto Smoothed Importance Sampling, Leave-One-Out Cross Validation (PSIS LOO) as implemented by the *loo* package (Vehtari et al., 2017). $\Delta\widehat{elpd}$ is the difference with respect to the best-fit model. $SE\left(\Delta\widehat{elpd}\right)$ is the estimate of the standard error of $\Delta\widehat{elpd}$. The effective number of parameters is calculated as the difference between $\widehat{elpd}$ and the non-cross-validated log predictive density; this quantity is analogous to the bias correction term in AIC. Sub-model 10 could not be effectively fit, hence the NAs; diagnostics indicated high Monte Carlo error and that the sampler did not converge.

Description	$\Delta\widehat{elpd}$	$SE\left(\Delta elpd\right)$	# Effective parameters
demographic stochasticity (oviposition), and demographic heterogeneity (oviposition)	0.00	0.00	48.18
demographic stochasticity (oviposition), sex-ratio stochasticity	-4.21	5.33	5.09
demographic stochasticity (oviposition and cannibalism), sex-ratio stochasticity	-4.68	5.26	5.24
demographic stochasticity (oviposition)	-12.89	3.05	4.86
demographic stochasticity (oviposition), sex-ratio stochasticity, and environmental stochasticity (oviposition)	-12.95	5.03	6.46
demographic stochasticity (oviposition), sex-ratio stochasticity, and demographic heterogeneity (oviposition)	-24.60	7.33	7.28
demographic stochasticity (oviposition) with temporal autocorrelation, sex-ratio stochasticity	-50.51	9.42	6.69
environmental stochasticity (oviposition), sex-ratio stochasticity	-119.93	19.56	2.26
environmental stochasticity (oviposition)	-297.65	20.74	5.41
demographic heterogeneity (oviposition)	-609.91	33.47	13.02
demographic heterogeneity (oviposition), sex-ratio stochasticity	-630.64	33.22	13.15

Table 3.4: Sub-model comparisons for the non-crash subset of Dataset 3 (# replicates = 107). The acronym "*elpd*" stands for expected log predictive density. $\widehat{elpd}$ is an estimate of elpd, computed using Pareto Smoothed Importance Sampling, Leave-One-Out Cross Validation (PSIS LOO) as implemented by the *loo* package (Vehtari et al., 2017). $\Delta\widehat{elpd}$ is the difference with respect to the best-fit model. $SE\left(\Delta\widehat{elpd}\right)$ is the estimate of the standard error of $\Delta\widehat{elpd}$. The effective number of parameters is calculated as the difference between $\widehat{elpd}$ and the non-cross-validated log predictive density; this quantity is analogous to the bias correction term in AIC. Sub-model 10 could not be effectively fit, hence the NAs; diagnostics indicated high Monte Carlo error and that the sampler did not converge.

Description	$\Delta\widehat{elpd}$	$SE\left(\Delta elpd\right)$	# Effective parameters
demographic heterogeneity (oviposition), sex-ratio stochasticity	0.00	0.00	4.24
demographic stochasticity (oviposition) with temporal autocorrelation, sex-ratio stochasticity	-0.21	1.36	4.36
demographic stochasticity (oviposition), sex-ratio stochasticity	-0.24	2.14	4.17
demographic stochasticity (oviposition and cannibalism), sex-ratio stochasticity	-0.81	2.52	4.57
demographic heterogeneity (oviposition)	-3.42	4.16	5.86
demographic stochasticity (oviposition), and demographic heterogeneity (oviposition)	-3.51	3.56	28.39
demographic stochasticity (oviposition), sex-ratio stochasticity, and environmental stochasticity (oviposition)	-4.29	4.03	7.40
demographic stochasticity (oviposition)	-6.74	6.96	6.30
environmental stochasticity (oviposition), sex-ratio stochasticity	-17.12	6.02	1.54
demographic stochasticity (oviposition), sex-ratio stochasticity, and demographic heterogeneity (oviposition)	-23.51	8.32	14.78
environmental stochasticity (oviposition)	-38.76	10.08	9.99

References

Allen, A. P., Li, B. L., & Charnov, E. L. (2001). Population fluctuations, power laws and mixtures of lognormal distributions. *Ecology Letters*, *4*(1), 1–3.

Anderson, S. C., Branch, T. A., Cooper, A. B., & Dulvy, N. K. (2017). Black-swan events in animal populations. *Proceedings of the National Academy of Sciences*, *114*(12), 3252–3257.

Anderson, S. C. (2015). *Variance and extreme events in population ecology* (Doctoral dissertation). Simon Fraser University.

Andreev, A. V. (1991). Winter adaptations in the willow ptarmigan. *Arctic*, *44*(2), 106–114.

Batt, R. D., Carpenter, S. R., & Ives, A. R. (2017). Extreme events in lake ecosystem time series. *Limnology and Oceanography Letters*, *2*(3), 63–69.

Benincà, E., Huisman, J., Heerkloss, R., Jöhnk, K. D., Branco, P., Van Nes, E. H., Scheffer, M., & Ellner, S. P. (2008). Chaos in a long-term experiment with a plankton community. *Nature*, *451*(7180), 822–825.

Boyce, J. M. (1946). The influence of fecundity and egg mortality on the population growth of tribolium confusum duval. *Ecology*, *27*(4), 290–302.

Bullock, M., Legault, G., & Melbourne, B. A. (2020). Interspecific Chemical Competition Between Tribolium castaneum and Tribolium confusum (Coleoptera: Tenebrionidae) Reduces Fecundity and Hastens Development Time. *Annals of the Entomological Society of America*, *113*(3), 216–222.

Chapman, R. N. (1928). The quantitative analysis of environmental factors. *Ecology*, *9*(2), 111–122.

Chapman, R. N. (1933). The causes of fluctuations of populations of insects. *Hawaiian Entomological Society*, *8*(2).

Costantino, R. F., Desharnais, R., Cushing, J. M., & Dennis, B. (1997). Chaotic dynamics in an insect population. *Science*, *275*(5298), 389–391.

Craig, D. M. (1986). Stimuli governing intraspecific egg predation in the flour beetles, Tribolium confusum and T. castaneum. *Researches on Population Ecology*, *28*(2), 173–183.

de Roos, A. M., & Persson, L. (2013). *Population and community ecology of ontogenetic development*. Princeton University Press.

Drake, J. M. (2005). Density-dependent demographic variation determines extinction rate of experimental populations. *PLoS Biology*, *3*(7), e222.

Drake, J. M. (2014). Tail probabilities of extinction time in a large number of experimental populations. *Ecology*, *95*(5), 1119–1126.

Gelman, A., Carlin, J. B., Stern, H. S., Dunson, D. B., Vehtari, A., & Rubin, D. B. (2014). *Bayesian data analysis* (3rd ed.). Chapman; Hall/CRC.

Gerber, L. R., & Hilborn, R. (2001). Catastrophic events and recovery from low densities in populations of otariids: Implications for disk of extinction. *Mammal Review*, *31*(2), 131–150.

Granéli, E., & Turner, J. T. (2006). *Ecology of harmful algae* (Vol. 189). Springer.

Gurney, W., Blythe, S., & Nisbet, R. (1980). Nicholson's blowflies revisited. *Nature*, *287*(5777), 17–21.

Hagstrum, D. W., & Smittle, B. J. (1980). Age-and sex-specific tunneling rates of adult tribolium castaneunm. *Annals of the Entomological Society of America*, *73*(1), 11–13.

Hassell, M., Latto, J., & May, R. (1989). Seeing the wood for the trees: Detecting density dependence from existing life-table studies. *The Journal of Animal Ecology*, 883–892.

Hastie, T., Tibshirani, R., & Friedman, J. (2009). *The elements of statistical learning: Data mining, inference, and prediction* (2nd ed.). Springer.

Hastings, A., & Powell, T. (1991). Chaos in a three-species food chain. *Ecology*, *72*(3), 896–903.

Hastings, A., & Costantino, R. F. (1991). Oscillations in population numbers: Age-dependent cannibalism. *The Journal of Animal Ecology*, 471–482.

Ho, F. K., & Dawson, P. S. (1966). Egg cannibalism by tribolium larvae. *Ecology*, *47*(2), 318–322.

Howe, R. (1956). The effect of temperature and humidity on the rate of development and mortality of tribolium castaneum (herbst)(coleoptera, tenebrionidae). *Annals of Applied Biology*, *44*(2), 356–368.

Howe, R. (1962). The effects of temperature and humidity on the oviposition rate of tribolium castaneum (hbst.)(coleoptera, tenebrionidae). *Bulletin of entomological Research*, *53*(2), 301–310.

Keitt, T. H., & Stanley, H. E. (1998). Dynamics of north american breeding bird populations. *Nature*, *393*(6682), 257–260.

Knape, J., & de Valpine, P. (2012). Are patterns of density dependence in the global population dynamics database driven by uncertainty about population abundance? *Ecology letters*, *15*(1), 17–23.

Lande, R., Engen, S., & Saether, B.-E. (2010). *Stochastic Population Dynamics in Ecology and Conservation*. Oxford University Press.

Mandelbrot, B., & Hudson, R. L. (2007). *The misbehavior of markets: A fractal view of financial turbulence.* Basic Books.

Mangel, M., & Tier, C. (1994). Four facts every conservation biologists should know about persistence. *Ecology*, *75*(3), 607–614.

Marquet, P. A., Quiñones, R. A., Abades, S., Labra, F., Tognelli, M., Arim, M., & Rivadeneira, M. (2005). Scaling and power-laws in ecological systems. *Journal of Experimental Biology*, *208*(9), 1749–1769.

May, R. M. (1976). Simple mathematical models with very complicated dynamics. *Nature*, *261*(5560), 459–467.

May, R. M., & Oster, G. F. (1976). Bifurcations and Dynamic Complexity in Simple Ecological Models. *The American Naturalist*, *110*(974), 573–599.

McGill, B. (2003). Strong and weak tests of macroecological theory. *Oikos*, *102*(3), 679–685.

Merkle, E. C., Furr, D., & Rabe-Hesketh, S. (2019). Bayesian comparison of latent variable models: Conditional versus marginal likelihoods. *Psychometrika*, *84*(3), 802–829.

Newman, M. E. J. (2005). Power laws, Pareto distributions and Zipf's law. *Power laws, Pareto distributions and Zipf's law. Contemporary physics*, *46*(5), 323–351.

Newton, I., Rothery, P., & Dale, L. C. (1998). Density-dependence in the bird populations of an oak wood over 22 years. *Ibis*, *140*(1), 131–136.

Ogden, L. E. (2018). Black Swans: Do Lessons from the Stock Market Apply to Animal Populations? *BioScience*, *68*(4), 312.

Park, T. (1934). Observations on the general biology of the flour beetle, tribolium confusum. *The Quarterly Review of Biology*, *9*(1), 36–54.

Park, T. (1935). Studies in population physiology. iv. some physiological effects of conditioned flour upon tribolium confusum duval and its populations. *Physiological Zoology*, *8*(1), 91–115.

Park, T., Mertz, D. B., Grodzinski, & Prus. (1965). Cannibalistic Predation in Populations of Flour Beetles. *Journal of Physics A: Mathematical and Theoretical*, *44*(8), 21–25.

Park, T., Ziegler, J. R., Ziegler, D. L., & Mertz, D. B. (1974). The cannibalism of eggs by tribolium larvae. *Physiological Zoology*, *47*(1), 37–58.

Potts, G., Coulson, J., & Deans, I. (1980). Population dynamics and breeding success of the shag, phalacrocorax aristotelis, on the farne islands, northumberland. *The Journal of Animal Ecology*, 465–484.

Prendergast, J., Bazeley-White, E., Smith, O., Lawton, J., Inchausti, P., Kidd, D., & Knight, S. (2010). The global population dynamics database.

Raffa, K. F., Aukema, B. H., Bentz, B. J., Carroll, A. L., Hicke, J. A., Turner, M. G., & Romme, W. H. (2008). Cross-scale drivers of natural disturbances prone to anthropogenic amplification: The dynamics of bark beetle eruptions. *Bioscience*, *58*(6), 501–517.

Ray, C., & Hastings, A. (1996). Density dependence: Are we searching at the wrong spatial scale? *Journal of Animal Ecology*, 556–566.

Reed, D. H., & Hobbs, G. R. (2004). The relationship between population size and temporal variability in population size. *Animal conservation forum*, *7*(1), 1–8.

Rich, E. R. (1956). Egg Cannibalism and Fecundity in Tribolium. *Ecology*, *37*(1), 109–120.

Ryan, M. F., & Nathanson, M. (1969). A relationship between handling and a developmental abnormality in the flour beetle, tribolium spp. *Bulletin of Entomological Research*, *59*(3), 435–440.

Saucy, F. (1994). Density dependence in time series of the fossorial form of the water vole, arvicola terrestris. *Oikos*, 381–392.

Schaffer, W. M. (1985). Order and chaos in ecological systems. *Ecology*, *66*(1), 93–106.

Schindelin, J., Arganda-Carreras, I., Frise, E., Kaynig, V., Longair, M., Pietzsch, T., Preibisch, S., Rueden, C., Saalfeld, S., Schmid, B., et al. (2012). Fiji: An open-source platform for biological-image analysis. *Nature methods*, *9*(7), 676–682.

Schmitt, F. G., Molinero, J. C., & Brizard, S. Z. (2008). Nonlinear dynamics and intermittency in a long-term copepod time series. *Communications in Nonlinear Science and Numerical Simulation*, *13*(2), 407–415.

Segura, A. M., Calliari, D., Fort, H., & Lan, B. L. (2013). Fat tails in marine microbial population fluctuations. *Oikos*, *122*(12), 1739–1745.

Segura, A. M., & Perera, G. (2019). The Metabolic Basis of Fat Tail Distributions in Populations and Community Fluctuations. *Frontiers in Ecology and Evolution*, *7*(May), 1–8.

Snyder, R. E., & Ellner, S. P. (2022). Snared in an evil time: How age-dependent environmental and demographic variability contribute to variance in lifetime outcomes. *The American Naturalist preprint doi:10.21203/rs.3.rs-888047/v1.*

Sokoloff, A. (1974). *The biology of tribolium with special emphasis on genetic aspects, vol. 2.* Oxford, Clarendon Press.

Solow, A. R. (2005). Power laws without complexity. *Ecology Letters*, *8*(4), 361–363.

Sonleitner, F. J. (1961). Factors Affecting Egg Cannibalism and Fecundity in Populations of Adult Tribolium castaneum Herbst. *Physiological Zoology*, *34*(3), 233–255.

Sonleitner, F. J., & Gutherie, J. (1991). Factors affecting oviposition rate in the flour beetle tribolium castaneum and the origin of the population regulation mechanism. *Population Ecology*, *33*(1), 1–11.

Stanley, J. (1942). A mathematical theory of the growth of populations of the flour beetle tribolium confusum duv. v. the relation between the limiting value of egg-populations in the absence of hatching and the sex-ratio of the group of adult beetles used in a culture. *Ecology*, *23*(1), 24–31.

Stone, L., & Hart, D. (1999). Effects of immigration on the dynamics of simple population models. *Theoretical Population Biology*, *55*(3), 227–234.

Strawbridge, D. W. (1953). *Population dynamics of the flour beetle tribolium castaneum herbst* (Doctoral dissertation). University of Chicago.

Strogatz, S. H. (1994). *Nonlinear dynamics and chaos: With applications to physics, biology, chemistry, and engineering*. CRC press.

Taleb, N. N. (2019). How much data do you need? an operational, pre-asymptotic metric for fat-tailedness. *International Journal of Forecasting*, *35*(2), 677–686.

Taleb, N. N. (2020). Statistical consequences of fat tails: Real world preasymptotics, epistemology, and applications. *arXiv preprint arXiv:2001.10488*.

Thibaut, L. M., & Connolly, S. R. (2020). Hierarchical modeling strengthens evidence for density dependence in observational time series of population dynamics. *Ecology*, *101*(1), e02893.

Thorson, J. T., Skaug, H. J., Kristensen, K., Shelton, A. O., Ward, E. J., Harms, J. H., & Benante, J. A. (2015). The importance of spatial models for estimating the strength of density dependence. *Ecology*, *96*(5), 1202–1212.

Vehtari, A., Gelman, A., & Gabry, J. (2017). Practical Bayesian model evaluation using leave-one-out cross-validation and WAIC. *Statistics and Computing*, *27*(5), 1413–1432.

Weron, R. (2001). Levy-stable distributions revisited: Tail index > 2 does not exclude the Levy-stable regime. *International Journal of Modern Physics C*, *12*(2), 209–223.

Wiens, J. A. (1977). On competition and variable environments: Populations may experience" ecological crunches" in variable climates, nullifying the assumptions of competition theory and limiting the usefulness of short-term studies of population patterns. *American Scientist*, *65*(5), 590–597.

Williams, G. (1954). Population fluctuations in some northern hemisphere game birds (tetraonidae). *The Journal of Animal Ecology*, 1–34.

Ziebarth, N. L., Abbott, K. C., & Ives, A. R. (2010). Weak population regulation in ecological time series. *Ecology letters*, *13*(1), 21–31.